N84-31514

DOE/NASA/0211-1
NASA CR-168244
ERC TR-83024

AC Propulsion System for an Electric Vehicle

Phase 2 Interim Report

James M. Slicker
Eaton Corporation
Engineering & Research Center

June 1983

Prepared for
NATIONAL AERONAUTICS AND SPACE ADMINISTRATION
Lewis Research Center
Under Contract DEN 3-211

for
U.S. DEPARTMENT OF ENERGY
Conservation and Renewable Energy
Office of Vehicle and Engine R&D

DOE/NASA/0211-1
NASA CR-168244
ERC TR #83024

AC PROPULSION SYSTEM FOR AN ELECTRIC VEHICLE: PHASE 2 INTERIM REPORT

COPY NO. _____

J. M. Slicker
Eaton Corporation
Engineering & Research Center
Southfield, MI 48037

June 1983

Prepared for:

National Aeronautics & Space Administration
Lewis Research Center
Cleveland, OH 44135
Under Contract DEN3-211

For:

U. S. Department of Energy
Conservation and Renewable Energy
Office of Transportation Programs
Washington, D.C. 20534

ACKNOWLEDGEMENT

The following people made major contributions to this report:

M. P. Bujold
D. Gritter
W. H. Garrett
S. Geppert
A. J. Hutchenreuther
I. Kalns
K. S. Williams

Technical Director: S. Geppert/J. M. Slicker

Program Manager: W. K. O'Neil

TABLE OF CONTENTS

TABLE OF CONTENTS

LIST OF FIGURES

LIST OF FIGURES (cont.)

LIST OF FIGURES (cont.)

1.0 SUMMARY

The object of this program was to develop and test an AC propulsion system, based on an earlier "Phase 1" prototype, in a test bed passenger vehicle. The system consists of a two-speed, mechanically-shifted (hydraulic clutches) automatic transaxle, an 18.65 kw (25 hp) rated AC traction induction motor, a pulse-width-modulated (PWM) transistorized inverter, and an overall microprocessor-based vehicle/drive controller. Integral with the inverter, and sharing circuitry, is a dual-mode (110 VAC or 220 VAC) battery charger and a 50 amp DC/DC converter for 12V system and vehicle loads.

The test bed vehicle, shown in Figure 1.1, was a modified 1981 Mercury-Lynx hatchback. The motor/transaxle assembly mounted under the hood and powered the front wheels. The inverter/controller mounted in a well beneath the rear seat. Two 96V lead-acid battery packs, one installed under the hood and the other under the luggage area (spare tire sacrificed), provided a nominal 192V traction system voltage.

Vehicle curb weight was 1364 kg (3000 lb.); test weight was typically 1636 kg (3600 lb.). Propulsion system weight was 139 kg (motor 55 kg, inverter 43 kg, transaxle 37 kg, and controller 3 kg).

Measured vehicle acceleration from 0 to 48 km/hr was 8.5 sec., and from 40 to 88 km/hr was 27 sec. Top speed was 104 km/hr. Creep speed gradeability was 16%, as derived from acceleration data.

Efficiency and performance tests were run with the propulsion system mounted on an instrumented dynamometer. Secondary efficiency data were gathered during the vehicle tests. A measured peak dc-to-mechanical system efficiency of 82% was achieved, and can be improved with continued transaxle developments. For vehicle tests, measured energy consumption at the battery terminals was .214 kwhr/mi at 25 mph, .225 kwhr/mi at 35 mph, and .266 kwhr/mi at 45 mph. Energy consumption of .320 kwhr/mi was measured at the battery terminals over the SAE J227a-D driving schedule. The above energy consumption figures reflect the high vehicle road load that was determined from coast-down and drawbar tests. Possible improvements in energy consumption with a lower road load are discussed in this report. Operation in both motoring and regenerative modes was tested.

The test results of the battery charger and DC/DC converter are included in this report along with dyno and vehicle results.

The work was performed under NASA Lewis Research Center (LeRC) Contract DEN3-211 for the U.S. Department of Energy from January 1, 1981 through January 17, 1983. A contract modification phase is continuing under Jet Propulsion Laboratory Contract #DE-AC08-81NV10320.

Figure 1.1 Electric Vehicle

2.0 INTRODUCTION

2.1 Background

This project was a follow-on effort to a "Phase 1" development program (ASCS1) which yielded a functional prototype AC propulsion system on a test frame. Although the broad system concept remained the same, the Phase 2 system (ACPS2) represents major refinements in all components. The Phase 1 system is described in NASA publication CR-165480 (DOE/NASA/0125-1) "AC Propulsion System for an Electric Vehicle - Phase 1 Final Report."

Whereas the Phase 1 proof-of-concept system was not intended for vehicle installation, the Phase 2 system was. This demanded more attention to weight, electronics packaging, and device cooling.

The main transaxle improvements were a 24% weight reduction, a volume reduction owing to a concentric intermediate and output shaft arrangement, and compact internal hydraulic lines.

The main motor improvements were a 17% weight reduction at identical power rating, much improved oil cooling paths, and production-oriented design. The motor top speed was raised from 9000 RPM in ACPS1 to 12,500 RPM in order to achieve greater utilization of motor power. This speed increase, combined with a transaxle gear ratio increase from ACPS1 also raised system efficiency in the vehicle 48 km/hr to 75 km/hr cruising range by operating at more efficient motor/inverter frequencies. Some marginal decrease in transaxle efficiency can be expected at a higher gear ratio; however the above advantages and the opportunity to obtain new information in the higher speed range outweigh this.

The main inverter improvements were a 20% weight reduction even with the addition of an integral automatic main battery charger and multiple output 850W DC/DC converter, a 50% volume reduction, higher efficiency at intermediate torques and speeds, a 33% increase in nominal battery bus voltage for reduced inverter currents, over 63% reduction in main transistor costs due to a new device availability, and much simplified snubber, current sensing, and switching energy recovery circuits due to a new circuit topology.

The main logic controller improvements were the elimination of all analog slip loop circuits with their attendent adjustments, integration of vehicle, inverter, and charger control software, simplified analog input circuits, better diagnostic capability, and an improved pulse width modulation (PWM) scheme. The PWM waveform generation scheme yields far better sinusoidal current waveforms than the "center 60o" notching method used in Phase 1 for reduced waveform harmonic content.

2.2 Purpose of Project

The purpose of the contracted effort was to prove the technical feasibility of a second-generation Eaton AC propulsion system in a subcompact test-bed vehicle. System efficiency improvements, integral battery charger, and more cost-effective design were major technical goals.

2.3 Scope of Project (as amended January 5, 1982)

One developmental inverter was built, followed by a second unit incorporating design changes from development work. Major parts and packaging for a third unit (or for spares) were built. Three logic controllers were built, with one unit carried forward with all changes. Three identical motors were fabricated. Two transaxles were completed. One test bed vehicle was completed for system testing. Computer simulations of motor, inverter (partial electrical and thermal), vehicle, and battery performance were carried out. A special-purpose, computerized dyno test stand was developed to aid in system development and verification. Two versatile portable diagnostic boxes which can monitor and control system operation were built.

2.4 Testing Overview

Testing was conducted over several levels. First, the controller was tested with simulated inputs in the electronics lab. Second, the motor/inverter/controller electrical subpackage was tested and debugged no load in the power lab. The charger and DC/DC converter were also developed in the power lab. Third, the electrical subpackage was tested on the dyno with the motor mounted on a torque table. The major system refinement occurred at this stage. Fourth, the transaxle was mated with the subpackage and the total system tested on the dyno test stand. Fifth, the system was installed in the test vehicle for system refinement and validation. Hardware and software improvements were continually being made throughout the test phases. Because of shortcomings in the transaxle, it was separately tested for efficiency on a dynamometer following the track tests.

3.0 SYSTEM OVERVIEW

3.1 System Concept

The AC propulsion system represents advanced electric traction drive technology. For consumer vehicles, the primary criteria are weight, efficiency, cost, size, ruggedness, and maintainability. Listed below are the fundamental technical decisions. They have not changed from the Phase 1 design.

1. The drive would use a three-phase AC induction motor. The advantages associated with the induction motor compared to a DC motor justify an AC approach. These advantages are smaller size, lighter weight, better mass production suitability, lower cost, brushless circuits, sealability, simpler rugged construction, and higher power density due to its higher speed capability.

2. The inverter would use transistors as the main switching devices. Transistors do not need commutation components and can be switched much faster than SCR's, leading to better waveform shape and less losses. As the price of power transistors continues to drop, overall costs for a 25 hp transistor drive are approaching an equivalent SCR drive.

3. A pulse width modulated inverter was chosen because of the fixed potential battery source. Alternative approaches, such as variable dc link voltage, require a front-end chopper and an inductor/capacitor dc bus filter and make regeneration difficult. In contrast, PWM is inherently regenerative and requires only a small capacitive bus filter. The generation of complex PWM waveforms, which has limited the application of PWM drives in the past, is easily accomplished with the microprocessor interface.

4. A two-speed transaxle assembly provides a direct mechanical link from motor shaft to vehicle drive wheels. The automatic shift prevents driver abuse and increases customer acceptance. Two gear ratios are provided to achieve reasonable low end torque for gradeability and acceleration without an oversized inverter and motor. Although a neutral gear is provided, it would not be used for Phase 2 vehicle testing. This omission from the test bed vehicle reduces complexity, because an additional speed sensor would be required for synchronizing the transaxle input and output shafts when using a neutral gear.

5. The microprocessor based controller would perform all aspects of the vehicle-motor control: motor waveform generation, shift commands, operator inputs, regenerative braking, battery charge mode control, and display

outputs. This approach allows for no limp-home capability upon microprocessor failure, and would need investigation in a production system. Redundant circuits with fault sensing would enhance reliability, but that approach was considered too complex for this design generation. Instead, self-checking, automatic restart, and extensive diagnostic/monitor software and hardware were included. The secondary functions included in the controller do not materially reduce its reliability in performing critical functions. Although a production system would need a speed direction sensor to achieve rapid forward-reverse operation through zero speed, this feature was not included on the test bed vehicle because of added complexity.

6. The drive would tolerate wide swings in DC supply voltage typical of battery systems.

7. The system would be sized for a small, all-electric car. As in Phase 1, continuous power (1 hour) would be 18.6 kw (25 hp) and maximum power (2 min) would be 33.6 kw (45 hp).

8. Maintaining the system concept of transaxle, motor, inverter, and controller would be important to optimize performance.

Figure 3.1.1 shows a block diagram of controller drive system functions. These functions are "invisible" to the operator.

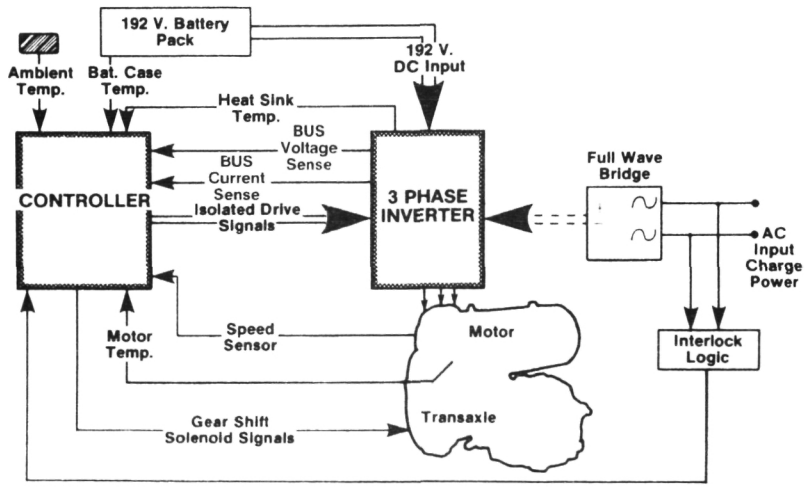

Figure 3.1.1 Controller Drive System Functions

The other aspect of system operation, Controller Vehicle/Operator Interface, is depicted in Figure 3.1.2. These two figures show all significant parts of the system except the DC/DC converter used to develop logic power and to charge the 12v vehicle accessory battery.

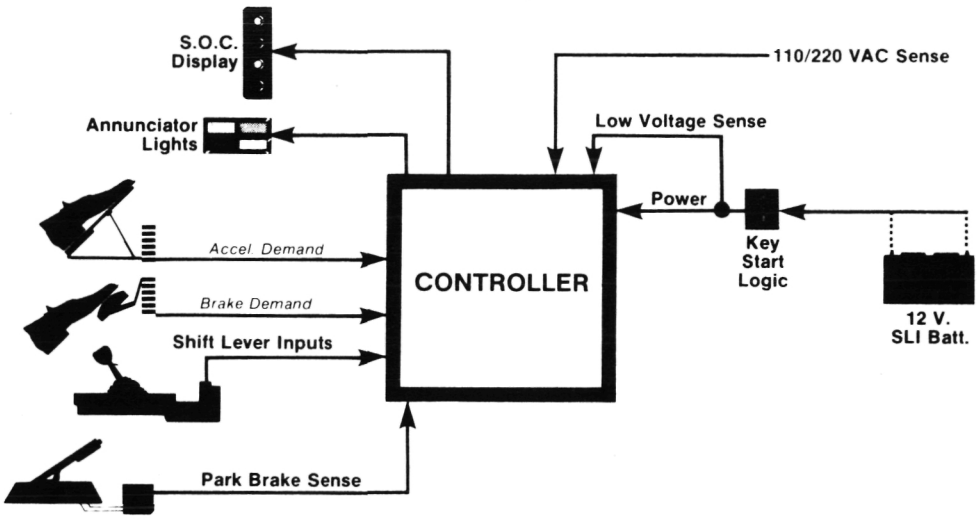

Eaton ACPS2

Figure 3.1.2 Controller Vehicle/Operator Interface

3.2 Component Specifications

Specifications (goal and achieved) for each of the four system components are listed in Table 3.2.1. Figures 3.2.1 through 3.2.4 show photos of each component. Table 3.2.2 summarizes component weights.

3.3 System Performance Goals in Specified Vehicle

Contract vehicle performance goals are listed in Table 3.3.1. Actual test weight during vehicle tests typically was 1636 kg (3600 lb). Battery-dependent parameters such as range are not specified among these goals. Energy consumption per km at various speeds and over a representative driving cycle were not given target values, but when obtained from the vehicle tests (Section 11.1) were compared with previously published results on the dc ETV-1 vehicle.

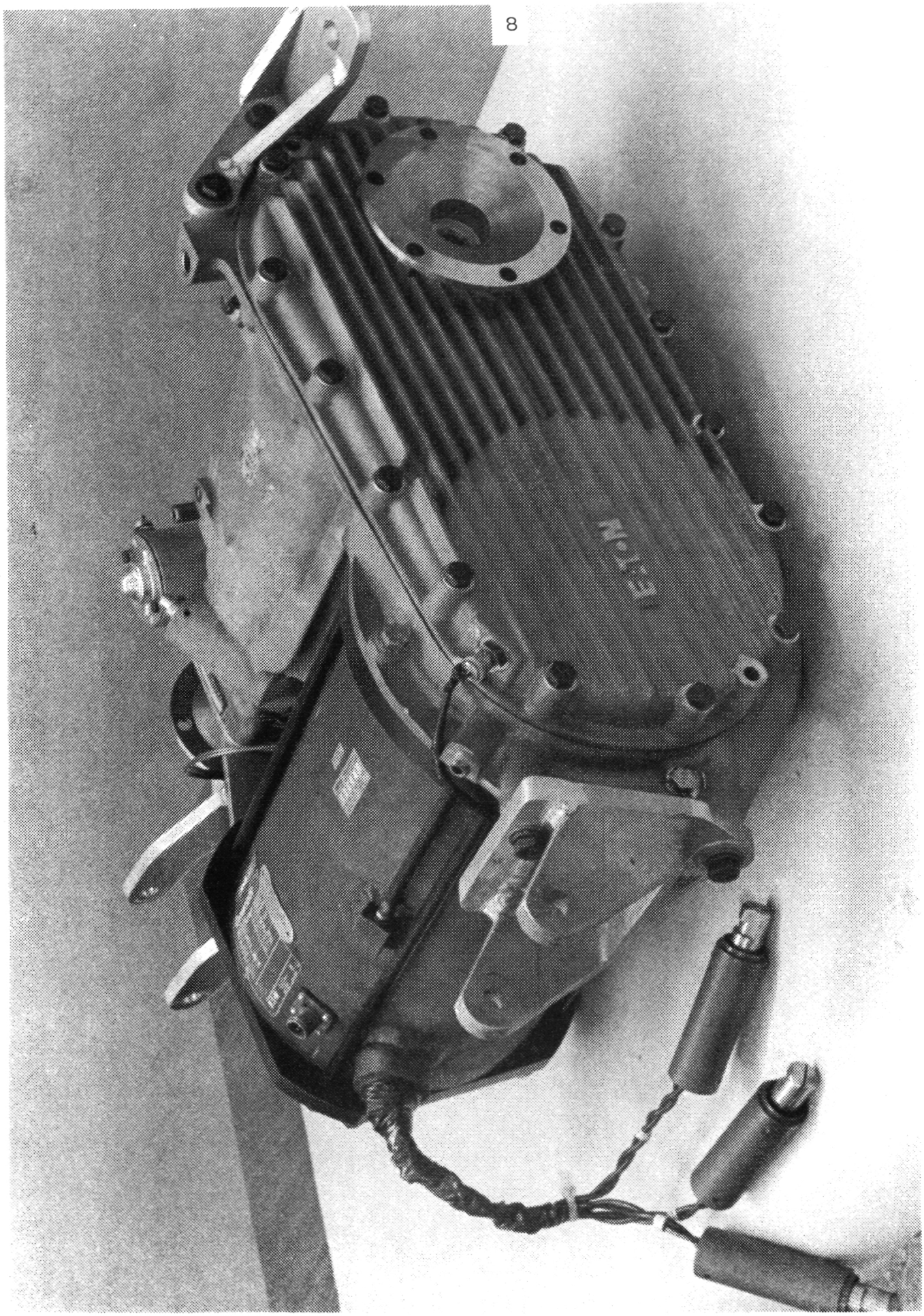

Figure 3.2.1 Trans/Axle Motor Assembly

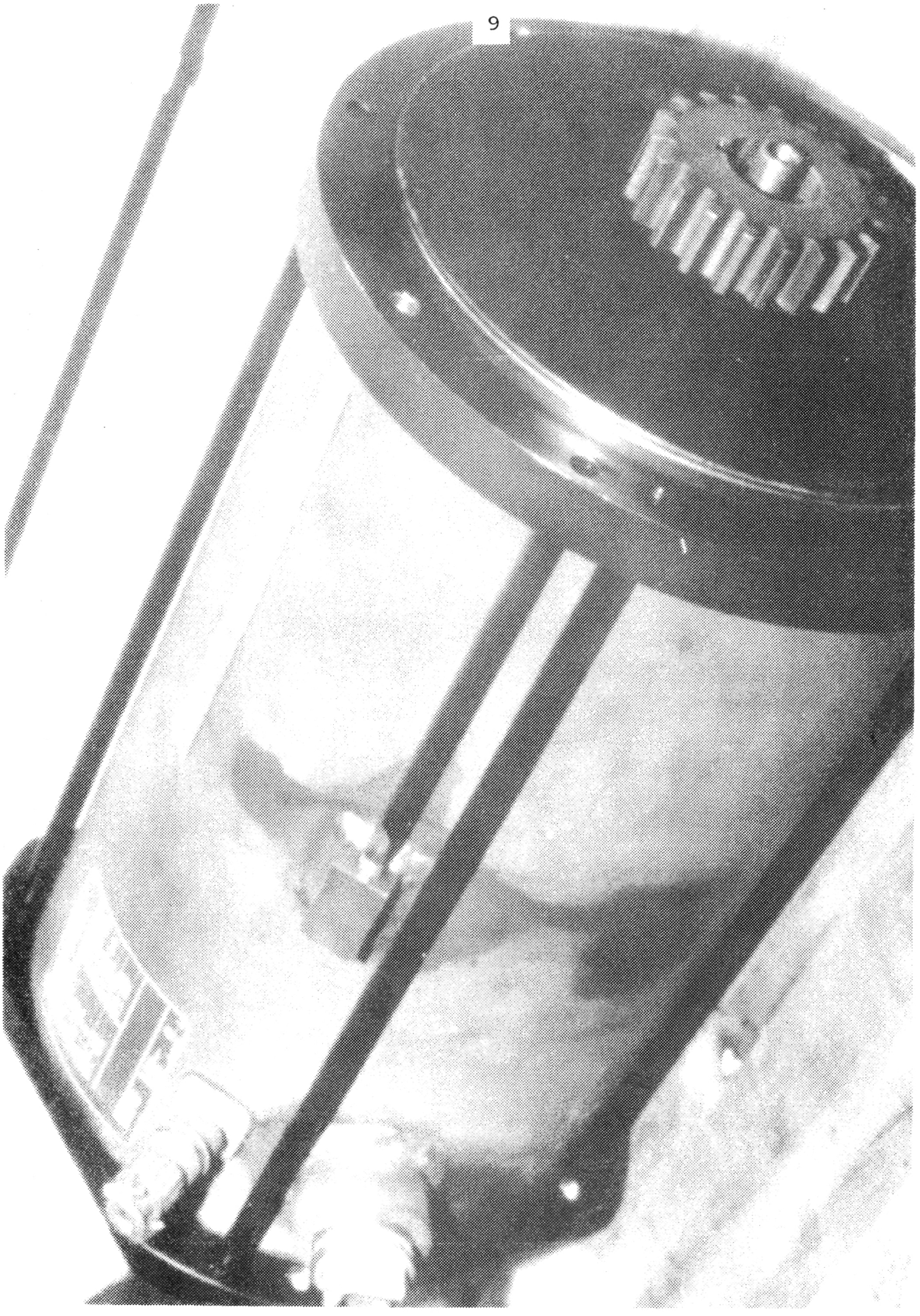

Figure 3.2.2 Motor

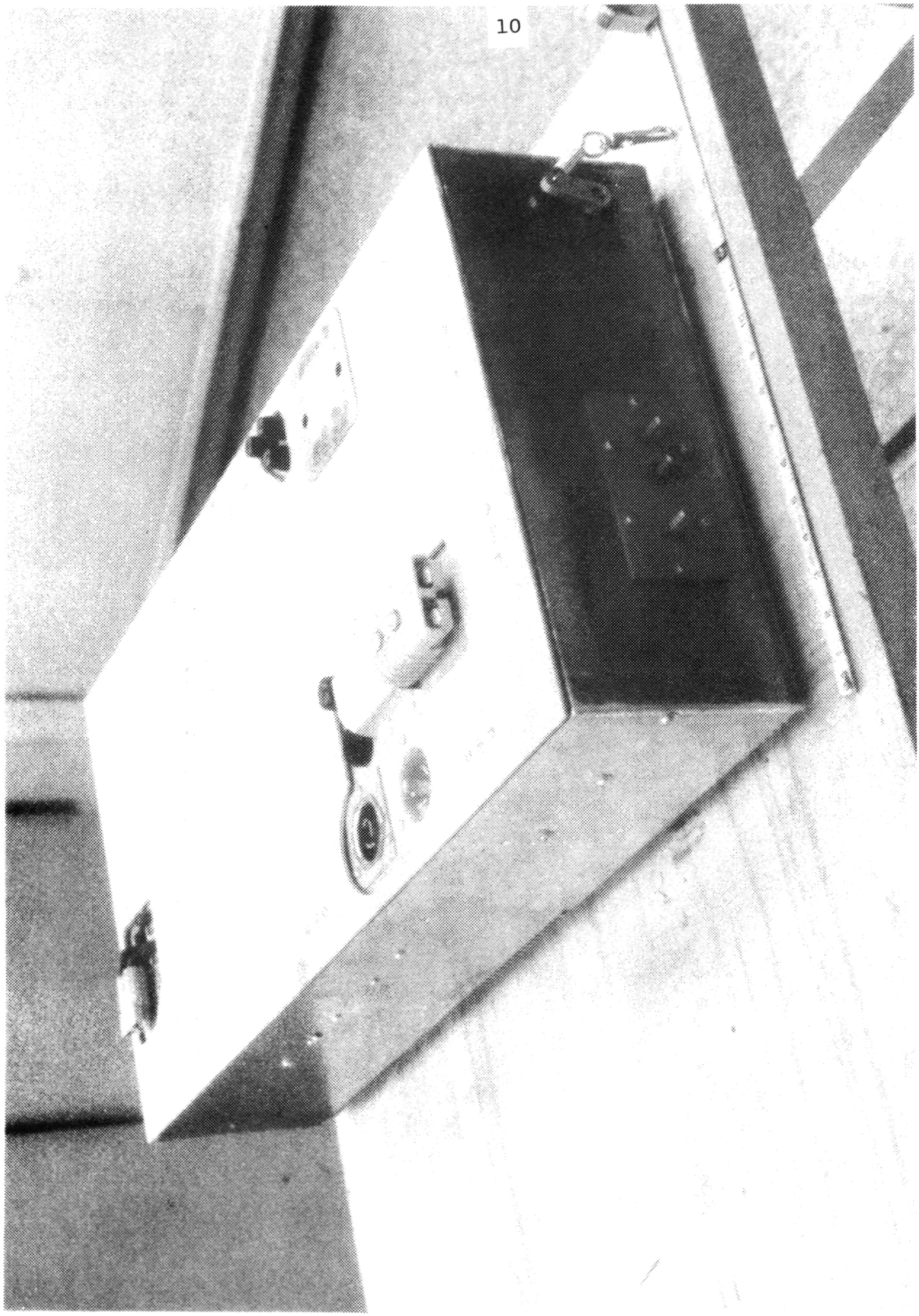

Figure 3.2.3 Inverter

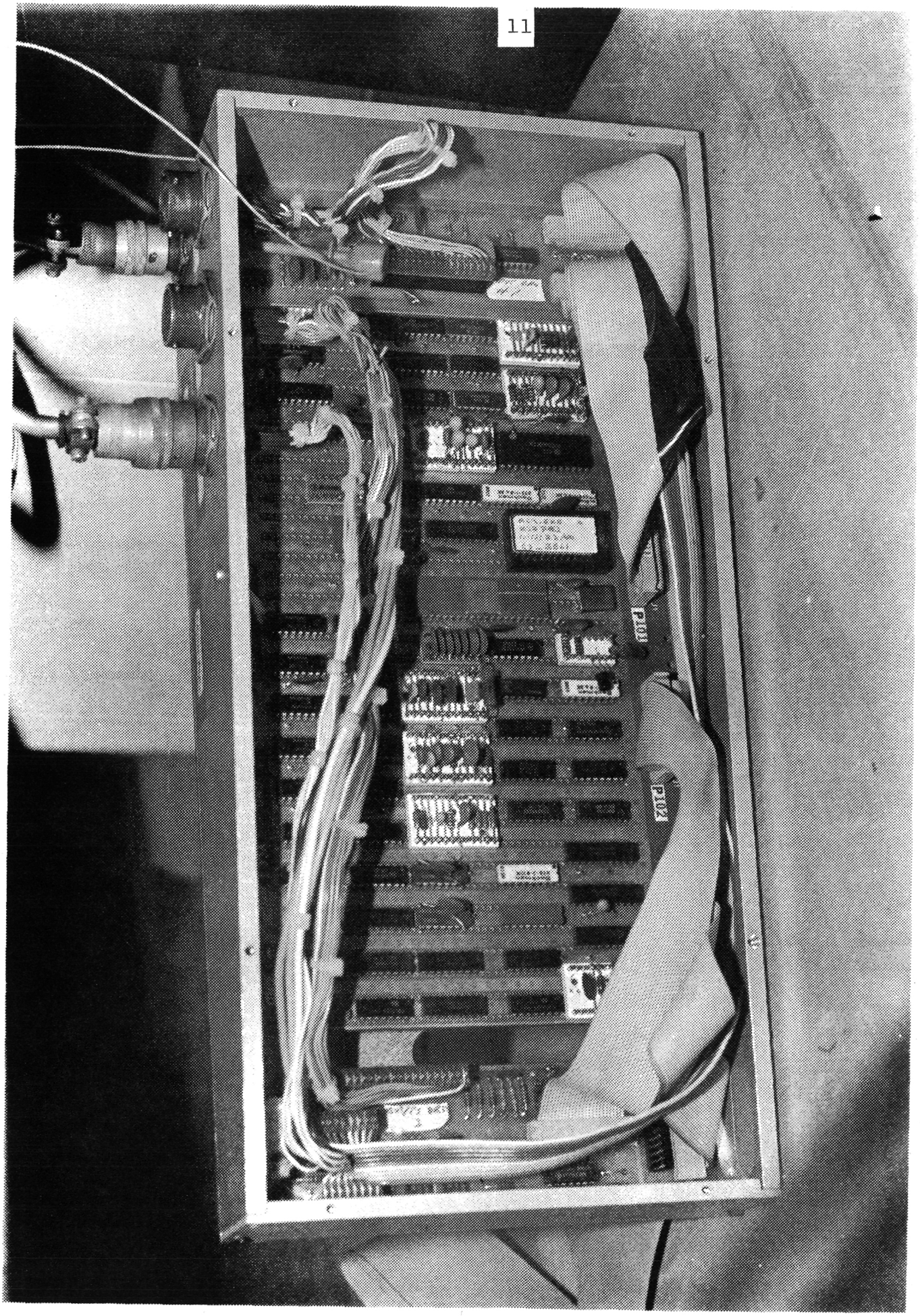

Figure 3.2.4 Controller

TABLE 3.2.1

PRIMARY SYSTEM SPECIFICATIONS OF PHASE 2 AC PROPULSION SYSTEM PROTOTYPE

	GOAL	ACHIEVED
TRANSAXLE		
Input power	18.6 kW (25 hp) continuous (motoring or 33.6 kW (45 hp) intermittent regen)	18.6 kW 33.6 kW
Max input speed	12,500 rpm	12,500 rpm
Max output speed	1,087 rpm	1,087 rpm
Max input torque	57 nm 42 lb-ft) intermittent	
Max output torque	1,741 nm (1,285 lb-ft) intermittent	
Reduction ratios	Low gear overall: 28.71 :	_____
	High gear overall: 10.75 :	_____
	Chain drive: 2.52 :	_____
	Suitable planetary: Low: 2.67 :	_____
	High: 1 :	_____
	Final output planetary: 4.267:1	_____
Design life, B-10	4,000 hrs or 160,000 km (100,000 mi)	Not tested
Weight w/pump, valves, oil	36 kg (80 lbs)	36.8 (81)

TABLE 3.2.1 (continued)

	GOAL	ACHIEVED
TRANSAXLE		
	Automatic with two hydraulic clutch packs under solenoid control	
Shift means hydraulic system	Pressure: 10.3 bar (150 psi) max	4.1 bar (60 psi) min
	Pump power: 0.25 kW (1/3 hp) @ 12V	.25 kW @ 192V
	Capacity: 3.8 ℓ (4 qts)	2.8 ℓ
	Fluid: GM Dexron II	GM Dexron II
MOTOR		
Type	AC induction traction	
Rating	18.6 kW (25 hp) for one hr @ base frequency and above	18.6 kW
	33.6 kW (45 hp) for two min @ base frequency	33.6 kW
	23.3 kW (36.5 hp) for two min @ maximum frequency	25 kW @ 11,000 rpm
Phases	3	
Poles	2	-
Base frequency	94 Hz (5,640 rpm synchronous)	
Max frequency	212 Hz (12,720 rpm synchronous)	-
Voltage at base frequency	133 Vrms line-line	-
Inverter drive	PWM transistorized. Nominal 192Vdc bus switching frequency to 5 KHz	
Frame	Special aluminum. Totally enclosed. Face mounting	-
Stator windings	Copper with Class H insulation. Thermister imbedded. Neutral brought out	-
Laminations	Transformer silicon steel	-
Rotor bars	Aluminum	-
Cooling	Dexron II oil. Nominal 1 gpm flow. External pump. Cooling passages	-
Ambient temperature	-40°C to +45°C	Not tested
Efficiency	90% sinewave at 60 Hz and rated torque	88.5%
Weight	55 kg (121 lb)	55.5 kg (122 lb)

TABLE 3.2.1 (Continued)

	GOAL	ACHIEVED
INVERTER (includes all power contactors and fuses)		
Type	PWM transistorized, 3 phase, six switch bridge using 2-100A Darlington/switch	-
Input voltage	192V nominal 125V minimum (reduced performance) 240V maximum (regen braking)	- 125V 240V
Power rating	20 kW continuous (1 hr) 36 kW peak (2 min)	20 kW 36 kW
Weight	41 kg (90 lb)	43 kg (95 lb)
Size L X W X S	-	78 cm x 38 cm x 18 cm
Packaging	Aluminum box totally enclosed non-ventilated	-
Switching rate	Up to 5 KHz	Up to 4 kHz
Protection	Fast phase current limits (Hall current sensors) Fast bus current limits (Hall current sensors) Fast inverter bus voltage limit Power up base-drive inhibit Heat sink temperature limit	All
Isolation	All high voltage circuitry isolated from case and logic controller. Switching commands opto-coupled	-
Cooling	Forced air over base extruded aluminum heat sink	
DC/DC converter	Supplies four ±7V floating base drive supplies @ $\pm^{+8}_{-2}$ amps Supplies one +14V accessory supply @ 50 amps (isolated)	4 x $\pm^{+8}_{-2}$ amps +14V @ 50 a
Battery charger	Integral to inverter switching circuits 220Vac: 6 kW max to battery 110Vac: No goal specified Overall efficiency over complete recharge cycle @ 220Vac (batteries initially 90% discharged): 90%	 4 kW to battery 1.5 kW to battery 80 %

TABLE 3.2.1 (continued)

	GOAL	ACHIEVED
CONTROLLER		
Type	Microprocessor-based, slip control scheme PWM voltage control strategy for 3ϕ induction motor Controls motor, charger, transaxle, and operator I/O	- Controls motor, charger, transaxle and operator I/O
Stator frequency range	0-220 Hz	0-250 Hz
Inputs	Driver accel/decel demand Motor speed Bus voltage Bus current Battery pack temp Motor case temp Main transistor heat sink temp Ambient temp Diagnostic input requests	0 to +2V each 0-13,000 rpm 0-255V range +250, -200 amp range 0-125°C range 160° to 200°C active range, motor stator temp 0-125°C range 0-125°C range -
Outputs	Inverter switching command signals @ stator frequency Gearshift command Alarm warn and shutdown Diagnostic data	
Slip control update rate	No spec	100 Hz
Voltage control update rate	No spec	Greater than 20 Hz
Weight	Less than 4.5 kg (10 lb)	2.8 kg (6.2 lb)
Size	7.6 cm x 38.1 cm x 17.8 cm (3" x 15" x 17")	7.6 cm x 38.1 cm x 17.8 cm
Power	10W max	9W
Temperature range	-20°C to +60°C operating	Not tested over range
Isolation	Totally isolated from traction battery (min 200KΩ)	Greater than 500KΩ
Enclosure	6-sided aluminum box with dust-sealed cover	6-sided aluminum box with dust-sealed cover

TABLE 3.2.2

AC PROPULSION SYSTEM COMPONENT WEIGHT DATA

COMPONENT	Kg	Lb
Transaxle w/oil, pump, pump motor, valves, brackets	36.8	81
Motor	55.5	122
Inverter w/dc/dc converter and battery charger	43	97
Controller	2.8	6.2
Controller Power Supply	1.0	2.5
Total	139.1	308.7

NOTES: Inverter-motor and inverter-battery cabling weight not included since length varies on vehicle installation. #2 welding cable used for both links.

Inverter cooling fan (2 kg) external to inverter, not included above.

Logic signal cable sensors, and connectors not included. Total less than 3 kg.

TABLE 3.3.1

TEST BED VEHICLE PERFORMANCE GOALS

Test weight not specified.

136 kg (30 lb) payload specified.

Acceleration:	0-48 km/m (0-30 mph) in 8 seconds.
	40-88 km/m (25-55 mph) in 16 seconds.
Gradeability:	Maintain 64 km/m (40 mph) on +4% continuous grade.
	Achieve 64 km/m (40 mph) in 305 m (1000 ft) on +4% grade.
Top Speed:	105 km/m (65 mph).

4.0 TRANSAXLE
4.1 Design
4.1.1 Major Design Considerations

The transaxle design, developed in Phase 1 of the program, demonstrated satisfactory function and performance in extensive dynamometer tests. However, some functional features necessary in a vehicle-mounted unit were deliberately omitted in that initial design or were provided external to the assembly. This was done in order to minimize the cost of verifying the basic transaxle concept and to provide a test bed for the complete AC system. It was felt that a much more detailed transaxle design at that stage could result in unnecessary effort, in case substantial changes in the configuration became necessary later.

The above Phase 1 approach was proven correct, as development tests and subsequent design evolution significantly changed the overall transaxle design. Considerable expense was also saved by providing a hydraulic system external to the transaxle assembly and by omitting all other features unnecessary for a unit only undergoing basic dynamometer tests on the test plate.

The Phase 2 design has been aimed at an optimized, self-contained transaxle assembly capable of achieving specified performance in a vehicle installation. The design objectives, therefore, were expanded correspondingly:

- Substantially reduce the size, weight, and manufacturing cost of the assembly.

- Retain all advantageous design features of the Phase 1 design: high mechanical efficiency, flexibility in motor-to-transaxle attitude, and relatively inexpensive adaptation to alternate motor sizes.

- Provide all design features required in a vehicle-mounted unit, such as integral hydraulics, parking latch mechanism, 3-point shock mounting, cooling fins, dipstick, lifting eye bosses, speed pickup, differential lock for dyno testing, convenient access to critical components, and easy maintenance.

- Provide a substantially increased overall gear reduction ratio to accommodate the 12,500 rpm maximum input speed of the second-generation AC motor. It was felt that Phase 2 should explore the higher speed range in search for optimal top motor transaxle input speed.

- Adapt existing automotive production hardware as much as possible in order to minimize prototype development time and cost.

- Bring function, appearance, and producibility closer to that of a manufactured product.

4.1.2 Phase 2 Transaxle Design

The initial attempt to incorporate these objectives in a revised Phase 1 design resulted in a considerable reduction in unit size. This was due to the elimination of the Belleville spring pack (originally intended for applying the low gear clutch), and elimination of double-bearing support for the input shaft. A section of the revised layout is shown in Figure 4.1.1. It became obvious, however, that even a substantial reduction in the length of the 2-speed transmission section did little to reduce the total envelope of the assembly. Arranging the axles and the differential in line with the transmission section would offer a far more substantial reduction in envelope size. Consequently, this idea was explored and adopted.

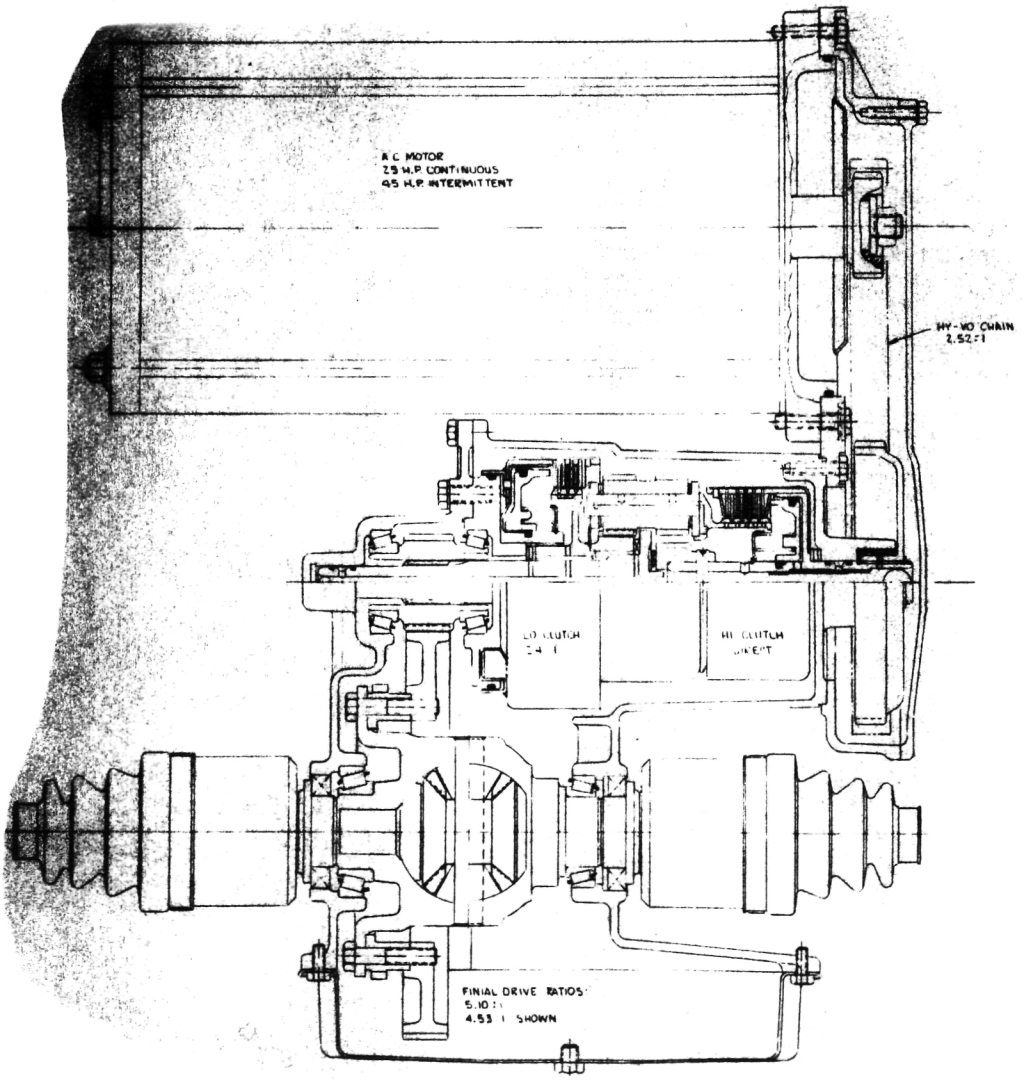

Figure 4.1.1 Revised Phase 1 Design Layout

The change represented a radically new approach in the transaxle design. The number of shaft centers was reduced from three (motor, transmission, differential) to two. The entire gearset was changed from a mixed planetary/countershaft arrangement to a pure coaxial basic planetary arrangement, with a substantially increased overall reduction ratio. An overrunning clutch was incorporated to serve as an alternate reaction member in the low-gear planetary.

The transaxle assembly, in addition to its basic function of transmitting mechanical power from the AC motor to the driving axles of the vehicle, also serves as structural support for the motor and a cooling means for much of the motor's rejected heat.

The Phase 2 transaxle is a two-speed, powershifted mechanical automatic, consisting of a chain drive reduction, a shiftable planetary gear and clutch assembly, a final drive planetary gearset, a differential head assembly, and a hydraulic system. A schematic of the powertrain is shown in Figure 4.1.2. A partial layout of the assembly is shown in Figure 4.1.3, and a photo of the motor/transaxle assembly in Figure 4.1.4.

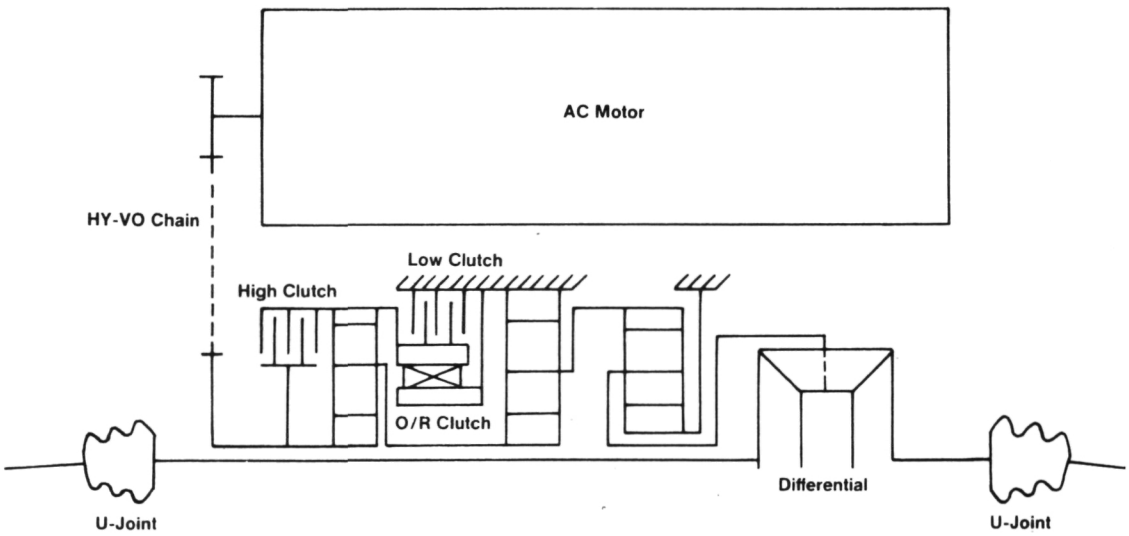

Figure 4.1.2 Phase 2 Drivetrain Schematic

Mechanical System

In the Phase 1 design, the chain drive reduction between the AC motor and the two-speed planetary transmission featured a Morse Hy-Vo Lite(R) chain. It was selected for its high efficiency, low noise, compact design, low weight and cost (compared to gears spanning the same shaft center distance). Also, the reduction ratio is easier to select and so is the

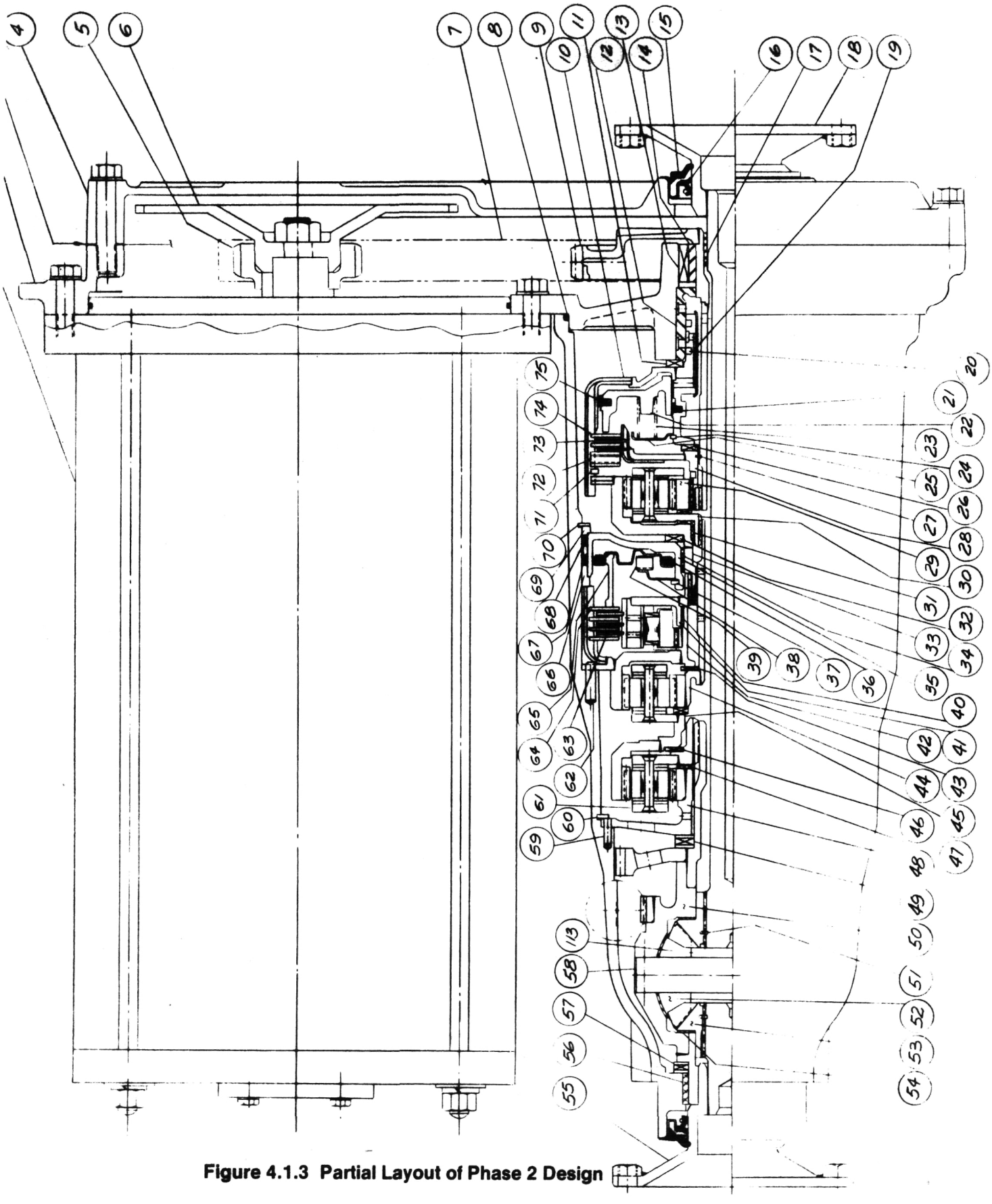

Figure 4.1.3 Partial Layout of Phase 2 Design

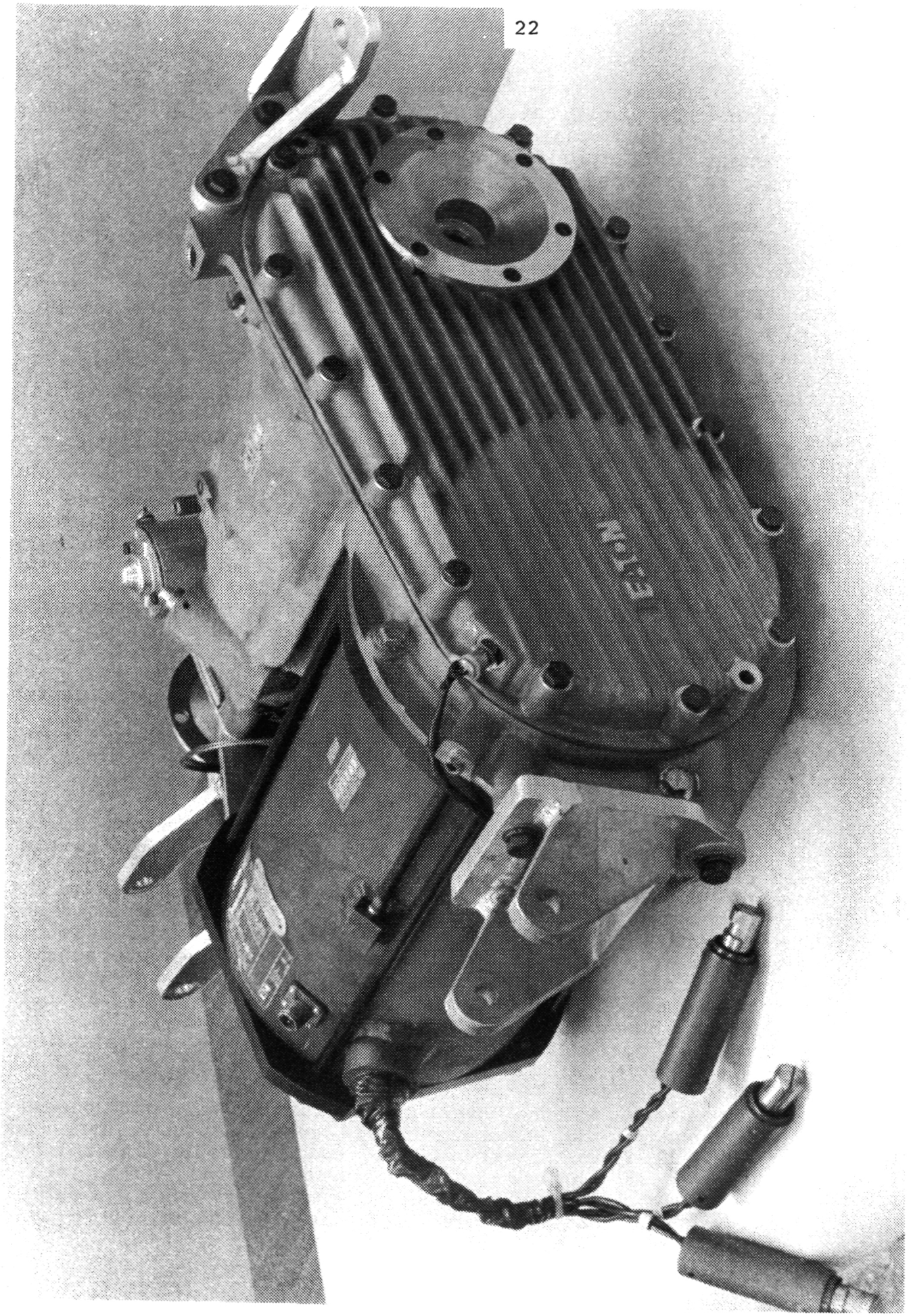

Figure 4.1.4 Trans/Axle/Motor Assembly

center distance (to accommodate a larger motor, for instance) by substituting alternate sprockets and/or chain housing. The chain drive is also less sensitive to component deflections and permits somewhat wider manufacturing tolerances.

The same 2.52:1 chain reduction between the AC motor and the transaxle has been retained in Phase 2 design. Attempts to substitute a timing belt were unsuccessful, as custom designs by Dayco Belt Research Center and by Gates Rubber Research engineers resulted in wider belts and larger sprockets than those of the present advanced Morse Hy-Vo(R) chain drive.

The two-speed planetary section uses a simple planetary for the 2.67:1 ratio, in place of the modified Ravigneaux set in the Phase 1 design. This results in more compactness, fewer parts, and improved gearset efficiency.

The final reduction comprises two simple planetaries in series, for a 4.27:1 overall reduction. This arrangement fits the available space better, is more efficient, and has wider alternate ratio flexibility than the single helical gear reduction of the Phase 1 design. The only difficulty with the coaxial, in-series arrangement of the Phase 2 design was the necessity of passing one of the two axle shafts through the center of the transmission. This required large sun gears in all three planetary sets. It has been possible, however, to adapt all gear and clutch elements, the parking latch mechanism, and the differential assembly from current production automatic transmissions through extensive rearrangement, modifications, and electron beam welding of the components.

The overrunning clutch has been incorporated in the design as an alternate means of holding the low gear reaction member, normally held by the low gear disk clutch. As the overrunning clutch adds noticeable drag to the system, it would be used only if the desired shift smoothness could not be attained through optimal overlap timing of the solenoid valves. The release and engagement of the overrunning clutch occur smoothly and automatically without any need for timing to achieve smooth shifts. The disk clutch is still necessary, however, for holding the reaction member when the vehicle is operated in reverse and during regeneration in low gear.

As the need for the overrunning clutch was not clearly established during Phase 2 vehicle testing, the clutch was not installed in either of the two transaxle assemblies. The incorporation of an overrunning clutch would entail considerable rework and increased complexity of the control system; hence, it has been left to the next development phase of the propulsion system.

A 3 in. diameter 192V DC motor-driven oil pump has been integrated into the main housing, along with all fluid passages, valving, and an accumulator. Mounting pads, cooling fins, lifting eye bosses, and a dipstick have also been provided.

The housing material has been changed to magnesium (AZ92A-T6) in order to obtain a one-third weight reduction without sacrifice in strength. Total weight of the four castings (machined) is 7.7 kg (17 lbs.).

Hydraulic System

The hydraulic system performs the cluch actuation functions and provides lube and cooling flow to the motor and trans-axle.

The small dc motor drives a gear pump, generating a minimum of 4.1 bar (60 psi) pressure. Oil flow beyond that required for the clutch actuation is directed to the lube and cooling circuits. A schematic of the hydraulic circuit is shown in Figure 4.1.5.

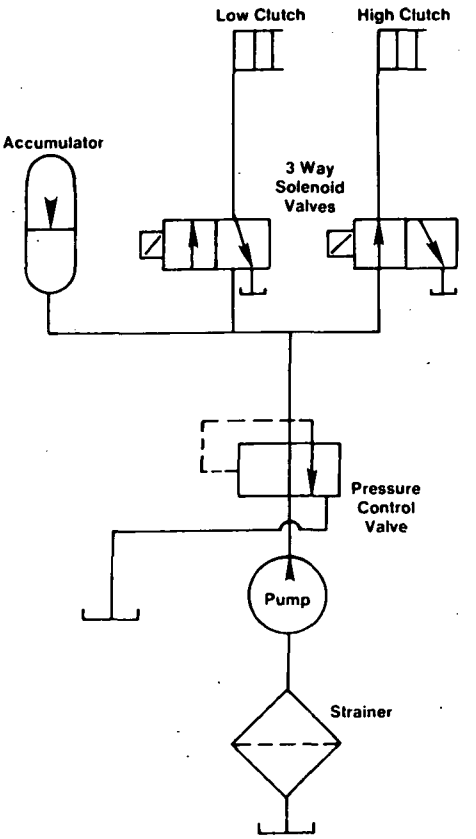

Figure 4.1.5 Transaxle Hydraulic System Schematic

An independently driven pump was chosen over a conventional, transmission input shaft-driven pump for the following reasons:

- Substantial pumping power loss is avoided at high input speeds.
- Cooling of traction motor is provided after vehicle is stopped, if necessary.
- Pump-reversing is avoided when traction motor is reversed.

Oil passages, made of aluminum tubing, are accommodated inside the main housing and oil pan. This was done, in preference to integrally cast passages, for the purpose of minimizing pattern equipment cost and to retain flexibility in modification of the circuitry as needed.

Transaxle Specification

Input power:	18.6 kw (25 hp) continuous 33.6 kw (45 hp) intermittent	
Maximum input speed:	12,500 rpm	
Maximum output speed:	1,160 rpm	
Maximum input torque:	57 Nm (42 lb-ft) intermittent	
Maximum output torque:	1,635 Nm (1,200 lb-ft) intermittent	
Design life, B-10:	4,000 hrs. or 160,000 km (100,000 mi.)	
Reduction ratios:	Overall, in low	28.7:1
	in high	10.75:1
	Chain drive	2.52:1
	Planetary (shiftable)	
	in low	2.67:1
	in high	1:1
	Planetary (final drive)	4.27:1
Actual weight (wet w/o traction motor):	36.8 kg (81 lbs.)	
Hydraulic system pressure, min.:	4.1 bar (60 psi)	
Hydraulic system fluid:	Dexron II	
Hydraulic system fluid capacity:	2.8 l (3 qts.)	

4.2 Transaxle Dynamometer Tests

Transaxle dynamometer tests were performed independently of the motor and controller on a separate test stand. Instrumentation was provided for recording input and output torques and speeds, temperature and oil pressure. The unit was then operated at various loads and pseeds in order to determine performance characteristics over a wide range of torques up to a maximum input speed of 5000 RPM, which was the dynamometer limit. Two sets of steady state tests were conducted on the transaxle in each gear range. These tests were drive performance and no-load losses. The efficiency results from these tests are shown in Figure 4.2.1 for low gear and 4.2.2 for high gear. The speed was limited by the test equipment. The test results do not include 160 watts in pump losses.

The overall accuracy of the equipment used in the determination of transaxle efficiency was approximately 1%. The torque sensors have a linear accuracy of 0.1% of full scale. The sensors were dead weight calibrated before and after each major test to ensure their accuracy.

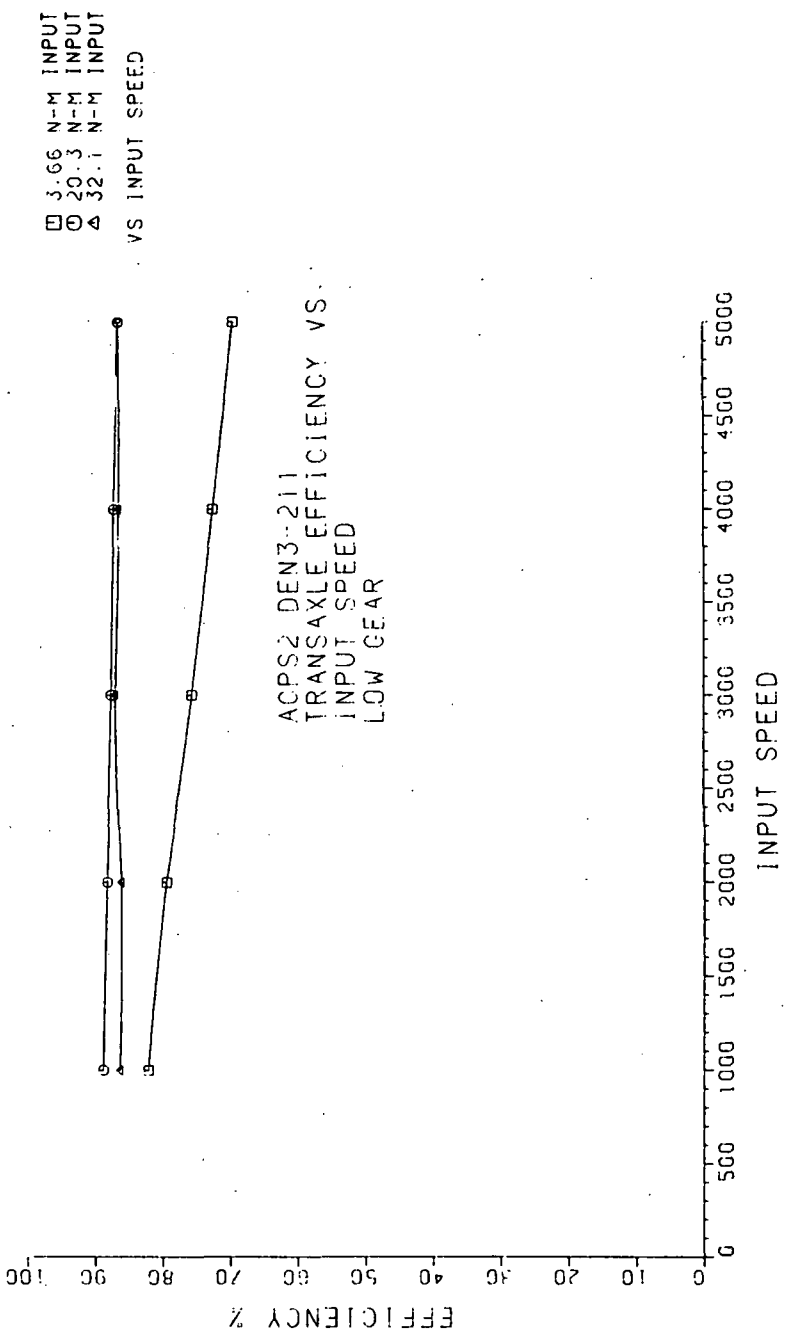
3.66 N-M INPUT
20.3 N-M INPUT
32.1 N-M INPUT
VS INPUT SPEED
ACPS2 DEN3--211
TRANSAXLE EFFICIENCY VS.
INPUT SPEED
LOW GEAR
EFFICIENCY %
INPUT SPEED
0
500
1000
1500
2000
2500
3000
3500
4000
4500
5000

Figure 4.2.1

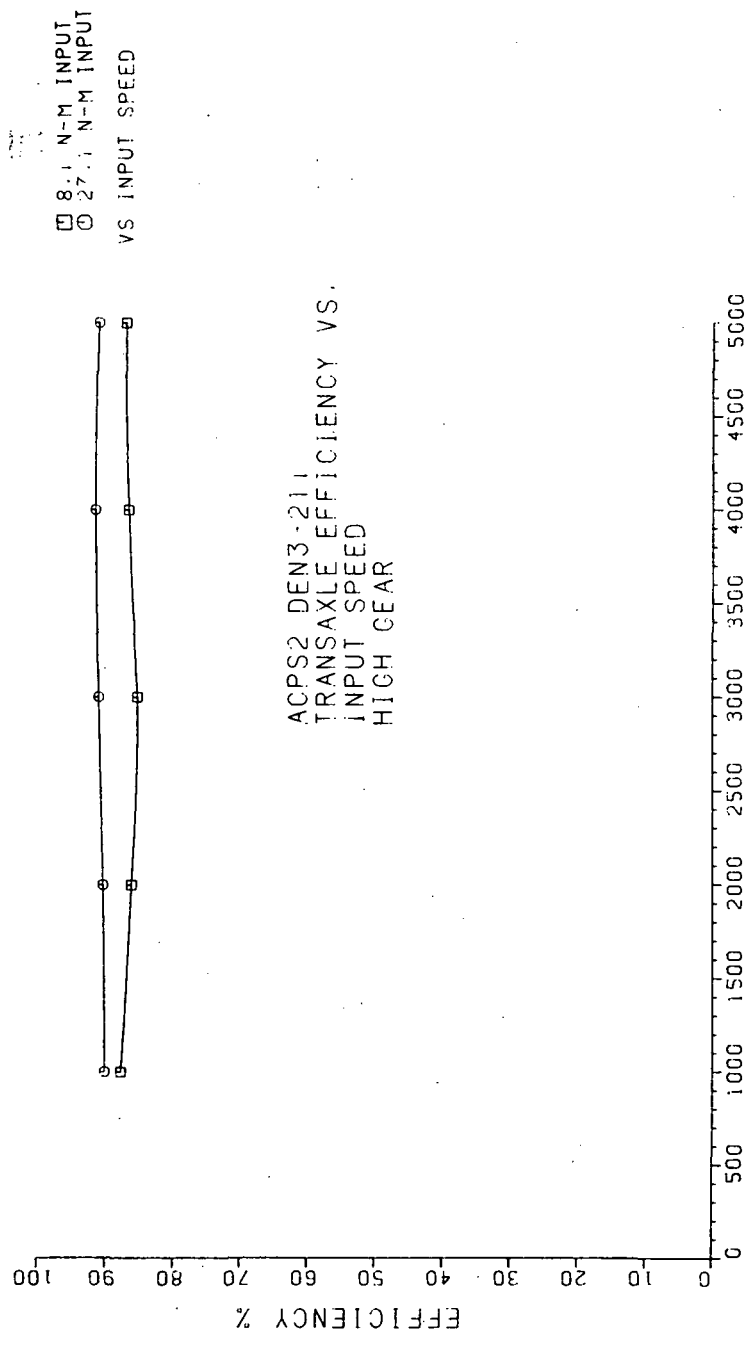
ACPS2 DEN3-211
TRANSAXLE EFFICIENCY VS.
INPUT SPEED
HIGH GEAR
8.1 N-M INPUT
27.1 N-M INPUT
VS INPUT SPEED
EFFICIENCY %
INPUT SPEED
0
10
20
30
40
50
60
70
80
90
100
0
500
1000
1500
2000
2500
3000
3500
4000
4500
5000

Figure 4.2.2

4.3 Discussion of Results
Test Observations

The transaxle design has satisfactorily met most of the design objectives, despite the very limited time available for transaxle modification development near the conclusion of the Phase 2 program.

The size and weight of the unit have been substantially reduced from those of the Phase 1 design (from 90 lb. to 69 lb.; 41 kg to 31.3 kg). The structural soundness, the heat dissipation capacity of main motor- and transaxle-rejected heat, freedom from excessive noise and vibrations throughout the speed range in each ratio, the function of the parking latch mechanism, and adequate lubrication of all components appear to be satisfactory, based on observations from the completed dynamometer and proving ground tests.

Overall mechanical efficiency and the duration of shifts, however, are in need of further improvement.

Some loss of Phase 2 transaxle efficiency could have been reasonably expected due to the 33% increase in both low gear and high gear overall reduction ratios. However, this fact does not sufficiently account for the drop in the efficiencies in both gear ratios of approximately five percentage points below those measured in Phase 1 tests. Although not verified, the causes have been explored, and potential remedies are discussed and proposed under the next heading.

Shift duration (elapsed time from initiation of release of one clutch until complete engagement of the ongoing clutch) in excess of two seconds was observed in vehicle tests. It would be desirable to bring this down to one second or less, provided that, in addition, the main drive motor speed changes can be electrically effected at corresponding rates.

Future Improvements

Mechanical efficiency improvement can be achieved through further refinement of design details.

For example, the plain thrust washers in the planetary gear-train (adapted with an original 2nd gear gearset from a production automatic) may be replaced by needle thrust bearings. Unlike the I.C. engine-powered drivetrain, the ac E.V. transaxle runs in low gear for extended time periods. Its final reduction double planetary gearset runs loaded all the time. Hence, reduced drag due to unbalanced thrust loads is bound to significantly improve the E.V.'s overall efficiency.

Similarly, the drag of the cast iron shaft seal rings may be substantially reduced through the use of advanced materials, such as Vespel(R), and induced pressure bleed across the rubbing surfaces.

Reduction in shift time duration may be achieved through breadboard modeling of the hydraulic system in order to study and optimize component and system characteristics. Improved oil flow, reduction of clutch fill volumes, reduction of solenoid valve pressure drop and response times are areas where significant improvements can be expected.

Overall performance improvements of the entire propulsion system are expected from closer integration of the electronic control and transaxle functions. For instance, vehicle starting and gradeability may be improved by rapid on-off cycling of low gear clutch, the frequency and duration to be electronically controlled in response to power demand. Similarly, up and downshift time duration and shift smoothness may be further improved through optimization of shift schedules and better matching of control and electro-hydraulic component response.

5.0 Induction Motor
5.1 Motor Design
5.1.1 Design Goals

Two generations of traction motors had been built prior to the ACPS2 program. This program's task was therefore seen as an improvement or evaluation of these previous designs rather than a ground-up motor design effort. Changes and/or improvements in the following areas were desired:

A. Higher voltage/lower current to allow a smaller, less expensive inverter to be designed.

B. A better utilization of the machine's speed-torque characteristics to allow better vehicle acceleration and improved efficiency in the 25 to 35 mph cruising range.

C. Improvement in overall motor efficiency. The increased voltage by itself would provide only marginal efficiency gain.

D. Reduced operating temperature.

5.1.2 Design Considerations

Motor Power Rating and Base Speed

The conclusions of the ACPS1 program, which require a 18.6 KW (25 hp) continuous motor rating and a (45 hp) inverter limit, remain valid. The 94 Hz base frequency chosen in Phase 1 results in a reasonable motor D^2 L (Diameter^2 x Length) in a frame, which, with proposed modifications, is more than adequate thermally. Any reduction in base frequency would result in a larger frame size and an excessively conservative oil-cooled thermal rating. An increase in base frequency would complicate the transaxle design and results in increased motor and inverter losses. Thus, the base frequency remained at 94 Hz for the new design.

Maximum Speed

A computer-generated motor design and analysis had indicated a base speed breakdown torque of at least 350% for the Phase 1 motors. If this torque is plotted in the constant horsepower region above base speed where breakdown torque is proportional to inverse speed squared, it intersects the inverter-limited 33.6 KW speed-torque curve at twice base speed, as shown in Figure 5.1.1. A plot of the continuous 18.6 KW thermally-limited speed-torque curve, also in Figure 5.1.1, indicates that rated constant horsepower operation up to a 2.5:1 speed ratio is possible.

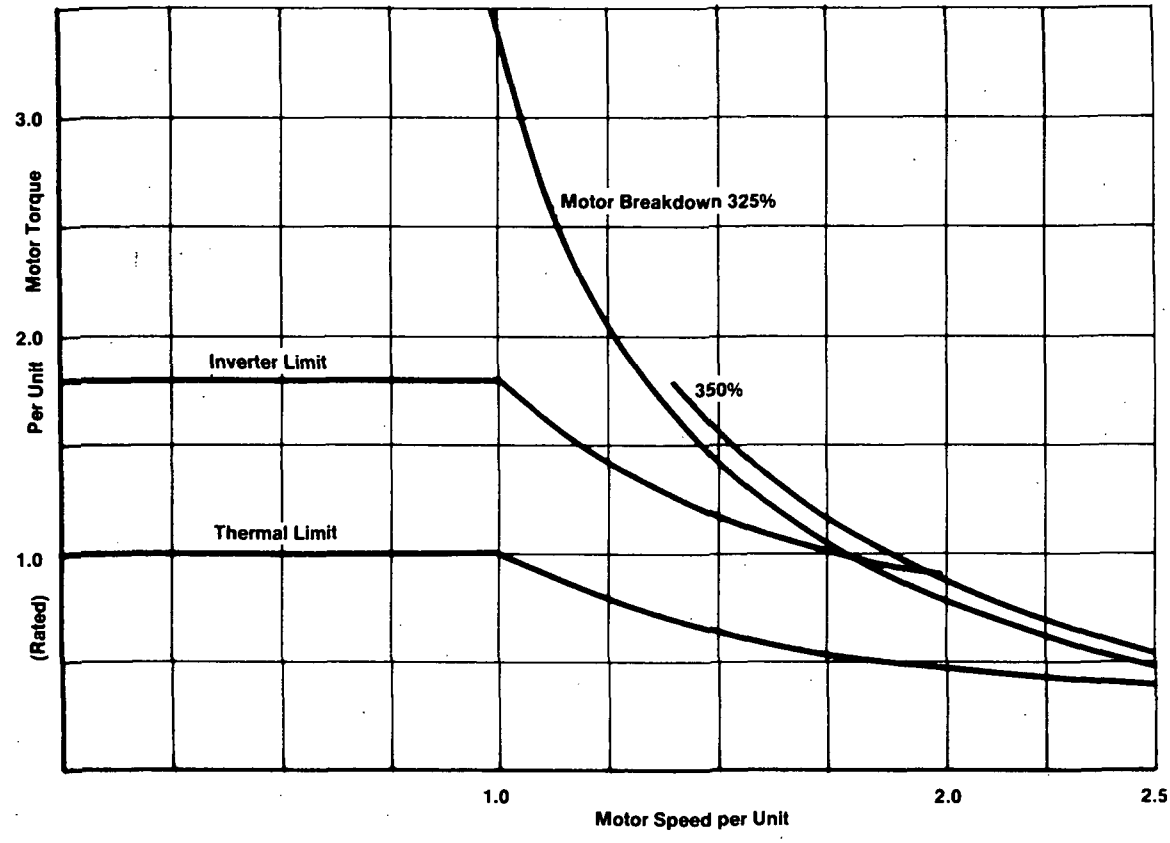

Figure 5.1.1 Motor Speed-Torque Curve

The motor efficiency at these high speeds will be acceptable. The iron losses are essentially equal to the losses at rated speed, since the magnetic flux decreases as speed increases. Furthermore, ACPS1 test results show high efficiencies in the constant power operating region. Figure 5.1.2 shows the predicted motor per unit slip at the thermal limit, inverter limit, and breakdown. While the inverter-limited slip increases to 6% at high speed, the thermally limited slip is relatively flat, indicating a maintained high efficiency over the entire speed range under normal steady-state loading. A design goal of 2.25:1 speed range for constant power operation was, therefore, chosen, resulting in better motor utilization than the Phase 1, 1.6:1 range. The top speed of 12,500 rpm was felt low enough to cause no problems in either the motor mechanics or transaxle designs.

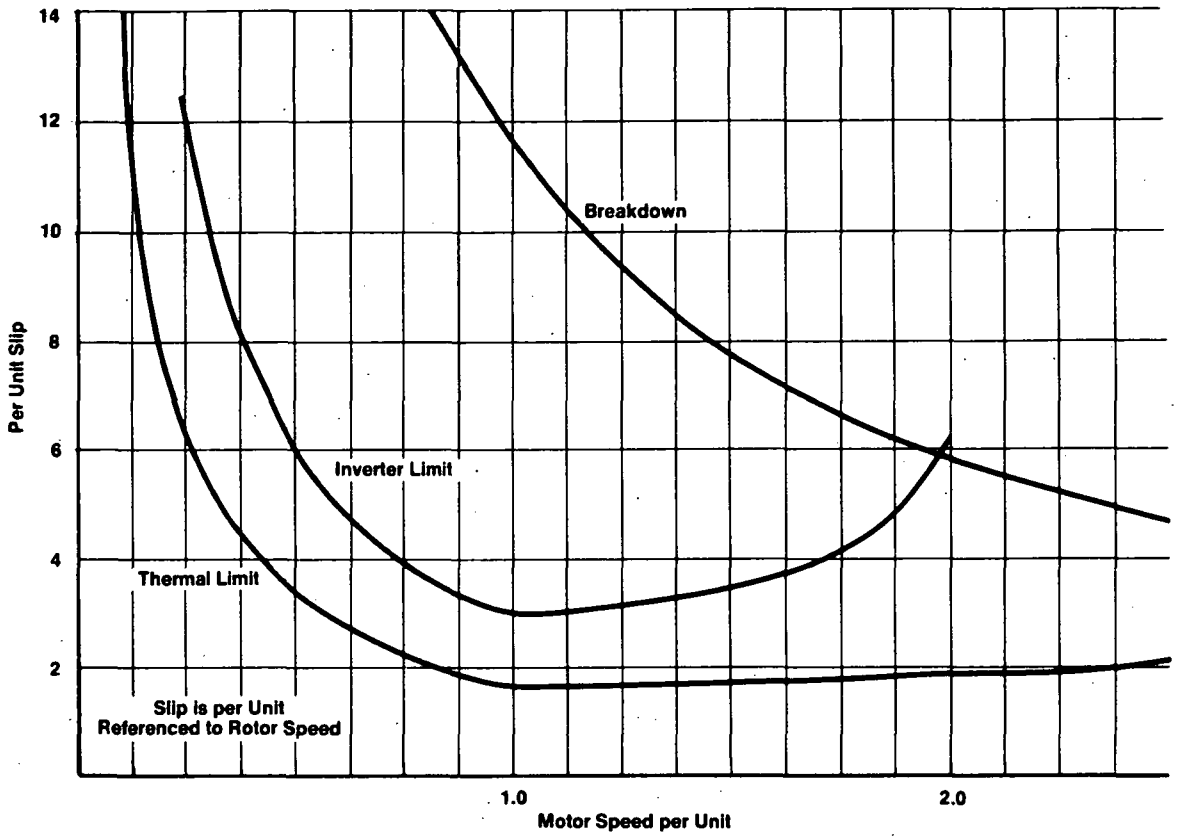

Figure 5.1.2 Predicted Motor per Unit Slip Limits

This wider constant power operating regime allows the transaxle ratio between low and high gears to be larger, giving more torque at the vehicle wheels in low gear for improved acceleration. High gear urban cruising at 25 to 35 mph may be centered around the base motor frequency for operating efficiency, as shown in Figure 5.1.3.

Motor Voltage

Rated voltage is chosen to allow operation from a 192 volt nominal battery voltage. If maximum performance is required when the batteries are discharged to 1.8 volts per cell and cabling and inverter voltage drops are included, a motor terminal voltage rating of 131 volts is required. However a design voltage of 133 volts RMS at 94 Hz was given to allow the motor winding to go from 3 turns at the previous 100-volt rating to 4 turns at 133 volts. Thus, no change in stack length was necessary.

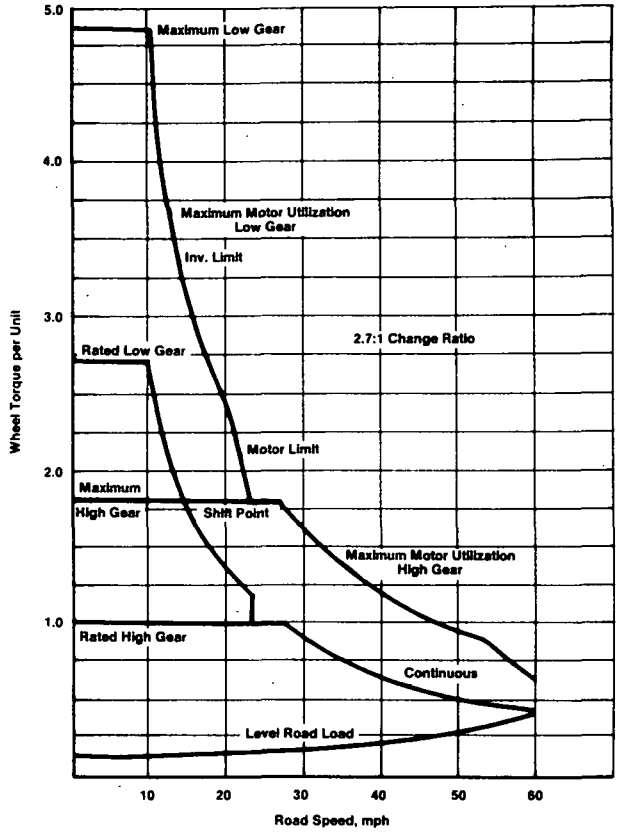

Figure 5.1.3 Gear Shift Torque-Speed Diagram

Electromagnetic Design

In order to improve the overall motor efficiency, the motor's air gap diameter was slightly reduced. The resulting 13% increase in stator winding area allowed a 10% decrease in per unit stator resistance. A similar reduction in rotor resistance was obtained by using nonstandard laminations. Magnetizing inductance decreases slightly, resulting in higher no-load currents. The overall effect of these changes was expected to effect a 2 to 3 percent increase in motor efficiency.

Thermal and Mechanical Design

Better heat transfer can be had by a redesign of the motor's oil cooling system. Testing of the Phase 1 motor showed that only a small percentage of the motor heat was being removed by the oil. Thus, the oil cooling system was

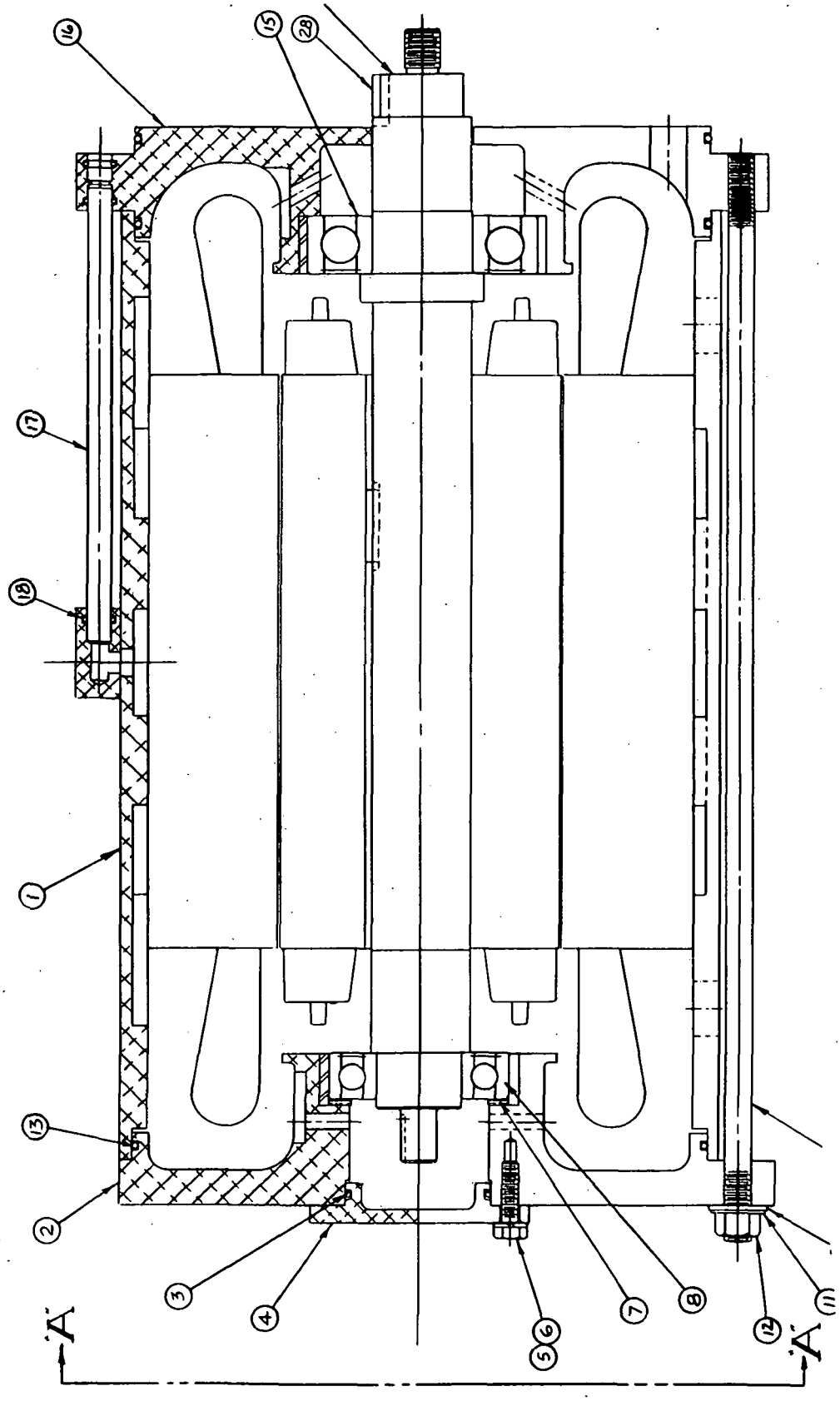

Figure 5.1.4 Motor Cross Section

changed to allow direct contact between the stator laminations and oil. This was accomplished by passing the oil through several channels machined into the inside of an aluminum motor shell. The stator laminations were sealed to prevent oil seepage into the air gap. After passing through these channels, the oil passes over the stator winding end turns and exits into the transaxle chain case.

Modifications to the frame include the use of an all-aluminum shell for reduced weight and external aluminum tie rods for simplified assembly. A 25-pound overall weight reduction was obtained, giving a new motor weight of 122 pounds.

A cross section drawing of the motor is shown in Figure 5.1.4.

5.2 Motor Testing

The motor was tested at manufacture on 60 Hz sine wave excitation to verify thermal capacity and check conformance to design. Later tests using sine wave modulated PWM excitation were performed at ERC to fully characterize motor performance over the expected operating range.

5.2.1 60 Hz Tests

The motor acceptance tests at the manufacturing division were run using 60 Hz sine wave excitation. Motor saturation, thermal, and 60 Hz efficiency characteristics were measured. The results of these tests are shown in Figure 5.2.1.

Efficiency at 60 Hz is about 2% higher than the Phase 1 machine. Furthermore, the separation of losses shows a different, more favorable distribution.

Loss Component	Phase 1	Phase 2	
Iron	222	371	
Stator Copper	711	555	
Rotor Copper	489	330	
Windage and Friction	13	13	(estimate)
Stray	406	295	
	1,841	1,563	
Efficiency	86.6	88.5	

Note that significant reduction in rotor copper loss and stray losses have been had through the use of nonstandard laminations. Stator copper loss has also been reduced; however, the iron losses are somewhat greater.

Thermal performance was considerably improved, as indicated:

1 Hr., 16 hp, 60 Hz Temperature Rise

	Phase 1 Motor	Phase 2 Motor
Case	51°C	19°C
Winding	87°C	55.5°C

Motor Testing to Specifications

Test No. 1372 Mfg'r. Eaton Mfg'r. Pro. No. 39476 Dyn. Pro.

HP 25 rpm 5640/12700 Volts 133 AMP 103 Phase 3 Cycles 94-212

Model 40-62184-0009 Serial No. 39476-1 Type TP-1 Frame 180 SPL

Ser. Factor 1.0°C Rise Duty 1 hr. Code NEMA Design Max. Amb. °C

Insul. Cl. H Rotor No. 77362-0100 Stator No. 79054-0100

WDG. Res. 0.0286 Ω @20°C. Instr. Weight 122.2 lbs.

Special Features: Stator Length 8.00 in.

Flow Rate ½ Gal./Min.
60 Hz Sine Wave
No. 758 Dyn.

W/2 Ft. Arm

ACPS2 Motor #1

							Idle Off Dyn.
Time	10:45	11:45	1:10		1:30	1:40	
Scale Lb.	12	12	11.25	11.25	13	13	0
Torque Lb. Ft.	24	24	22.5	22.5	26	26	0
% of Rated Torque							0
R.P.M.	3526	3502	3533	3520	3502	3496	3598
HP	16.12	16	15.14	15.08	17.34	17.31	
Volt.							
I In	21	26	21	22	23	23	
I Out	21	41	22	32	32	35	
Voltage	85	85	85	85	85	85	85
Ammeter Reading	5.14	5.13	4.9	4.85	5.57	5.56	1.88
Multiply by Ratio	20	20	20	20	20	20	20
Amperes	102.8	102.6	98	97	111.4	111.2	37.6
Wattmeter Reading	672	675	637	631	740	743	21
Multiply by Ratio	20	20	20	20	20	20	20
X2 for Half Volt.							
X4 for Full Volt.							
Final Multiplier							
Watts	8440	13500	12740	12620	14800	14860	420
Eff. % Calc. From	89.5	88.5	88.7	89.2	87.4	86.9	
P.F. % Wattmeter	88.8	89.4	88.3	88.4	90.2	90.8	
Res. Ω		0.0352					
Res. Ration R_H/R_C		1.23					
Temp. Rise °C		55.5					
Ambient Air °C	22	23	22	23	23	23	
HSG. Temp. °C	24	42	21	32	32	36	

Date: 9/17/81 Test by

Figure 5.2.1

A greater percentage of the heat was carried by the oil in the new design.

	Phase 1	Phase 2
Oil Inlet Temp.	26°C	40°C
Oil Temp. Rise	3.5°C	15°C
Heat in Oil	234 watts	1003 watts
Total Heat	1841 watts	1564 watts
T, Case to Oil Inlet	36°C	16°C
Percentage of Heat Carried by Oil	13%	64%

The motor will, therefore, run with a considerably lower temperature rise than the Phase 1 design and yield a several percent efficiency improvement when operated from the sine wave modulated PWM inverter.

5.2.2 PWM Tests

Dynamometer testing with the ACPS2, PWM inverter revealed a significantly higher efficiency than in Phase 1. This increase resulted from two important contributions:

1. improved motor design, as described above, and

2. an improved pulse width modulation scheme combined with higher inverter operating frequencies to reduce motor harmonic currents.

The motor efficiencies vs. torque for the PWM tests are plotted in Figure 5.2.2. For comparison, the Phase I motor efficiency, taken on the same test setup, at 56 Hz is shown as a dashed line in Figure 5.2.2. The Phase 2 curve at 40 Hz is shown to be 5% above the 56 Hz curve taken in Phase 1.

The test setup for the PWM tests is described in Section 10 and Appendix A.

5.3 Discussion and Conclusions

The Phase 2 design has met all design goals to provide a potentially low-cost, lightweight, high-efficiency traction motor for integration into the vehicle propulsion system. Sustained high efficiency well into the constant power operating range allows for efficient cruising over a wide speed range in which the inverter is at or close to 100 percent voltage output and thus operating at low switching rates.

Future design efforts might address the reduction of no-load motor current by increasing magnetizing inductance. This would improve the light load efficiency.

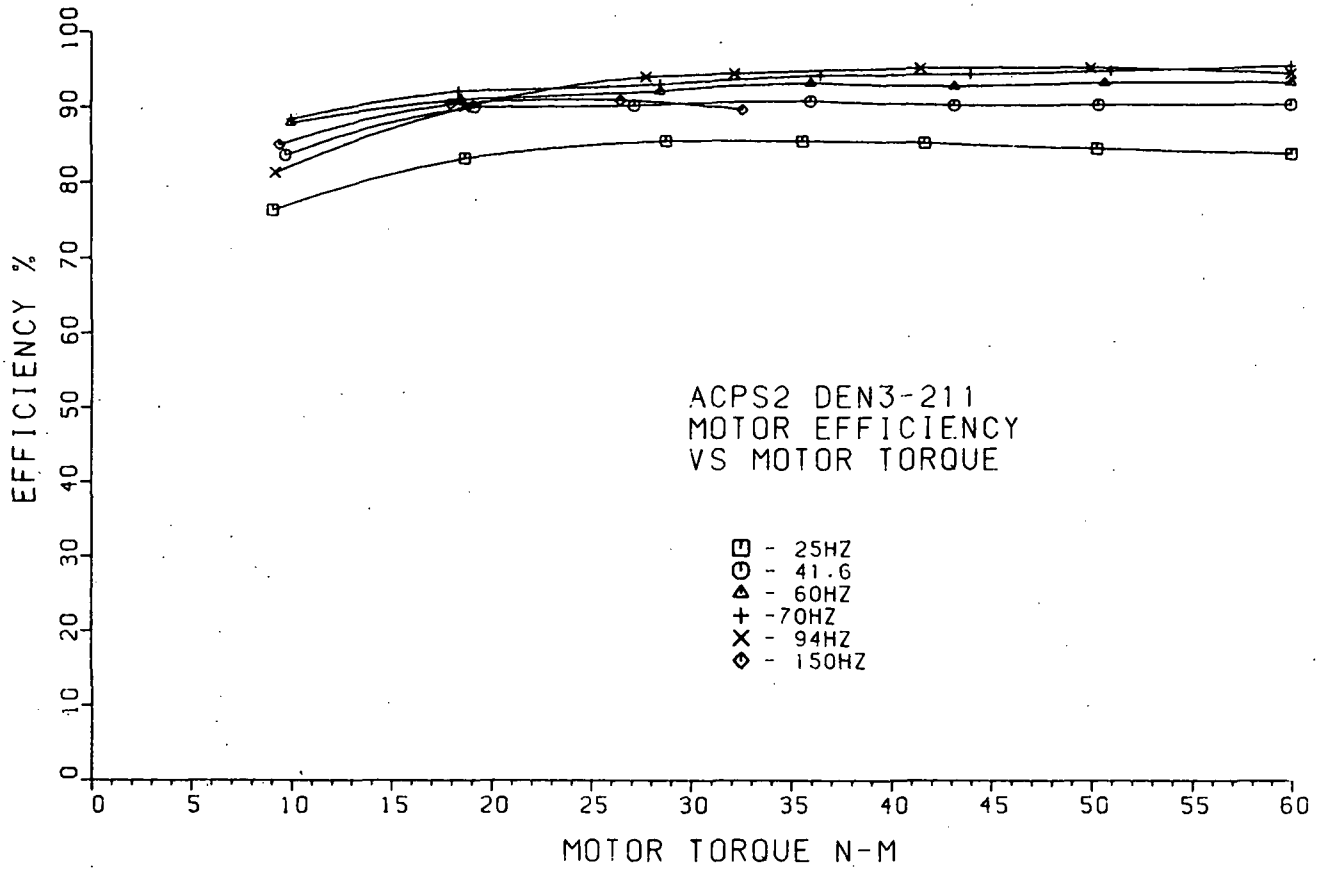

Figure 5.2.2 Motor Efficiency Vs Torque with PWM Inverter

A slightly higher breakdown torque or lower maximum speed would avoid the efficiency reduction at the top of the speed range. Increased breakdown torque would require reduced leakage inductance, but that reduction would probably increase the motor's harmonic currents.

A lower maximum speed would require a lower transaxle gear ratio and would sacrifice some of the significant system efficiency improvements that were realized in the moderate 48 km/hr to 75 km/hr speed range. Information gained from this project at the higher speed range has provided a broader data base for final determination of the best maximum speed. This determination is a function of motor and transaxle efficiency and system power tradeoffs throughout the vehicle speed range.

The motor thermal design is more than adequate, indicating that a further reduction in motor size is feasible if efficiency were not adversely effected. A reduction in stack length and corresponding increase in base speed would be the preferred approach.

6.0 TRACTION INVERTER/BATTERY CHARGER/AUXILIARY CONVERTER

The inverter power section was designed for a high level of integration among the motor bridge circuit, battery charger, and low-level power supplies to obtain economies in size and number of components. These economies are most evident in the inverter/battery charger design, where the integration of both functions into one circuit has significantly reduced the number of power devices required.

First, from an inverter perspective, it was possible to achieve the desired power levels using two paralleled Darlington transistors per switch. However, using two instead of three devices added a requirement for a DC bus series choke for inverter di/dt limiting and also required a higher power level in the base drive circuitry. These added costs, particularly the series choke with its associated energy recovery circuitry, would have weighed in favor of three transistors per switch.

However, by integrating the onboard battery charger into this choke, the necessary di/dt limit was obtained at little extra cost, and it was possible to parallel only two transistors per switch in the inverter circuit.

From the charger standpoint, a low-cost, compact, onboard battery charger was realized with no active devices not already contained in the inverter.

Additional component reductions were obtained by integrating the 12-volt vehicle auxiliary power supply and the base drive power supplies into one multi-output, regulated, switching, DC-DC converter. This supply was further cost-reduced by combining individual filter chokes on each low-level output with a single, multiple winding, coupled inductor on the converter input section.

A summary of the main inverter features is given in Table 6.0.1. The nominal battery voltage has been increased to 192 volts from the 144 volts used in the Phase 1 system. Use of higher voltage transistors and the above combination of circuit functions has resulted in a total weight for the inverter/battery charger/auxiliary power converter of only 95 pounds vs. 135 pounds for the Phase 1 inverter which had no battery charger and converter.

6.1 Inverter Design

The major design considerations and a description of the inverter operation is given in the following paragraphs.

MAIN FEATURES OF INVERTER

-Input Voltage:	**192V Nominal: Reduced Performance to 125V; Regenerative Braking to 240V**
-Power Rating:	**20KW Continuous (1 Hour); 36 KW Peak (2 Min)**
-Weight:	**43 KG (95 Lb.)**
-Three-Phase, 12 Transistor Bridge using 100A Monolithic Darlingtons	
-Protection:	**Fast Local Protection at Base Drive Level**
-Interface:	**Optoisolators at Controller/Inverter Interface**
-Packaging:	**Totally Enclosed Non-Ventilated**
-Switching Rate:	**4 KHZ**
-50 Amp, 12 Volt Auxiliary Power Supply	
-Battery Charger Features:	**-Onboard 4KW Utilizing Inverter Bridge Transistors** **-220V Input Line; 110V Input at Reduced Power** **-Charge Rate Controlled by Vehicle Microprocessor**

Table 6.0.1

6.1.1 Battery Voltage Selection

Battery voltage selection was based upon favorable cost and efficiency tradeoffs between the battery pack and the system electrical components. Although the transistorized PWM inverter concept was demonstrated in Phase 1 with a 144-volt bus, this voltage is a poor choice for existing lead-acid batteries. Use of twelve 12-volt batteries at 144 volts results in an undersized power source and unacceptable vehicle range. However, the option of twenty-four 6-volt batteries is overruled by size and weight limitations of a passenger vehicle. Thus, the only reasonable choices for battery voltage are a conventional 96 volts to 108 volts using 6-volt units or a much higher 192 volts to 208 volts using 12-volt batteries.

The choice of the higher 192-volt bus was based upon the overriding weight, efficiency, and cost penalties incurred in the high-current, low-voltage system. The cost and weight penalties are especially evident in the 3-phase power inverter, where higher current switching requirements are necessary for 6 separate switching elements. Thus, if two transistors are to be paralleled in the 192-volt system for a 12-transistor bridge, 24 transistors are needed at the lower voltage.

The choice of 192 volts provides additional cost and weight savings for contactors, wiring, and the induction motor. In addition, the system efficiency can be made higher at the higher bus voltage.

6.1.2 Transistor Selection

Computer simulations of motor currents at the higher bus voltage showed that a peak motor current of 320 amps could be expected at the maximum 2 minute, 33.6 kw rating of the motor and that 175 amps peak were required at the 1 hour, 18.6 kw level. For these requirements, "Building Block" transistors manufactured by Fuji Electric Corp. were chosen. Paralleling of two of these transistors per switch is sufficient for achieving the above average ratings and would result in a 63% cost savings from the Phase 1 transistors. Other advantages of this transistor are:

- The "building block" style package permits bolting to a heat sink surface with no need for expensive clamps and two-sided heat sinks.

- A reverse bias safe operating area (RBSOA) rating for increased ruggedness compared to previous high power transistors would allow them to be switched without snubber circuitry.

- A self-contained back diode is included for cost and package size savings.

- They are easily paralleled for flexibility in inverter sizing.

Although the above features are now available from other transistor manufacturers, the Fuji device, #ET-127, was the only transistor that could claim all these advantages at the time. Figure 6.1.1 shows the device ratings, Figure 6.1.2 shows the typical gain characteristics, Figure 6.1.3 shows the saturation characteristics, Figure 6.1.4 shows the device reverse bias safe operating area (RBSOA), and Figure 6.1.5 shows the forward bias safe operating area (FBSOA) for this transistor.

ET127-09

1. Absolute Maximum Ratings (TC=25°C)

Item		Symbol	Maximum Rating	Units
Collector Base Voltage		V_{CBO}	600	V
Collector Emitter Voltage		$V_{CEO(SUS)}$	450	V
Emitter Base Voltage		V_{EBO}	6	V
Collector Current	DC	I_C	100	A
	1ms	I_C	250	A
	DC	$-I_C$	100	A
Base Current	DC	I_B	5	A
	1ms	I_B	15	A
Collector Disspation		P_C	960	W
Operating Temperature		T_j	+ 150	°C
Storage Temperature		T_{stg}	-40 ~ +125	°C

2. Electrical Characteristics (TC=25°C)

Item	Symbol	Condition	Limits MIN	Limits MAX	Units
Collector Emitter Voltage	$V_{CEO(SUS)}$	IC=1A	450		V
Collector Cut off Current	I_{CBO}	VCB=600V		1.0	mA
Emitter Cut off Current	I_{EBO}	VEB=6V		300	mA
Collector Emitter Voltage	$-V_{CEO}$	-IC=80A		1.6	V
DC Current Gain	h_{FE}	IC=100A, VCE=5V	100		
		IC=100A, VCE=2V	50		
Collector Satulation Voltage	$V_{CE(sat)}$	IC=100A		2.0	V
Base Satulation Voltage	$V_{BE(sat)}$	IB= 2A		3.0	V
Switching time	ton	IC=100A, RL=3Ω		4.0	μs
	tstg	+IB=2A, -IB=2A		10.0	μs
	tf	PW=50μs		3.0	μs
Thermal Resistance	Rth(j-c)	Junction-Case		0.13	°C/W
Thermal Resistance	Rth(j-c)	Junction-case(Diode)		0.60	°C/W

	DATE	NAME
DRAWN	Oct	
CHECKED	-25-80	S.Furuta / Sekiya

REVISIONS

開発課

MT5M 2855 1/12

Fuji Electric Co.,Ltd.

Figure 6.1.1

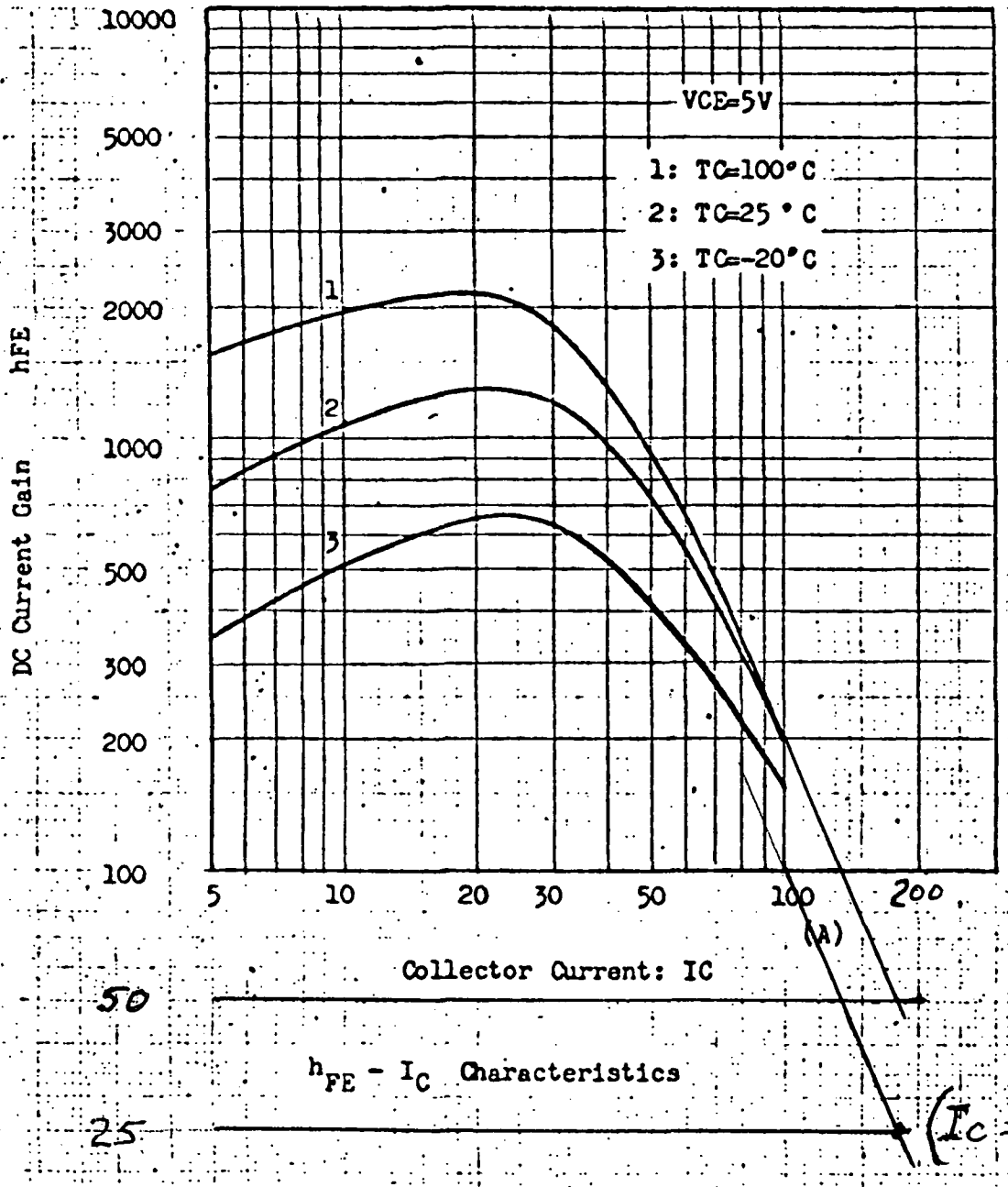

h_{FE} - I_C Characteristics

(I_C = 175, h_{FE} = 25)

Figure 6.1.2

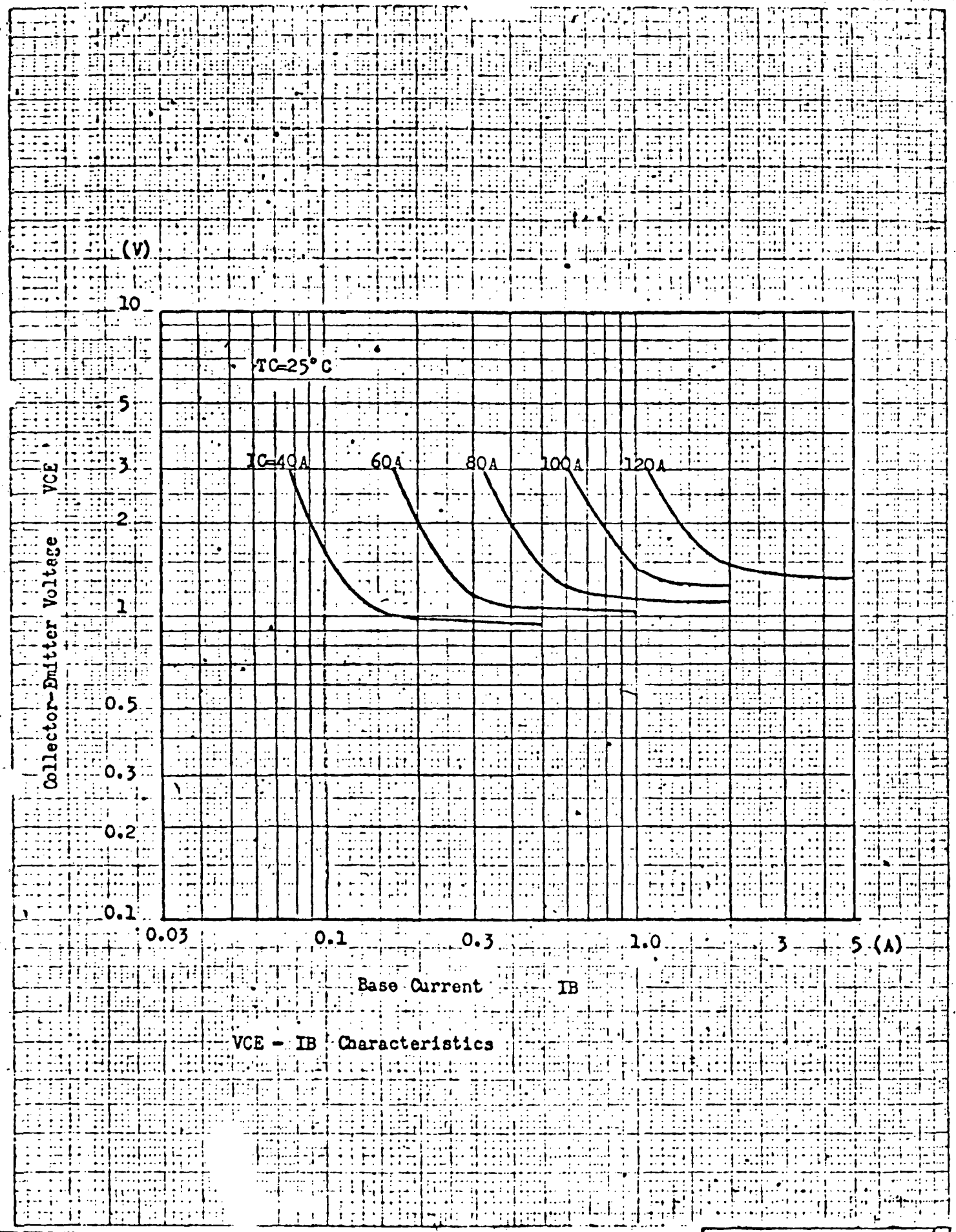

VCE - IB Characteristics

Figure 6.1.3

ET127
ET133

REVERSE BIAS SAFE OPERATING AREA

$T_{CASE} \leqq 125°C$

$-V_{BE} \leqq 6V$

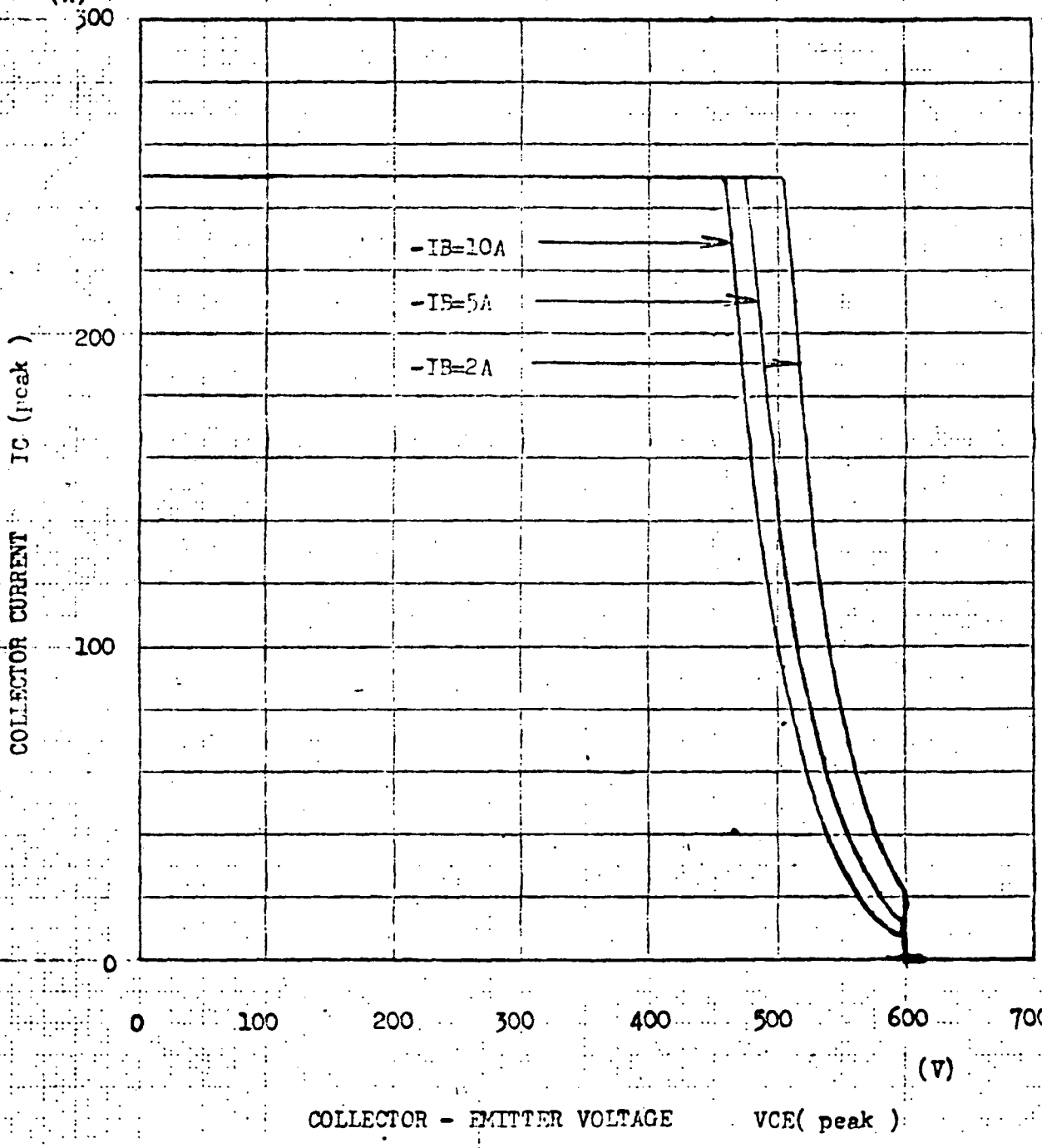

Figure 6.1.4

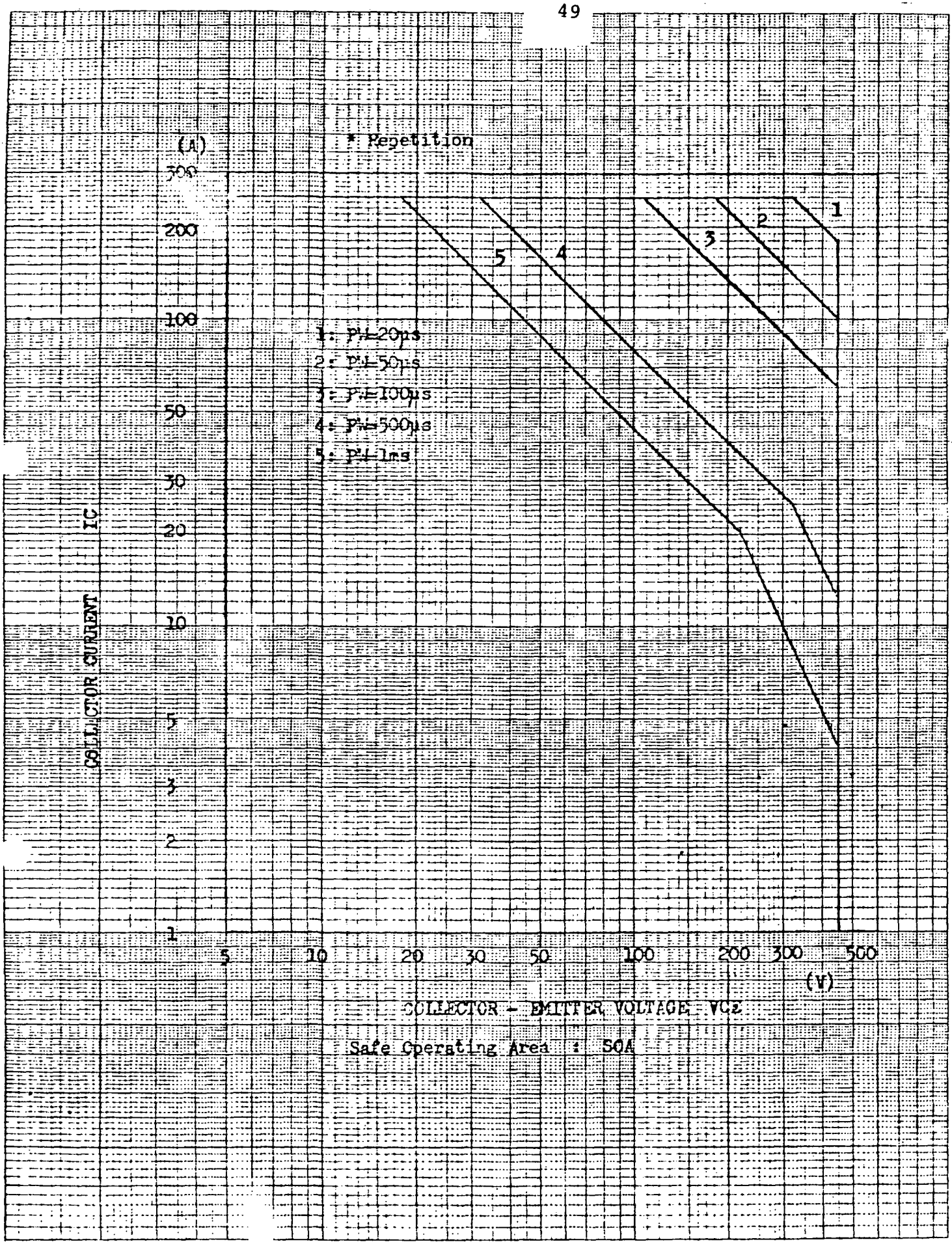

Figure 6.1.5

MT5M 2855 8/12

Referring to Figures 6.1.4 and 6.1.5 for transistor forward and reverse bias safe operating area, it is seen that the ET-127 can be operated safely up to 250 amps peak current. The transistor's reverse bias safe operating area (Figure 6.1.4) can be relied upon under most operating/conditions, and, thus, the turn off of 250 amps peak current by this device can be assured. However, acceptable operation under forward bias conditions is not solely a function of the device FBSOA, but also depends upon case temperature and DC current gain (hfe).

Transistor case temperature is determined from load estimates and thermal packaging considerations, which are discussed in a separate section.

The transistor current gain is a concern because, from Figures 6.1.2 and 6.1.3, it is seen that no information is provided about the transistor "on" characteristics above 120 amps collector current. With an expected peak motor current of 320 amps, or 175 amps (allow for 2 transistors being paralleled and a 10% expected current mismatch between paralleled devices) per device, it was necessary to extrapolate the published data to determine base drive requirements and verify safe operation. This gain extrapolation is done in Figure 6.1.5 by drawing a line parallel to the typical DC current gain; but through the guaranteed minimum gain point of hfe-100 at 100 amps. This extrapolation shows that a "worst case" gain of 25 could be expected, requiring a peak base current of 7 amps per transistor at the peak 175 amp transistor current. This base current level is within the device peak allowable base current level as given in Figure 6.1.1 and is within the capability of a reasonably sized base drive circuit.

6.1.3 Bridge Circuit Design

Operation of the transistors in their extended range, as described above, places additional requirements on the final inverter design. These requirements are as follows:

1. Base Drive. Although a peak base current of 7 amps per transistor (14 amps total for two paralleled transistors) is required to achieve the inverter 2-minute peak power rating, Figure 6.1.3 shows that less than 1 amp is required under most other conditions. In order to reduce the base drive power dissipation for normal conditions and reduce low level power supply size, a proportional (current regulated) base drive circuit is needed.

2. Base Drive Power Supply. The PWM mode of operation combines with the 14-amp peak base current requirement to place a severe current step response requirement on the base drive power supply. This requirement

necessitates a special topology in the auxiliary power supply and will be discussed in section 6.1.7.

3. Inverter Passive Protection. Driving the bridge transistors at this base current level places added stress on them during short circuit conditions, as they are no longer gain limited. Thus, it is now possible, without some passive di/dt protection, to achieve currents well beyond the transistor one-time peak current rating. This failure mode would occur even with active current limit protection, since the destructive current level can be attained before the transistor storage time has passed (Ref. #1).

This last consideration results in a requirement for a series bus inductor and associated energy recovery circuitry. This inductor is, hitherto, not required as the large transistor RBSOA permits the transistors to turn off during normal operation without capacitive snubber components, and thus, no transistor turn-on di/dt limit would have been necessary (Ref. #2).

The requirements for the series bus inductor and the other considerations listed above would have weighed in favor of paralleling a third transistor in order to avoid these problems. However, by integrating the main battery charger into the bridge circuit, the series inductor can be added for little extra cost, and only a 12-transistor bridge is needed.

The bridge circuit schematic diagram is shown in Figure 6.1.6 The key element of this circuit is Transformer T501, which is seen to have three windings, P1, P2, and S. In the inverter mode of operation, P1 is connected to the main battery and P2 is disconnected by means of Relay 500. In this configuration, P1 serves as the passive di/dt limit inductor which uses winding S for trapped energy recovery.

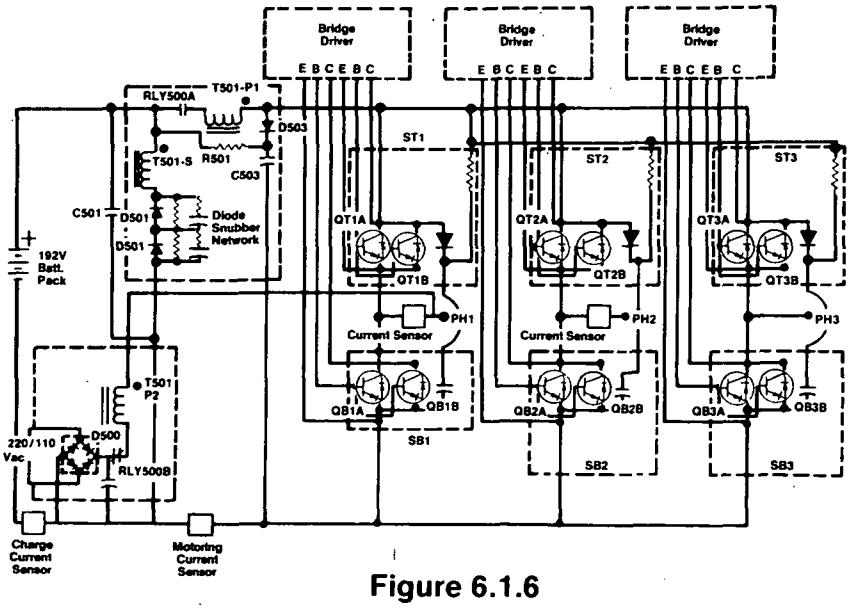

Figure 6.1.6

In the battery charging mode, P2 is connected to either the 220 v. or 110 v. AC lines, and P1 is disconnected. In this configuration, P2 combines with S and transistors SB1 to form a "flyback" type, 4 kw AC-DC battery charger.

Use of a flyback type converter is normally avoided at this power level, because of poor transistor and transformer utilization and the resulting high cost. The disadvantage of poor transistor utilization is overcome by using an existing bridge transistor; and, although the transformer is larger than that required by other type converters which are unregulated, the requirement for current and voltage regulation in this converter would necessitate an output filter inductor for many other topologies. An output filter inductor is inherent in the main transformer of the flyback converter, and, thus, the total transformer requirements in this circuit are not excessive.

In addition, the flyback converter, adapts to both the 110 volt and 220 volt input line voltages with no additional power components. Another major advantage of this charger topology is that, by using only one leg of the inverter bridge, the EV motor can remain connected, and thus, no large contactor is required for disconnecting the motor during charging.

Although in normal operation, the transistors can be switched without local capacitive snubber circuitry, some means of clamping the peak bridge voltage is required due to leakage inductance in Transformer T501 and other stray wire inductance. This clamp is provided by the network R501, C501, and D503. When in charge mode, this clamp is active through the internal inverse parallel diodes in transistor ST1. By eliminating local R-C-D snubbers, inverter switching losses are greatly reduced from Phase 1, and the allowable switching frequency in motoring is raised to 4 kHz from the maximum Phase 1 switching frequency of 650 Hz.

It is important to note that the above tradeoffs between a DC bus inductor and additional transistors are specifically applicable to the particular power transistors being used and to the peak power and bus voltage requirements for this drive. The future availability of higher current transistors or a change in power or voltage power requirement could preclude the need for a series bus inductor and result in a simpler configuration. However, the integration of the battery charger into this circuit is viable even without the series bus inductor.

6.1.4 Base Drive Circuit Design

Four requirements were placed upon the base drive circuit.

1. Regulated voltage source so that power is not wasted during 2:1 excursion of main battery voltage

2. Maximum output current of 14 amps (7 amps/transistor) to meet inverter peak power requirements

3. Regulated base current output so that power is conserved during light inverter loading

4. Bipolar output so that reverse bias ratings of bridge transistor can be utilized.

The first requirement is met by integrating the base drive power supply into the regulated DC-DC auxiliary converter and is discussed in Section 6.1.7. The last three requirements are met with the circuit shown in Figure 6.1.7. While the positive output transistor is capable of a peak 15 amps, if required, base current is regulated to low levels by the antisaturation circuit consisting of Diodes D402, D403, and D404. These diodes keep the Vce saturation voltage of the output transistor within ($V_{BE_{Bridge\ Tr}}$ + $V_{BE_{Q1}}$ + $V_{BE_{Q2}}$ - $3V_{f_{diode}}$) or approximately $V_{BE_{fuji}}$ - 0.7 volts.

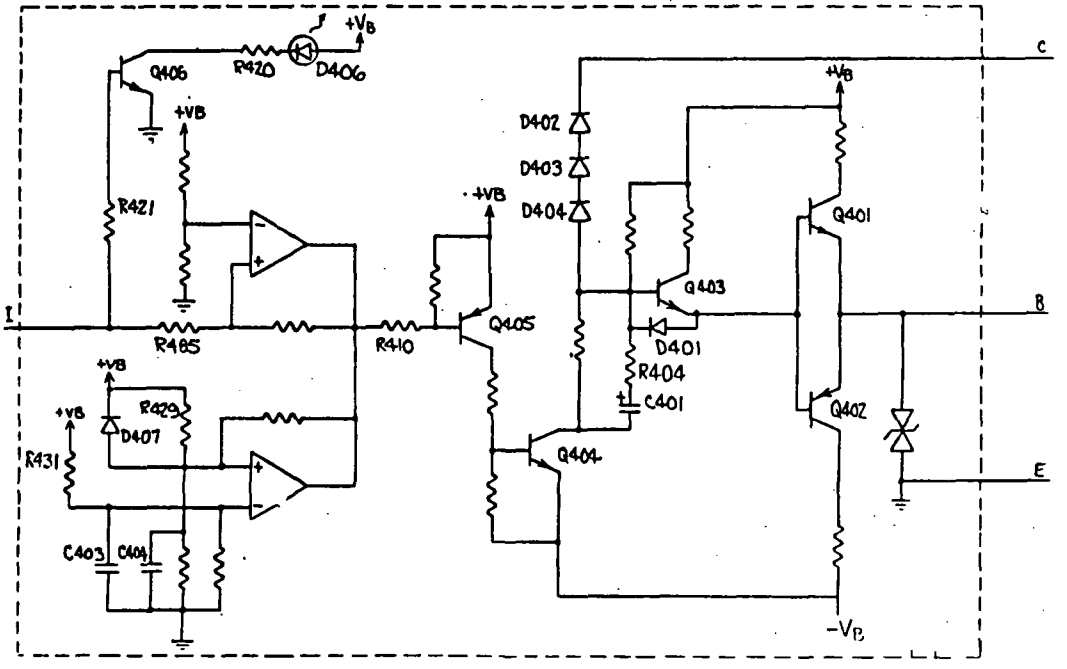

Figure 6.1.7 Base Drive Circuit

Other types of clamping circuits clamp the Vce saturation voltage to the V_{BE} saturation voltage of a transistor; however, at rated motor current of 100 amps, this additional 0.7-volt drop adds 270 watts to the inverter conduction losses and is intolerable.

The negative base drive output is capable of sinking 5 amps (2.5 amps per transistor) to achieve short bridge transistor storage times and make best use of this transistor's RBSOA (Figure 6.1.4), which is seen to have its largest safe area at -2 amps I_b.

6.1.5 Base Drive Logic

The overall logic scheme is shown in Figure 6.1.8. Controller permissives for the enabling of any transistor are: the steering command, the bridge enable, and a charger "off" signal. In the battery charge mode, only the bottom transistor on Phase 1, will be enabled.

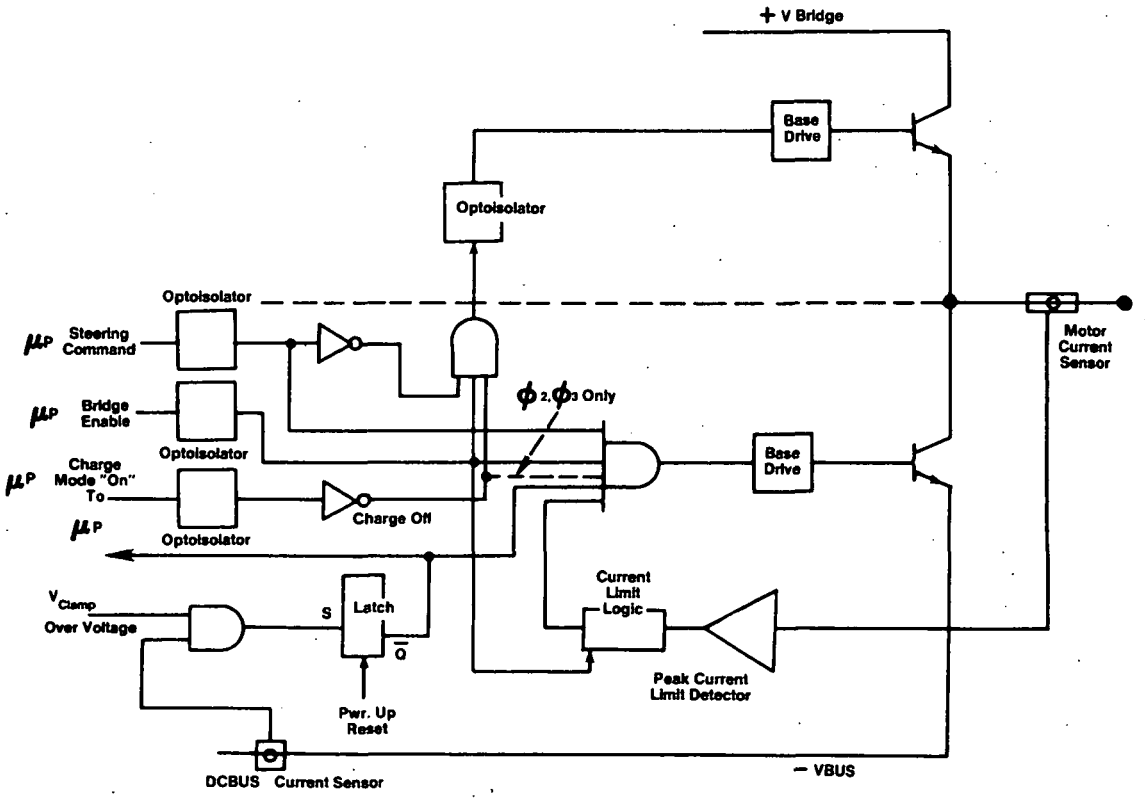

Figure 6.1.8 Base Drive Logic Functional Schematic

The drive local protection is derived from an overvoltage sensor at the bus clamping capacitor and current sensing devices at two of the motor leads and on the DC bus.

Detection of either an overvoltage or an overcurrent trip on the DC bus indicates a failure and will shut the inverter down. The only way to re-enable after these types of trips is to turn the system off and then power up again. Detection of a motor current trip during motoring will shut the system down. However, in this case, the inverter can be re-enabled from the diagnostic box or by bringing the vehicle to a complete stop. The motoring current limits are set at 400 amps.

In the charge mode configuration, the Phase 1 motor current sensor is set up to detect the peak current in the primary winding of transformer T501. Detection of a current limit in this case will shut the SB1 transistors down for the duration of existing "on" command, but the transistor will be re-enabled upon receiving the next "on" command from the controller. This strategy allows the inverter to run in a repetitive peak current limit mode when charging the battery. In the charge mode, the transistor instantaneous current limit is set at 110 amps.

The above method of drive protection with instantaneous current tripout proved adequate for the purpose of preventing catastrophic failures. However, when combined with the slip control scheme that was used in the controller, operational deficiencies became evident in the form of occasional nuisance inverter current tripouts during startup and gearshifting. An area for further work is to develop a method of continuous current limit control for the system.

6.1.6 Transformer Design and Battery Charger Considerations

As performance of the T501 3-winding transformer is crucial to the operation of the inverter/battery charger, considerable time was spent in the development of this component. Various initial designs were tested with different core sizes and winding configurations before the final version was arrived at. This last design is not yet optimized, and further work would be needed to produce a product-worthy transformer.

The following basic considerations were involved in the final design:

1. Core Type. A 4-mil laminated silicon steel core was chosen for low cost, high flux density, and moderate power loss. Although ferrite is usually the choice in high frequency applications, its low flux density would have resulted in unacceptable size and increased winding loss due to longer turn length involved. In addition,

although the power loss per unit volume is lower in ferrite, low flux density and resulting larger volume result in the same total loss. It was believed that, by operating at high enough frequencies with the flyback configuration (the so-called "continuous conduction" mode), the transformer flux excursions, and thus core loss, could be kept down. Other type core materials were ruled out as being too expensive for automotive applications.

2. Operating Mode. The circuit mode of operation affects both the transformer design and the system operating losses. Two basic modes of operation exist for operating a flyback converter.[5] The first mode, shown in Figure 6.1.9, calls for complete transfer of the energy stored in the transformer on every pulse. In the second mode of operation, shown in Figure 6.1.10, complete energy transfer is not accomplished on every pulse since, while energy is still stored in the inductor, the driving transistor turns back on. The second mode was chosen for the charger, because experimentation on earlier versions of the transformer showed that transformer core losses were reduced in this mode. In addition, the second mode requires a lower peak energy storage and, thus, a smaller core than the first mode of operation. Although power loss from commutation of transformer leakage energy is higher in the second mode, these losses are more easily dissipated through power resistors, are compensated by the reduced core loss, and can be made small by minimizing the transformer leakage inductance.

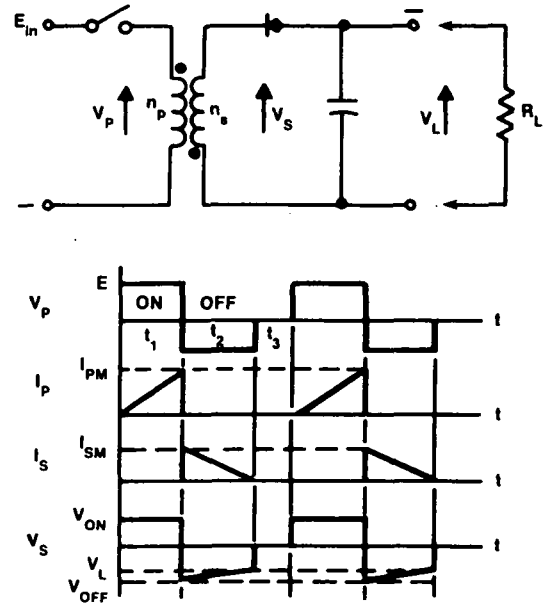

Figure 6.1.9 Battery Charger Operating Mode #1

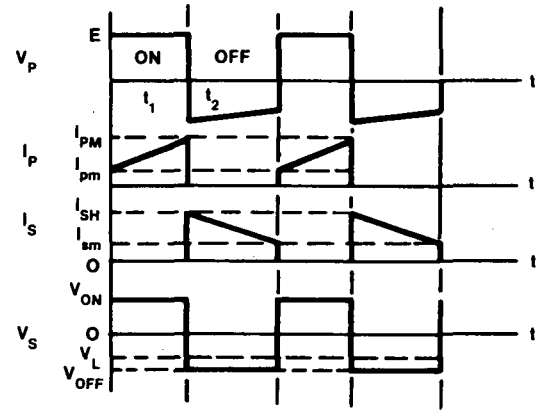

Figure 6.1.10 Operating Mode #2

3. Primary Inductance. A large transformer primary inductance is desired to reduce transistor peak currents, reduce transistor switching frequency, and minimize ac line disturbances and bus capacitor requirements. However, a large inductance increases energy storage and requires a larger transformer. With a switching frequency of 10 kHz, it was found that a 160 μh primary inductance was adequate to keep the transistor peak currents under 150 amps at the rated charger load. The resulting energy storage requirement results in a transformer of acceptable size as determined below.

4. Transformer Size. Core size was determined by "area product" method.[3] This method will yield the core size as measured by its window area, A_W times its cross sectional area, A_i, by the following relation:

$$A_p = A_i \times A_W = \frac{L_p \cdot I_p \cdot I_{rms} \cdot 1{,}550}{\frac{n}{N} \cdot B_{pk} \cdot J}$$

where L is transformer primary inductance, I_p is the peak primary current, I_{rms} is the maximum effective input current, n is the winding packing efficiency, N is

the number of windings, B_{pk} is the peak flux density, and J is the winding current density. Table 6.1.1 shows the values used in the above equation. It is seen that the winding packing efficiency is quite low and is due to the need for Litz wire in this high frequency application.

L_p - 160 μh
I_p - 150 amps
I_{rms} - 25 amps
n - .4
N - 3
B_{pk} - 1.2 tesla
J - 1000 amps/in^2

Table 6.1.1
T501 design parameters used in determination of transformer size.

Solving the above equation for Ap with the values in Table 6.1.1 gives an area product of 8.06. Thus, the core designated AH-393 from Arnold Engineering, having an Ap of 8.44 and weighing 8.12 lbs. was selected.

5. Turns Ratio. The transformer turns ratio for charge mode was designed around the maximum voltage ratings of the drive transistor ($V_{ce_{sus}}$ = 450 v., V_{cbo} = 600 v.). This design requirement originates from the fact that, when the drive transistor is off, the transformer secondary is conducting current to the main battery and is, thus, clamped to the battery voltage. During this period, the primary winding will reflect onto the SB1 transistor collector a portion of this voltage determined by the transformer turns ratio in a direction which adds to the line voltage.

Assuming a peak voltage of 340 volts on the 220-volt ac line and a peak charging voltage of 240 volts on the main battery, it is seen that a turns ratio of 0.43 will keep the total transistor voltage (line voltage plus reflected voltage) under the transistor 450-volt sustaining voltage as follows:

$$V_{ce} = 340 \text{ v.} + \left(\frac{np}{ns} \cdot 240 \text{ v.}\right) = 442 \text{ v.}$$

This turns ratio leaves a 160-volt margin available from the transistor reverse bias rating of 600 volts for absorbing transformer leakage spikes at transistor turn-off.

The transformer turns ratio when motoring is determined by the voltage rating of the blocking diode on the transformer secondary. This diode must withstand the main battery voltage plus the voltage that is reflected on the secondary when all of the main battery voltage is

impressed upon the snubber inductor winding. Assuming a peak battery voltage of 240 v., the diode reverse voltage in this condition can be expressed as:

$$V_r = 240 + (n \times 240)$$

where n is the turns ratio between the transformer secondary on the snubber inductor winding.

By connecting two 1,000-volt diodes in series, a withstand voltage of 2,000 v. is obtainable for blocking the secondary. By letting n = 7, it is seen above that Vr_{pk} is 1,920 volts. In order to achieve this voltage rating with 2 series 1,000-volt diodes, a resistor/capacitor snubber network was needed to ensure equal voltage sharing.

6. Determination of transformer turns. The number of primary turns was determined from the following relation:[3]

$$N = \frac{L\ I_{pk}}{B_{pk}\ A_i} \times 1{,}550$$

where B_{pk} is the peak flux density and A_i is the core cross sectional area in square inches. Using the numbers in Table 6.1.1 for the core selected, the primary winding gets 9 turns; and using the turns ratio of 0.43, the secondary gets 21 turns.

The number of turns for the snubber inductor winding is now calculated to be 3 turns, using its turns ratio of 1/7.

7. Winding the Transformer. In winding the transformer, the main objective was to minimize transformer leakage inductance. The energy stored in the leakage inductance is not transferable to the output and must be dissipated in power resistors. The final winding configuration is shown in Figure 6.1.11. The battery charger primary winding has been sandwiched between two layers of the secondary winding to improve transformer coupling in the charger mode. Litz wire was used for the battery charger primary winding and for the secondary in order to reduce losses from skin effect at high frequency (10 kHz). Since Litz wire increased the wire buildup and raised leakage inductance, it is recommended that other winding techniques be tried for this transformer.

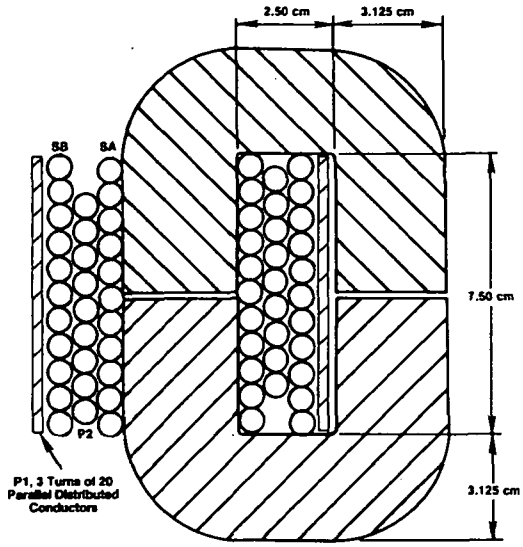

Figure 6.1.11 T501 Cross Section

The battery charger primary inductance was measured at 148 μh and the leakage inductance with the secondary shorted was measured at 2 μh. This 1.35% leakage inductance, considered good in many applications, was too high for the 10 kHz frequency used in this converter and lowered the peak charger efficiency to 80%. Transformer leakage inductance would have to be reduced on production versions of this circuit.

6.1.7 Auxiliary Power Supply

The auxiliary power supply is a multiple output, DC-DC converter, which supplies up to 50 amps to the 12-volt vehicle auxiliary system and also provides 4 isolated ±7-volt outputs for inverter base drive power. The specifications for this supply are given in Table 6.1.3. The most severe requirement on this supply is for nearly instantaneous 14-amp step response on the base drive outputs. Good base drive step response is necessary in PWM-type inverters because, at certain times in the PWM cycle, the bridge transistors are required to conduct full motor current immediately upon turning on. This requirement is more difficult on this inverter because the transistor power throughput is being stretched, as described in Section 6.1.2 and, thus, high step base currents are required.

Input Voltage: 240/125 v DC

Outputs:
1. 50 amp continuous, 13.5 volt for vehicle auxiliary
2. Three, ± 7 volt, 15 amp peak, 2 amp average outputs for the three top base drive circuits
3. One, ±7 volt, 15 amp peak, 6 amp average output for the three bottom base drive circuits

Duty factor: 50 amps from output #1, 20 amps from (2 + 3 + 4 + 5)

Maximum output power: 825 watts
Maximum input power: 900 watts at 90% efficiency
Tape of Supply: Coupled inductor, current driven topology

Frequency: 26 kHz

Protection: Operating current limit of 50 amps on output #1. Fast peak current shutdown and soft restart, for input faults.

Isolation: All outputs isolated from input bus and from each other through transformers

Control: Voltage and current control with pusle-width modulated integrated circuit.

Table 6.1.3 Auxiliary dc-dc Converter Specification

The basic converter configuration for the auxiliary power supply is shown in Figure 6.1.12. This circuit features a coupled inductor (T1) whose primary is on the input side of and in series with the converter input and whose multiple secondaries are in parallel with each of the supply outputs. Operation of this circuit is described as follows.

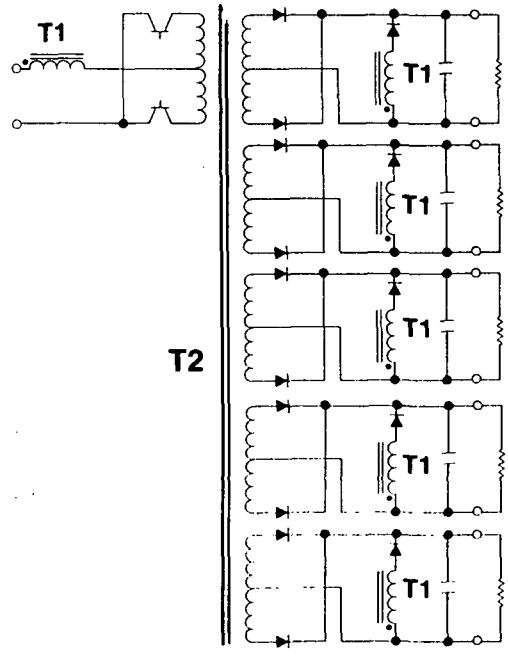

Figure 6.1.12 Aux. Converter Configuration

When both transistors are off, no primary current can flow. Energy which is trapped in the coupled inductor primary is seen as current in each of the coupled inductor secondaries thus, each secondary is clamped to its output voltage. In this mode of operation, if any output is loaded more heavily than the other outputs, its T1 secondary winding will "hog" the energy stored in T1, since its secondary voltage will tend to be lower than the other secondaries voltages.

When either transistor is on, current flows through the inductor primary to the transformer primary, T2. In this mode of operation, the T1 inductor secondary voltages are reversed and, thus, are blocked off by their series diodes. Current is supplied to the outputs by the T2 transformer secondaries which, when conducting, are also voltage clamped to their outputs. Thus, if any output is more heavily loaded than the other outputs, it will likewise "hog" current from the other outputs.

In either of the above cases, step changes in the load at any output are immediately seen and responded to by inductive elements in the input section. In addition, if these step load changes occur on unregulated outputs, the load current supplied to the regulated output will undergo a step change and, thus, the regulator section immediately sees and responds to load changes on the unregulated outputs.

This excellent cross regulation between multiple outputs as described above is ideally suited to the severe step response requirements for this drive. During motor load changes, the energy level in the T1 inductor builds slowly, but not more slowly than load changes in the induction motor. So, as induction motor load increases, the T1 stored energy also increases and, thus, can distribute power immediately to any base drive output requiring it.

Other advantages to this type converter are as follows.

- Input current rate of change is limited by T1 so the transistors are not subjected to current spikes.

- Transistor on-time and storage-time matching is not critical, as the T1 inductor protects the drive against slight volt-second mismatch in the T2 primary halves.

- The output current is continuous, so output capacitor requirements are small.

- The T1 primary winding blocks all but the minimum design bus voltage from the T2 primary and, thus, maximum transformer utilization is achieved on T2.

- Low peak inverse voltages occur on the output rectifiers and, thus, low dissipation Schotky rectifiers can be used in the 12-volt auxiliary output.

More complete descriptions of this converter topology are given in references 5 and 6.

The overall schematic for the auxiliary power supply is shown in Figure 6.1.13. It is seen that the negative base drive outputs have no coupled secondary on the input inductor, as their step requirements are not severe. The supply voltage regulation is performed by the TL-494 PWM voltage-regulating integrated circuit. This regulator has an operational current limit override, which is derived from the feedback shunt resistor on the 12-volt output.

In addition to the operating current limit, instantaneous shorts on the primary side of the converter are sensed by a "Hall" effect sensor, which immediately retriggers the circuit "soft start" sequence.

Low-level power for regulation and base drive is provided by the 12-volt auxiliary system. Isolation between the output transistor bases and their power source is provided by transformer T3.

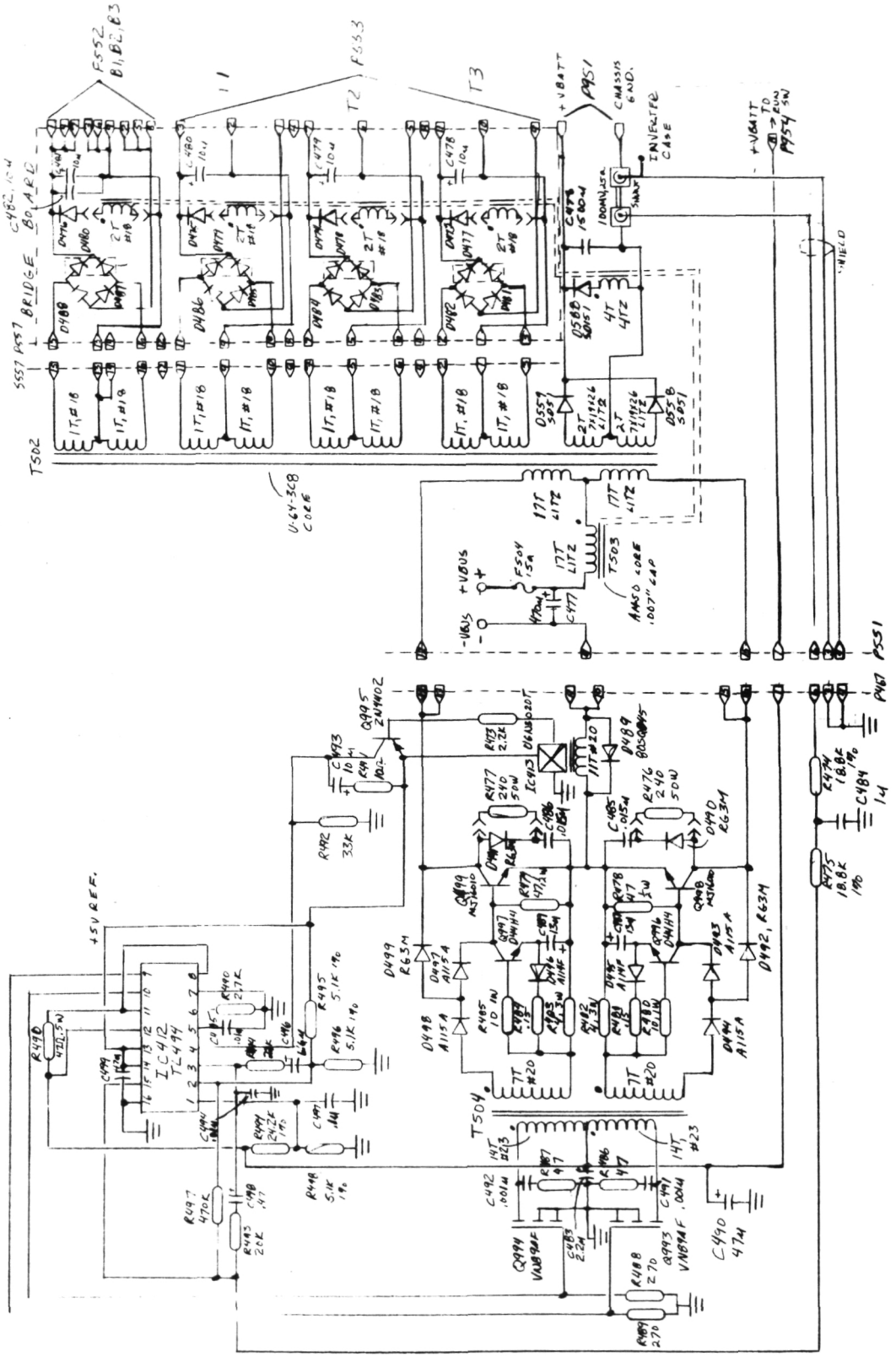

Figure 6.1.13 ACPS 2 Inverter Power Supply

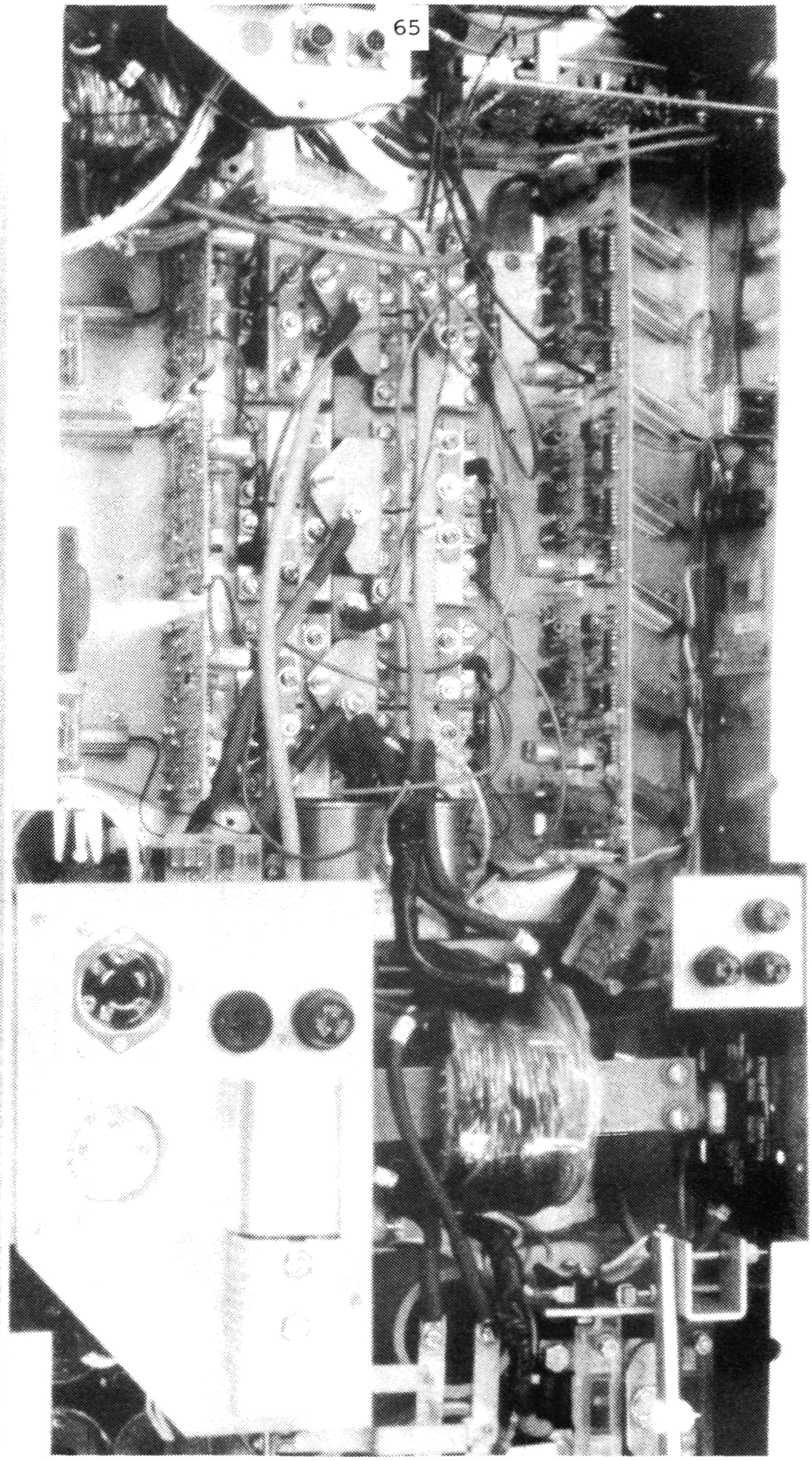

Figure 6.1.14 Inverter - Top View

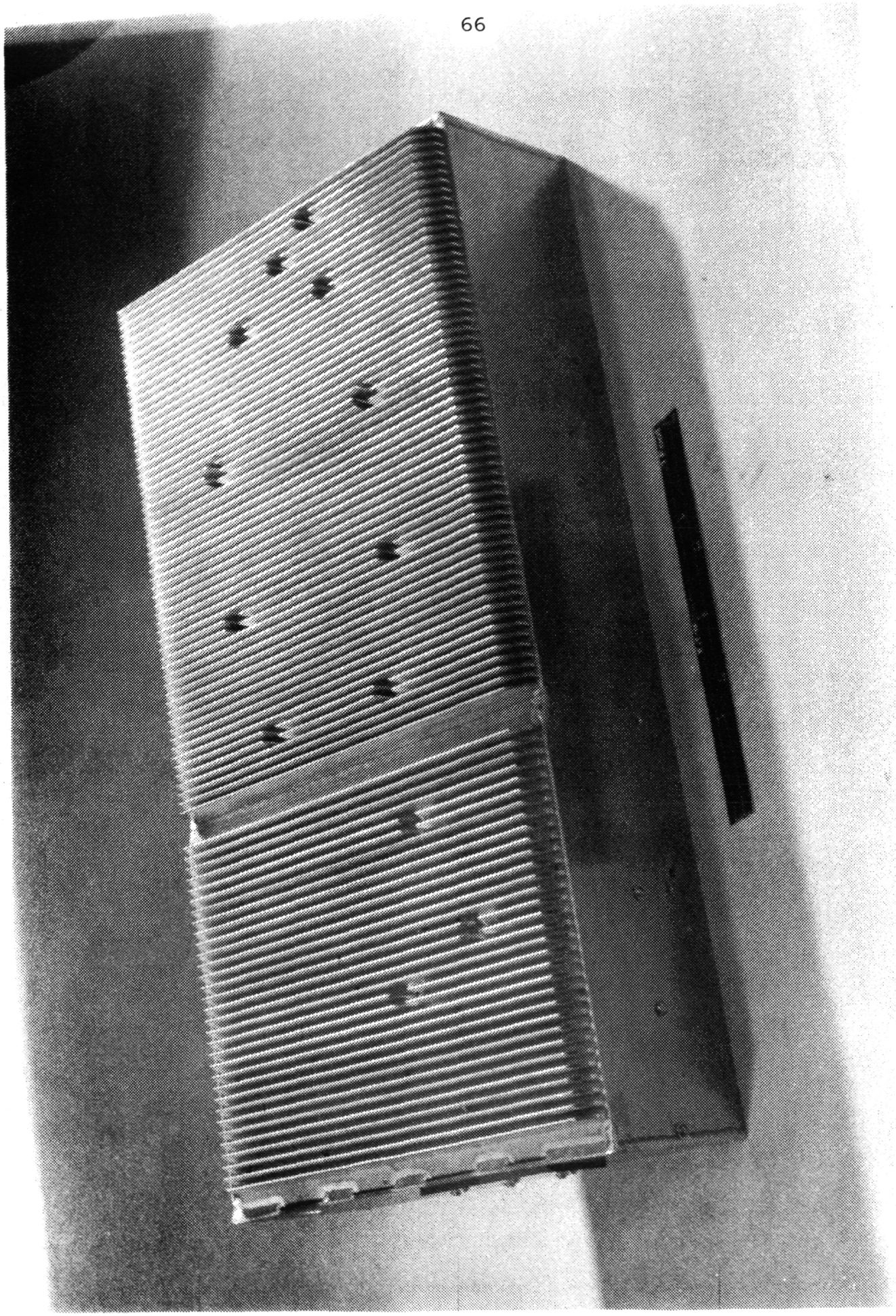

Figure 6.1.15 Bottom of Inverter

6.1.8 Packaging and Thermal Analysis

A top view of the final inverter package is shown in Figure 6.1.14. The general power flow from the battery is from the left side through the main contactor and Transformer T1 to the 12-transistor bridge and back out to the motor. The auxiliary power supply components are located at the far right.

The transistors are placed as closely together as possible to minimize wire inductances.

All heat dissipative components, including power transistors, diodes, base drive transistors, snubber resistors, and transformers, are placed in good thermal contact with the package bottom, which can be seen from Figure 6.1.15 to be entirely heat sink material. Electrical isolation between the bridge transistors and power diodes from the heat sink material is achieved with thermally conductive gaskets and electrically insulated mounting bolts.

In order to verify safe thermal performance of the inverter and to determine air flow requirements when placed under the rear seat, a computer-based thermal analysis was performed. This analysis resulted in numerous suggestions for improvements in packaging and specified the minimum air flow needed for safe operation in the vehicle. A detailed description of the thermal analysis is given in Appendix D.

6.2 Inverter Performance

Oscilloscope waveforms were taken to ensure safe operation of the bridge transistors and to verify inverter operation. The oscillograms shown below were taken at 3,600 rpm, 1.8 x rated torque, and a 192-volt bus. The chop frequency was 48 x the stator frequency or 2,880 Hz. This operating point corresponds to the most stressful inverter conditions in motoring.

The basic motor current waveform, showing the improved PWM scheme is shown in Figure 6.2. For 1.8 x rated torque at this speed, the peak current is seen to be 285 amps.

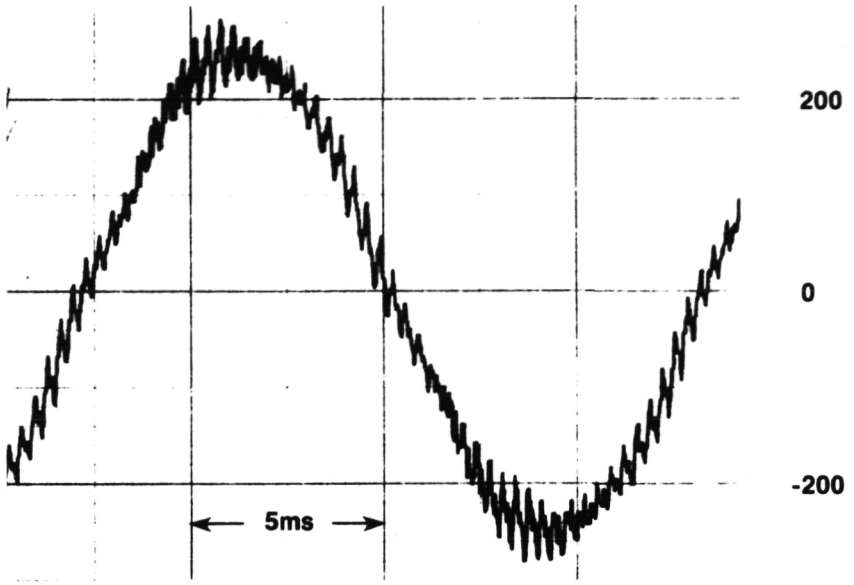

Figure 6.2. Motor ϕ_1 amps Vs. Time 3600 rpm, 1.8 P.U. Torque

I_m = 200 a/Div., t = 5ms/Div.

6.2.1 Safe Switching

Safe switching can be verified from Figure 6.2.1 (a & b), which shows the Phase 1 bottom transistor collector-emitter voltage (SB1-V_{ce}) vs. the Phase 1 motor current for one pulse of the PWM waveform. From 6.2.1.a, it is seen that the transistor is kept safely in saturation for the entire "on" time for motor currents up to 300 amps.

The expanded view in Figure 6.2.1b shows the turn-on and turn-off of B1 for 278 amps motor current. It was not possible to monitor the transistor collector current because introduction of a coaxial shunt into the circuit for this purpose would have a detrimental effect on the V_{ce} waveform. However, safe transistor operation at turn-off is ensured from examination of 6.2.1b and from the transistor published RBSOA, Figure 6.1.4.

The RBSOA provides the conditions for guaranteed safe turn-off of a transistor without having access to the actual time locus of collector voltage and current. From Figure 6.1.4, it is seen that, if the reverse base current during turn-off is -2 amps and the maximum collector voltage is clamped under 600 volts, then the maximum current of 250 amps can be repetitively switched. These conditions are easily met at peak load on this drive, as the two paralleled transistors are seen to switch 275 amps (approximately 138 amps each) while clamping the V_{ce} to 285 volts. The above voltage

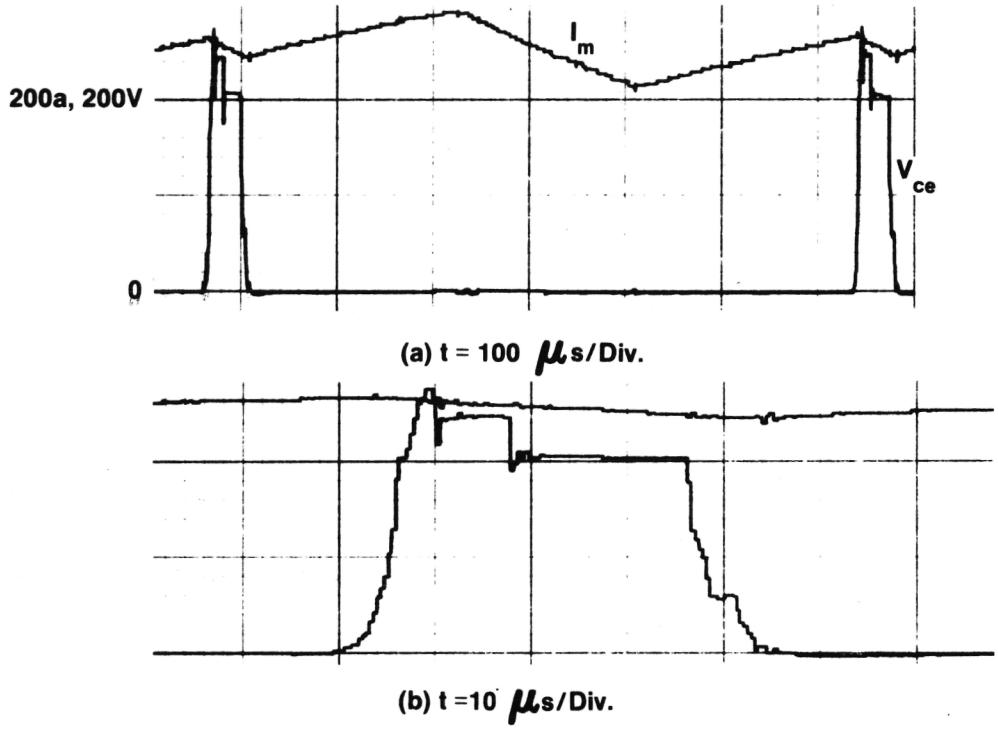

Figure 6.2.1 Q 501 Collector Voltage and ϕ_1 Motor Current, Vs. Time , 3600 rmp, 1.8P.U. Torque V_{ce} = 200 a/Div., I = 200 a/Div.

margin provides for switching fault currents in excess of 500 amps on a nonrepetitive basis. This margin can be assured by the large clamp capacitor provided (C501 = 16 μf) from the following analysis:

After turn-off, two "shelf" voltages can be seen on Figure 6.2.1b. The first voltage of 256 volts, is the nominal clamp voltage on C501. This voltage is a "worst case" condition, as the 3,600 rpm point corresponds to the maximum inverter switching frequency. The reserve energy storage capability on C501 for absorbing non-repetitive fault currents can be calculated as follows.

For a maximum allowable V_{pk} of 500 volts and for C501 = 16 μf, the reserve energy storage capability, E, is:

$$E = \frac{C(V_{pk}^2 - 256V^2)}{2} = 1.5 \text{ joules}$$

Assuming a conservative stray inductance of 7 μh (including leakage inductance of 5 μh in T501), the maximum fault current is:

$$i = \sqrt{\frac{2E}{L}} = 649 \text{ amps}$$

which is greater than inverter fault current allowed by the current sensors.

The second shelf voltage of 214 volts is reflected from the coupled inductor action and is discussed in the next section.

It is interesting to note a minor aspect of Figure 6.2.1a, which is that the bridge transistors are not required to switch the peak motor current of 304 amps that occurs in the middle of the transistor "on" pulse. This side benefit is a result of the PWM scheme being used. The peak motor current is brought down as a result of switching the other two motor phases, which are conducting considerably less current at this time.

It was not possible to monitor collector current during transistor turn-on for the same reasons noted above for turn-off. However, although turn-on load lines were not taken, safe turn-on is assured from the manufacturer's recommendation for the use of this transistor in PWM drive applications. Examination of the turn-on portion of the voltage waveform in Figure 6.2.1b reveals the most stressful portion of turn-on is the 64-volt "shelf" persisting for 1.5 μs. This shelf is caused by recovered charge on the complementary transistor's inverse parallel diode, which had been conducting motor current. This diode, which is internal to the drive transistor, is specified by the transistor manufacturer as a fast recovery type for PWM applications.

6.2.2 Series Choke Operation

Installation of the series bus inductor with its energy recovery winding raises issues regarding added inverter power loss and overall circuit operation. Inductor-related power losses arise from T501 core losses, transformer leakage energy loss which is dissipated in resistors, and snubber losses from the two series diodes on the energy recovery return winding (D501, D502). The above losses have been estimated at 250 watts under peak loading conditions

and will reduce inverter efficiency by about 1% below motor base speed. As the motor approaches base speed and pulses in the PWM waveform merge (lower switching frequency), these losses become negligible.

Overall bridge operation with the series choke is revealed in Figure 6.2.2, which shows the Phase 1 motor current, the DC bus current, the transistor bridge voltage, the D501 return diode blocking voltage, and the T501 coupled secondary current.

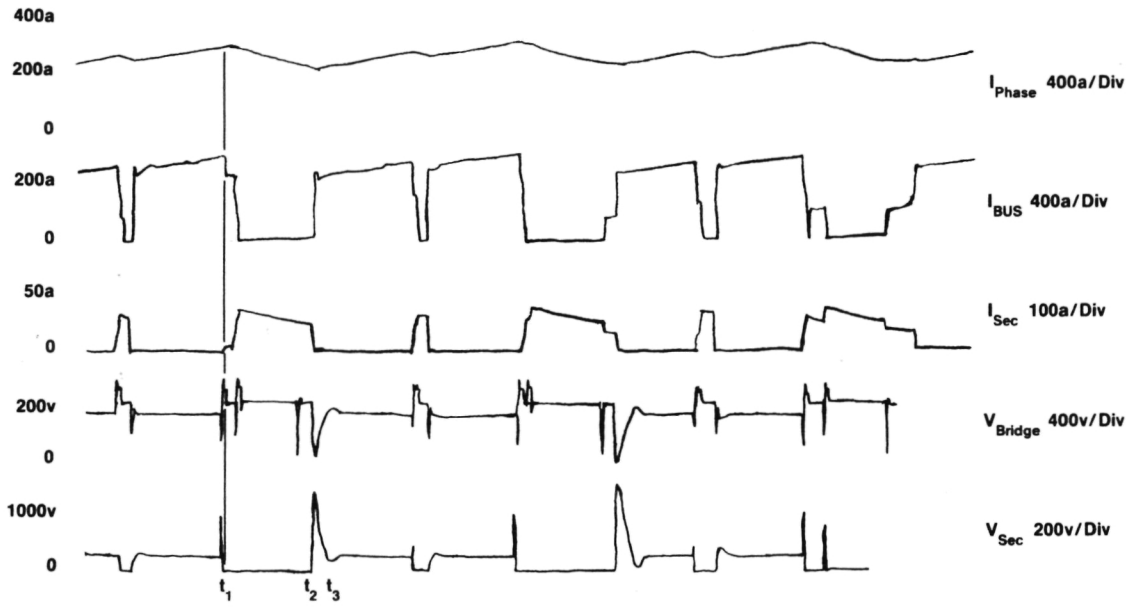

Figure 6.2.2 Inverter Bridge Operation 3600 rpm, 1.8 p.u. Torque

The complexity of these waveforms is due to the action of the series choke. Two intervals in 6.2.2 are noteworthy: From times t1 to t2, the return of stored energy in T501 can be seen from the transformer secondary current. At this point, the secondary is clamped to the battery voltage and the bridge voltage can be calculated from the T501 turns ratio to be:

$$V_{Bridge} = V_{Bat} + \left(\frac{3}{21}\right) V_{Bat} = 214 \text{ v}$$

If this interval is long enough, then significant energy is taken from T501. Thus, when a transistor switches to increase motor current, a mismatch occurs between motor current and T501 primary current. This action is shown in the t2 to t3 interval, where the bridge voltage is pulled to ground until the T501 current can be raised to equal motor phase current. As the entire bus voltage appears across the T501 primary at this point, the D501, D502 series blocking diodes see a peak of 1,600 volts from the T501 secondary.

This condition is the reason for needing 2,000 volts blocking capability on these diodes. This transformer action has a limiting effect on the power that can be transmitted to the motor, since a portion of the transformer energy is always being returned to the bus. However, this effect is only significant below base speed where the PWM duty cycle is below 100% and, thus, it can be overcome by raising the duty cycle.

Although the above problems with the series bus inductor configuration resulted in slightly degraded performance and increased cost, they were more than compensated by savings of six main power transistors in the bridge.

6.2.3 Base Drive Performance

Performance of the proportional base drive circuit is shown in Figure 6.2.3 (a & b) which show transistor base current vs. motor phase current at heavy inverter loading. From Figure 6.2.3a, it is seen that, over a motor cycle, peak base current is required for only a fraction of the cycle. Although the peak base current is 5.7 amps at this high load level, at light loads, the proportional base drive contains base current to less than two amps. This peak 5.7 amp base current level is well below the 14 amps projected in section 6.1.2, because the projected current was derived from the transistor worst case current gain characteristics.

Base current during transistor turn-on and turn-off is shown in Figure 6.2.3b. A negative base current of 5.6 amps (2.8 amps per transistor) can be observed, which reduces transistor storage time to 6 s and also makes good use of the transistor RBSOA, which was shown to be maximized at -2 amps base current at turn-off. A fast turn-on is achieved by this proportional drive circuit by sourcing a peak of 14 amps during the initial transistor turn-on. After transistor turn-on, the base drive circuit is shown to go immediately back into regulation.

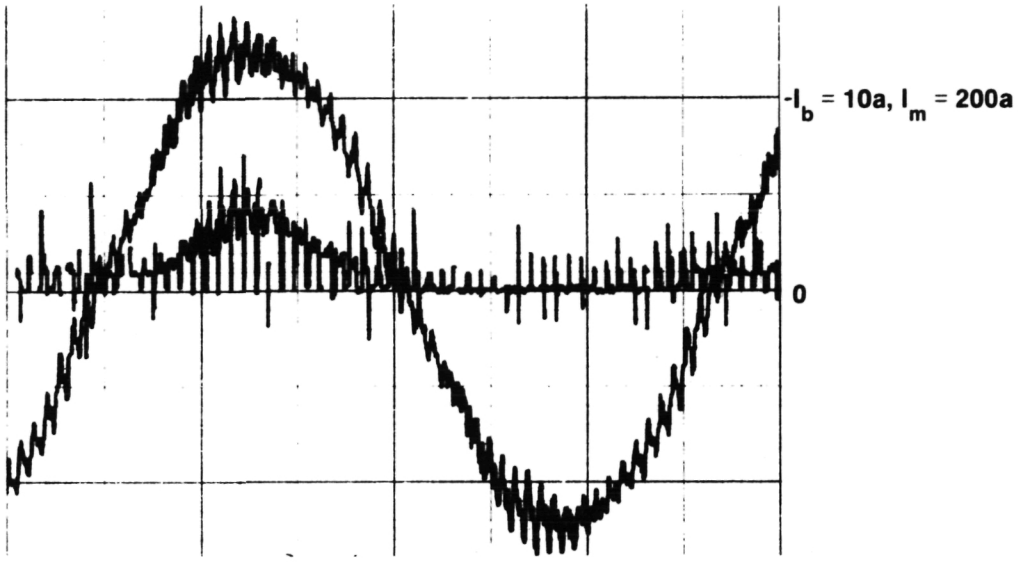

(a) t = 5ms/Div.

I_m =200 a/Div. I_b = 10 a/Div. t = 5ms/Div.

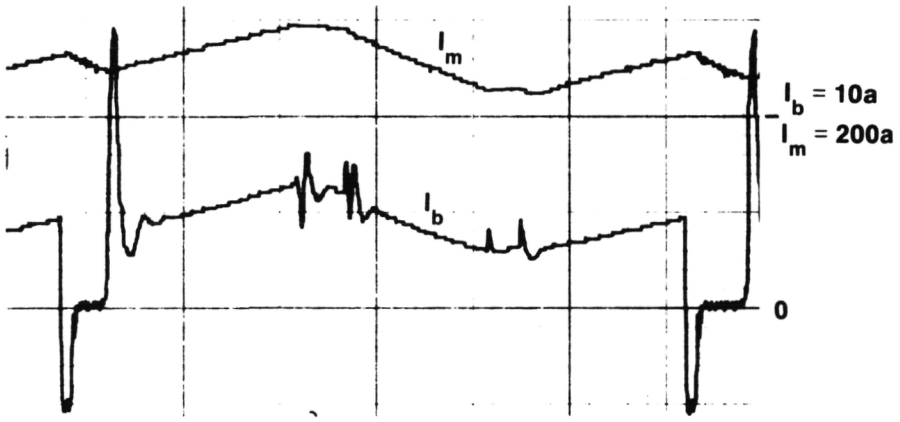

(b) t = 100μs/Div.

I_m =200 a/Div. I_b = 10 a/Div. t = 100ms/Div.

Figure 6.2.3 Motor ϕ_1 amps and Q501 Base Current Vs. Time. I_m = 200 a/Div., I_b = 10 a/Div.

6.2.4 Battery Charger Performance

Battery charger waveforms were taken at 16 amps charge current with the battery packs at 220 volts. The input line voltage was 208 volts.

The transformer primary current vs. transistor collector voltage is in Figure 6.2.4. The ac line frequency is evident, due to the minimal bus capacitance being used on the charger input. A peak transistor current of 110 amps is observed. This current level is the trip point for the base drive current limit and indicates operation of the charger in repetitive peak current mode. This 110 amp level is slightly below that required to achieve the peak power goal of 4 kw and is limited by the power dissipation capability of voltage clamping circuit. Scheduling limitations prevented pushing this power level higher.

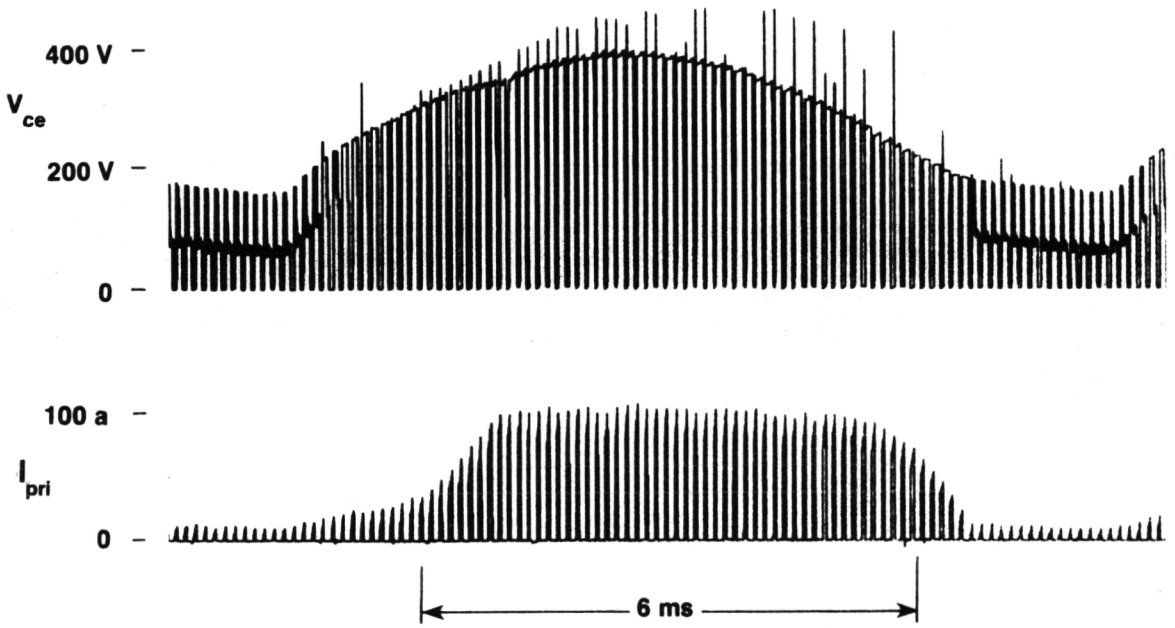

Figure 6.2.4.1 Q501 Collector Voltage Vs. T501 Primary Charge Current, Charge Mode

One pulse of the waveform in Figure 6.2.4 is shown in Figure 6.2.5, where the transistor is observed switching 112 amps. At this charge current level, the peak V_{ce} is seen to be 500 volts until stray wire inductance to the bus clamp capacitor, C501, is overcome. The clamp voltage of 458 volts on C501 can then be observed. Although the energy stored on C501 must be dissipated in resistors, these resistors are tied to the positive side of the main battery so that the current through them contributes to total charge current. Thus, not all of the T501 leakage energy is lost.

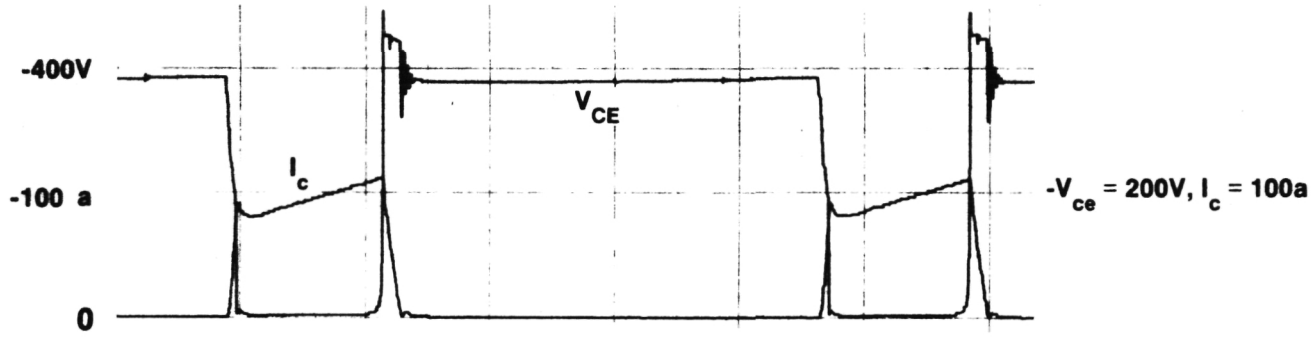

Figure 6.2.5 Q501 Collector Voltage Vs. T501 Primary Charge Current, Charge Mode
V_{ce} = 200 V/Div., I_{pri} =100 a/Div., t = 2μs/Div.

The transformer secondary voltage and current is shown in Figure 6.2.6. This rectangular current waveform is smoothed out by the main bus capacitors so that high frequency currents are not seen by the battery. A peak voltage of 900 volts, which must be blocked by D501, and D502, is observed on the T501 secondary.

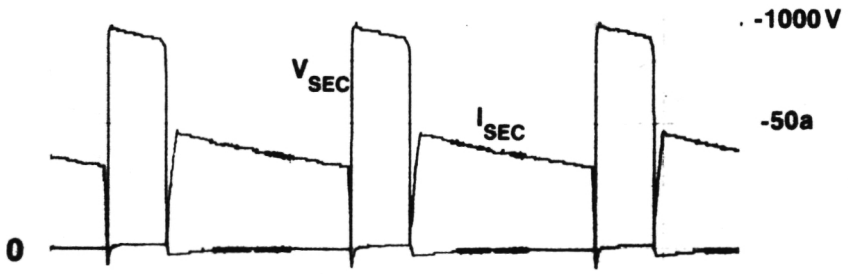

Figure 6.2.6 T501 Secondary Voltage and Current Charge Mode

V_{sec} = 500 V/Div., I_{sec} =50 a/Div., t = 50μs/Div.

The ac input voltage and current are shown in Figure 6.2.7. The high frequency operation is seen to produce little distortion on the ac line. In addition, a high power factor can be construed from the two waveforms.

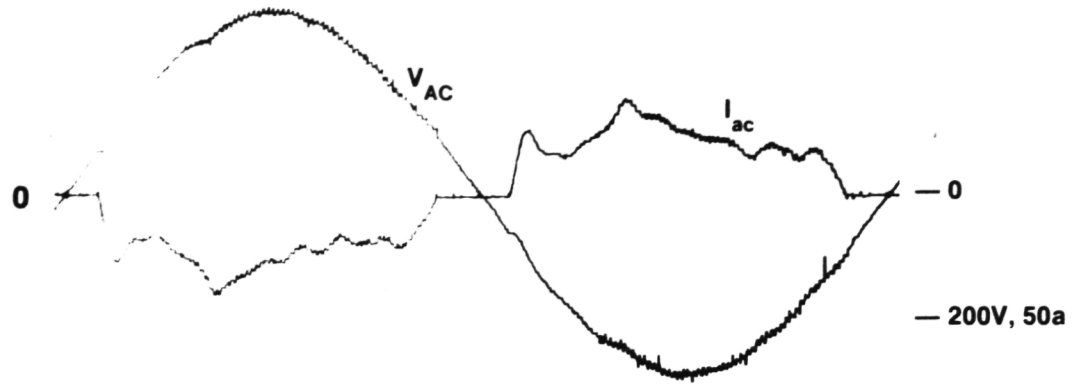

Figure 6.2.7 AC Line Voltage and Current, V_{AC} = 200 V/Div., I_{AC} = 50 a/Div., t = 2.5 ms/Div., Charge Mode

Battery charge current is observed in Figure 6.2.8. Although the 120 Hz related line frequency is evident, the 10 kHz chop frequency is missing, having been filtered by the main bus capacitors.

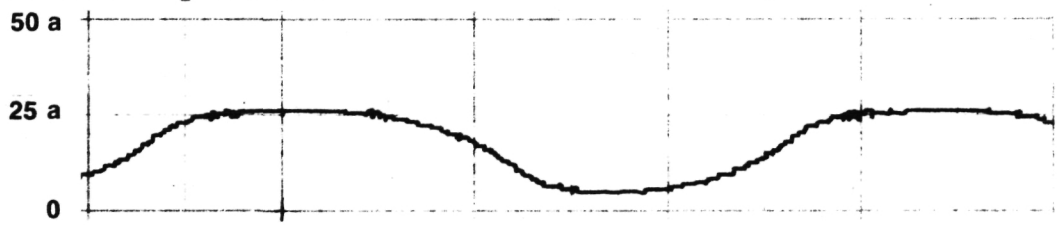

Figure 6.2.8 Battery Charge Current, Charge Mode I = 50 a/Div., t = 2.5 ms/Div.

6.2.5 Inverter/Charger Efficiency Results

Inverter efficiency measurements were taken during a dynamometer test sequence which is described in Section 10. The efficiencies versus motor torque are shown in Figure 6.2.9. The efficiency values shown include 160 watts of losses from the auxiliary power supply and the inverter fan, which were measured separately during the tests.

Efficiencies shown are significantly higher than those in Phase 1, having benefited from the following improvements:

- Elimination of snubber capacitors which added significant loss to the Phase 1 inverter
- Raising the battery voltage from 144 volts to 192 volts to achieve lower conduction losses
- A proportional base drive, which conserves power at light loads

Future improvements to inverter efficiency will be small and would be possible mainly by eliminating the series bus inductor.

Battery charger efficiency vs. power output is shown in Figure 6.2.10. These efficiencies include 150 watts of auxiliary power supply losses. It is seen that charger efficiency is poor at low power levels and only climbs to a peak of 80% at 3.5 kw. Although disappointing, it is believed that improvements similar to those achieved in the Phase 2 inverter are possible. These improvements would come from the following areas.

1. A scheme for reducing auxiliary power supply output during charging. The present 150 watts in loss is 4% of output power at 3.5 kw and increases to 15% at 1 kw output.

2. Improved design of the T501 transformer is needed. Significant losses arising from high leakage inductance and core hysteresis exists. This design could be improved, first, by eliminating the series inductor winding, which would allow more winding area for the battery charger windings. Thus, primary inductance could be increased, allowing for slower chop frequency and reduced hysteresis loss in the core. Leakage inductance could be reduced through improved winding techniques, which may require some computer modeling of transformer flux paths. In addition, an alternative to the use of Litz wire is needed because its low packing density increases leakage inductance.

3. Improved, low-cost core materials may become available with significantly lower core loss specifications. One candidate in this area is metallic glass.[7]

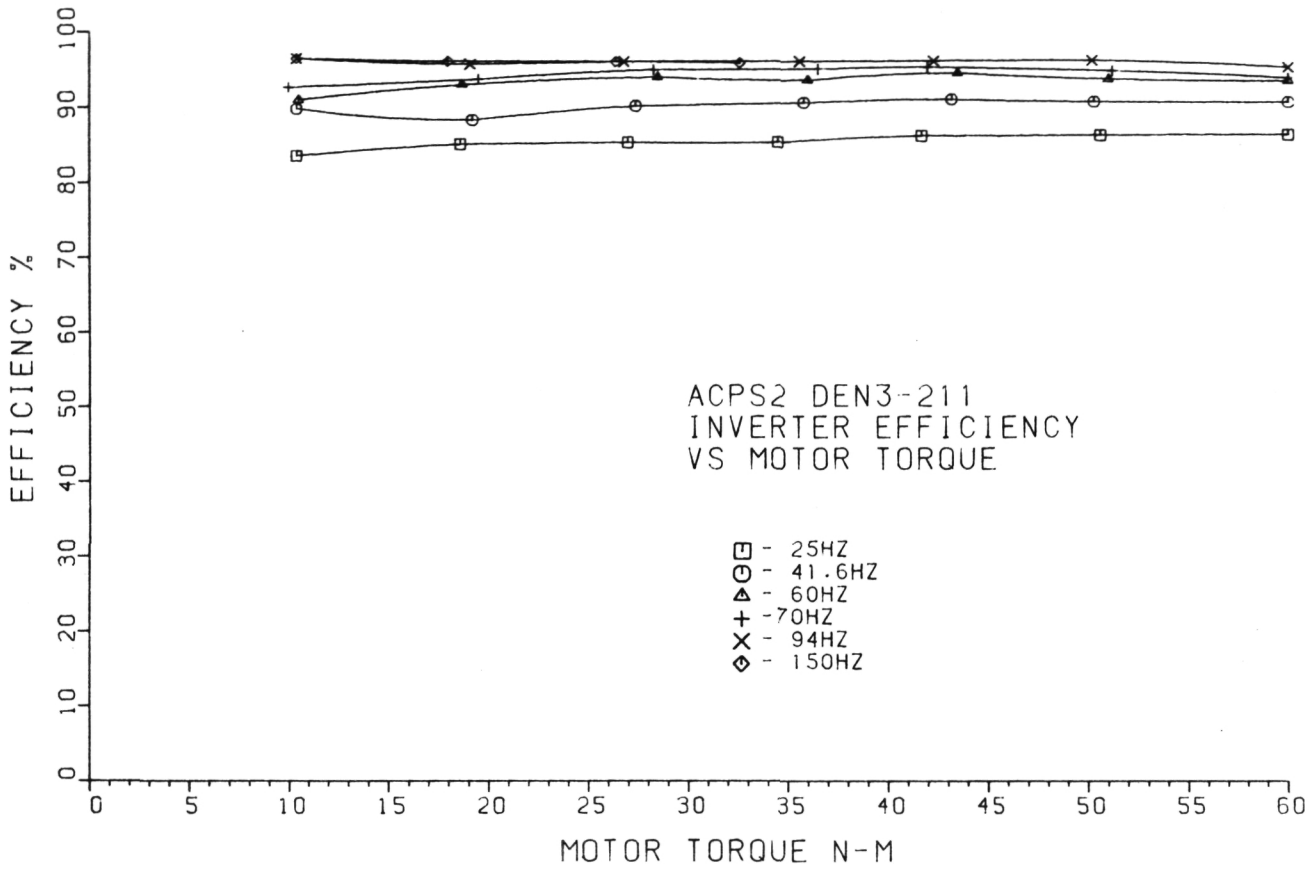

Figure 6.2.9 Inverter Efficiency Vs Motor Torque

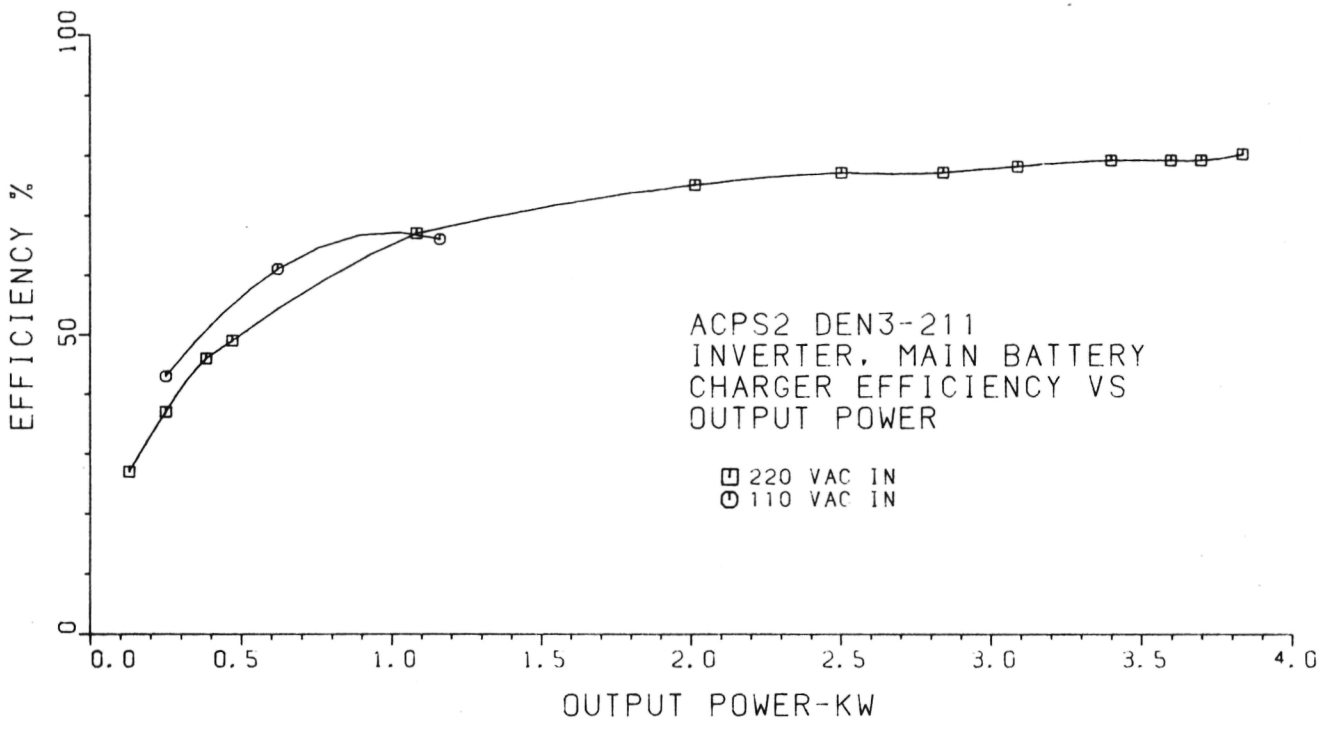

Figure 6.2.10 Battery Charger Efficiency Vs Output Power

6.3 Conclusions

1. A large step toward achieving cost competitiveness with DC systems was taken in this second phase of inverter development. Advances in lower cost, more rugged power transistors permitted the design of a significantly more compact and efficient inverter than in ACPS1.

2. The integration of the battery charger and DC bus series inductor into the inverter via the T501, 3-winding transformer, results in a cost effective circuit with many advantages. However, the future availability of higher current transistor or any change in peak power or bus voltage requirements would necessitate a reevaluation of the tradeoffs discussed in section 6.1.3. Although the need for the series bus choke could possibly be eliminated in a differently sized system, the concept of using the bridge transistors in the battery charger circuit is still viable.

3. Paralleling of low power transistors to achieve a higher inverter rating is possible with few attendant problems.

4. The current regulated base drive circuit worked well and resulted in a conservation of base drive power without significant increase in transistor conduction losses.

5. Although the base drive level protection logic is adequate for safe inverter operation, a method of smooth recovery from current limiting conditions must be devised in order to avoid intolerable inverter tripouts when driving.

6. The operation of the 3-winding inverter transformer, T501, was functionally adequate, but design improvement to reduce core losses and lower leakage inductance would be necessary in a production unit.

7. A special converter topology for the auxiliary power supply was needed to achieve fast step response on the base drive outputs. This power supply combined the base drive outputs and vehicle auxiliary output into one circuit for considerable cost and size savings. The 50 amp peak load capability on the vehicle auxiliary output could result in significant reduction in the size requirement on the 12-volt service battery.

8. The inverter efficiency is raised from Phase I to the point where only small future efficiency improvements could be expected. Future increases in charger efficiency can be obtained, principally, by design improvements to the T501 transformer.

7.0 LOGIC CONTROLLER

7.1 Design Summary

The logic controller handles all functions of vehicle operation:

A. inverter/motor control
B. transaxle gear shift
C. driver inputs
D. selected dashboard displays
E. battery charging
F. diagnostics

A. Inverter/Motor Control

The system philosophy is torque control, so that pressing down the accelerator has generally the same effect in an EV as in a conventional vehicle. Therefore, the primary vehicle "outer loop" controller input is torque demand. The primary inverter/motor "inner loop" controller input is motor rotor frequency. This feedback variable is obtained from reading rotor speed from a pulse pickup. The controller always adjusts internally generated stator frequency so that the desired slip frequency is maintained. This "slip loop" is kept as fast as practical for stability. Torque demand (+ or -) is mapped into a slip command along with an RMS motor voltage command. The voltage update rate is much slower than the stator frequency update. Voltage cannot change, nor does it need to change, as rapidly as slip to maintain stability.

Both motor stator frequency and RMS motor voltage must be controlled to efficiently run an induction motor over a speed and torque range. The controller generates a multiple of stator frequency which is used to clock three-phase PWM switching commands to the inverter. The pulse width modulated 3-phase switching waveforms are synthesized by an algorithm which causes nearly sinusoidal current waveforms in the motor.

Figure 7.1.1 shows the block diagram of the generation of FSMLT, the multiple of stator frequency. The system uses motor slip as feedback control by measuring motor speed 100 times a second, digitally adding (+ or -) slip within the software of the microprocessor, generating a resultant frequency, FSSUB, proportional to stator frequency in real time, and finally developing FSMLT which clocks switching commands to the inverter at the effective stator frequency rate. The slip loop is entirely digital with no drift. Although the microprocessor is in the loop, the stator frequency related activities are interrupt driven to assure an 100 Hz update rate. This was considered adequate compared to

the 10 to 15 Hz motor/vehicle response. The phase lock loop (PLL) governs the slip loop response. Since slip can be less than 1% of stator frequency, stability and accuracy are essential for a scheme such as this to function properly. This is why the digital approach is used.

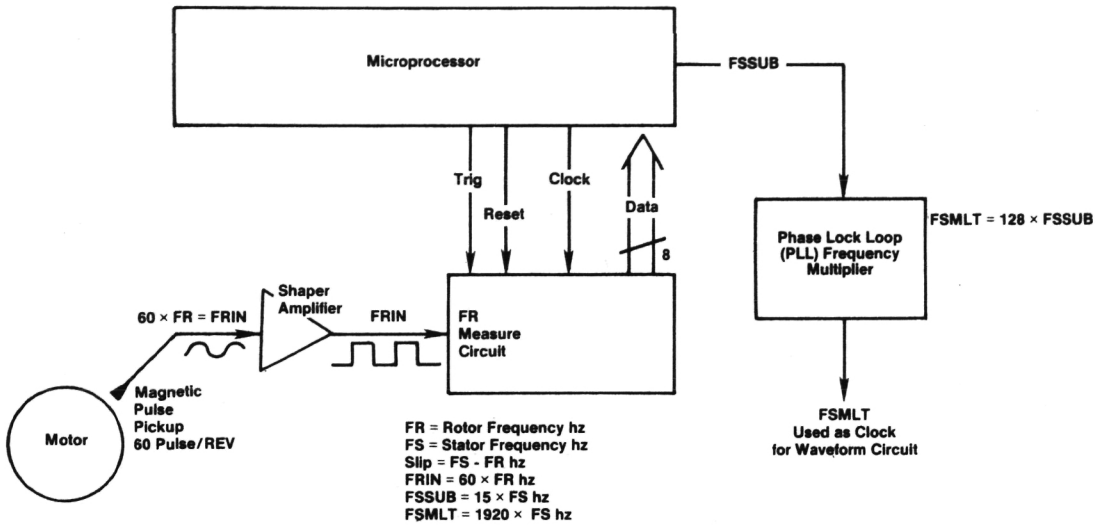

Figure 7.1.1 FSMLT Generation for Slip Control

Figure 7.1.2 shows a block diagram of the waveform generation scheme. The three final switching command lines, Ø3F, Ø2F, Ø1F, are identical except for being displaced $\pm 120^{o}$ from each other. These lines drive optocouplers in the inverter. One stator frequency period is divided into 1920 segments. Each segment for each phase is allocated one unique address in the Buffer and Master RAMS. Thus, the PWM waveforms can be synthesized with a resolution of one part in 1920 (0.187^{o} steps).

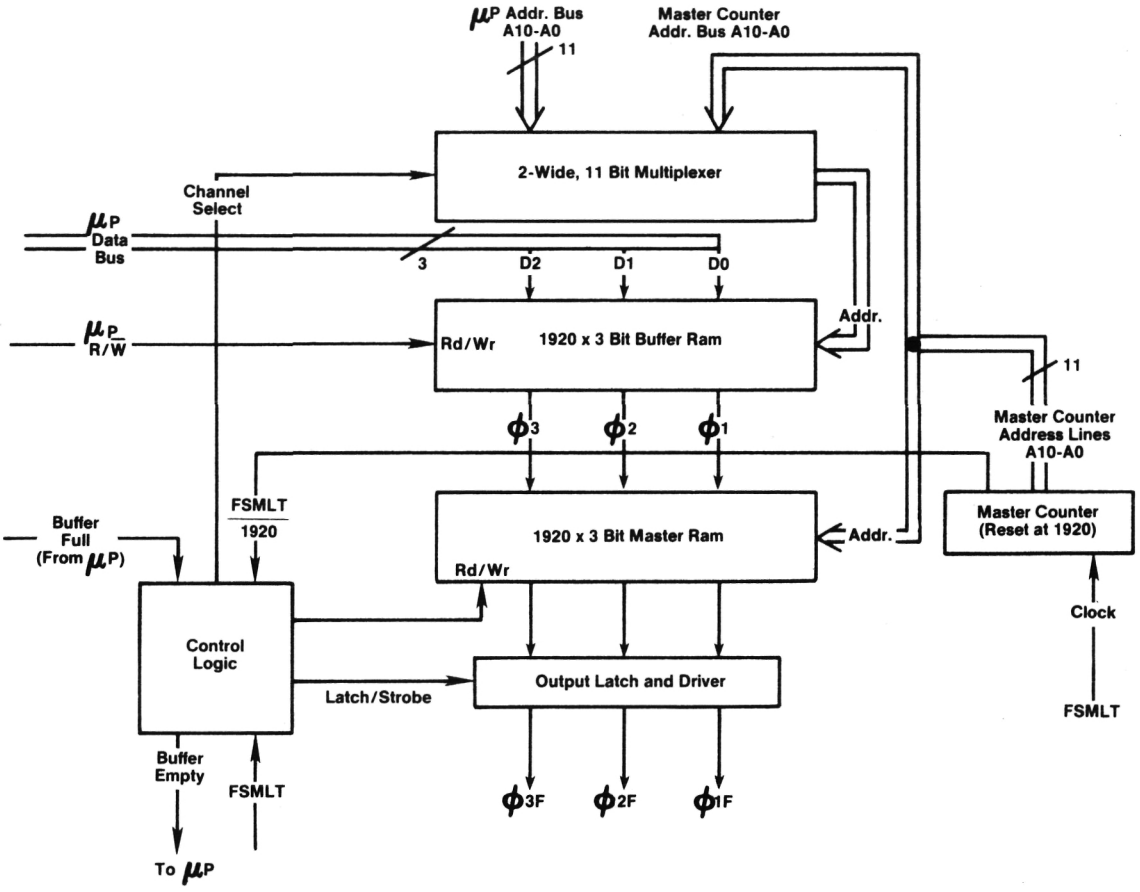

Figure 7.1.2 PWM Waveform Generation Scheme

Upon receipt of a "Buffer Empty" signal, the processor, through a programmed alogrithm using desired motor volts as input, generates three serial bit streams representing the main switching transistor commands over one stator frequency cycle. These three streams are simultaneously written to the Buffer RAM as 3-bit words at a rate asynchronous to stator frequency (FS). The waveform is loaded onto the Buffer RAM with an arbitrary reference point (0^{o} on Phase 1). The Master RAM is always clocked by FSMLT through the Master Counter which acts as an address generator. Since 1920 RAM locations constitute one stator frequency period, and FSMLT = FS x 1920, the Master RAM output represents three complex digital waveforms at stator frequency rate.

After writing 1920 triplets to the Buffer RAM, the processor issues a "Buffer Full" signal to the control logic. The new waveform cannot be transferred from Buffer RAM to Master RAM until the Master RAM returns to a reference synchronizing point. The point chosen is when the master counter folds over from address 1919 to

0. At this point, the multiplexer switches the Buffer RAM address bus over to the Master Counter, and Master and Buffer RAM's are synchronous for one FS cycle. During this cycle, the 3-bit data words are written from Buffer to Master and also to the output. Thus, the Master RAM is transparent during an update cycle. After the update cycle, the control logic issues a "Buffer Empty" signal to the processor and reverts the Buffer RAM address bus back onto the processor address bus. The Buffer is ready to receive a new waveform.

This scheme relieves the processor of real time waveform generation to the inverter, and yet allows waveform flexibility limited only by resolution and software. If the processor were to create the waveform in real time, it would need to tend to the task as often as once every 3 µs, impractical with present designs. The output latch prevents glitches from the Master RAM (as addresses change) from reaching the output.

Four temperatures are sensed:

. motor stator temperature (thermistor in winding)

. inverter heat sink temperature (National LM235 sensor)

. battery electrolyte temperature (National LM235 sensor in sealed Teflon tube)

. ambient temperature in controller box (National LM235 sensor)

These temperatures are read by the controller and act as torque demand limiters if excessive.

Bus voltage and bus current are also read through isolation amplifiers (AD290A's). Both can limit torque and shut down the drive if outside limits.

B. Transaxle Gear Shift

The gear shift is controlled by high and low gear hydraulic clutch packs. The packs are engaged or disengaged by solenoid valves excited from the controller. The controller determines when to upshift or downshift based on motor speed. During a shift, the motor speed is controlled to synchronous speed with the new ratio. Close synchronism is not needed since the clutches can safely slip momentarily. Hysteresis in shift point is provided in software. A discrete logic circuit prevents the controller from commanding both high and low clutches simultaneously for more than 1.2 seconds (some overlap is desired) in the event the processor malfunctions. Downshifts are prevented if motor overspeed would result.

C. Driver Inputs

The driver has five inputs to the controller:

- accel demand pedal (potentiometer on pedal)
- brake demand pedal (potentiometer on pedal)
- shift lever (switch closures: reverse, neutral, low and drive)
- parking brake status
- ignition key status

The function of these inputs is covered in Section 7.3.

D. Selected Dashboard Displays

The controller drives two dashboard displays:

- State-of-Charge (SOC) display. This is a string of seven LED's mounted in an arc. The lit LED indicates traction battery capacity remaining, as computed from an algorithm by the processor. Upon power up, the initial SOC is deduced from battery open-circuit voltage. During operation, amp-hours into and out of the battery are digitally integrated. A battery temperature factor is included in the SOC calculation.
- Annunciator display. This consists of four LED's:
  1. System Fail (drive shut down)
  2. System Limit (torque output limited by some parameter)
  3. Aux. battery low (indicate DC/DC converter failure and imminent controller malfunction)
  4. Charge mode (indicate system is configured to charge batteries from line input power)

The remaining dashboard displays are conventional and not linked to the controller.

E. Battery Charging

Figure 7.1.3 shows the essentials of the charge mode scheme. The system can accept single phase AC power at 110 VAC or 220 VAC $\pm$10%. Plugs are located behind the "gas filler door" of the test vehicle. The controller senses input voltage and adjusts limit points

accordingly. If the vehicle is at rest, the charge door is open, AC voltage is present, the main bus contactor to the bridge is off, the key is removed from the ignition switch, and no fault is sensed, the controller automatically enters "charge mode." As discussed in Section 6.1, the charger is a flyback transformer type with the bottom transistor of Phase 1 of the bridge acting as the chopper element.

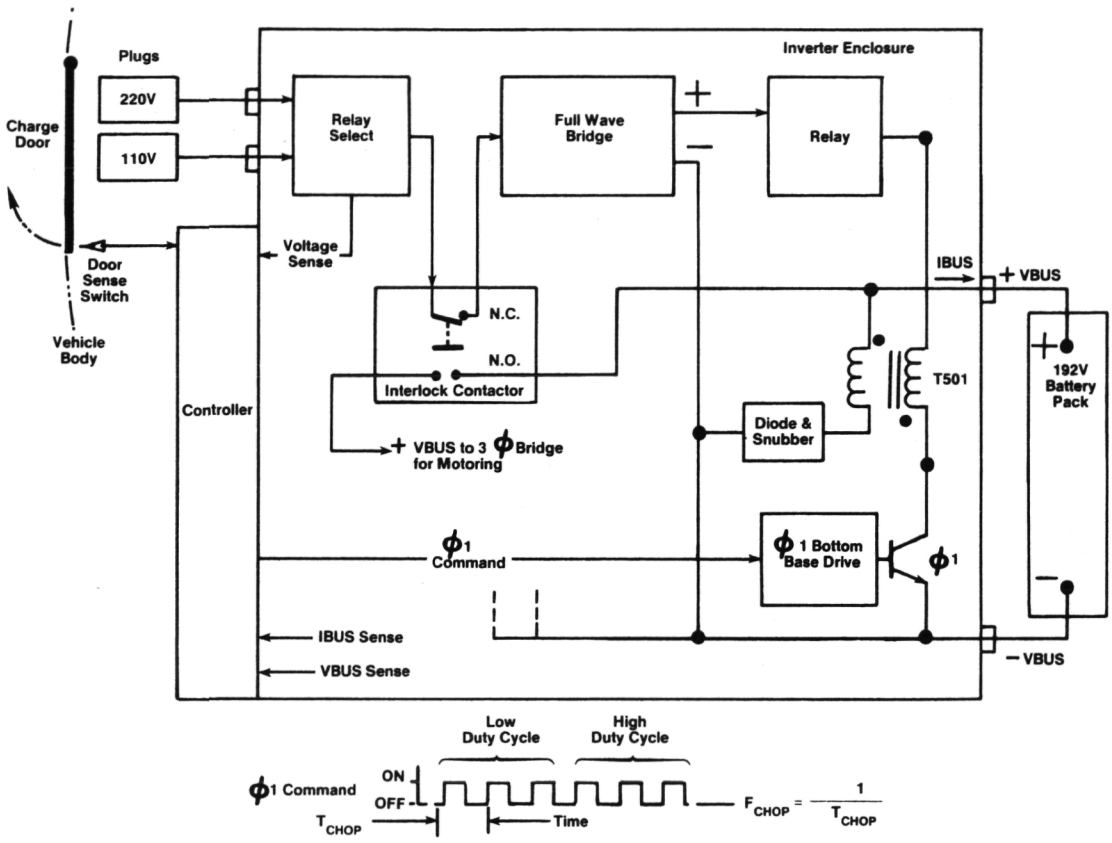

Figure 7.1.3 Charge Mode Scheme

The controller inhibits bridge legs Ø2 and Ø3, and begins to send a constant frequency Ø1 command at a minimum duty cycle (see Figure 7.1.3). The same circuitry used to generate motor waveforms is used here, except FSMLT is replaced by an internally generated carrier frequency, FCHARG (614.4 kHz). Again, a single period of the Ø1 command is divided into 1920 parts. After experimentation, it was determined that a chop frequency, FCHOP, to the transistor of 10.24 kHz was suitable. This implies that each FCHOP period contains 614.4/10.24 = 60 bits. By adjusting the ratio:

$$\frac{\text{Bits Hi}}{60}\text{; where Bits Hi + Bits Lo = 60,}$$

the effective on time, or duty cycle, to the switching transistor can be varied. As the duty cycle is increased, charge current increases. FCHOP is asynchronous with the 60 Hz or 50 Hz line frequency. A synchronizing scheme was used at first in an attempt to smooth out current pulses. Duty cycle was modulated to be a minimum at the crest of the line input voltage. However, this synchronous scheme yielded poor power factor as proportionally more current was drawn at low instantaneous input voltages. At 10.24 kHz chop frequency, peak currents are not severe and power factor is above 0.9.

The controller slowly increments the duty cycle while monitoring battery voltage and current. If battery voltage reaches the "crossover voltage," VBUSCR (a function of battery type and electrolyte temperature), the duty cycle is adjusted to maintain that voltage. Current tapers as required. Until the crossover voltage is reached, the charger is in current limit mode. The proper limit for 115VAC input (assume 15a service) or 220VAC input (assume 20a service) is automatically selected. In the present design, no final cutoff is provided. The current just tapers to a small maintenance value.

The "constant I - constant V" charging method described above is entirely under software control. During charging, heatsink, battery, and ambient temperatures are monitored and current is reduced if excessive temperatures are noted. A fault monitor routine for overcurrent, overvoltage, extreme temperatures, loss of sensors, and abnormal duty cycles is performed concurrently. 110VAC brushless muffin fans vent the battery boxes during charge. A transformer supplies 110VAC when primary voltage is 220VAC.

F. Diagnostics

Software in the controller has been included to allow two-way communication with a purpose-built, portable diagnostic box. Variables can be viewed and modified in real time. Several status and fault words are generated to pinpoint the cause of a shutdown and to indicate the state of the system at a given moment.

An LED is mounted in the controller which flashes when the program is cycling properly. This provides a quick check that the controller is functioning during lab tests.

7.2 Hardware Description

The controller can be divided into six parts:

A. processor board
B. input board
C. output/power supply board
D. driver board
E. connectors and harness assemblies
F. case

A functional block diagram is shown in Figure 7.2.1.

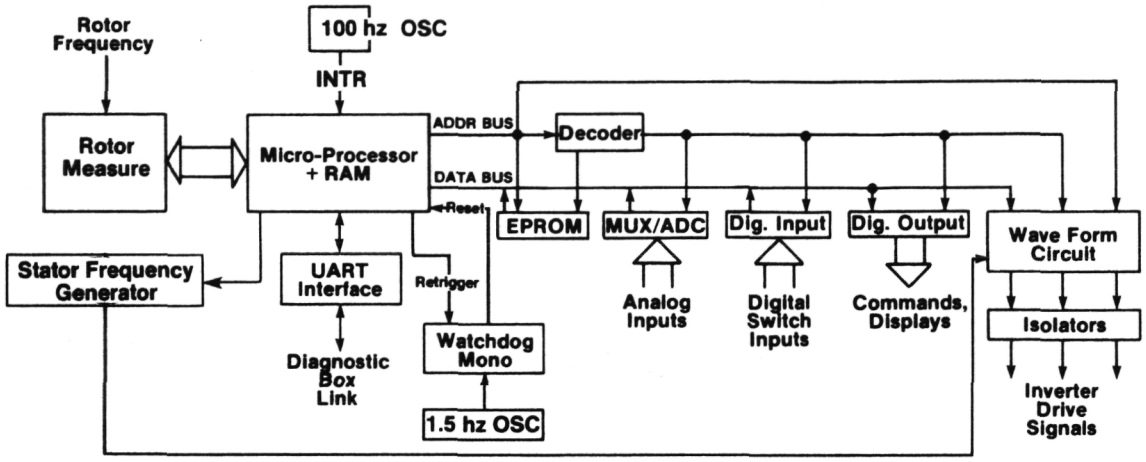

Figure 7.2.1 Controller Function Block Diagram

A. Processor Board

This 17 cm x 28 cm wirewrap board carries all the logic and most of the analog circuits. The system is based on a Motorola MC6801L1 microcomputer. MC6801L1 was chosen because its on-chip resources matched the functional needs. It has 128 bytes of RAM, a Serial Communication Interface (SCI), parallel I/O ports, a three function timer, and a multi-level interrupt structure. All these functions are utilized. "Mode 2" of the MC6801L1 is used to make use of the internal RAM and external EPROM.

Memory needs are fulfilled by a 128 x 8 external RAM (Motorola 68A10L) and a 4k x 8 EPROM (Intel I2732). All address decoding and other processor support functions are on the board.

A special counter circuit was developed to measure rotor frequency FR. For good slip control, 12 bit accuracy on FR is needed over a wide 1 to 212 Hz range. Further, measurement time should be less than 6 ms. to achieve an adequate update rate. The input frequency, FRIN, varies from 0 to 13 KHz. The information rate is too slow to use simple gated counting. Figure 7.2.2 shows the FR circuit.

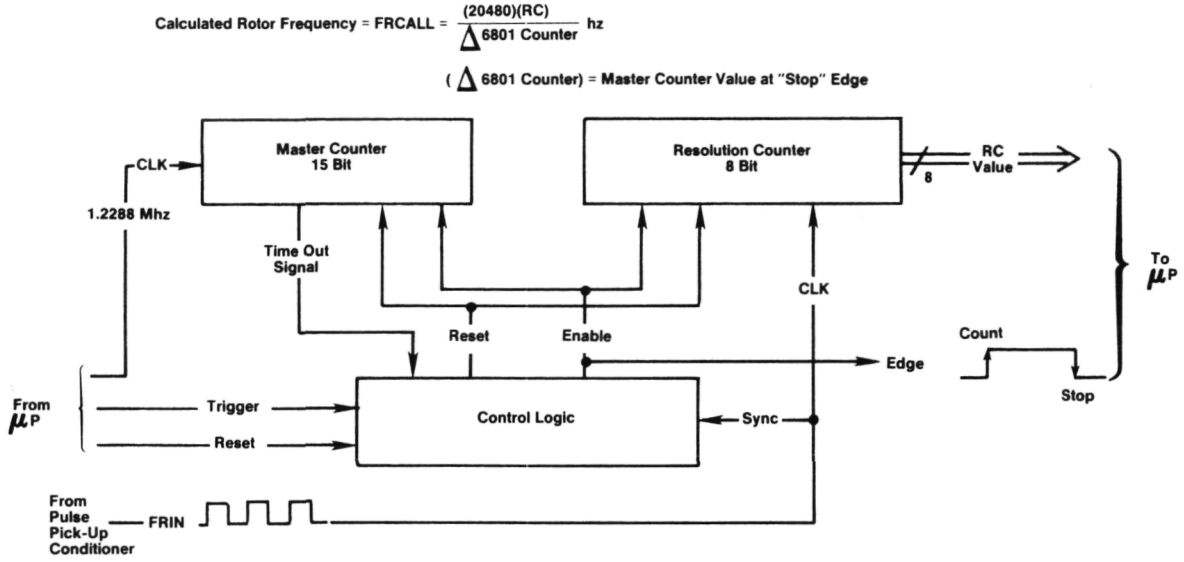

Figure 7.2.2. FR Measure Circuit

Every 10 ms., an interrupt routine is invoked which strobes a reset and then a trigger pulse to the FR measure circuit. Upon the next rising edge of input frequency FRIN after the TRIGGER, both counters are enabled. The internal MC6801 counter is also enabled by the EDGE rising transistion. The Resolution Counter accumulates FRIN pulses. Eventually the Master Counter issues a TIME OUT SIGNAL, which is independent of FRIN. Both counters and the internal MC6801 counter are disabled on the next rising edge of FRIN. The rotor frequency is calculated from the equation:

$$\text{Calc. rotor frequency} = \text{FRCALC} = \frac{(20480)(RC)}{6801 \text{ ctr.}} \quad \text{Hz},$$

where RC = contents of Resolution Counter after disabled and 6801 = effective contents of MC6801 internal counter when disabled (the internal counter is not actually disabled, but the effect of the EDGE pulse is as such).

Two features are essential for this circuit to work successfully. First, the ENABLE signal must be synchronized with FRIN edges so that the ±1 count uncertainty is eliminated. Second, the circuit allows for variable number of FRIN periods to be counted as the permissible convert time allows. This gives high accuracy over the full frequency range since the resolution of the Master Counter, clocked by a crystal-derived frequency, is always held to at least 1 part in 4096.

The microcomputer generates a multiple of stator frequency at a toggling output port. This frequency is then increased 128X by a conventional multiplying phase

lock loop. A CMOS 4046 type PLL with a CMOS 4024 7-stage divider is used. The resultant frequency, FSMLT, is used in the waveform circuit on the processor board (see Section 7.1 and Figure 7.1.2).

The heart of the analog section is an 8-channel multiplexer-analog-to-digital converter (MUX-ADC, National Semiconductor ADC 0808CCN IC). This IC converts 8 DC analog signals to 8-bit digital words read by the microcomputer. A small DC/DC converter steps up the logic 5 volts to 15 volts. The 15 volts is regulated by a precision regulator to 5.00 volts, which serves as the MUX-ADC reference. The logic 5 volts level is not stable enough. The 15-volt line is also used to power the isolation amplifiers for bus voltage and bus current signals.

None of the analog signals have any significant preconditioning on the processor board. Simple RC filters are used to reduce noise. Whenever practical, pull-up or pull-down resistors are incorporated on the inputs to put the input to a failsafe/shutdown state if the input line opens. Table 7.2.1 lists the controller I/O. Digital inputs and outputs are straightforward. Note that "Neutral Select" is the absence of any other gear mode select. This was a failsafe measure.

TABLE 7.2.1

CONTROLLER INPUTS/OUTPUTS

ANALOG

INPUTS	ADC SENSITIVITY
Ambient temperature (in controller)	2°C/increment
Battery electrolyte temperature	2°C/increment
Heat sink temperature (sensor mounted on stud into ϕ1 inverter heat sink)	2°C/increment
Motor temperature (thermister mounted on surface of stator winding)	2°C/increment
Accel Demand (from pedal pot)	1% steps from 0 to max + torque
Decel demand (from pedal pot)	1% steps from 0 to max - torque
Bus voltage (sensed on inverter bus	2V/increment
Bus current (sensed on -IBUS line)	2a/increment

DIGITAL

INPUTS	OUTPUTS
Rotor pulse pick-up frequency	Inverter inhibit control
Parking brake status	Charge mode status/indicator line
Reverse selected	Inverter blower control
Low gear only selected	Low gear solenoid control
Drive (shift enable) selected	High gear solenoid control
12V auxiliary battery status (low or OK)	Battery state of charge (3 bit word)
Charging door status (open or closed)	Auxiliary battery indicator line
110Vac charge input	System fault indicator line
220Vac charge input	3ϕ inverter switching command lines

A "watchdog timer" is included to restart the processor if it "crashes" due to a transient or glitch. The timer consists of a dual-input retriggerable monostable oscillator. One input receives a stream of pulses if the program is cycling properly. The other input is a 1.5 Hz pulse generator. The output connects to the MC6801 reset line and also directly to the inverter inhibit line. If the computer goes awry, the timer times out, resets the system, and shuts off the inverter. Within 0.7 sec., the timer allows a restart. If the restart is successful, the stream of watchdog triggers will resume and the system will stay enabled. If no watchdog triggers occur in 17 ms., the system resets and tries again in 0.7 sec.

The MC6801L1 SCI port is used to communicate with the diagnostic box. When the box is not connected, the system ignores the port.

One trim pot is on the board to adjust the ADC reference voltage to 5.000 v $\pm$ 5 mv.

B. Input Board

This 5 cm x 17 cm printed circuit board acts as an interface between all external inputs and the processor board.

The bus current signal from the remote isolation amplifier is scaled and offset by a low drift RCA CA3160AE op. amp. The offset is needed since the current signal is bipolar, and the controller analog section is unipolar (0-5 v). Zero current is set at 2.00 v. nominal to the ADC. A trim pot is included to adjust the offset.

A one volt regulator/driver is included to drive the thermistor on the motor stator. A resistor in series with the thermistor is used to linearize output in the area of interest = 160^{o} to 180^{o}C. Below 80^{o}C, accuracy is poor. An op. amp with a span trim pot scales the thermistor output.

All other inputs feed through the input board unchanged. The ambient temperature sensor (10 mv/^{o}C output) is mounted on this board.

C. Output/Power Supply Board

This 5 cm x 17 cm printed circuit board acts as an interface between all processor board outputs and the external system. It also handles logic and diagnostic box input power.

The following signals are opto-coupled on the board to the outside:

- low gear clutch command (5 to 12 v. level shift)
- high gear clutch command (5 to 12 v. level shift)
- inverter cooling blower command (5 to 12 v. level shift)

Digital buffers are included for FS, FSMLT÷32, and FRIN frequencies monitored in lab test work. Buffers for "charge command" to the inverter and for the serial output to the diagnostic box are also included. For circuit convenience, one input opto-coupler for the incoming diagnostic box data is put on the board.

D. Driver Board

This 2.8 cm x 5.7 cm printed circuit board carries three power Darlington transistors and collector-emitter transient suppressors for low clutch solenoid, high clutch solenoid, and blower drive. The base drive is from the opto-coupler on the output/power supply board via a ribbon cable.

E. Connectors and Harness Assemblies

The processor board has four 26-pin ribbon connector headers. Two headers, P100 and P101, connect with the input board via ribbon cable. The other two, P102 and P103, connect to the output/power supply board.

The input board has two additional discrete wire headers. Connector P303 links the board with an 18-pin Bendix circular connector (S403) on the case. All input signals from points remote from the inverter pass through this connector. Connector P302 passes all input signals from the inverter enclosure.

The output board has five additional headers. Connector P204 passes bridge switching command signals to the inverter. Connector P205 links the board with a 6-pin Bendix circular connector (P405) on the case. All controller and diagnostic power passes through this connector. Also, the auxiliary 12 v. low warning signal enters here. Connector P206 links the board with an 8-pin Bendix circular connector (S406) on the case. All diagnostic box signals and power pass through this connector. Connector P207 links all controller outputs to remote system points to a 19-pin Bendix circular connector (S407) on the case. Connector P208 links the driver board to the output/power supply board. All links between the bulkhead-mount Bendix connectors and the board header are either ribbon or bundled wires. Links between the inverter and controller are discrete

cables which pass through aligning slots between controller and inverter cases and fan out as required in the inverter. The controller mounts on one end of the inverter case.

F. Case

The controller case is seen in Figure 7.2.3. It is a purpose-built aluminum box with internal grooves to hold the three main boards. The driver board mounts on a side to utilize the aluminum plate as a heat sink. Figure 7.2.3(a) is a sketch of the controller case. Figure 7.2.3(b) shows the controller mounted to the inverter. The controller has studs on the bottom face which bolt to the inverter side plate. A gasket is used to help seal the mating surface, since through slots are provided for signal wires between inverter and controller.

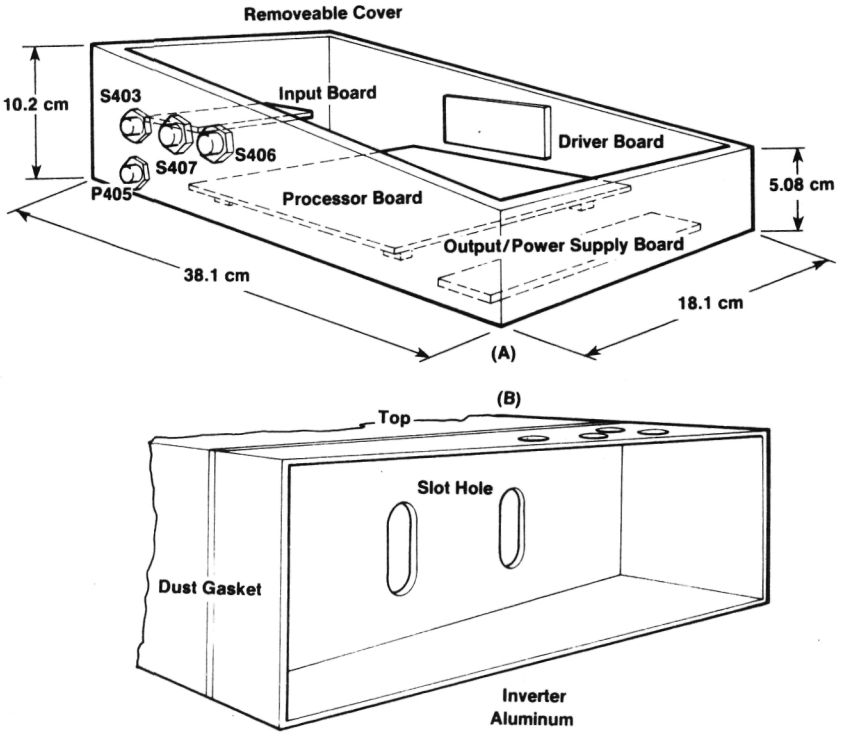

Figure 7.2.3 Controller Case

7.3 Software Description

(Appendix B contains pseudo-code descriptions)

The program is organized into functional blocks called modules. The modules are linked together with chunks of executive code. Figure 7.3.1 shows the overall program

EATON-ERC 26201 NORTHWESTERN HWY SOUTHFIELD, MICHIGAN 48037	TITLE: OVERALL LOGIC FLOW PROJECT: 400406--ELECTRIC VEHICLE AC2PS SHEET: _1 OF _2

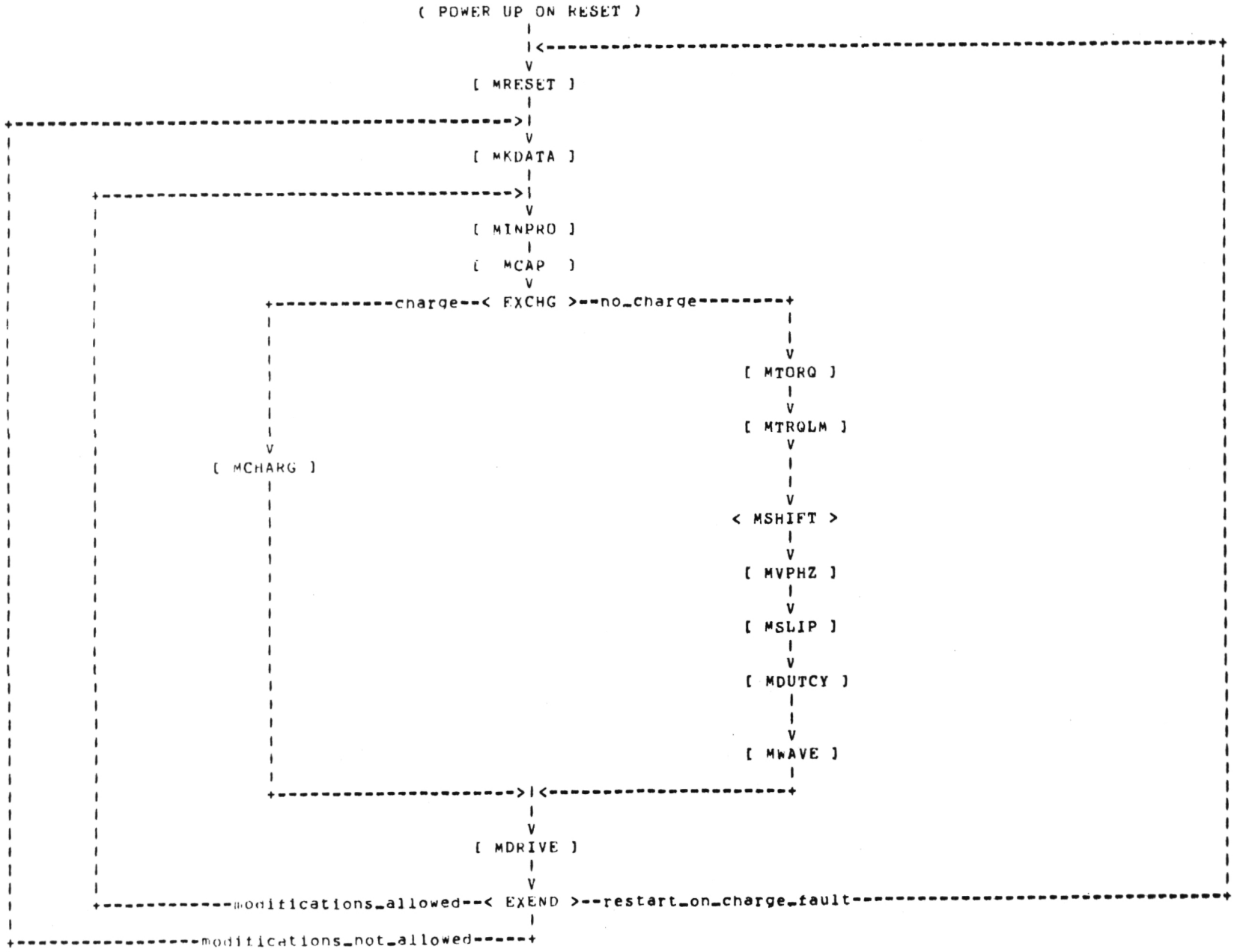

flow. The following discussion will cover each module in turn as depicted in Figure 7.3.1.

After power-up, the watchdog restart circuit resets the MC6801L1 and sets in Motorola "Mode 2" microcomputer configuration. The reset vector puts the program to module MRESET. MRESET initializes ports, does a RAM functional check, sets up internal registers, and exercises all dashboard LED's as a lamp check.

One feature of the diagnostic box is that important constants used in the program can be modified through a keypad as the system is operating. Module MKDATA transfers those constants from EPROM (where they are not modifiable without burning a new EPROM) to RAM (where they can be readily modified any time). The program always accesses the constants from the RAM locations.

MINPRO handles all input acquisition and processing. The digital port and 8 analog channels are read. Each variable is sampled a programmable number of times and averaged. The averaged value is then scaled as required and compared to limits. Appropriate action is taken, depending on the variable, if a limit is exceeded. The diagnostic box can insert a "dummy" value for any input variable upon command. This substitution takes place in this module.

MCAP estimates the battery state of charge. Since no non-volatile memory to store current amp-hours remaining in the battery is available, the hybrid approach of integrating from a state variable starting point was chosen. Exchanging batteries or shutting the system down does not entail resetting the capacity meter. If bus current is less than 4 amps for a specified time, bus voltage is used to compute state of charge. The "open circuit bus voltage" is related to battery capacity remaining. This relationship is nearly independent of temperature for lead-acid batteries. When less than 4 amps are flowing, the voltage is close to the open circuit value. When bus current is equal to or greater than 4 amps, MCAP calculates + or - amp-hours out of or into the battery and updates the accumulation every 10 ms. The net computed amp-hours is continuously added (+ or -) to the capacity determined from the last calculation using "open circuit voltage." The result is modified by electrolyte temperature, quantized to one of seven levels, and sent to the dashboard display to turn on one of seven LED's. MCAP is active during motoring, regeneration, and battery charging.

EXCHG is a linking section which transfers the system to "charge mode" if conditions are proper. The following conditions are needed:

- charge door open
- inverter disabled
- zero motor speed

Further, inverter hardwire interlocks require that the main bridge contactor be off, the key be out of the ignition, and AC input power be present before input voltage can reach the chopper transistor.

If conditions are met, the controller enters MCHARG. A check on input voltage is made. If the voltage has changed (between 110 vac and 220 vac) since the last loop, or MCHARG is being entered initially, a charge start sequence is initiated. A "charge" light on the dash is turned on. After a relay settling delay, a minimum duty cycle waveform is loaded into the Buffer RAM. Section 7.1.-E describes the subsequent MCHARG activity.

Two motoring operating modes are available--"Manual" and "Normal."

"Manual" is implemented in MMANL. It allows independent manual control of slip, duty cycle, and notch number through the diagnostic box. These variables control the torque and current peaks to the motor. Manual mode bypasses the "outer loop" involving operator torque demand, and gives direct access to "inner loop" variables. During lab development, manual mode is essential to map the drive limits and optimize slip-duty cycle scheduling as a function of torque and speed. MMANL is entered initially only if the inverter is disabled, the motor is at rest, and the mode is requested from the diagnostic box. Once in manual mode, exit requires that the inverter is disabled, the motor is at rest, and normal mode is requested. All fault monitoring and diagnostics are available in either mode.

In a vehicle, normal mode is used. Here the input is + or - torque demand, and inner loop variables are determined by the program. MTORQ module modifies operator torque <u>command</u> to yield motor torque <u>demand</u>.

MTORQ starts by checking the accel pedal position. If the pedal is depressed, and the system has just been powered up (a flag bit is set the first executive loop out of MRESET), the inverter is kept disabled. The pedal must be released before the system can be enabled. Next, motor speed is checked. If speed is below a cutoff value (corresponds to vehicle speed of 5 km/hr in low gear) and the accelerator pedal is released, the drive is turned off. If speed is above the cutoff value, the program determines if accel or decel is requested. Decel overrides above a minimum decel value. If neither pedal is pressed, a programmable coast decel command is inserted.

The torque command is then limited as necessary by four temperature roll-off schedules. The most restricting of ambient, heat sink, battery, and motor temperature schedules dominates.

A series of torque roll-off schedules follow for regenerative overvoltage and overcurrent (negative), motoring undervoltage (droop) and overcurrent (positive), and overspeed.

Next, the rate of change of command is checked. If excessive, the rate is limited to a maximum value.

Finally, torque demand is set to zero if the following conditions exist:

- park brake on
- neutral selected
- park latch on

At MTORQ exit, a torque demand is determined. A status word, CWRN, is developed in MTORQ which shows any active limits on torque command. If a limit exists, a "limit" light on the dash is turned on.

MSHIFT handles the gear shift sequencing and forward/reverse control. Upshifts and downshifts are allowed only if motor speed remains below at safe limit. Unlike an ICE vehicle, the shift point need not be modulated by torque demand. Peak torque does not occur at the higher speeds, but remains essentially constant up to 44% of maximum motor speed. From 44% to 100% speed, available torque falls off substantially.

Upon reaching a shift point, MSHIFT starts a timed clutch overlap and overrides torque demand with a programmable value selected so that the motor will reach roughly synchronous speed by the time the oncoming clutch engages. Some slippage is expected.

Upshift and downshift speeds are different to prevent hunting. After an upshift, the same torque demand present before the shift yields less torque at the wheels by the gear step amount. The opposite is true on downshift.

Reverse can be selected only at rest. For reverse, the motor reverses direction and only low gear is allowed. "Low Only" and neutral postions have interlock logic to prevent damage if selected at an inopportune time.

Now the program starts calculating the inner loop variables needed to actually control the inverter switching waveform shape and frequency.

Module MVPHZ calculates the effective motor volts per stator frequency hertz using torque and a predetermined curve:

volts/Hz = (constant 1)(torque demand) + constant 2 = VPHZCH

The schedule is determined by lab tests to give proper stator excitation over the torque range and to maximize efficiency.

VPHZCH is limited to min/max values. The inverter only "sees" the motor terminal voltage. The effective motor excitation voltage is different due to stator resistance voltage drop. During motoring, the effective voltage is less than the terminal voltage. During regeneration (motor is an alternator), the opposite is true. Thus, separate volts/Hz schedules are used for accel and decel. MVPHZ ends with a value, VPHZI, determined.

Module MSLIP determines motor slip frequency from torque demand and VPHZI from the simplified induction motor torque equation:

$$\text{Torque} = (\text{constant})(\text{slip})(\text{VPHZI})^2$$

or

$$\text{Slip} = \frac{(\text{Torque demand})}{(\text{Constant})(\text{VPHZI})^2}$$

A special slip computation is done at low start-up speeds. Smoother start-up occurs if the slip is kept larger than the above formula provides and volts per Hz is modulated to control torque. If stator frequency is below a threshold, the slip is boosted, and VPHZI is adjusted to develop the demand torque.

MSLIP ends with a slip determined, and modified volts per Hz if under start-up conditions.

Now the waveform duty cycle can be computed. The actual waveshape is determined by the duty cycle. MDUTCY calculates duty cycle from the equation:

$$\text{Duty cycle} = \frac{(\text{stator frequency})(\text{volts per Hz})(\text{constant})}{(\text{bus voltage} - \text{bridge drop})}$$

MWAVE uses the duty cycle to calculate the waveform bit pattern for the three phases spaced 120^{o} apart. The modulation algorithm (Appendix C) yields nearly sinusoidal motor currents with minimal harmonic losses over a wide motor voltage range. The three waveforms are concurrently loaded in the buffer RAM. When loading is completed, MWAVE issues a "Buffer RAM Full" signal.

Another variable, notch number, enters in here. This parameter determines the effective inverter chopping rate as it synthesizes the motor waveforms. Through testing, it was found that only one notch number, 24, was needed over the dynamic range. This is so because the waveform algorithm automatically "melts" notches together as speed increases to lower the effective switching rate.

The final module is MDRIVE. This module performs a final check of fault words and a controller status word before enabling the inverter. It also provides some glitch tolerance. A fault must be present for a set number of executive loops before the inverter is disabled. If a shutdown occurs, the "Fail" light on the dash is turned on. Since major inverter faults have fast shutdown circuits independent of the controller, the delay (about 140 ms.) in controller shutdown is tolerable. All diagnostics remain after a shutdown to aid in tracing causes. MDRIVE also updates the controller output latches.

EXEND is a block of executive code which does several functions. It flashes the LED on the processor board to indicate normal cycling. It controls a timer in charge mode which attempts a controller restart if an AC line momentary dropout or glitch tripped out the charger. Restart is attempted eight minutes after a fault trip. If the fault still exists, the system shuts down again. Finally, a "modify flag bit" is tested. The bit is fixed in EPROM, and allows or disallows modification of the various program constants through the diagnostic box. If real-time tampering with the software is to be prohibited, this bit is put to zero when the EPROM is programmed.

The interrupt structure does not show up in the software flowchart, but it is absolutely essential for system operation. Four interrupts are used. Each will now be discussed.

Maskable interrupt, IRQ1, is driven by a 100 Hz oscillator. Thus the IRQ1 routine is executed every 10 ms. The routine first decrements several counters used as timers in the program. Then it performs the amp-hr. accumulation update used in MCAP. Finally it resets and then triggers the FR measure circuit.

Input capture interrupt, ICF, is an internal MC6801 interrupt associated with the 16-bit internal counter/timer. It responds to the "Edge" output of the FR measure circuit (Fig. 7.2.2) and enables the routine to determine the number of internal clock cycles to the timer between the two "Edge" transistions. The routine reads resolution counter RC (see section 7.2-A) and computes rotor frequency. The timing is designed so that every IRQ1 is followed by an ICF before IRQ1 repeats. Therefore, an updated rotor frequency is available every 10 ms.

Output compare interrupt, OCF, is another internal interrupt associated with the internal counter/timer. The OCF routine toggles an output line at a multiple of stator frequency (FSSUB, see Figure 7.1.1). Frequency is determined by the increment added to the output compare register after each counter/register match. The larger the increment, the slower the frequency, since the free running counter is clocked at a fixed frequency. The OCF routine must be very fast since it can be called as fast as once every 300 μsec.

The processor could spend nearly all its time in OCF if the routine approached 300 μsec. Therefore, the routine simply adds the increment to the compare register, sets flags, and returns. The increment value is computed in ICF.

Serial communication interrupt, SCI, is used to link the controller with the diagnostic box. It handles incoming and outgoing data.

The program sets up an interrupt priority as follows:

Top priority	1.	OCF
	2.	IRQ1
	3.	ICF
Bottom priority	4.	SCI

Timing and worst-case execution intervals have been computed to insure no damaging conflicts occur. Worst-case total interrupt overhead to the main program is about 45%. This occurs at 220 Hz rotor frequency.

7.4 Logic Power Supply

This 18.4 cm x 12.1 cm x 5.7 cm aluminum box holds a 12v to 5v DC/DC converter rated at 5a output. The regulated, isolated 5v is the single controller logic voltage. The power supply operates from 11 to 16 volts input and is polarity protected. Input voltage is from the vehicle 12v auxiliary battery which is kept charged by a 14v regulated DC/DC converter working from the main battery.

Also in the box is the low auxiliary battery voltage sense relay. This sensing is important because if the auxiliary battery voltage drops too far due to some fault, the controller could malfunction and shut down in a disorderly way. The voltage sense allows for an operator warning light on the dash to activate well before a malfunction would occur.

The harness to the controller contains the 12v input lines to reference the clutch solenoids, blower, and diagnostic box if connected.

Input current draw without the diagnostic box is typically 0.6a @ 14v. With the diagnostic box, it is 2.2a @ 14v. The blower draws an additional 4a, and each clutch solenoid draws 1a.

The controller is completely electrically isolated from both the 192v traction circuits and the 12v vehicle circuits. Isolation amplifiers, transformers, and optocouplers are used to provide signal and power isolation.

7.5 Diagnostic Computer

A photo of the diagnostic computer box is shown in Figure 7.5.1. This "Diagbox" is a Motorola 6800 microprocessor-based unit used with the controller to display, monitor, and modify controller variables real-time. It has an 80-character alphanumeric display, eight potentiometers for simulated sensor inputs, a hexidecimal keyboard with function buttons and a Manual/Normal select switch, four noncommitted digital-to-analog (DAC) output ports, and an inverter inhibit switch. The diagbox is connected to the controller by a single cable. Communication is a serial 9600 baud link. Power (11 to 16b @ 1.6a) is supplied from the controller. The diagbox is isolated from the 5v. controller logic by optocouplers on the serial data lines. In the test vehicle, an extension cable from the controller is used with a bulkhead connector near the rear seat for easy diagbox connection.

The unit is packaged as a small portable console that will easily ride on an operator's lap in either the front or rear seat. It is approximately 36 cm wide, 28 cm deep, and 25 cm high.

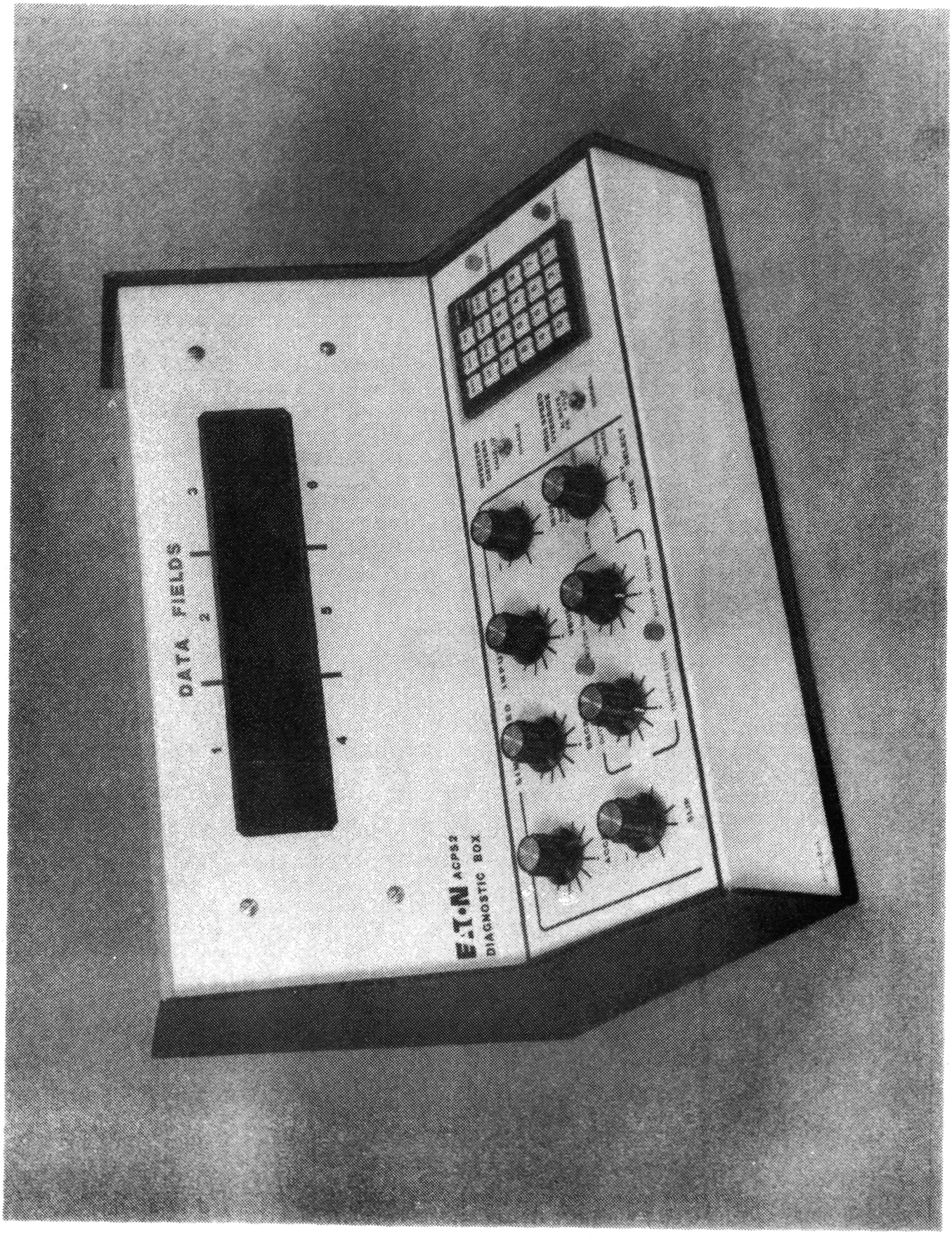

Figure 7.5.1 Diagnostics Computer

The diagbox functions as an engineering tool for design development and testing of controller software and hardware. When "Manual" mode is selected, slip, duty cycle, and waveform notch number are input directly from the diagbox using the appropriate knobs. The values being sent are shown on the display, along with any other four variables requested. Seventy-five controller variables and constants are available for display. The diagbox must be connected to operate in "Manual" mode.

When "Normal" mode is selected, controller algorithms calculate slip and duty cycle from input torque demand. If the box is disconnected, the controller defaults to normal mode upon power-up. In normal mode, the diagbox can monitor up to six variables simultaneously. The selected data is displayed in hexidecimal and decimal format along with its identifying index number. Many critical variables are displayed with proper scaling and units symbols for clarity.

The critical scaling and control constants used in the various software modules are modifiable through the diagbox. Up to 13 constants can be modified at a time. An "M" flashes in front of each modified variable displayed to act as a reminder it has been modified. The original data can be reinstated anytime. This modify feature allows "trimming" of system operation while the system is operating.

For test and debug purposes, all system inputs except one can be simulated by the diagbox. The exception is "charge door" open/closed. This was omitted intentionally since accidental entry into "charge" mode without the hardware interlocks normally present could be damaging. The simulated inputs can be used one at a time or in any combination. Active simulated inputs override the corresponding actual system inputs.

Finally, a function is provided to change a variable from a digital word (0 - FF_H) to an equivalent voltage (0 -2.55V) through a DAC. Up to four variables can be monitored or recorded as analog output from four BNC connectors on the diagbox. Update rate is around 50 Hz, which is sufficient for almost all variables of interest.

Two diagbox units were built.

7.6 Lab Test Results

A series of test were run on the controller alone in the lab to verify function. These tests did not include environmental tests.

Stator Frequency Generator

The most critical accuracy requirement concerns the stator frequency generator circuit. Stator frequency range is 1 to 216 Hz. The slip range is $\pm$4 Hz (the controller has a $\pm$8 Hz dynamic slip range to give plenty of margin). For smooth control, slip resolution and accuracy should be held to at least 0.1% of maximum stator frequency. By design, the controller holds slip resolution to 0.062 Hz over the entire speed range. A precision frequency generator and counter were used to verify the rotor frequency measurement circuit and the companion FSSUB frequency generator. Worst-case overall measured error in stator frequency from the ideal was 0.08%. Usually the error is less than 0.05%, but at certain frequencies digital trunctation errors peak. The benefit of a digital approach is clear, since accuracy is locked in and will not drift. No adjustment or calibration is needed.

The multiplying phase lock loop used to create FSMLT (Figure 7.1.1) dominates slip loop response. The PLL filter was adjusted to attenuate rotor frequency jitter, but still provide adequate response for vehicle dynamics and stability. The final parameters are

Natural frequency W_n = 66 rad/sec
Damping constant = 1.1

Settling time $T_s = \frac{4}{W_n} = .06$ sec.

Simulated rotor input tests verified that the input sensor amplifier and all stator frequency circuits can lock on to rotor frequency from 2 to 250 Hz. The 2 Hz low limit is permissible since start-up slip is always programmed greater than 2 Hz.

Analog Inputs

Table 7.6.1 summarizes the performance of the eight analog input channels. Bus current, IBUS, is the only input needing relatively high accuracy below 30 a, since the battery charging routine relies on IBUS for feedback control. The scaling is set for maximum + and -motoring and regeneration currents, but full-scale charging currents are only 8% of those. Bus voltage, VBUS, is used in determining waveform duty cycle and in the charge mode routine. All eight inputs are used as limiters on torque and system shutdown triggers if any inputs become excessive. Since temperature inputs are influential only in abnormal conditions, the rather crude accuracy is acceptable. Once digitized, input variable accuracy experiences negligible degradation due to digital processing.

All trim pots were run end to end to check for adequate adjustment range and settability.

Digital Inputs

The eight quasi-static digital status lines (see Table 7.2.1) were all exercised to assure proper input to the controller. The diagbox can monitor the RAM image of the input port.

TABLE 7.6.1

ANALOG INPUT PERFORMANCE

INPUT VARIABLE	MNEUMONIC	UNITS	ACTIVE RANGE	RESOLUTION	MEASURED ACCURACY OVER RANGE	SENSOR	COMMENT
Battery bus voltage	VBUS	Volts	100 to 250	2	±2V	Resister divider	Cal. trim pots for zero and span on isolator amplifier in inverter
Battery bus current	IBUS	Amps	-200 to +250	2	±4a*	Hall effect sensor	Cal. at Hall sensor amplifier and offset adj. on Controller Input board
Accel demand	VACCEL	% of rated	0 to 198	2	-	Pot on accel pedal	Accuracy not critical. Conductive plastic pot. element for life, resolution
Decel demand	VDECEL	% of rated	0 to 198	2	-	Pot on brake pedal	Conductive plastic pot element
Ambient temperature	AMBTP	°C	o to 70	2	±3°C	Nat. LM235 sensor	Solid-state sensor. 10mv/°C located in controller box
Battery electrolyte temperature	BATTP	°C	0 to 70	2	+0°C -4°C	Nat. LM235 sensor	Sealed Teflon tube houses sensor and emersed in battery electrolyte of selected center cell of front vehicle pack
Inverter heat sink temperature	HSTP	°C	0 to 120	2	±3°C	Nat. LM235 sensor	Electrically isolated. Mounted rear #1¢ bridge transistors
Motor stator temperature	MOTTP	°C	160 to 190	2	±5°C	Fenwal KT41J3 thermister	Span trim pot on input board. Cal at 180°C. Linearized

* at constant temperature

Rotor pulse pickup sensitivity was measured at 100 mv peak-to-peak @ 10 Hz. The Electro Model 3015HTB magnetic pickup gaped at 0.25 mm to a steel 60-tooth wheel has at least 180 mv peak-to-peak at that speed, providing adequate margin. At higher speeds, pickup output is very large and a voltage clipper and frequency roll-off characteristic on the input circuit protects the amplifier and reduces stray high frequency noise. The pickup circuit was tested to assure a clean, square wave output over a 0.5 to 220 Hz rotor frequency range.

Digital Outputs

All digital outputs (see Table 7.2.1) were exercised by diagbox commands. Most signals are low level logic and were tested with actual loads to assure integrity. The three 12v power control lines (high and low clutch solenoids @ 1a, cooling blower @ 4.5a) were checked under load to assure adequate drive and heat sinking of the power transistors. The 3Ø switching command lines were examined very closely for glitches or false bits. The waveforms were clean with rise and fall times under 2 μs.

Processor Board Logic and Voltage

The 5v power plane was checked at 12 places over the board and found to be constant within 40 mv and have a worse case spike ripple of 120 mv peak-to-peak. RMS ripple was well under 30 mv. The spikes on the 5v net are primarily due to the DC/DC converter transformer power supply.

All important internal clock frequencies, pulse widths, and phase timing were checked and found acceptable. Microcomputer data and address buses were checked for proper TTL and/or CMOS levels.

Stability over time (checked over about 2 months) of the 5.00v analog reference voltage was 2 mv. The represents 0.1 of an ADC increment. Measured temperature sensitivity over a 5^{o}C to 70^{o}C range was 0.3 mv/^{o}C, or one ADC increment over the range.

Software Verification

Each software module was checked using the diagbox and simulated inputs where necessary. Some modules were simulated on a main frame computer for detailed examination of output (e.g., MWAVE). System operation, of course, is an excellent overall test in itself.

The following summarizes checkout data collected in the lab on various modules.

MCHARG: Charge mode operates in current limit until a critical battery voltage, VBUSCR, is achieved. VBUSCR is a function of battery electrolyte temperature, BATTPF. When VBUSCR is reached, the charger operates in constant voltage mode. Figure 7.6.1a plots the VBUSCR vs BATTPF curve used. (192v nominal bus voltage)

Three temperatures can limit maximum charge current: ambient, heatsink, and battery. Figures 7.6.1b, c, d show these roll-off curves. MXICH is the maximum average charge current allowed into the battery. Overriding fixed maximum current limits apply to Figures 7.6.1b, c, d, but they do not show up on the curves. KI110 is maximum current @ 110 VAC input. KI220 is maximum current @ 220 VAC input. These values limit MXICH regardless of any temperature. The controller follows there curves within 14%. Bus current resolution limits accuracy.

MTORQ: Commanded motor torque is limited by nine roll-off curves. The most restrictive curve dominates. Figures 7.6.1e, f, g, h, show maximum torque allowed vs. ambient, heatsink, battery, and motor stator temperatures respectively.

Figure 7.6.1j shows the torque roll-off curve for excessive bus voltage VBUS. This curve is active during regen (decel, braking) if the batteries are highly charged.

Figure 7.6.1k shows the torque roll-off curve for deficient bus voltage VBUS. If the batteries droop too far during motoring, this schedule limits torque to prevent voltage from decaying further.

Figure 7.6.1l shows the torque roll-off curve for excessive negative battery current (IBUS) encountered during regen.

Figure 7.6.1m shows the torque roll-off curve for excessive positive battery current encountered during motoring.

Allowable torque is reduced if a motor overspeed is detected. Figure 7.6.1n shows this schedule.

All input parameters are filtered and averaged in MINPRO to reduce jitter which could cause objectionable torque pulsations if a limit curve were active.

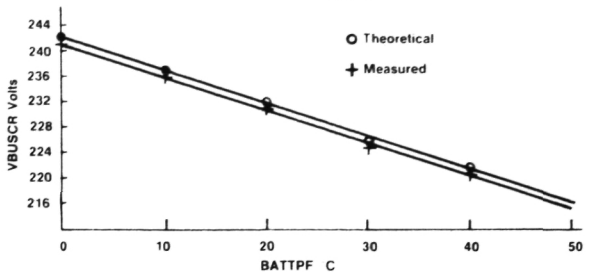

Figure 7.6.1a VBUSCR Vs. BATTPF

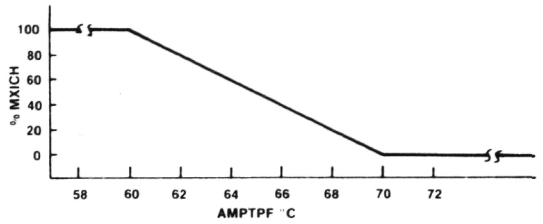

Figure 7.6.1b % MXICH Vs. Ambient Temp. AMPTPF

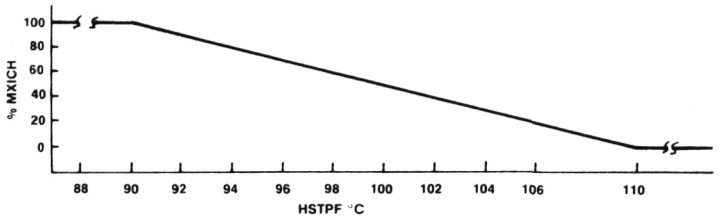

Figure 7.6.1c % MXICH Vs. Inverter Heat Sink Temp. HSTPF

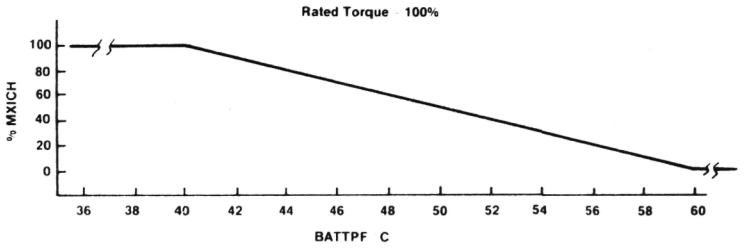

Figure 7.6.1d % MXICH Vs. Battery Electrolyte Temp. BATTPF

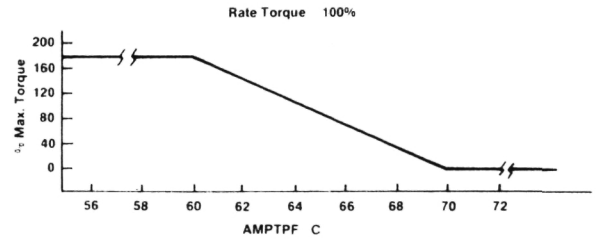

Figure 7.6.1e % Max. Torque Allowed Vs. Ambient Temp. AMBTPF

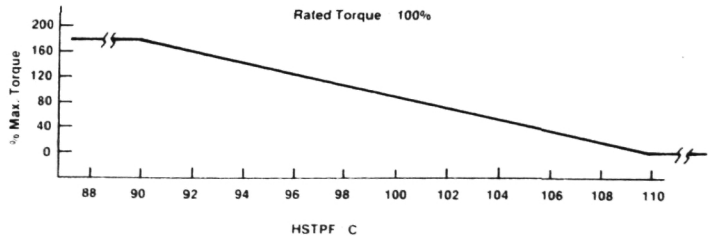

Figure 7.6.1f % Max. Torque Allowed Vs. Heat Sink Temp. HSTPF

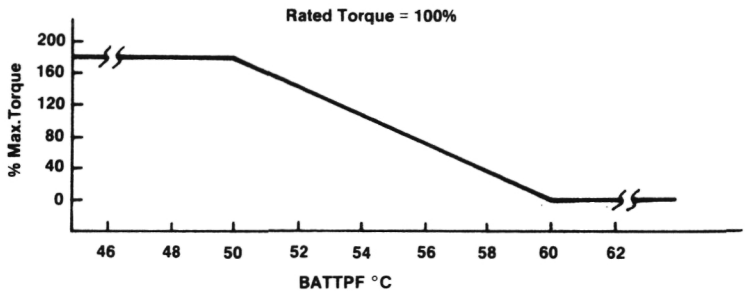

Figure 7.6.1g % Max. Torque Allowed Vs. Battery Temp. BATTPF

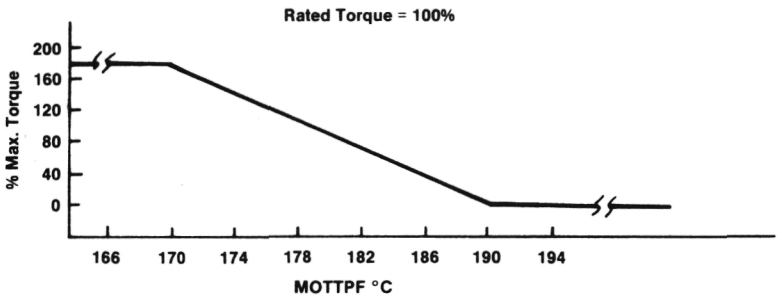

Figure 7.6.1h % Max. Torque Allowed Vs. Motor Temp. MOTTPF

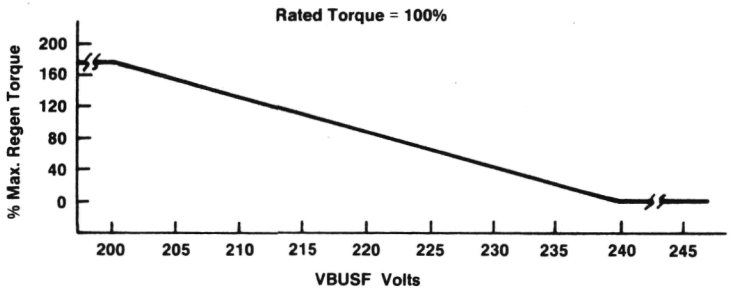

Figure 7.6.1j % Max. Regen Torque Allowed Vs. VBUSF Volts

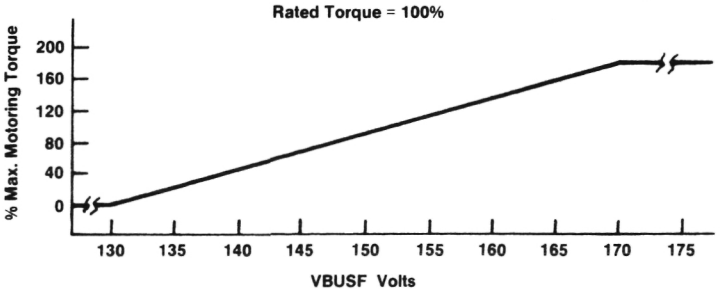

Figure 7.6.1k % Max. Motoring Torque Allowed Vs. VBUSF Volts

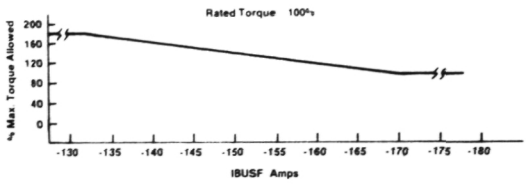

Figure 7.6.1l % Max. Torque Allowed Vs. BUS amps Regen

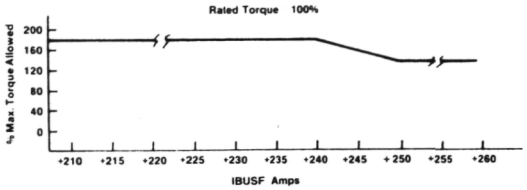

Figure 7.6.1m % Max. Torque Allowed Vs. BUS amps Motoring

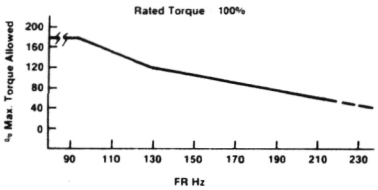

Figure 7.6.1n % Max. Torque Allowed Vs. Rotor Frequency FR

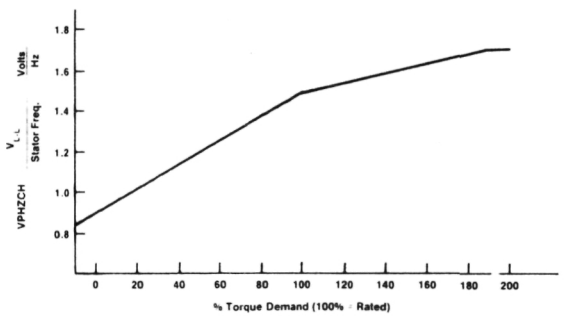

Figure 7.6.1o Motoring Chart Volts per Hz Vs. Torque Demand

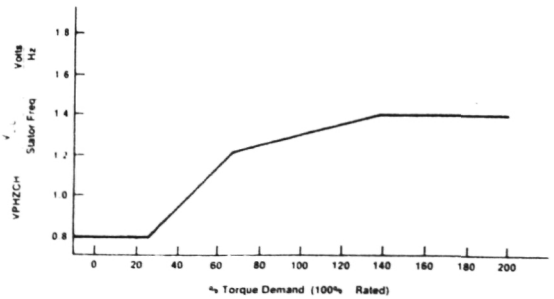

Figure 7.6.1p Regen Chart Volts per Hz Vs. % Torque Demand

MVPHZ: The initial motor volts per Hz value is determined as a function of torque demand. The curves shown in Figures 7.6.1o and 7.6.1p for motoring and regenerating were determined from empirical system tests to optimize efficiency. The routine follows this curve to obtain an initial volts per Hz value called "chart" VPHZ, or VPHZCH. This curve is used during motoring when motor terminal voltage is higher than the "effective motor voltage" due to stator voltage drop.

MSLIP: A special volts per Hz/slip calculation is done during motor start-up from rest. At very slow rotor speeds (present transiently during startup), the PLL stator frequency circuit is unstable. Further, steps in volts per Hz are coarse because the frequency is near zero. Finally, stator resistance is more prominent since little counter EMF is being generated. This requires a volts per Hz boost.

During startup the minimum stator frequency is at 3Hz and the duty cycle is set at 4%. These values are allowed to increase as the motor speeds up. A digital filter inserted in the duty cycle calculation keeps the motor flux from changing abruptly in this region.

In summary, the following sequence determines the motor parameters duty cycle and slip:

- Torque demand is determined from input torque command.
- Motor excitation volts per hertz (VPHZ) is determined from a schedule of VPHZ vs. torque command.
- Slip is determined from VPHZ and torque demand. Scaling yields optimum slip values determined from lab tests.
- Waveform duty cycle is determined from VPHZ and bus voltage. Duty cycle translates a desired motor VPHZ into a waveshape which can yield that value. The duty cycle calculation is scaled so that it yields optimum values as determined from lab tests.

As shown in section 6.4, the highest efficiency points of the motor/inverter system do not require precise slip/duty cycle pairings. Efficiency suffers if the pairings deviate 10 to 20% from optimum. This tolerance eases the accuracy requirement of the VPHZ, slip, and duty cycle routines.

Every branch in the program as reflected in the code of Appendix B has been exercised. Table 7.6.2 lists the various limit values used in the software as of March 31, 1983.

8.0 VEHICLE

8.1 Vehicle Selection Rationale

In addition to demonstrating the feasibility of an AC propulsion system, it was desired through the implementation of a vehicle conversion to demonstrate a practical vehicle with utility and safety generally comparable with its internal combustion engine counterpart. For accessibility of pertinent design information necessary to make the conversion, a domestic vehicle was preferred.

A number of preliminary objectives were established for the conversion vehicle. These are summarized in Figure 8.1.1. Overlaying these objectives on the characteristics of domestic vehicles yielded two prime candidates. These were the Omni/Horizon vehicles produced by Chrysler Corporation, and the Escort/Lynx vehicles produced by Ford Motor Company.

Preliminary battery packaging studies were conducted on both vehicles. While packaging sixteen traction batteries was deemed feasible for both vehicles, the Escort offered slightly greater space and packaging flexibility. With the Escort, it was deemed feasible to have identical battery packs in the front and rear of the vehicle and to have all batteries within each pack on a single elevation. This reduced the cost of the battery packs, improved the overall vehicle serviceability, and simplified the ventilation system for the battery packs themselves.

A second important criteria was vehicle weight. Figure 8.1.2 compares the weight of the Escort/Lynx with the Omni/Horizon. Although the production vehicles are almost equivalent in weight, the Ford powerplant is somewhat heavier than Chrysler's. Subtracting out the weight of the powerplant and the spare tire yields a 123 lb. weight advantage for the Escort/Lynx vehicles.

It was assumed that comparable cooperation could be achieved with Ford or Chrysler in supplying needed design and engineering information to assist with the conversion process. However, based on the weight advantage and the improved battery packaging flexibility, the Escort/Lynx vehicle was selected.

8.2 Mechanical Modifications by Subcontractor (Triad Engineering)

The program concept called for packaging of an Eaton designed front wheel drive power train together with two battery packs, each containing eight EV 800 batteries, with provision for using EV 1300 batteries should they be available.

Structural bogies for the vehicles were established as being equivalent to the base Lynx vehicle in bending stiffness and cashworthiness with added structure to carry the additional loading induced by the battery packs.

Certain other structural modifications would be required as a result of changes to the rear suspension.

Ride and Handling requirements were specified as being comparable to the base vehicle.

FIGURE 8.1.1

PRELIMINARY SPECIFICATION OF PROPOSED TEST VEHICLES

PARAMETER	OBJECTIVE
1. Vehicle Type	Sedan - Compact 2 or 4 door
2. Seating Capacity	Maintain existing four passenger arrangement
3. Maximum Curb Weight: - vehicle without batteries and propulsion - total vehicle (improved lead acid) - total vehicle (EV-800 batteries)	 1600# 3400# 3050#
4. Weight Distribution Range	50% front, 50% rear to 62% front, 38% rear
5. Driving Wheels	Front
6. Propulsion	Solid state inverter driving 25 hp AC motor
7. Drivetrain	Two-speed transaxle (automatic)
8. Tire Size	P165 R13 radial or eliptical section with equivalent rolling radius
9. Rolling Resistance, lb/lb	.011 maximum
10. Spare Tire	Not required
11. Payload (passenger and luggage)	700 lbs
12. Ride Frequency with Two Front Seated Passengers (300#)	1.20 Hz front, 1.30 Hz rear
13. Handling	Similar to current production ICE powered vehicles
14. Brakes	- Regenerative through drive wheels - 30 Hp maximum - Disc front, drum rear foundation brakes - Adaptive control system to modulate above - Braking performance meeting current FMVSS 105-75 requirements is desired

FIGURE 8.1.1

PARAMETER	OBJECTIVE
15. Battery Requirements	14 to 16 traction batteries and one service battery with flexibility for either of the following: Improved Lead Acid (for traction only) 10.8"H x 7.4"W x 12.7"L x 75# per battery Globe Union EV-800 8.9"H x 6.8"W x 12.7"L x 54# battery
16. Heater	Gasoline fired liquid heater and circulation pump to circulate fluid through existing heater core. Air distribution and window defrost will be standard production hardware with the possible exception of the heater blower
17. Motor Cooling	Ram air directed over motor/transaxle assembly
18. Crash Integrity	Vehicle not required to pass specific crash tests. Design analysis will show consideration for retention loads on battery hold-downs and containment of acid outside of passenger compartment
19. Bumpers	Production energy-absorbing bumpers will be used but not altered for increased GVW
20. Vehicle Finish	All internal and external surfaces to be generally consistent as far as possible with current production vehicle standards. All mechanical modifications to be documented with detail drawings.
21. Driver Instrumentation	State of charge, auxiliary battery voltage, propulsion system status indicator lights.
22. Air Conditioning	Not planned
23. Power Steering	Not planned

FIGURE 8.1.2

WEIGHT COMPARISON

	ESCORT/LYNX*	OMNI/HORISON**
Curb Weight	2,140 lb	2,154 lb
Power Plant		
Engine/transaxle	499	366
Cooling system	31	25
Exhaust system	38	26
Fuel system	52	97
Subtotal	620 lb	514 lb
Spare tire	31 lb	28 lb
Body shell weight w/interior	1,489 lb	1,612 lb

*Based on actual weights

**Based on published weights

Vehicle System Design Optimization Study
by J. L. Gilmour, April 1980
JPL Contract No. 955498

8.2.1 **Weight Distribution Analysis**
Base Vehicle

Curb Weight Condition (Actual weight of Vehicle "b")
WR_C = 1400 lb.
WR_C = 740 lb.
Design Weight Condition (Design = Curb + pass. + 50 lb. luggage)

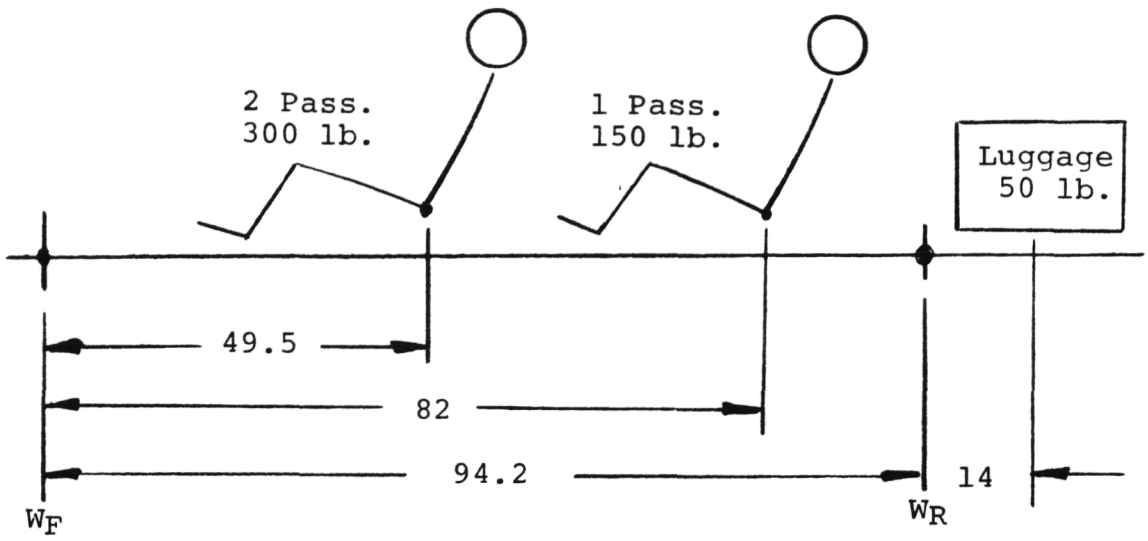

Figure 8.2.1 Diagram of Weight Distribution

Design Wt. = 2140 + 450 + 50 = 2640 lb.

$$\text{Distribution } W_R + \frac{(300 \times 49.5)+(150 \times 82)+(50 \times 108)}{94} = 740$$

WR_d = 1086
WF_d = 1554
GVWR (Design + 1 pass. + 50 lb. luggage)
GVWR = 2640 + 150 + 50 = 2840
Distribution:

$$WR - \frac{(150 \times 82) + (50 + 108)}{94} = 1086$$

WR_G = 1274 lb.
WF_G = 1566 lb.

ELECTRIC LYNX

Differential for Base Vehicle (lb.)

Delete	Total	Front	Rear
Exhaust	38	19	19
Cooling	31	36	-5
Engine	323	346	-23
Transmission	176	176	0
Fuel	52	7	45
Spare Wheel & Tools	31	-4	35
Rear Suspension	61	2	59
Body Parts	12	7	5
Heater	2	2	0
Total	726	591	135
Add			
Motor and Transmission	210	225	-15
Batteries Front (EV130) (1)*	600	648	-48
Batteries Rear (EV 1300) (1)*	600	-102	702
Battery Box Front	40	43	-3
Battery Box Rear	40	-7	47
Converter	100	13	87
Heater & Tank & Fuel	24	22	2
Ducting & Blower	5	4	1
Structure	40	25	15
Wire & Connectors	30	15	15
Rear Suspension	100	1	99
Total	1789	887	902

Curb = 2140 - 726 + 1789 = 3203 (2)

Design = 3203 + 500 = 3703

GVWR = 3703 + 200 = 3903

Distribution

	Total	Front	Rear
Curb	3203	1696	1507
Design	3703	1850	1853
GVWR	3903	1862	2041

*NOTE: Numbers in brackets () refer to explanatory notes in Appendix E

UNSPRUNG WEIGHT

Front (Production Lynx and Electric)

	Total Weight	Unsprung Weight
Lower Control Arm	3.6	1.8
Strut	20.8	17.0
Hub	3.7	3.7
Caliper	6.7	6.7
Disc	9.9	9.9
Wheel and Tire	31.2	31.2
Drive Axle	9.5	4.0
Spring	4.5	2.3
Stab. Bar	13.4	2.0
Total (per side)		78.6 lb.
Total		157.2 lb.

Rear (Production Lynx)

	Total Weight	Unsprung Weight
Wheel and Tire - 2	62.4	62.4
Brake Assembly - 2	12.0	12.0
Drum & Hub Assembly - 2	22.0	22.0
Control Arm - 2	19.0	9.5
Spring - 2	11.0	5.5
Shock Strut - 2	13.0	11.0
Trailing Arm - 2	7.0	3.5
Total		125.9

Rear Electric Lynx)

	Total Weight	Unsprung Weight
Wheel and Tire - 2	62.4	62.4
Brake - 2	14.0	14.0
Brake Drum - 2	11.0	11.0
Axle	45.6	40.0
Track Bar	3.81	1.20
Spring - 2	18.0	6.0
Hub and Bearing	10.5	10.5
Shock Absorber - 2	6.5	4.0
Total		149.1

SPRUNG WEIGHT COMPARISON WITH EV 1300 BATTERIES

	Production	Electric	% Change
Curb - Total	1857	2897	+ 56
Front	1243	1539	+ 24
Rear	614	1358	+121
Design - Total	2358	3397	+ 44
Front	1397	1693	+ 21
Rear	961	1704	+ 77
GVW - Total	2557	3597	+ 41
Front	1409	1705	+ 21
Rear	1148	1892	+ 65

SPRUNG WEIGHT COMPARISON WITH EV 800 BATTERIES

	Production	Electric	% Change
Curb - Total	1857	2513	+ 35
Front	1243	1336	+ 7
Rear	614	1177	+ 92
Design - Total	2358	3013	+ 28
Front	1397	1488	+ 7
Rear	961	1525	+ 59
GVW - Total	2557	3213	+ 26
Front	1409	1500	+ 6
Rear	1148	1713	+ 49

Figure 8.2.2 Front End, Right Side Structural Modification

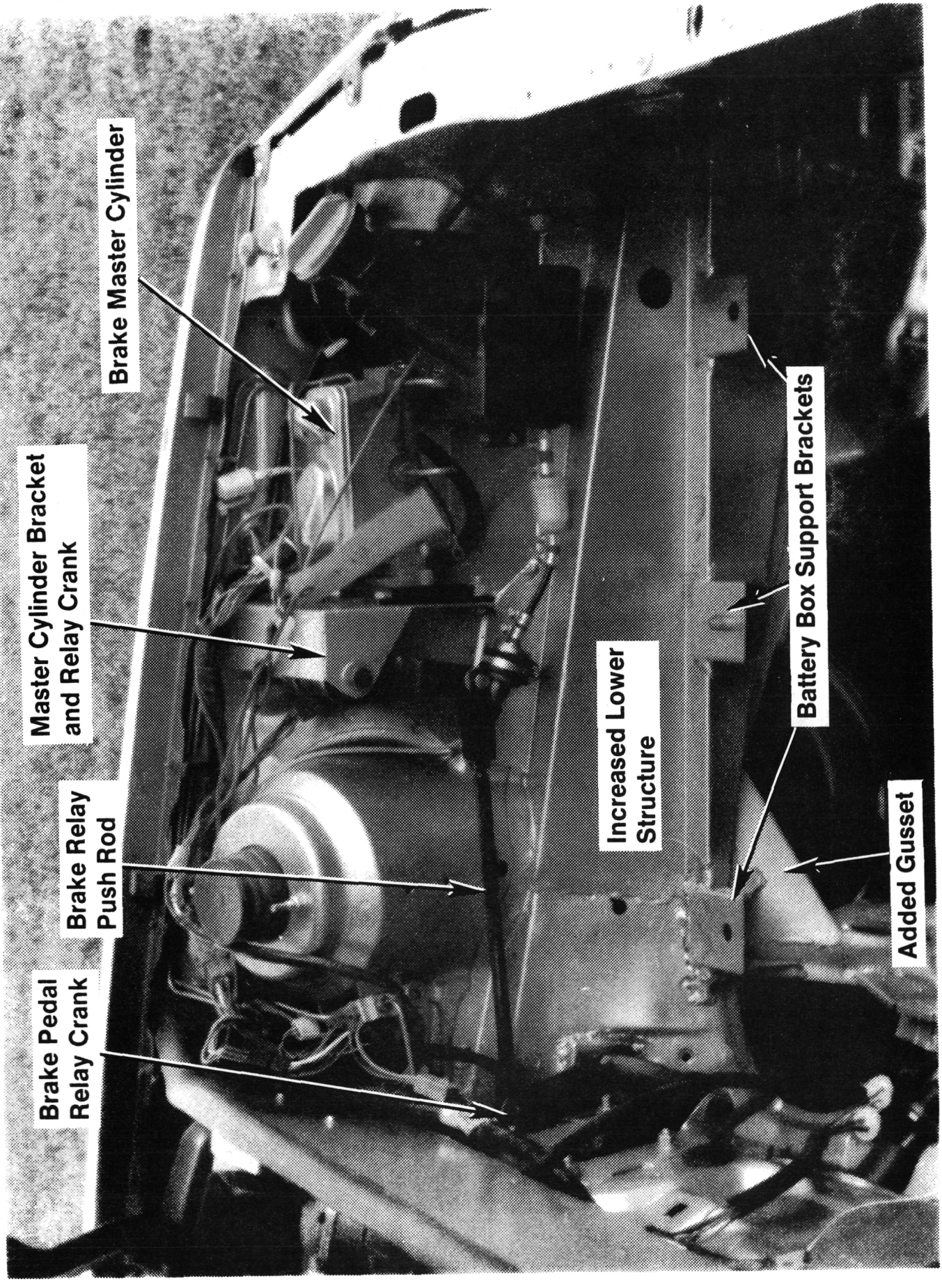

Figure 8.2.3 Front End, Left Structual Modification

8.2.2 Structural Considerations

The vehicle structure was treated as two separate units, dash panel forward and rear seat kick up rearward. After this the total vehicle was studied in a beaming stiffness mode.

8.2.2.1 Front End

The front end weight of the electric version increased only 148 lb. per side over the base vehicle as received. The base vehicle is, however, available with power brakes, power steering, air conditioning, etc., which will reduce the weight increase over the max GVW of the Lynx model. The axial loading in an impact mode, however, increases with the total vehicle load, not only front end loading. The assumption was made that the structure modifications required to absorb the energy at the desired rate would also handle the vertical and lateral load increases. See Figures 8.2.2 and 8.2.3.

Impact Analysis
Assumptions

- The lower structural beams absorb 50% of the total energy.
- Front battery pack will break away and dissipate its energy into the barrier. (This has been witnessed on other vehicle program barrier tests.)
- The electric motor and transmission will act in a similar way as the heat engine would and will dissipate its energy into the barrier.

Vehicle Mass

To decelerate the vehicle in the same distance as the production vehicle the structure stiffness must be increased proportionally to the mass to be stopped.

Mass to be stopped after battery pack and drive has contacted barrier is:

Production Vehicle - Design Wt.	2640	
Less - Engine & Trans.	470	
	2170	lb.
Electric Vehicle - Design Wt.	3703	
Less - Frt. Batt. Pk.	640	
Less - Motor & Trans.	210	
	2853	lb.

Mass Increase - 2853 - 2170 = 683 lb.

Proportion of mass handled by upper and lower structure in the production vehicle is 2170 x 0.50 = 1085 lb. each.

Therefore, lower structure in the electric vehicle must carry 1085 + 683 = 1768 lb.

Increase Ratio $\frac{1768}{1085} = 1.63$

Energy Absorption

The specific energy absorption of a beam is dependent upon the volume of material. The volume is proportional to the cross section area.

CSA of Production Beam = 1.65 in^2
CSA of Modified Beam = 2.62 in^2

These areas were measured from the layout (54646-R) @ sect. 1600 mm

Increase Ratio $\frac{2.62}{1.65} = 1.59$ (acceptable)

Buckling Load

The critical load for a beam is obtained from:

$$P/A = S_y - C_3 (L/k)^2 \quad (3)$$

where P = critical load
A = CSA
S_y & C_3 = constants obtained from imperical data for structural steel with a safety factor and the type of beam end restraint (Ref. Mechanics of Materials; Higdon, Ohlsen, Stiles Page 350-351.
L = length to spring tower
k = radius of gyration of section @ sect. 1600 (these were obtained by computer analysis).

therefore P for the production version = 24,120 lb.

and P for modified version = 40,129 lb.
Increase ratio = 1.66 (acceptable)

Passenger Compartment Intrusion

The crush length of a production Lynx is established at 24 inches (this length allows the proposed FMVSS 208 to be met for deceleration levels and is the target distance for most manufacturers).(Appendix E) As the length from the front of the vehicle to the

dash panel is 40.75 inches, the distance from the barrier to the dash panel after impact is 16.75 inches.

From previous programs batteries are known to crush approximately 1/3 of their length from their own inertia;(Appendix E) therefore, the battery box length after impact can be calculated as:

$$L_B = (12.56 \times 2 \times \frac{2}{3} + (0.1 \times 2) + 0.50) = 17.44^{(6)}$$

It can be seen, therefore, that the battery pack will depress the dash panel by 0.69". In a dynamic condition an additional two inches of deformation can be expected(Appendix E). However, the additional 2.69" intrusion is unlikely to separate the panel joints or to damage the windshield. Dash panel deformation of 10 inches has been observed in some vehicles.

8.2.2.2 Rear End

The rear end of the vehicle required changes to accomplish not only the packaging of the battery pack but also the change from an independent rear suspension to a beam axle type. The suspension change did not drastically alter the location of the load input to the structure; however, many changes were required to provide clearances to the various axle locating members. It was, therefore, considered that the forces induced by the suspension would be increased by the ratio of the vehicle weight and that the floor structure should be increased by the same ratio.

The battery pack induced loads are reacted by the entire rear end of the vehicle; however, the rear floor contributes at least 70% of the structure due to the hatchback configuration.

Analysis
Suspension Induced Loading

Rear end sprung weight increase is 65% @ GVW (section 8.2.1). Moment of inertia of production Lynx main longitudinal structure member is 1.2437 (computer calculated).

The moment of inertia required for the same stiffness is:

$$1.2437 \times 1.65 = 2.052$$

The section of the beam was increased from 2.50" deep to 3.50". This increases the moment of inertia by

2.744 times, resulting in an I of 3.413, which is more than required.

Battery Pack Induced Loading

The static deflection of the rear structure with the battery box installed can be approximated as shown.

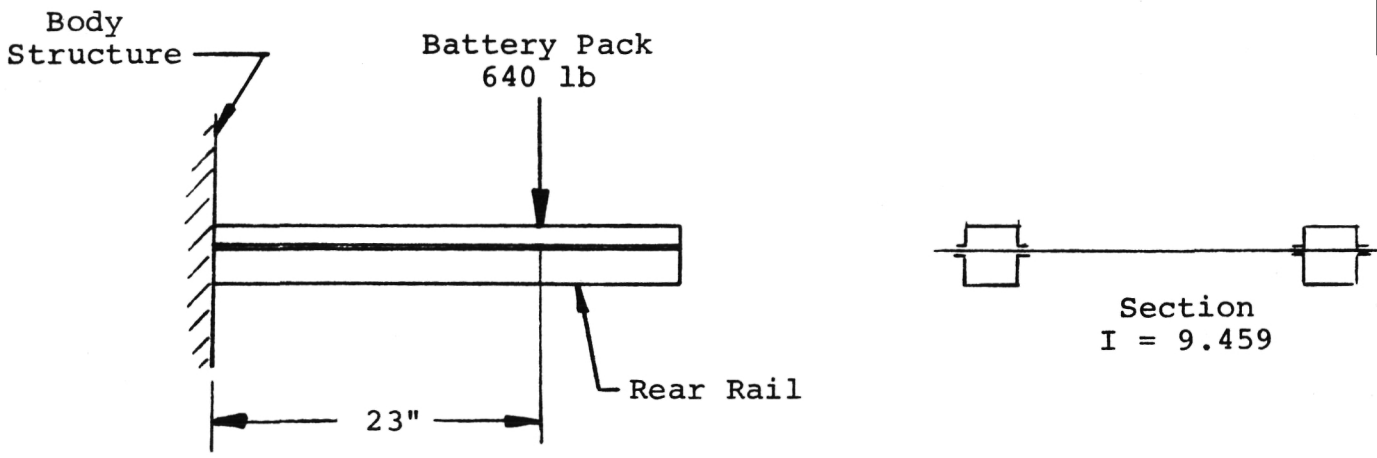

Figure 8.2.4 Battery Pack Induced Loading Diagram

$$I \text{ for total vehicle} = \frac{9.459}{0.7} = 13.51^{(9)}$$

deflection at point of load is y

$$y = \frac{Pl^3}{3EI}$$

$$= \frac{640 \times 23^3}{3 \times 30 \times 10^6 \times 13.51}$$

$$= 0.006$$

Dynamically (3_g loading) the deflection will be 0.018". This is considered to be acceptable.

Behavior of Rear Battery Pack Upon Impact
Frontal Impact

At 30_g deceleration the battery box will exert a force of 19200 lb. into its attachments. (For EV 1300 batteries.) The worst condition occurs if the attachments are loose and no clamping action is available. The bolts and locating pins will sheer under these conditions; however, the supports are set in channels which will prevent movement. See Figure 8.2.5. The box is again riveted to the channel

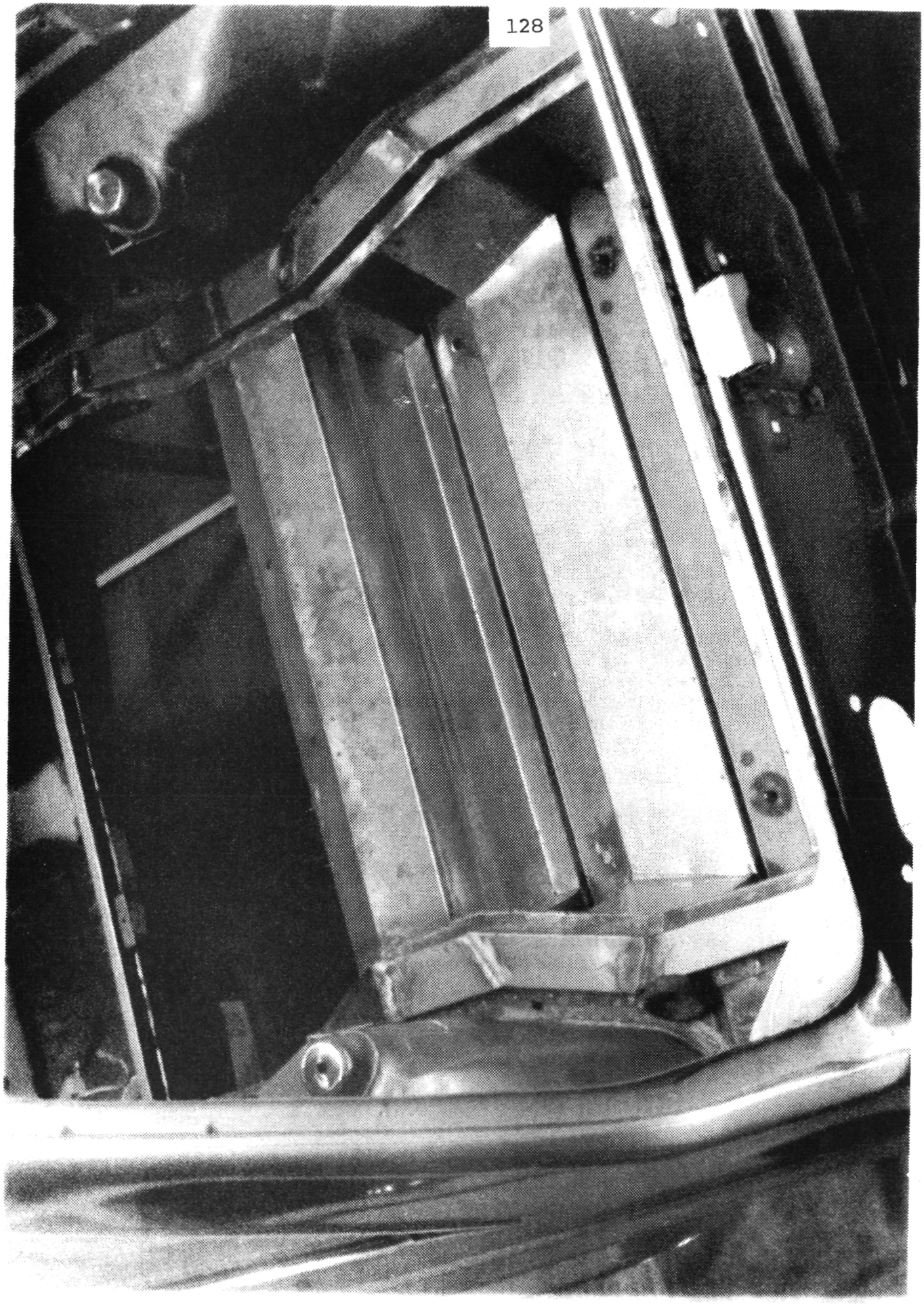

Figure 8.2.5 Rear Battery Box Supports

supports with 66 rivets of 0.18 dia., these rivets will not shear under the applied load. It can, therefore, be assumed that the box will not move from its location.

Rear Impact

In order to protect the vehicle occupants from injury from acid during a rear impact, the following action has been taken.

- The rear structure has been increased to decrease the amount of deformation.
- The batteries are in a sealed box.
- The box is in a covered compartment in the vehicle trunk.
- The trunk cover has been retained to provide an additional barrier.

We believe this to be sufficient protection for the occupants eyes from acid injury.

8.2.2.3 Total Vehicle

The bending stiffness of the total vehicle was studied by separating the vehicle into major components with the remainder taken as a uniform distributed load. The loading and bending moment diagrams are shown in Figure 8.2.6.

It can be seen that the center section of the body is loaded less in the electric version than for the production Lynx. Therefore, no changes were made in this area.

The large increase in bending moment takes place at the center lines of the wheels. These areas have been discussed in Sections 8.2.1 and 8.2.2.

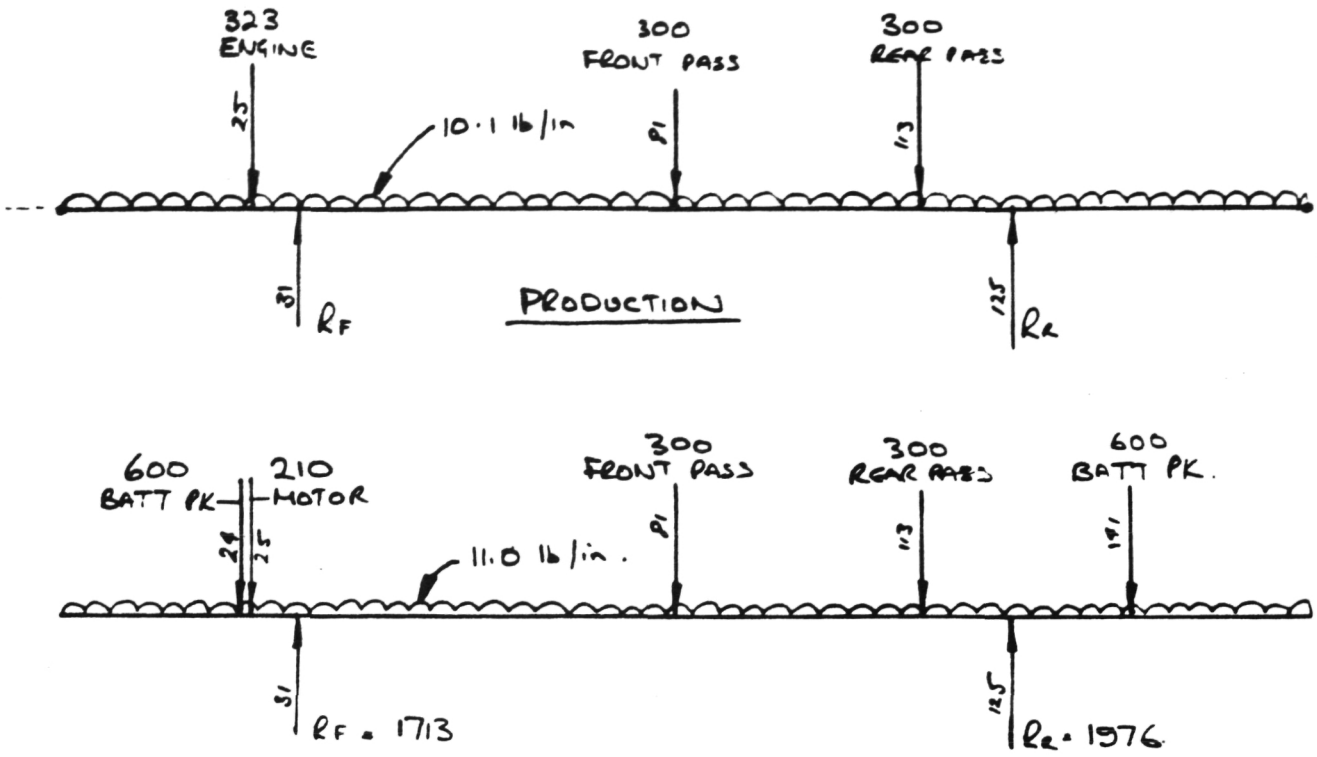

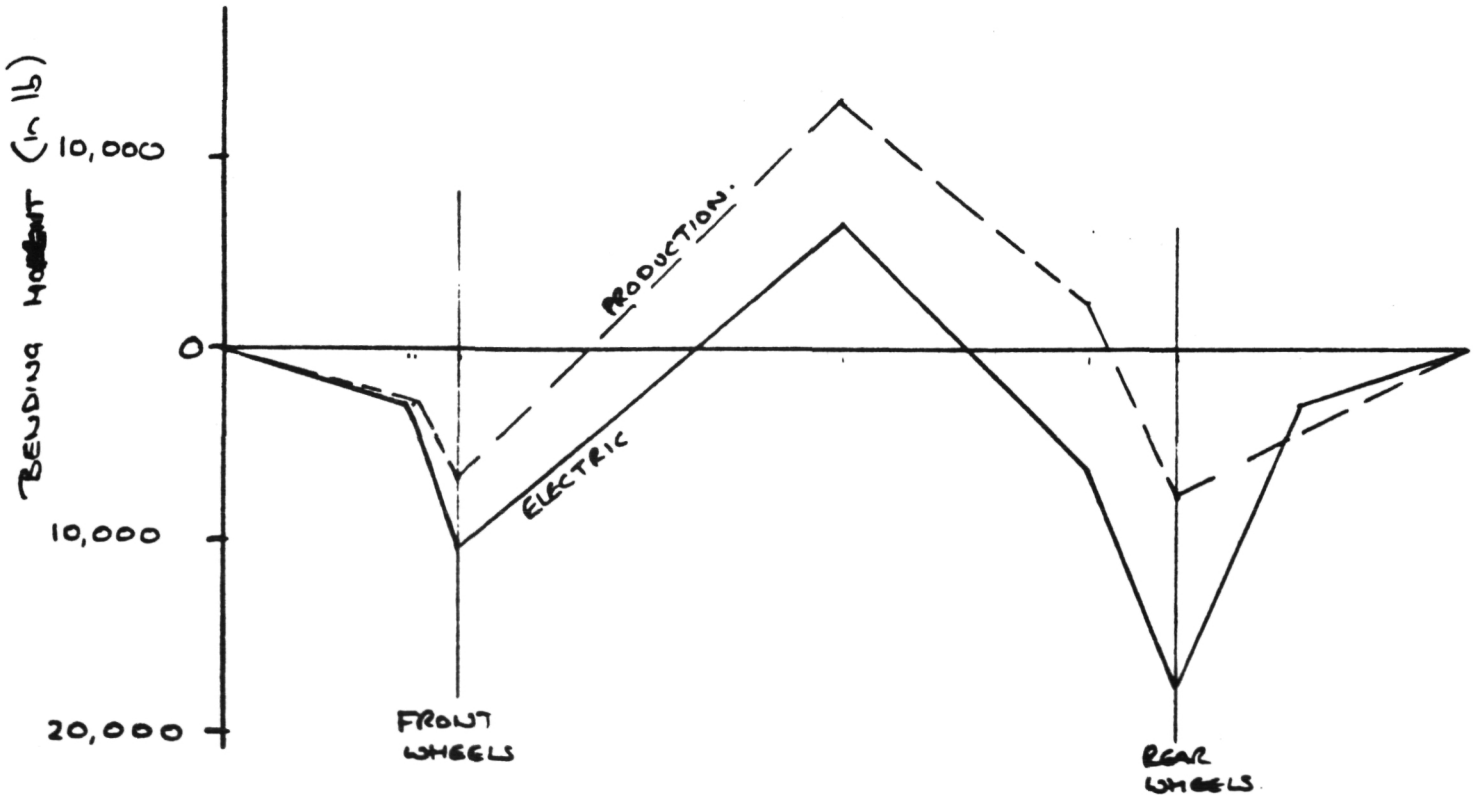

LOADING & BENDING MOMENT DIAGRAMS

Figure 8.2.6

8.2.3 Component Selection and Packaging

8.2.3.1 Power Train

The power train assembly was provided by Eaton as an assembly.

The unit was positioned in the vehicle with the transmission output shafts equally spaced about the centerline of the vehicle. This enabled equal length axle shafts to be used. Additionally, by sizing the flange width correctly it was possible to use the L.H. production shaft on both sides. The advantages of this were both part availability and equal torque reaction at each wheel. The mounting system for a 4-cylinder gasoline engine is far more complex than that required of an electric drive unit due to the inherent out of balance and pulsating load problems associated with a piston engine. For this reason, the production mounts contain excessive amounts of rubber. Although these properties are not necessary for the electric motor mounting, they are not detrimental to an electric drive. The production insulators were found to be suitable from a packaging standpoint and were therefore incorporated.

8.2.3.2 Battery Packs

A study of the battery pack layout indicated that a symmetrical arrangement was possible and that the same box could be used front and rear.

Previous experience had shown that a fiberglass box with sealed lid gave very good structural properties and allowed the batteries to be held in place with little mechanical hold downs, hence providing easy access.

The box can also be of sufficient strength to allow removal from the vehicle without removal of the batteries. The hold downs consist of rubber blocks attached to the lid which contact the batteries on their edges. A purge blower was mounted to the box on the R.H. side with an outlet in the L.H. side of the lid. The purged air/gas mixture was piped to the edge of the hood in the front and to behind the bumper in the rear.

8.2.3.3 Rear Suspension

For the reasons explained in Section 8.2.2, the GM X-car rear suspension was chosen for adaptation to the Lynx.

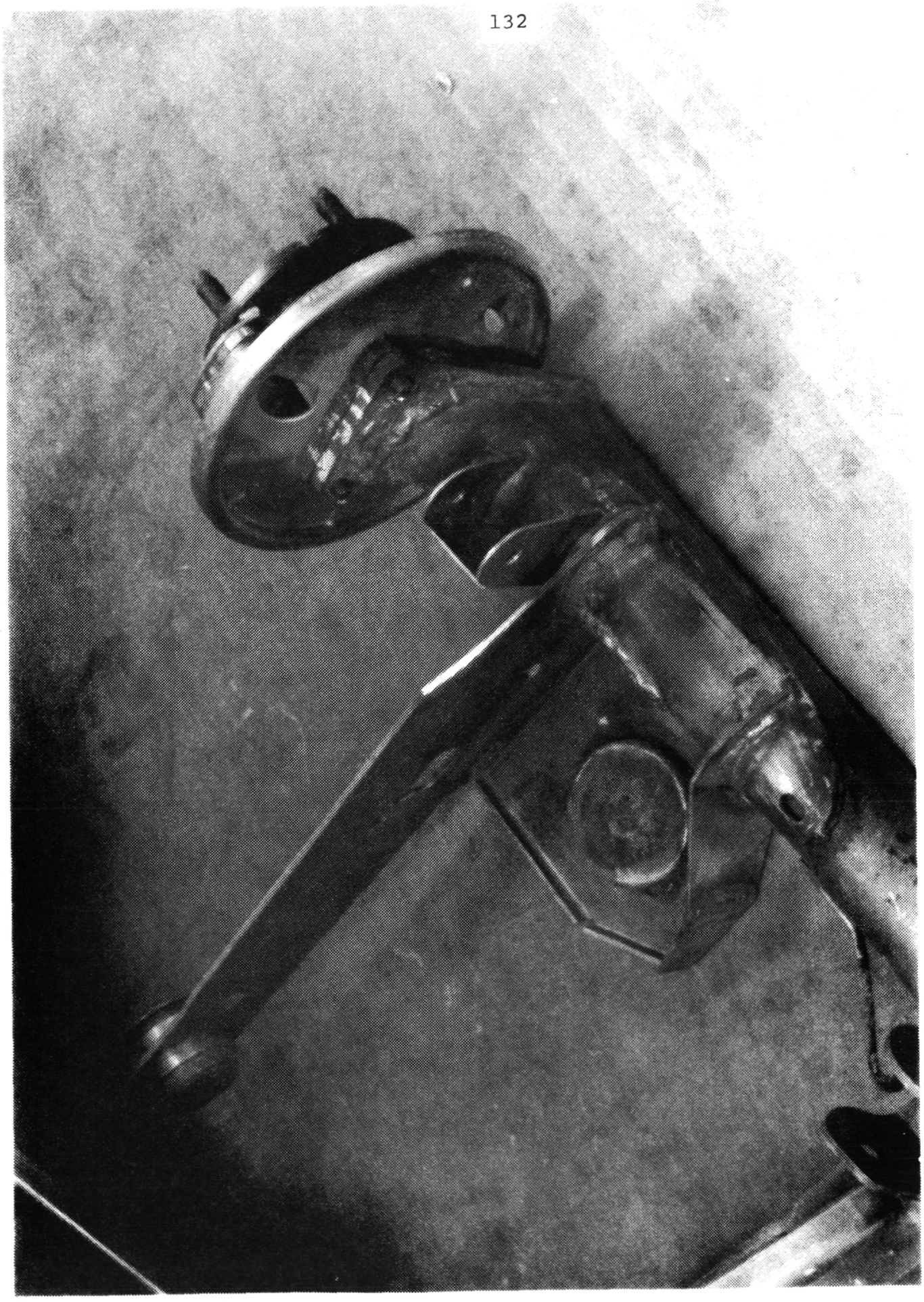

Figure 8.2.7 Rear Axle Detail

Analysis of the X-car weights shows the wheel load to be 867 lb. compared to 946 lb. for the electric Lynx. This increase was considered to be acceptable for use considering the lower speed range of the electric version.

Analysis of the axle beam was based upon the following assumptions.

Torsional Loading - The axle geometry is unchanged; therefore, the resultant torsional stresses will not exceed those experienced by GM on the X-car.

Brake Torque - Braking torque is at a maximum during spike stops. The maximum level is determined by brake dia., coefficient of friction, energizing force and wheel and tire inertia. All of these have remained the same with the exception of the wheel and tire inertia which has been reduced. Therefore, the axle will experience lower loadings than which it was designed.

Jounce Loading - Jouncing the suspension causes a bending stress to occur at the shock absorber attachment to the axle. In order to package the axle in the vehicle it required shortening and also relocation of the shock bracket closer to the axle end (see Figure 8.2.7). The bending stress is proportional to both the load increase and the aforementioned distance.

Therefore: X-car = 867 x 5.5 = 4768.5 in. lb.
Electric = 946 x 3.7 = 3500.2 in. lb.

Therefore, the electric vehicle sees a lower jounce loading induced by bending stress.

8.2.3.4 Front Suspension

The sprung curb weight increase experienced by the front suspension was found to be 148 lb. per side. From discussions with Ford engineers it was found that Ford plans on using this suspension unchanged on a 1983 vehicle which has a front sprung weight increase of 100 lb. per side without options over the Lynx. With the addition of A/C, power steering and brakes the 148 lb. per side is probably comparable.

For this reason no changes were made to the front suspension with the exception of the front springs which were changed to maintain the ride height and ride frequency.

8.2.4 Ride and Handling Analysis

Increasing the weight of the vehicle and changing its distribution by the amounts required to achieve the conversion would have had significant impact on the handling if the production suspension arrangement had been retained.

An analysis of the production vehicle was made using a Triad Services, Inc. computer program which predict vehicle steady state gains as well as its transient response characteristics. The suspension data was gathered from a production Escort; the tire data was extrapolated from previously obtained tire data on tires of similar construction but different size. The results of the analysis are shown in this table:

	Reference (14) Steer Angle (Deg/g)	Total Understeer (Deg/g)	Yaw Velocity Response Time (Sec)	Lateral Acceleration Response Time (Sec)
Production Lynx	5.9	4.1	0.16	0.39
Modified Weight and Distribution	3.5	1.6	0.38	0.76
Typical Limits	-	3 min.	0.25 max.	0.50 max.

It can be seen that the modified vehicle has little understeer quality and excessive response times. The long response times are partly attributed to the high yaw inertia of the vehicle resulting from position of the battery packs.

In order to reduce the response times and to increase the total understeer of the vehicle, it was necessary to modify the deflection steer characteristics of the rear suspension and to alter the geometry to improve the roll steer characteristics.

In addition to the above geometry changes, it was obvious that the rear weight increase would be too great for the suspension components including the wheel bearings and brakes. Consequently, it became obvious that a complete change of suspension was needed and that a GM X-body, beam axle type rear end would provide both the desired geometry and increased size and strength components.

The computer was again programmed with data obtained from the GM X-car and the following handling projections were made:

Reference Steer Angle (Deg/g)	Total Understeer (Deg/g)	Yaw Velocity Response Time (Sec)	Lateral Acceleration Response Time (Sec)
5.3	3.4	0.24	0.49

These characteristics were considered to be very suitable for the vehicle and were considered to be manageable within the requirements of the program.

8.3 Mechanical Modifications Performed by Eaton

Service Brakes

The hydraulic brake system for the Lynx conversion was part of the G.M. X-car (Citation) rear suspension which has one inch diameter larger drum brakes to compensate for the added vehicle weight. Performance tests were conducted separately on the Lynx front disc and the X-car rear drum brakes to obtain a front to rear torque ratio. From this data, performance parameters such as brake pressure, torque and pedal force versus deceleration were plotted. See Figures 8.3.1 and 8.3.2. Also, a front to rear brake split curve was computed to indicate proportioning valve characteristics, i.e., the knee and the slope to ensure rear wheel tracking if a skid situation exists. See Figure 8.3.3.

To accommodate the X-car rear brake, the parking brake cable lever required modification to accept the Lynx cable end. Also, the wheel studs were revised from a five bolt to the Lynx four bolt pattern. These tasks were completed by Triad Services.

The brake master cylinder has been moved from the normal dash-mounted position to an area forward of the left side spring tower. This was done to make room for the front battery box which then could be identical to the rear battery box. The system of relay levers and push rod is shown in Figure 8.2.3 and was designed and fabricated by Triad Services.

Regenerative Braking

For regenerative braking, a special link connecting the brake pedal to the relay rod crank was made, a positive return spring was installed, and a linkage stop was added. The special link (see Figure 8.3.4) is slotted at the inboard or brake pedal end to allow for regenerative brake travel of about one and one half inches at the pedal before engaging the hydraulic system. A linear potentiometer (NEI type 50 LMF-125) is connected to the brake lever at a point which generates a quarter of an inch travel before the service brakes are engaged. The return spring ensures positive positioning against the stop to permit a fine adjustment of the potentiometer. The return spring is a stock Lee spring (P/N LE 115J-5) which produces a pedal force of 6 lbs at the start of travel and reaches 8 lbs at full regenerative travel. If a greater regenerative pedal force is desirable, a custom spring could be employed.

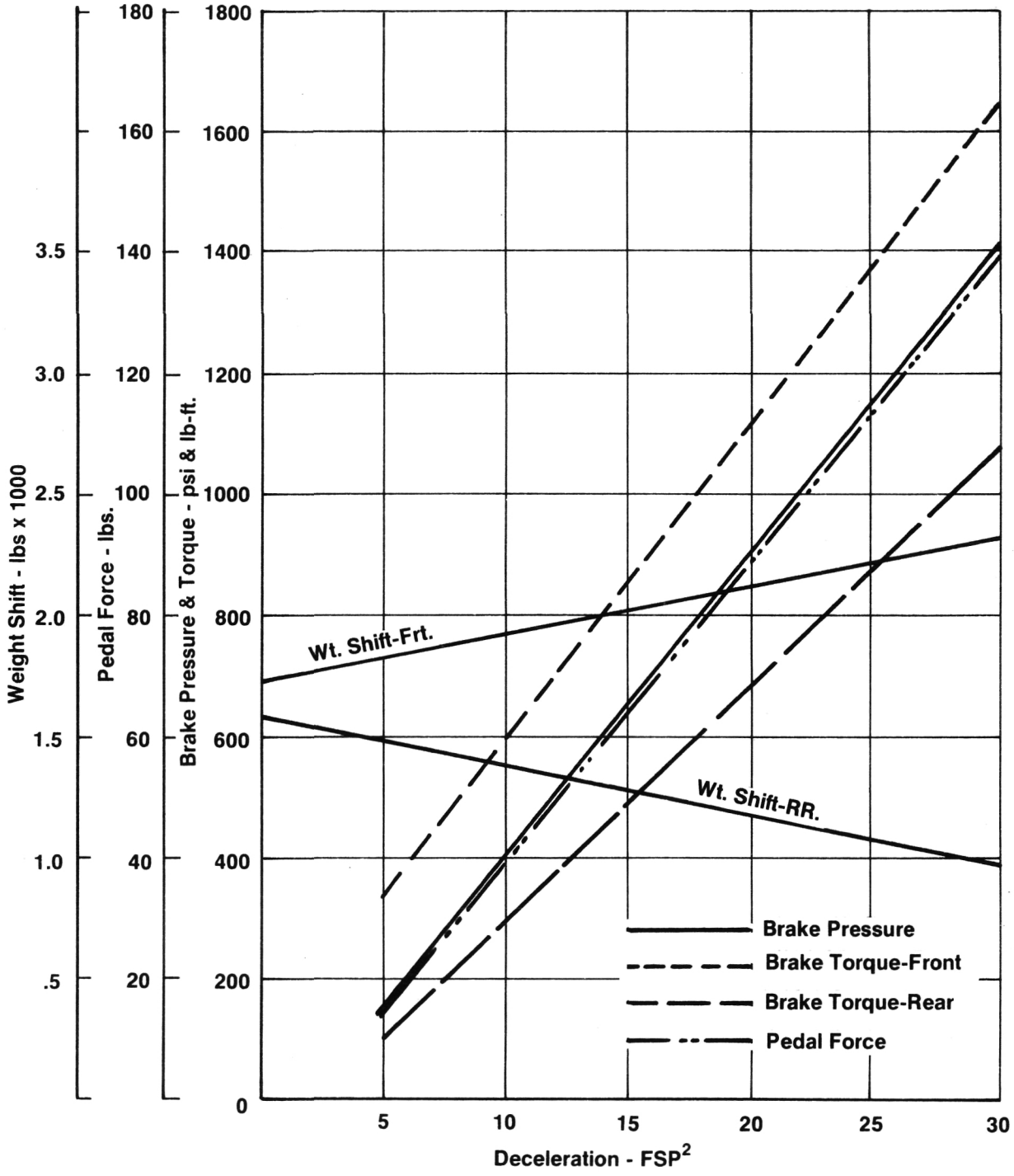

Figure 8.3.1 Weight Shift, Pedal Force, Brake Pressure, Brake Torque Vs. Deceleration ACPS2 Test Vehicle @ 1 Pass. Load

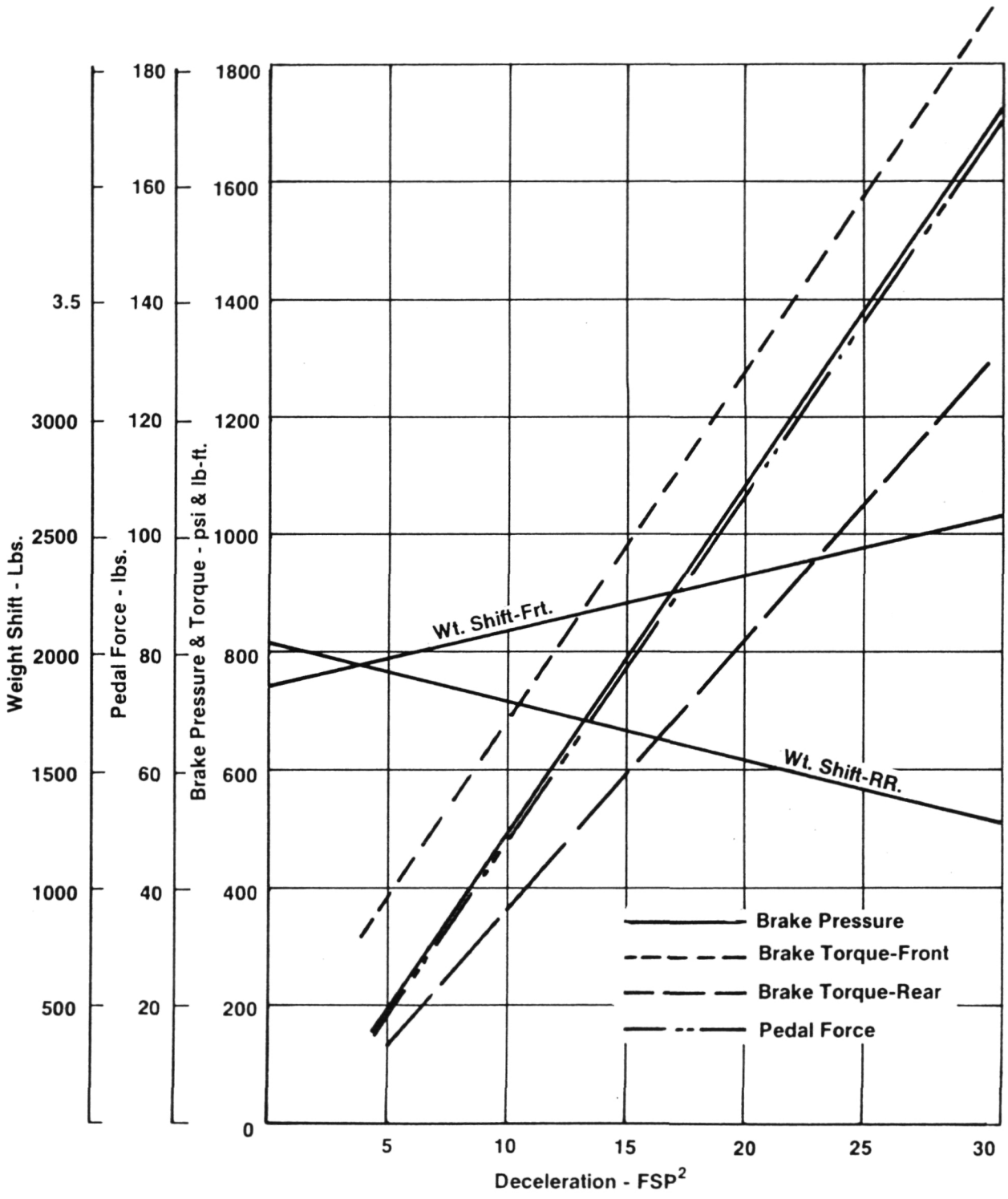

Figure 8.3.2 Weight Shift, Pedal Force, Brake Pressure, Brake Torque Vs. Deceleration ACPS2 Test Vehicle @ Max. GVW

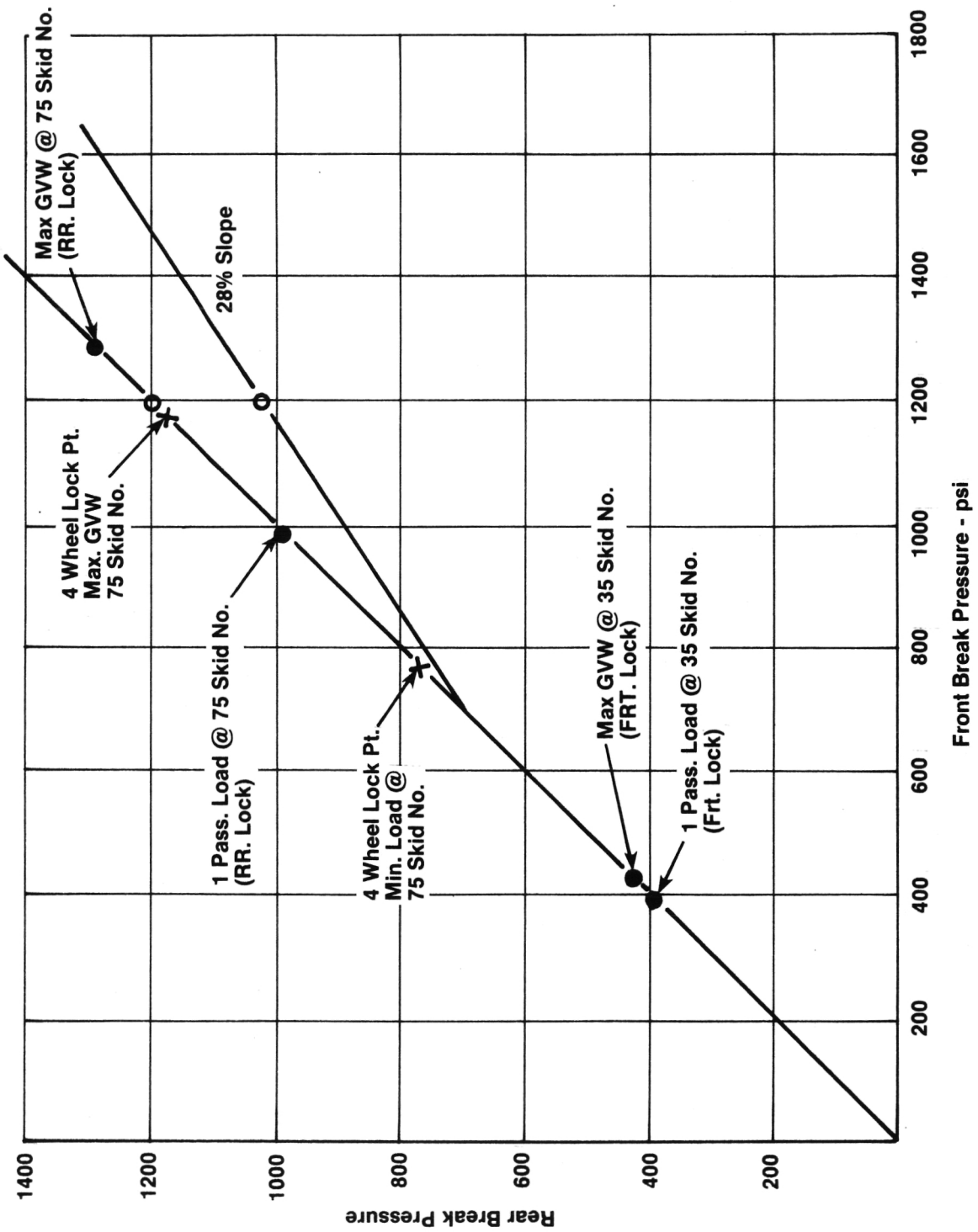

Figure 8.3.3 Front Vs. Rear Brake Pressures

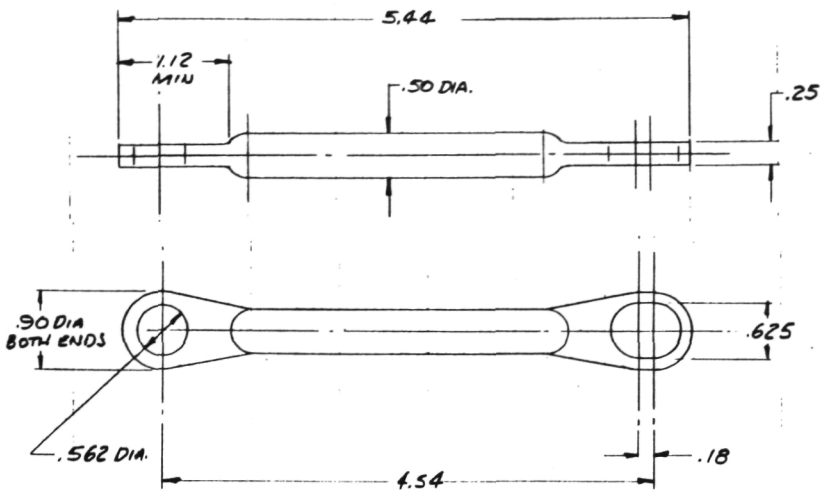

Figure 8.3.4 Brake Link

The potentiometer is connected to the brake lever through a spring loaded slip device which protects it from damage due to overtravel, if full pedal travel occurs.

A linkage stop was installed to give consistency to the brake lever rest position so that the potentiometer can be adjusted accurately. The stop is a rubber pad which, in time, may take a set and may require potentiometer adjustment.

An auxiliary lever was welded to the brake pedal cross tube to geometrically accommodate the return spring and the potentiometer mount. A special anchor bracket was made which fits under the dash panel. This bracket is the ground for both the return spring and the potentiometer.

The spring and potentiometer are placed well above the normal foot position so that the likelihood of damage is slight. The spring is placed between the driver's shoe and the potentiometer as a means of protection, and in normal braking action the shoe would never contact the spring.

Brake performance was monitored, especially the transition from regenerative braking to service braking, where some "tuning" adjustments were made in the inverter/controller. Regenerative braking is superimposed on the service brake until the drive wheel speed approaches zero, at which point the regen. effect is lifted. The amount of regen. braking depends on pedal position,[1] road surface skid number and the state of charge of the batteries. If premature drive wheel locking occurs, a software program can be introduced into the controller to alleviate the problem.

[1]It should be noted that full regen. is reached by the time the service brake is applied and the potentiometer resistance remains constant throughout the remaining pedal travel.

Accelerator Pedal

The accelerator or speed control pedal was reworked to include a return spring and a means of attaching a linear potentiometer (NEI type 50 LMF-125). The return spring is a Lee extension spring (P/N LE-115J-8) which is attached to the pedal two inches below the pivot. A turnbuckle in series with the spring allows a pedal force adjustment of about 5-1/2 to 8 lbs. The full travel load increases only 1/2 lbs due to the geometry change and the low spring rate. A pedal force of 6 lbs appears to give an acceptable feel.

The speed control potentiometer rod travels a quarter of an inch by design of its lever attachment point. Since the return spring positions the lever against its production stop, the potentiometer can be finely adjusted to its proper setting. In this arrangement, as with the brake lever, the potentiometer is placed above the return spring to assure damage protection from the driver's shoe. However, under normal conditions, the shoe could not contact the spring.

Parking Brake To Contactor Control

For the vehicle starting sequence, the parking brake must be on. Contactors in the controller box must be manually activated by positioning the parking brake lever in the engaged position. This is accomplished by using a boden cable attached to an added lever in the parking brake mechanism. Also, as part of the start sequence, a microswitch is added which senses the engaged position. This switch is mounted in tandem with the parking brake warning light switch.

Transmission Shift Lever Control

The gear selection of the transaxle is accomplished electrically rather than mechanically; therefore, a series of small microswitches are used for this purpose. The switches are mounted on a quadrant where a metal spring leaf mounted to the select lever activates a switch according to which position the lever is moved. Switches are mounted for reverse, drive and low gears with no switch assigned to neutral.

For park, a modified production boden cable is attached to the park detent lever via a bell crank on the transaxle and is activated by the gear selector lever. Because of space limitations due to the inverter cooling duct, the transaxle pawl lever direction of travel was opposite to the travel of the selector boden cable. Therefore, a bell crank was added to transmit the proper geometry. Detent positions for park, reverse and neutral were provided, those of drive and low having been positively located by the shifter gate.

Inverter Cooling

The requirement to cool the inverter especially during the charging mode was dictated by the heat generation of some of the components enclosed. An aluminum heat sink which formed the base of the inverter enclosure required air flow across its fins to dissipate the heat. A blower was mounted on the front panel of the vehicle for this purpose. Ducting was designed to direct the air to the heat sink and exhaust at its after end. Triad Services designed and built the ducting from the fan, over the motor and transaxle, down under the floor pan to the rear seat area where the inverter is mounted. See Figure 8.3.5 for cooling air to inverter heat sink flow diagram. Eaton completed the ducting and necessary shrouds to assure that the cooling air was properly directed to the inverter heat sink. A special cover was built by Triad to seal the inverter area from the passenger compartment. See Figure 8.3.6. A controlled amount of cooing air is directed over the top of the inverter housing which is accomplished by placing vent holes in the baffles that seal the top half of the chamber. The air passes between the inverter housing top and the cover and is exhausted aft.

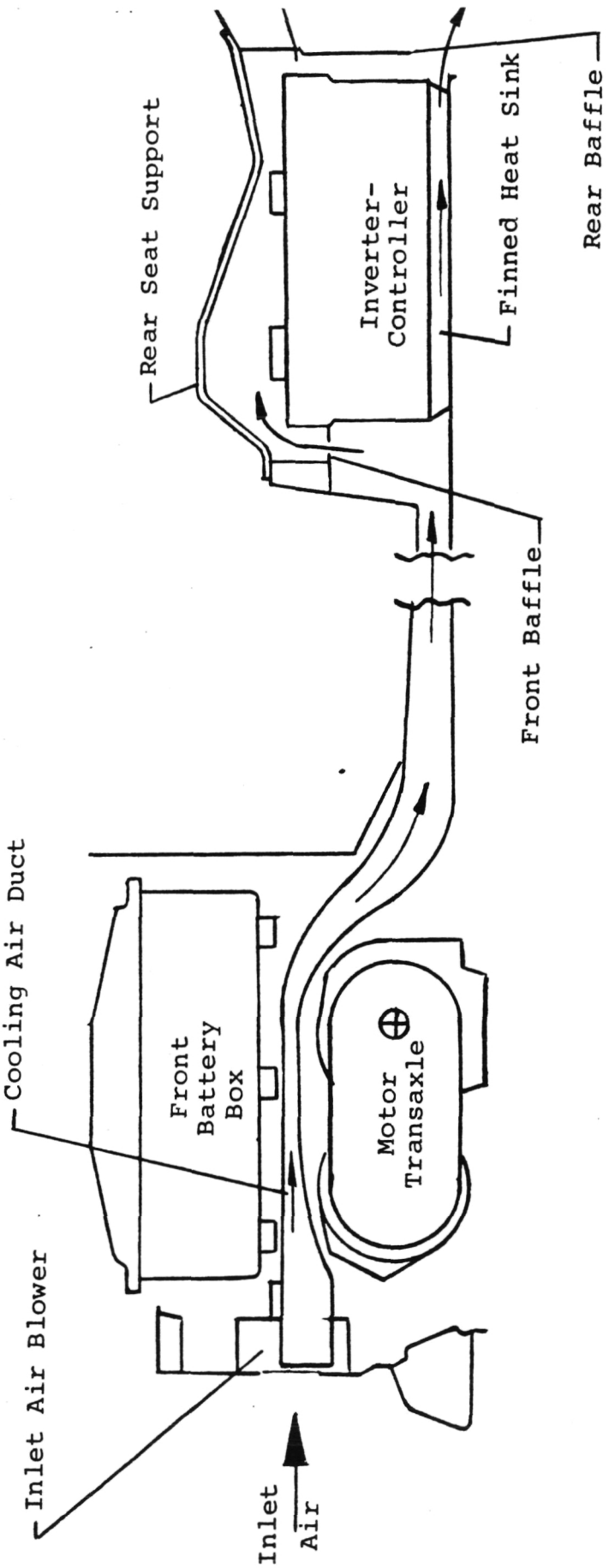

INVERTER COOLING AIR SCHEMATIC

Figure 8.3.5

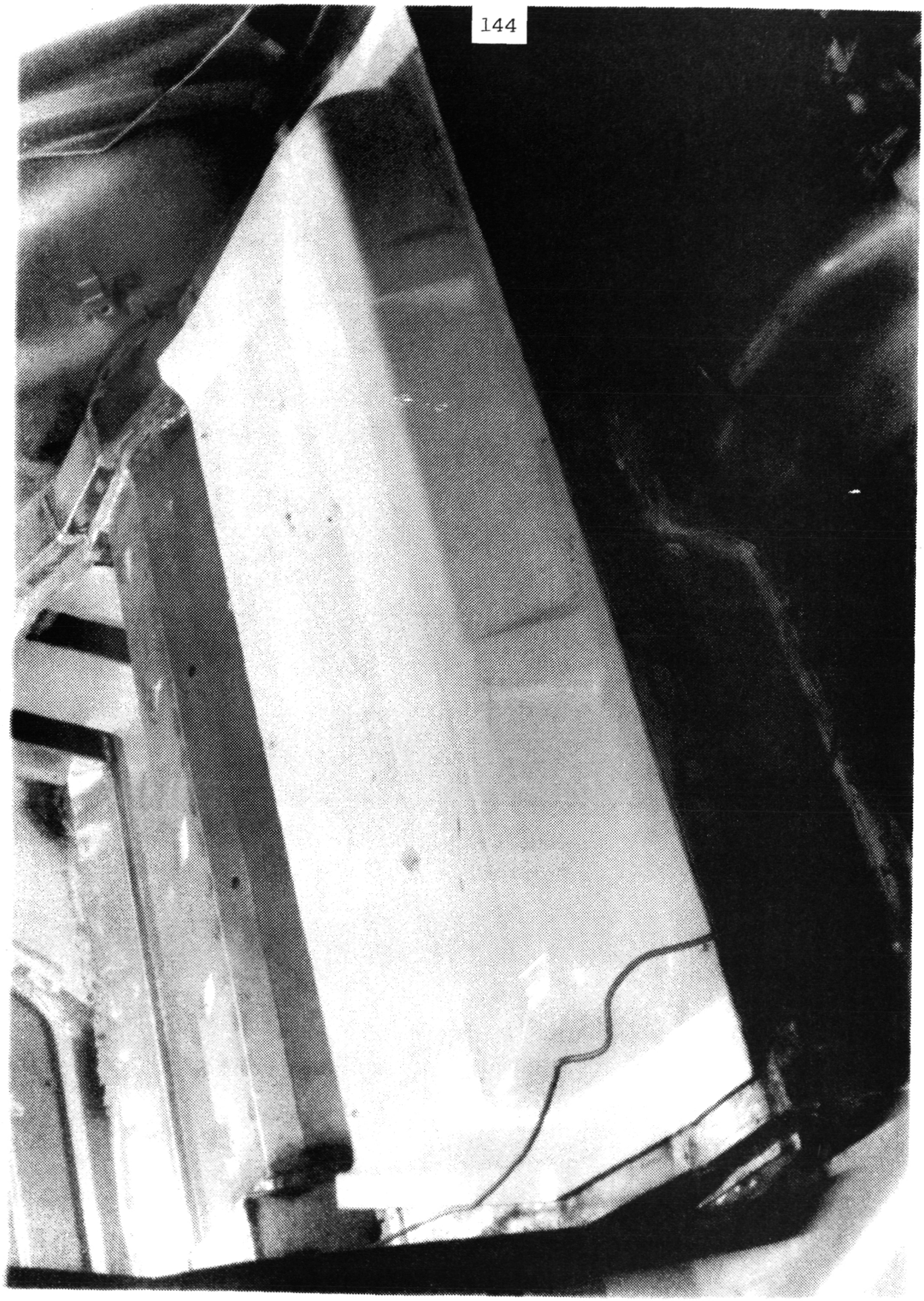

Figure 8.3.6 Inverter/Passenger Compartment Barrier

The cooling air flow through the heat sink was done empirically in the lab. A mock-up was made of the vehicle underbody plenum and shrouds surrounding the heat sink fins. Air flow was initiated from a Dayton model 2C 646 12-volt d.c. blower which is used in the car. A hot wire anemometer, an Anemotherm Mini Mite, was used to measure air flow in feet per minute at the discharge end of the heat sink. An analysis was made of component heat dissipation into the heat sink whereby an air flow of 1140 feet per minute at 50°C (122°F) was determined to be adequate. The lab test results are shown in Table 8.3.1 which indicates that sufficient air flow is available which can be directed, with proper shrouding, to the required hot spot areas.

Position	Flow-ft/min.
L5	925
L4	950
L3	1025
L2	950
L1	800
0	1450
R1	1450
R2	1350
R3	1275
R4	1075
R5	825

Table 8.3.1

8.4 Electrical Modifications

All OEM alternator/charger parts and associated harnessing were removed. The 12V vehicle auxiliary battery was moved from the left front to right front area to allow for placement of the brake master cylinder. The hatchback area courtesy light was deactivated. All other 12V lighting, radio, and accessory circuits are operational.

The two 96V battery packs are linked by #2 welding cable which run through the vehicle center tunnel. The three motor leads are also #2 welding cable and run through the tunnel area. Total cable loss at maximum power is calculated at 330W, or about 1% of the 33.6 KW maximum system power.

The 50 A dc/dc converter packaged in the inverter enclosure feeds 14V dc to the auxiliary battery via two #6 gauge wires. A ground return wire was included rather than relying on the steel car frame to ensure overall low circuit resistance. A 1 a/mv shunt and 60 A fuse are mounted in the +14V charger lead near the 12V battery. The shunt allows measurement of vehicle electrical loads. The load reflects back to main battery bus current.

The OEM fuse block was retained with the following circuits added:

- Fuse 9 feeds the transaxle pump if a 12V pump motor is used. The fuse is switched by the ignition key. If a 180V pump motor is used (140 to 220V operating range), power is supplied from the inverter side of the main bus contactor through a connector and fuse on the inverter box.

- Fuse 16 is unswitched and feeds the inverter blower. The blower is controlled by a transistor switch to vehicle ground. This switch is computer controlled. Fuse 16 also feeds power to the controller during charge mode, when the ignition key must be removed.

- Fuse 18 is switched and feeds the controller during vehicle operation.

The ignition key switch was rewired so that only the "RUN," "OFF," and "LOCK" positions interface with the ac propulsion system. The accessory "ACCY" position still works the OEM 12V loads as in the production Lynx. The key switch assembly has a contact which activates when the key is in the ignition. This is used to activate a warning reminder buzzer if the driver door is opened. The contact was wired to also activate a relay which prevents battery charger operation with the key in the switch. This is an extra level of protection to insure no inverter operation or attempted vehicle operation while charging.

Since the battery charger is integral with the inverter, the 110 and 220 VAC plugs must be accessible. The plugs were mounted behind the original gasoline filler door. A door open/closed sense switch was also installed. In order to enter "charge mode," the door must be sensed open. The ac lines are enclosed in flexible conduit to the inverter. The conduit runs in the right rear wheel well and under the frame. The chassis is electrically tied to the ac ground wire.

In order to pull in the main contactor, powering up the inverter, three conditions are necessary:

1. Ignition switch in "RUN" position
2. Charge plug door closed (thus charge cable disconnected)
3. Parking brake on.

The main contactor requires mechanical pretravel before it pulls in. This pretravel is supplied by the parking brake lever via a sheathed cable which connects to a lever on the inverter.

The controller power supply mounts on top of the inverter and plugs into a 12V feed from switched fuse 18. During charging, the controller gets power from unswitched fuse 16 via a relay in the inverter.

Each battery box has a 110 VAC vent fan. The fan motors receive power via line cord from connector on the inverter. Controller signal input leads are routed along the right door sill to separate them from the power wiring. The following external input signals are wired from various vehicle locations to controller input connector S403:

- Motor speed pulse pickup
- Motor stator temperature sensor
- Front battery pack sample cell electrolyte temperature
- Parking brake sense switch
- Charge door sense switch
- Automatic gear shift select sense switches (PRNDL lever)
- Accel and brake pedal position sensing potentiometers.

Shielded signal cable was used for all analog inputs. Controller external signal output leads are routed as required from controller output connector S407. The output signals are:

- High and low gear clutch solenoid commands
- Inverter blower control
- Dash display. The original vehicle tachometer was replaced by a display consisting of two sets of light emitting diodes (LED's). The first set of four red LED's indicate system failure, system in torque limit, auxiliary 12V battery low, and charge mode active. The

second set of seven LED's display main battery state of charge. Each LED represents a certain percentage band of capacity remaining. Figure 8.4.1 shows the special dash display.

An Espar Model D3L kerosene, 11,000 BTU heater is mounted on the firewall in the motor compartment. A small fuel tank is located in the front left corner of the vehicle under the hood. The OEM gasoline level sender was modified and installed in the heater fuel tank. The dash "gas gauge" now indicates heater fuel. The hot air heater ties into the OEM heat ducts and baffles. Minor changes in the heater actuation levers and addition of switches allowed interface to the Espar heater without adding any new controls to the dash panel. When running, the heater draws 45W at 12V and consumes 0.38 l/hr. of fuel.

8.5 Safety Considerations

Emphasis has been placed on system and vehicle safety. Listed below are items included for operational safety in both motoring and charging modes for the test vehicle.

Motoring Mode

- 12V vehicle circuits isolated from 192V propulsion system circuits.
- Special dashboard displays isolated from 192V propulsion system circuits.
- All circuits are fused.
- All fuses (except 12V auxiliary charger fuse) enclosed and protected.
- All high power connectors insulated and/or enclosed.
- All creep distances on 192V circuits at least 6 mm.
- Any propulsion system components exposed to road splash are sealed to prevent water intrusion.
- Two main 192V battery pack fuses are used, one each mounted within each pack. This arrangement protects against high current discharges if a power cable short occurs anywhere in the system. Also, protection against terminal shorts is afforded when handling packs outside the car.
- The battery boxes are self-supporting and nonconducting fiberglass. They are not sealed, but the mounting location of both packs is such that a bulkhead exists between the boxes and the passenger compartment. The

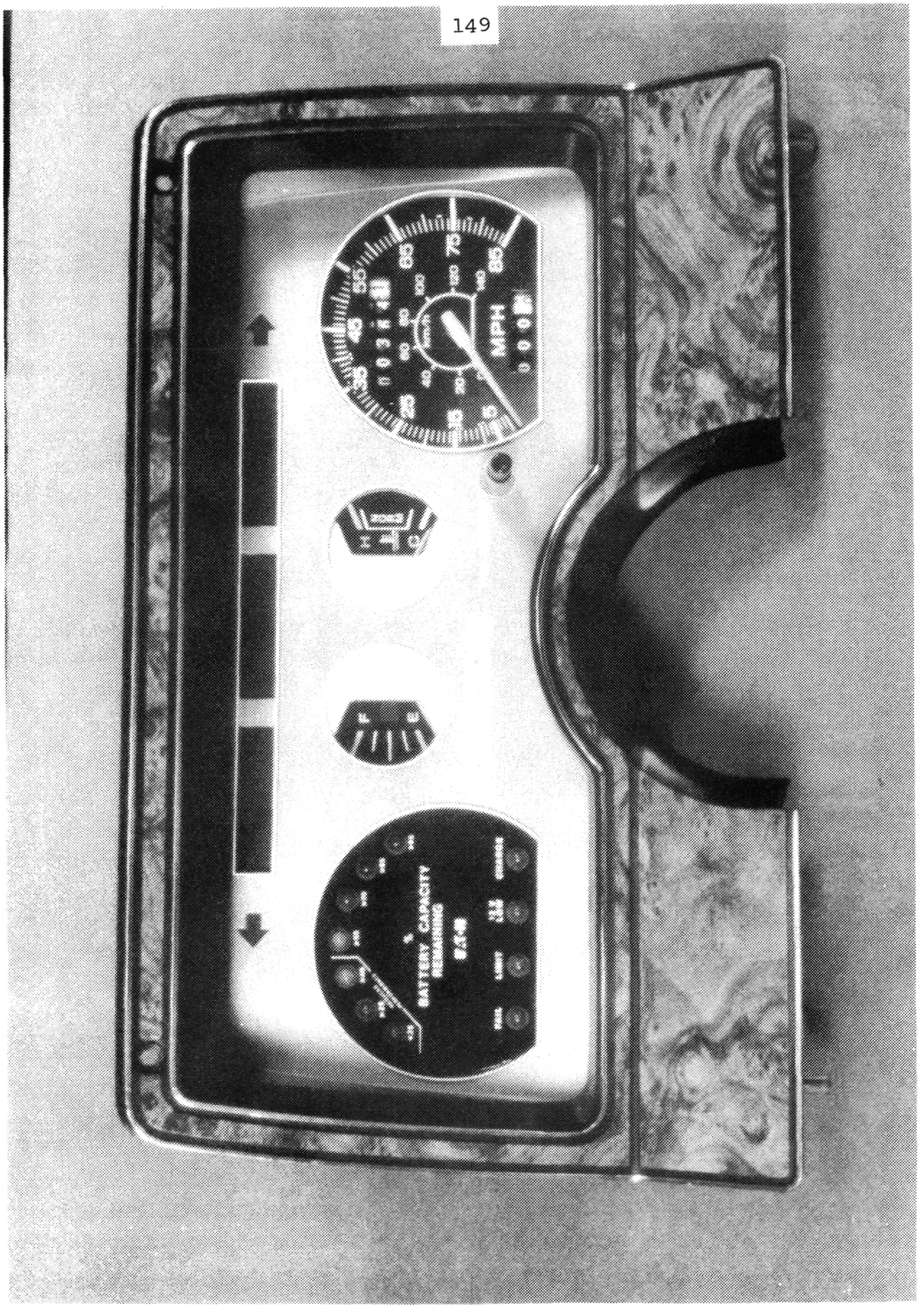

Figure 8.4.1 Dash Display

design is intended to prevent battery acid penetration into the passenger compartment for a 49 km/hr (30 mph) frontal or 25 km/hr (15 mph) rear collision. Crush design should prevent any serious pack intrusion into the passenger compartment.

- A main battery disconnect contactor is provided which has an interlock switch to prevent charging and motoring from occurring simultaneously.

- All sensor and driver control circuits are configured so that a severed or disconnected cable causes the system to failsafe. This typically means the drive turns off (vehicle coasts with service brakes fully operational) or the drive will not start initially.

- Motor temperature, controller temperature, inverter heat sink temperature, and battery electrolyte temperatures are sensed and output power is smoothly reduced to derate the system above appropriate threshold temperatures. At maximum limits, the drive is shut down. A warning "limit" light on the dash informs the driver the system is in derate mode. This feature not only protects hardware, but also reduces the chance of a sudden, unexpected failure on the road.

- Traction battery voltage and current are sensed continuously. This reduces the risk of sudden failure since the controller reduces power if excessive voltage or current occurs.

- The drive will not start if the charge receptacle door is open. The door must be open for either 110 VAC or 220 VAC cable to be plugged in.

- The car will not start initially upon "ignition key" action unless the accelerator pedal is fully released.

- Above a low speed threshold, the brake command overrides the accelerator command.

- Vehicle stability is designed to allow evasive manuevers with no unexpected or unusual response characteristics. The modification design provides for adequate strength of spindles, wheels, and suspension members to withstand severe cornering and panic stop situations.

- All sensitive signal lines are shielded to reduce likelihood of erratic behavior due to RF fields encountered on the road.

- Seat belt buzzer, key-in-ignition buzzer (when driver door ajar) and door ajar buzzer are retained from the production Lynx.

- The controller checks random access memory at every power-up. If a faulty bit is detected, the drive is inhibited.

- If a transient pulse causes the controller to fail, the drive turns off (vehicle coast) for a maximum of two seconds while the logic attempts to reinitialize. If restart is successful, the accelerator pedal must be momentarily released and then applied to regain torque. This forces operator acknowledgment of the restart. The brake pedal does not need to be released. Service brakes are available at all times.

- The controller is powered from the 12V auxiliary battery through an isolated power supply. If the battery drops below 10 volts, controller operation is not assured. Since the controller is critical to vehicle operation, a warning light on the dash activates if voltage drops below 11V. This gives advance warning. A dc/dc converter keeps the auxiliary battery charged at a nominal 14V.

- All Lynx electrical safety systems (lights, flashers, wipers) are left intact. The dc/dc converter powered from the traction battery keeps the 12V auxiliary battery charged under worst case loads. Headlamps are kept at full brightness.

- Loss of hydraulic solenoid electrical power causes the transaxle to default to high gear. This is always a safe shift at any motor speed, and allows for limp-home capability.

- A hardware circuit apart from the microprocessor prevents simultaneous high and low clutch actuation beyond a maximum one second overlap time.

- The motor cannot be powered with either the parking brake or parking latch set.

- The heater is sized to give satisfactory defrosting/defogging performance to improve visibility.

- All occupant interior mechanical safety features are left unchanged.

Charging Mode

- Ignition key must be removed before ac main power applied to charger. Interlock prevents possible car motoring attempt when charging.

- Vehicle chassis is grounded to earth through the charge plug recepticle.

- Battery vent fans (one per pack) provide over 10 air changes per minute to prevent hydrogen buildup in packs.
- Charger shuts down if overcurrent sensed due to a fault. If severe overcurrent, main fuses blow.
- Either 110 VAC or 220 VAC can be applied. A relay prevents any short circuit if both plugs are inserted simultaneously. System defaults to lower current 110 VAC feed. Both sides of both 110 VAC and 220 VAC feeds are fused in the inverter enclosure.
- All interlocks remain in force even if a utility power failure occurs.
- A line transient suppressor reduces risk of arc over due to line surges.
- 110 VAC, 220 VAC, and 192V dc inverter connectors must be disconnected before the inverter cover can be physically removed.
- All batteries have flame arrester caps.
- The battery box covers are sloped with the vent at the peak. Vent hoses slope upward from box to outside vents. This encourages natural convection venting if a fan fails.
- The charger monitors bus voltage and electrolyte temperature to regulate current to prevent excessive gassing.
- The controller automatically senses the mains voltage and adjusts peak current accordingly.

9.0 TRACTION BATTERY

9.1 Specification

The Eaton Proplusion System does not formally include the battery. However, traction battery choice is important for overall vehicle performance. The following were the selection criteria:

- 12V module. At 192V bus voltage, any available 6V unit leads to a package too big for a compact car. The small car has always been the target vehicle style for the propulsion system.

- Adequate power density. Power density is important to enable road testing to the system's power limit. The overall drive can be easily battery-limited in acceleration if power density is not high enough. Further, the power density should be maintained at an adequate level down to 50% D.O.D. for testing convenience.

- Adequate energy density. This is a secondary consideration as far as the propulsion system is concerned. The system is to be as efficient as feasible, so better batteries simply reflect increased range.

- Availability. Spare batteries must be readily available.

- Performance information. This project is not concerned with battery development, and risk in that area is to be minimized. The chosen battery should have performance data derived from test.

Lead-acid seemed the preferred choice at this stage. Further, the Globe-Union EV-800 12V battery appeared to best meet the criteria.

- BCI Group 27 package (12.1" x 6.8" x 8.8")
- 12V
- 54 lb.
- 14.4 whr/lb. @ 3 hr. rate
- 62 amp hr. @ 2 hr. rate
- 68 amp hr. @ 3 hr. rate
- 75 amp for 45 minutes
- Basically a heavy-duty marine battery.

This battery yields a realistic total pack energy of about 12 kwh, which is far from spectacular. Effective kwh capacity depends on discharge profile, age, and temperature. Nevertheless, range is tolerable for test and demonstration purposes.

In case the power density of the EV-800 batteries proved inadequate, another battery was considered. The Globe-Union EV-1300 was developed for the DOE-GE hybrid car project, and is essentially a scaled-down version of the Globe-Union ISOA lead acid battery. Admittedly, this 12V battery is in prototype development, but most testing to date is encouraging. It incorporates acid recirculation which benefits power density at reduced states of charge. This feature does add complexity.

Specifications on the EV-1300 are:

- custom package (12.7" x 7.4" x 10.8")
- 12V
- 75 lb.
- 16.9 whr/lb. with acid circulation system factored in
- 106 amp hr. @ 3 hr. rate

This battery yields a realistic total pack energy of 21 kwhr. Range would be improved both due to increased capacity and increased energy density, which overshadow the increased weight.

The main advantage of the EV-1300 over the EV-800 is its power density. At 100% state of charge, the EV-1300 is about 25% better, according to Globe-Union. At lower states of charge, the margin increases.

Due to cost of the EV-1300 prototype packs, they were not purchased. However, the battery enclosures were designed to accommodate either battery type.

9.2 Performance Modeling

A computer model was developed to predict the range of the vehicle with two different battery sets. Two batteries manufactured by Globe-Union were compared, model numbers EV-800 and EV-1300. The computer simulation used for comparison was a customized version of the Boeing Computer Services (BCS) HEAVY program.

The Eaton transaxle was modeled using Fortran statements. The model implemented utilizes a piecewise linear representation of transaxle torque losses, dependent on torque and speed. The model was based on data collected at the ERC during EV propulsion system phase 1 (DEN3-125) testing.

The BCS HEAVY implementation of the Bozek Averaging Battery Model was carefully studied through the HEAVY Users Guide and the HEAVY source code. The HEAVY implementation was found to be inappropriate for comparing the batteries using the battery data available. The approach used in the Bozek

battery model is a time-averaged, fractional utilization model. The model obtains the predicted battery capacities from a Puekert's curve. The Puekert's curves for the batteries of interest were obtained from Globe-Union and are shown in Figure 9.2.1. As can be seen from the figure, the two curves are straight lines on a log-log plot. The default equation for the Puekert's curve implemented in HEAVY gives a straight line on a semi-log plot. It was found that the equation constants could not be adjusted so that the curves fit the manufacturer supplied data well enough to perform a capacity comparison. Therefore, a Peukert equation as described by Bozek was implemented. This implementation allowed accurate comparison of the batteries using the manufacturer supplied data.

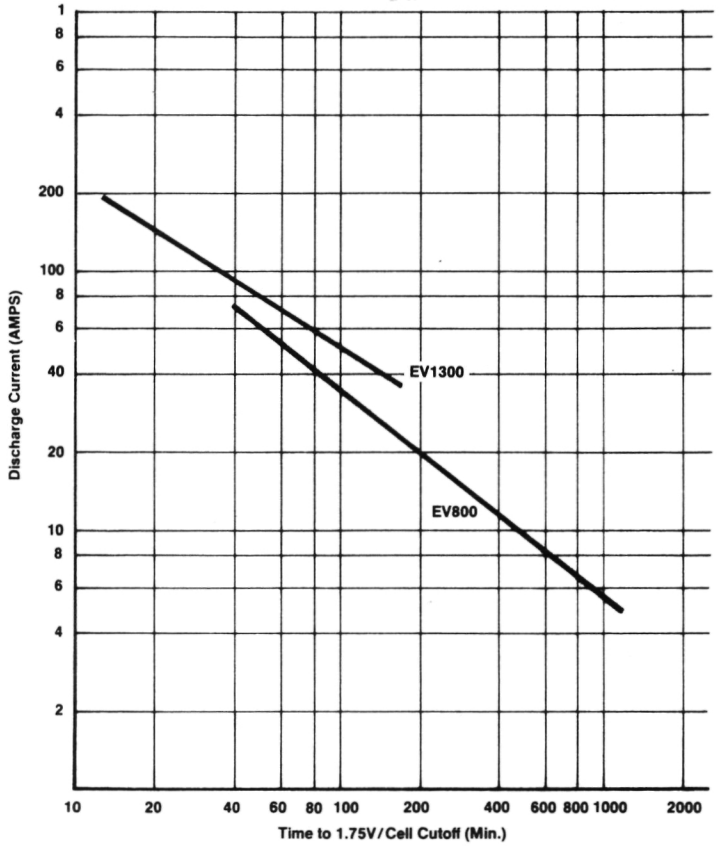

Figure 9.2.1 Puerkert's Curve

Data describing voltage versus time for various constant current draws (voltage signature curve) is needed to completely describe the terminal characteristics of batteries with the HEAVY battery model. This data was not available for either battery under study. Thus the assumption was made the the "voltage signature curves" for the two batteries are the same and the HEAVY default data (signature of an EV-106 cell) was used. This is a conservative assumption for this study. The EV-1300 is the "stiffest" (maintains its voltage under load the best). The EV-106 is the least "stiff" (voltage droops the most for decreasing

capacity) and the EV-800 is in-between. This assumption will lead to a conservative prediction for the EV-1300 relative to the EV-800. Moreover, this assumption will affect the comparison even less due to the fact that the simulation used predicts the vehicle range by performance during one cycle (as suggested by Bozek).

The BCS HEAVY simulation uses data collected and compiled at the Eaton Engineering & Research Center for the induction motor/inverter drive system. The data is for a 144V system with a maximum motor output speed of 943 rad/sec. In order to utilize this data for studying the present vehicle system, with a 192V bus and a top motor speed of 1332 rad/sec, two assumptions were made: firstly, the efficiency gains of the motor and the inverter due to higher voltage (thus lower current) operation were neglected; secondly, the gain/loss due to the higher system frequency operation was neglected. These are reasonable assumptions for this study since the purpose is not so much for absolute vehicle range prediction as for relative vehicle range comparison. The model was not rerun when actual Phase 2 efficiency data was measured due to time and budget constraints.

The vehicle propulsion system and battery constants used in the study are summarized in Table 9.2.1. The results of the study were obtained from two simulation runs using the SAE j227aD cycle with the fixed vehicle and propulsion data. The resultant predicted ranges for the vehicle using the two battery sets are also shown in Table 9.2.1 and are 92.7 km (57.6 mi.) for the EV-800 battery set and 142.4 km (88.5 mi.) for the EV-1300 battery set. These ranges are obtained from well-tuned models, as discussed above. As such, they are the best predictions using the data and models available, but they are approximate. The predicted ranges are good measures of relative improvements over a base case. That is, the study shows that the EV-1300 will provide a 54% range improvement over the EV-800 base.

Table 9.2.1 Summary of Battery Range Comparison

Vehicle Simulation Used: Boeing Computer Services HEAVY with battery and transmission components modified by Eaton.

Vehicle Simulated: 1981 Mercury Lynx (modified for EV) Inverter/ Induction Machine on 192 V bus with two 96V battery sets

Assumptions Made:

1) Inverter and motor efficiency gains over 144 V system not modeled.
2) Gain/Loss from higher frequency of operation than Phase 1 system negelected.
3) Battery signature curve assumed to be the same.

Simulation Parameters:

- Driving Cycle: SAE j227aD
- Constant Accessory Load: 200 watts
- Controller and Inverter: Eaton PWM
  - Weight - 45.36 kg (100 lbs.)
- Induction Machine & Cables: Eaton Squirrel Cage
  - Weight - 60.78 kg (134 lbs.)
  - Inertia - 0.0129 kgm^2 (0.306 $lb\text{-}ft^2$)
- Transaxle: Eaton 2-speed automatic
  - Weight - 39.0 kg (86 lbs.)
  - Inertia - 0.002202 kgm^2 (0.0524 $lb\text{-}ft^2$)
- Vehicle: Mercury Lynx (modified for EV)
  - Weight - 796.53 kg (1,756 lbs.)
  - Drag Coefficient - Cd = 0.46
  - Presented Area - A=1.821 m^2 (19.6 ft^2)
  - Wheel Radius - 0.2667 m (10.5 in.)
  - Payload - 2 passengers, 138 kg (304 lbs.)

Two simulations were made with the above fixed vehicle data, changing the battery data for comparison of the two battery sets.

	EV 800 Simulation	EV 1300 Simulation
Number of Cells:	96	96
Number of Batteries:	16	16
Weight per Battery:	24.494 kg (54 lbs.)	34.02 kg (75 lbs.)
Weight of Battery Set: (structure included in vehicle)	391.91 kg (864 lbs.)	544.32 kg (1,200 lbs.)
Peukert Curve:	Supplied by Globe Union	Supplied by Globe Union

SIMULATION RESULTS

	Vehicle With EV-800 Set	Vehicle With EV-1300 Set
Predicted Range:	92.7 km (57.6 mi.)	142.4 km (88.5 mi.)
Relative Improvement over EV-800:	1.00	1.54

NOTE: The above range predictions are approximate, but they are good as measures of relative improvements over a base case.

Range tests were not included in the vehicle test plan since energy consumption per km. is the best measure of propulsion system performance. Therefore, experimental data to compare with the model result is not available.

9.3 Battery Box

Each battery box contains eight 12V batteries for a nominal 96V pack voltage. The front and rear boxes are identical. The box is made of fiberglass with three steel "C" channel beams for bottom support. Holes on the channels line up with locating pins on the vehicle frame, and four through bolts tie down the box. The box is approximately 83 cm wide, 71 cm deep, and 38 cm high. With a full complement of batteries, the box weighs 218 kg (480 lb). The interior is coated with epoxy paint. Drain holes are provided so the batteries can be washed down. Figure 9.3.1 shows the box with cover, and Figure 9.3.2 shows the box with cover removed.

The top cover has rubber blocks spaced to clamp down on the batteries. Four eyebolts can attach to the bottom frame with tie rods. A special lifting frame (shown in Figure 9.3.1) and harness fastens to the eyebolts for easy pack removal. Both front and rear packs can be lifted straight up out of the vehicle using an overhead hoist. The cover is sloped with a vent at the apex. A small brushless muffin fan mounted on the box side pushes air through the box and out the vent during charging.

The battery interconnect links (#2 welding cable) have clamp-on post connectors which are burned on to the battery posts for better integrity. A 200a fuse is mounted on an interior wall and is connected between batteries 4 and 5 (mid-voltage). The fuse element is enclosed and presents no external arc if it blows. The output connector is an Anderson SB-175 attached to #2 welding cable pigtail leads which exit the side of the box through grommetted holes.

A solid-state temperature sensor IC is used to sense electrolyte temperature. The IC is placed at the end of a blind hole in a teflon tube and sealed with silicon sealant. The tube is mounted to a battery cap such that when installed, the tube is emersed in electrolyte. The cap is placed on a cell in the middle of the pack on the assumption that heat buildup should be greatest there. Only one representative cell temperature out of 96 is monitored by the controller. The system does not detect gradients. The test vehicle used the front pack sensor. The sensor leads exit the side of the box and terminate in a push-on connector. A mating cable goes to the controller. No special insulation or thermal management design was used in the box design. The main criteria were physical integrity and ease of box interchange.

Figure 9.3.1 Battery Box - Cover On

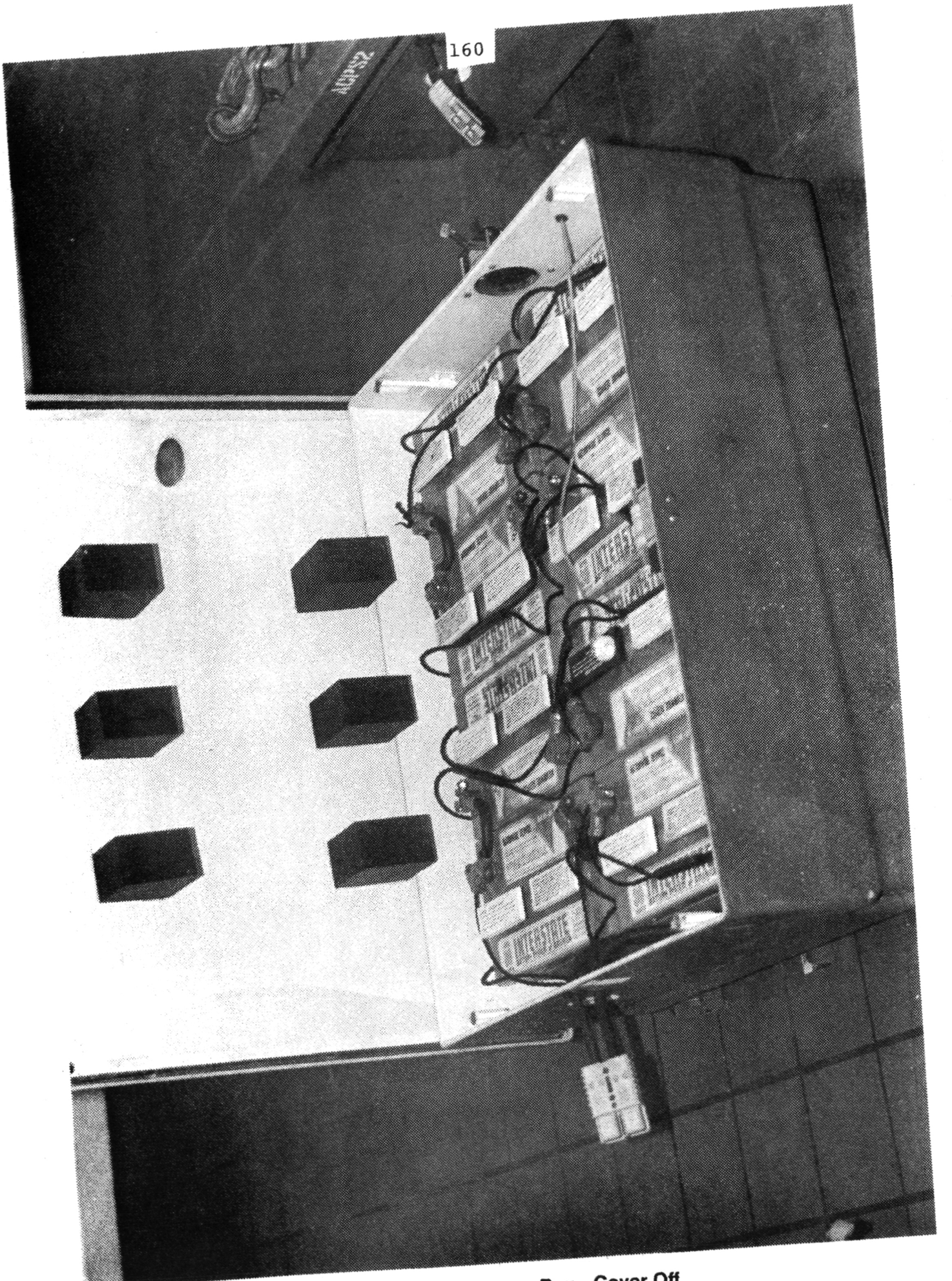

Figure 9.3.2 Battery Box - Cover Off

9.4 Battery Support Cart

For operating convenience, a portable cart based on a hand dolly was built to aid in battery charging and maintenance. The cart has utility type watt-hour meters for 110 and 220 VAC, circuit breakers, ac voltage and current waveform acquisition, and all necessary hook-up cables. A storage box holds a hydrometer, distilled water, and miscellaneous items. Figure 9.4.1 is a photo of the cart.

Figure 9.4.1 Battery Support Cart

10.0 SYSTEM TESING ON THE DYNAMOMETER

10.1 Overview of Tests

The system tests in the dynamometer were intended for verification of the performance of the controller, inverter, motor, and transaxle prior to installation in the test vehicle and cover the following specific efforts:

1. Motor mounted on torque table and driven by inverter and controller. This "torque table" test sequence was used as a preliminary step to full system integration with the transaxle. Motor speed-torque limits were determined; transistor safe switching was verified. Motor and inverter efficiency was optimized for notch number and V/Hz and the motor and inverter thermal performance was checked.

2. AC drivetrain testing and characterization. These tests were run on the total propulsion system controller/inverter/motor/transaxle. The total system efficiency was measured, and the gearshift sequence was tested before installation on the vehicle. This test sequence was cut short in order to meet a deadline for installation of the propulsion system into the vehicle. Thus, not all the required data was collected. However, a separate dynamometer test of the transaxle alone was performed and helped fill gaps in the system efficiency maps.

10.2 Test Setup

10.2.1 Power Lab Testing

Equipment in the Power Lab for performing the testing on the base drive and auxiliary power supply consists of standard laboratory instruments, including a digital Nicolet oscilloscope for documenting waveforms. Test accuracies in the power lab can be kept within 2%.

10.2.2 Dynamometer Test Setup

The dynamometer test system was designed to characterize the AC propulsion system. These tests were performed with the apparatus described in this section.

The test stand was designed with two work stations. One work station tested the motor and inverter alone, while the other station tested the motor, transaxle, and inverter as a system. The test stand is driven by a 45/60 hp driving/absorbing dynamometer which is capable of supplying a load or driving the motor in a regenerative condition. The setup is shown in Figure 10.2.1. For the torque table tests the dynamometer shaft undergoes a 2/1 speed reduction from the motor on the torque table through a set of HY-VO chains so that a maximum motor speed of 12,000 rpm can be

attained. The torque table measures the reaction torque on the motor housing. Two speed sensors were installed on the motor and dynamometer shafts to sense the system speeds. An oil lubrication system was used to lubricate and cool the motor while an oil mist system was used to lubricate the chain. The motor was outfitted with thermocouples to monitor oil inlet, oil outlet and case hotspot temperature. The inverter controller was located on the control console positioned on the bedplate for the m jority of the tests. This was necessary to minimize the lead length losses for accurate motor efficiency readings.

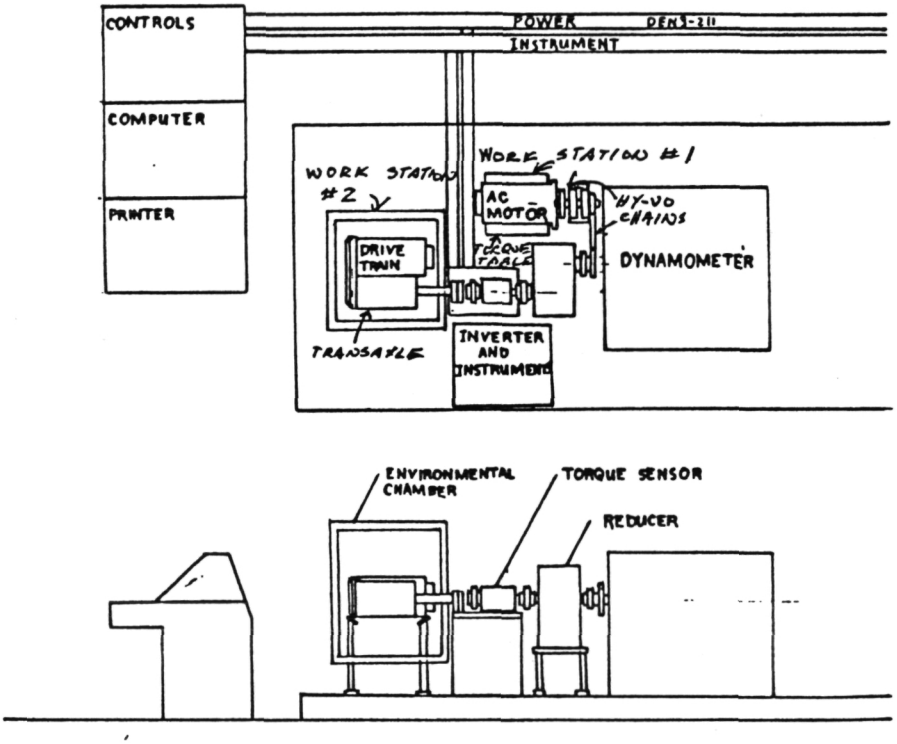

Figure 10.2.1 Mechanical Test Setup

The motor, transaxle, and inverter controller work station were designed to test the total system performance. The system is powered by the 45/60 hp dynamometer which can be operated as an absorber or drive for the system. The dynamometer shaft was aligned to a 6:1 speed reducer. The reducer supplies the proper speed ratio in order to match the dynamometer torque-speed curve to the drivetrain torque-speed requirements. The output shaft of the transaxle was coupled to the reducer through a rotary transformer torque sensor. A special removeable shaft was inserted in the unused transaxle output to lock up the differential. The torque sensor monitors output torque of the transaxle which along with output speed yields the power out of the system. A standard Ford Escort drive axle has been adapted to fit between the transaxle and torque sensor shaft. A major

consideration in the selection of these components was to keep the bedplate installation as close to the vehicle installation as possible. In view of that, the motor/transaxle were supported from three posts which extend up from the bedplate. The posts were located at the same position and use the same motor mounts, and brackets as the vehicle installation. The motor and transaxle have been instrumented with pressure and temperature sensors to monitor clutch and line pressures as well as critical drivetrain temperatures.

The inverter and motor controller rested on a control console located on the bedplate. A blower and shroud has been constructed around the inverter to insure that the proper air flow was supplied during the tests. The fan and shroud was chosen so that it would simulate actual vehicle air flows as closely as possible.

10.2.3 Computer and Instrumentation

The following description applies to the steady state propulsion system data acquisition system described in Appendix A.

Calibration of the test stand is necessary to achieve the stated accuracy goals. Proper calibration is ensured for each test run by providing a computer program to perform an on-line calibration of the analog channels at the start of each test run. The purpose of the program is to measure gain drifts and zero offsets in the instrumentation so that their effects may be removed from the acquisition system displayed data. Other calibration procedures to verify sensor scale factors and instrumentation voltages are performed in the course of test stand checkout.

The on-line calibration software measures offsets and drifts in the instrumentation by inserting known zero and calibration voltages at the inputs of the isolation electronics described in Appendix A. Calibration measurements are displayed on the test stand terminal and printer for review by the engineer prior to running a test. These measurements are applied by the data acquisition programs when converting A/D converter data to engineering unit values. Test stand calibration, performed after a minimum warm-up period of one hour, was demonstrated to remain stable for at least eight hours. Figure 10.2.2 is a sample calibration display.

CURRENT CALIBRATION DATA VALUES 5/5/82 10:15

LABEL		ADC CHANNEL NUMBER	PRECAL ZERO (VOLTS)	CAL MAGNITUDE (VOLTS)	SPAN (VOLTS)	CAL POINT (ENG UNITS)
VDC	BATT VOLTS	8	0.005	7.489	7.484	196.50
ADC	BATT AMPS	7	0.015	7.167	7.152	-194.60
N-M	TORQUE	1	3.325	0.034	-3.291	46.21
VRMS	LINE VOLTS	16	0.015	8.080	8.065	255.40
ARMS	LINE CURRENT	15	0.015	5.532	5.517	144.30
%	DUTY CYCLE	2	0.010	7.450	7.440	100.00
	NOTCH NO.	3	-0.596	7.494	8.090	24.00
VDC	AUX BATT VOLTS	5	0.005	7.362	7.357	12.40
ADC	AUX BATT AMPS	6	0.010	7.753	7.743	79.30

Figure 10.2.2 Sample Calibration Display

When performing calibration and steady state measurements, the acquisition system averages samples collected over eight 0.1 second intervals. This applies to the wattmeter channels and all analog input channels. The rate measurements for motor speed and stator frequency are made over one second intervals with input frequencies of one pulse per RPM. Thermocouple inputs are scanned at the rate of one measurement per thermocouple per screen update.

Table 10.1 lists displayed propulsion system variables and valid dynamic ranges, Figure 10.2.3 is a typical data acquisition system display. Variables which are measured directly are: motor speed, battery voltage and current, motor watts, Volts/Hz, line-to-line AC voltage, single phase current, stator frequency, auxiliary battery voltage and current, duty cycle and notch number. The last two variables are digital signals converted to analog form by the propulsion system diagnostic computer. Variables whose values are computed include: transaxle speed, slip, efficiencies (3), powers (4), and dynamometer speed.

```
ELECT. VEHICLE PROPULSION SYSTEM        ACPS-2 DEN3-211 PROJ: 4004-06
TEST NO.          204                    6/17/82
STATUS:     ffif                         OPERATOR: JMS
TEST 3.2.2.5 MOT/INV EFF                 UNIT ID:  2/2/-

  4209.68 RPM    MOT SPEED                    29.00 DEG C  T1-MOTOR CASE
          RPM    T/A SPEED                    34.00 DEG C  T2-FUJI CASE
                 GEAR                         31.00 DEG C  T3-TR-HT SNK
   194.57 VDC    BATT VOLTS                   22.00 DEG C  T4-T501 HT SNK
    50.07 ADC    BATT AMPS                    30.00 DEG C  T5-T501 TOP
    19.07 N-M    TORQUE                       44.00 DEG C  T6-T502 CORE
  2640.00 WATTS  WATTMETER 1                  36.00 DEG C  T7-FRONT HT SN
  6800.00 WATTS  WATTMETER 2                  26.00 DEG C  T8-BACK HT SNK
     1.30 V/HZ   VOLTS/HZ                     19.00 DEG C  T9-D501, D502
          VRMS   LINE VOLTS                   22.00 DEG C  T10-BOTTOM HS
          ARMS   LINE CURRENT                 27.00 DEG C  T11-T501 BOTTOi
     0.75 HZ     SLIP                         19.00 DEG C  T12-ROOM TEMP
    70.91 HZ     STATOR FREQUENCY          -123.12 WATTS   PWR AUX BATT
    70.20 %      DUTY CYCLE                9744.02 WATTS   PWR DC
     6.00        NOTCH NO.                 9440.00 WATTS   PWR AC
    14.30 VDC    AUX BATT VOLTS            8410.96 WATTS   PWR MECH
    -8.61 ADC    AUX BATT AMPS
  2104.84 RPM    DYNO SPEED
    89.09 %      EFF MOTOR
    96.87 %      EFF INVERTER
    86.31 %      EFF OVERALL
```

Figure 10.2.3 Sample Output Display

Definitions of the computed variables given here:

1. Battery power
   battery power = battery volts * battery current

2. Inverter power ("two wattmeter method")
   inverter power = Phase 1 watts + Phase 2 watts

3. Mechanical output power
   mechanical power = (2* /60) * $\frac{\text{motor RPM}}{\text{gear ratio}}$ * transaxle torque

4. Auxiliary battery power
   aux. battery power = aux. battery volts * aux. battery current

5. Mechanical efficiency
   mechanical eff. (%) = (mechanical power/inverter power) * 100

6. Inverter efficiency
   inverter efficiency (%) = (inverter power/battery power) * 100

7. Overall efficiency
   overall efficiency (%) = (mechanical power/battery power) * 100

8. Slip
   slip = stator frequency - (motor RPM/60)

9. Transaxle speed
   transaxle speed = motor RPM/gear ratio
   gear ratios: 28.8:1 and 10.75:1

TABLE 10.1
PROPULSION SYSTEM VARIABLES AND DYNAMIC RANGES

NAME	RANGE	UNITS
Motor Speed	0-12,700	RPM
Transaxle Speed	0-1,508	RPM
Battery Voltage	125-300	VDC avg.
Battery Current	± 300	ADC avg.
Motor Torque [1]	± 60	NM
Transaxle Torque [2]	± 1,600	NM
Watts (1 & 2)	± 40,000	Watts
Volts-per-Hertz	3.00	V/HZ
Line-to-Line Voltage	0-150	VRMS
Single Phase Current	0-250	ARMS
Stator Frequency	0-400	Hz
Slip	± 8	Hz
Duty Cycle	0-100	Percent
Gear	Low, High, Neutral	
Temperature (10)	0-300	°C
Notch Number	0-32	Notches
Efficiency (3)	0-110	Percent
Power (4)	50,000	Watts
Aux. Battery Voltage	0-16	VDC avg.
Aux. Battery Current	0-±50	ADC avg.
Dyno Speed	0-6000	RPM

Notes:
1. Available on torque table only.
2. Two transducer ranges available.
3. Precision at slow update rate (update 1/sec).

10.3 Test Results

Detailed tests performed under this task are described below.

10.3.1 Torque Table Tests

During these tests, the basic electrical system performance was verified. Specific areas of testing on the torque table are listed below.

- The motor/inverter torque vs. speed limits were determined for motoring and regenerating. Inverter peak currents were determined at the torque limits.
- Bridge transistor safe switching was verified for extreme conditions. The correct snubber requirements were determined.
- Adequate system protection for overloads and cutouts under microprocessor control were verified.
- The motor and inverter steady-state efficiency was optimized for V/Hz, slip, and notch number over the system operating range. Final motor/inverter efficiencies were documented.
- The inverter thermal performance was verified.

10.3.1.1 Inverter Development Tests

The purpose of these tests was to verify the operation of the inverter bridge circuitry when driving the motor. The concept of the DC bus snubber inductor with the coupled energy recovery winding was tested. Final performance tests for this phase were conducted at peak torque. Although the tests were conducted in this phase, the relevant waveforms are presented and discussed in Section 6 on the inverter.

As a result of this development testing, the final base drive protection strategy was resolved. Specifically, the need for an overvoltage sensor on the C501 bus clamping capacitor was determined, and the strategy of shutting the inverter down upon detecting a motor current peak was worked out. The overvoltage sensor is needed because erratic system operation during motoring and heavy loading during regeneration or battery charging can cause this capacitor voltage to rise above safe levels. The need for a permanent shutdown for peak motor current tripouts was discovered when it was found that the system cannot run in a repetitive peak current limit mode with the new PWM scheme.

A further result of these development tests was that the ability of the inverter to run without local snubber capacitors was proven. Elimination of these snubbers results in a considerable improvement in inverter efficiency.

10.3.1.2 Motor/Inverter Torque vs. Speed Performance Tests

The purpose of this test was to verify the peak torque capability of the motor under inverter power as a function of motor speed. Peak transistor currents were recorded, along with transistor voltage waveforms during these tests.

The system was run both with the test stand battery charger on (in order to determine maximum system capability) and with the battery alone to determine system degradation vs. battery voltage.

The torque vs. speed curve obtained at the nominal 192-volt bus is shown in Figure 10.3.1. It is seen that 2 x rated torque was achieved between 10 Hz and 94 Hz. This torque level, being achieved at 192 volts, is adequate for vehicle operation at the 1.8 x rated torque goal down to 172 volts bus. Beyond the 94 Hz base frequency, the constant 45 hp operation can be seen in Figure 10.3.1, which is also sufficient.

However, a significant drop in torque is exhibited below 10 Hz and is due to instabilities in the motor currents causing inverter current trips. These instabilities must be corrected with future controller improvements in order to achieve adequate vehicle starting torques.

For the system running at 48 pulses of the PWM waveform per stator cycle and for the torques shown in Figure 10.3.1, the peak current was measured at 320 amps and is well within the inverter peak current capability.

10.3.1.3 Motor/Inverter Efficiency Optimization

This test was intended to empirically determine the most efficient operating curves for the combination motor and inverter as a function of V/Hz, slip, and notch number. The optimum curves are stored in controller memory for use in the driving cycle. These tests were run as follows.

- To eliminate temperature effects, the motor was run until motor temperature reached a stable state. To eliminate the effect of DC bus voltage changes, the DC bus was supported with the battery charger.

- For rotor frequencies of 25, 50, 75, 94, 125, 150, and 200 Hz, the motor was run from zero to maximum torque in 25 Hz increments.

- For each condition above, the V/Hz, slip, and notch number were adjusted to get maximum combined motor and inverter efficiency.

- Representative efficiency data points around the optimum were collected in order to plot the degradation. For each point, all CRT data displayed by the computer was collected and stored.

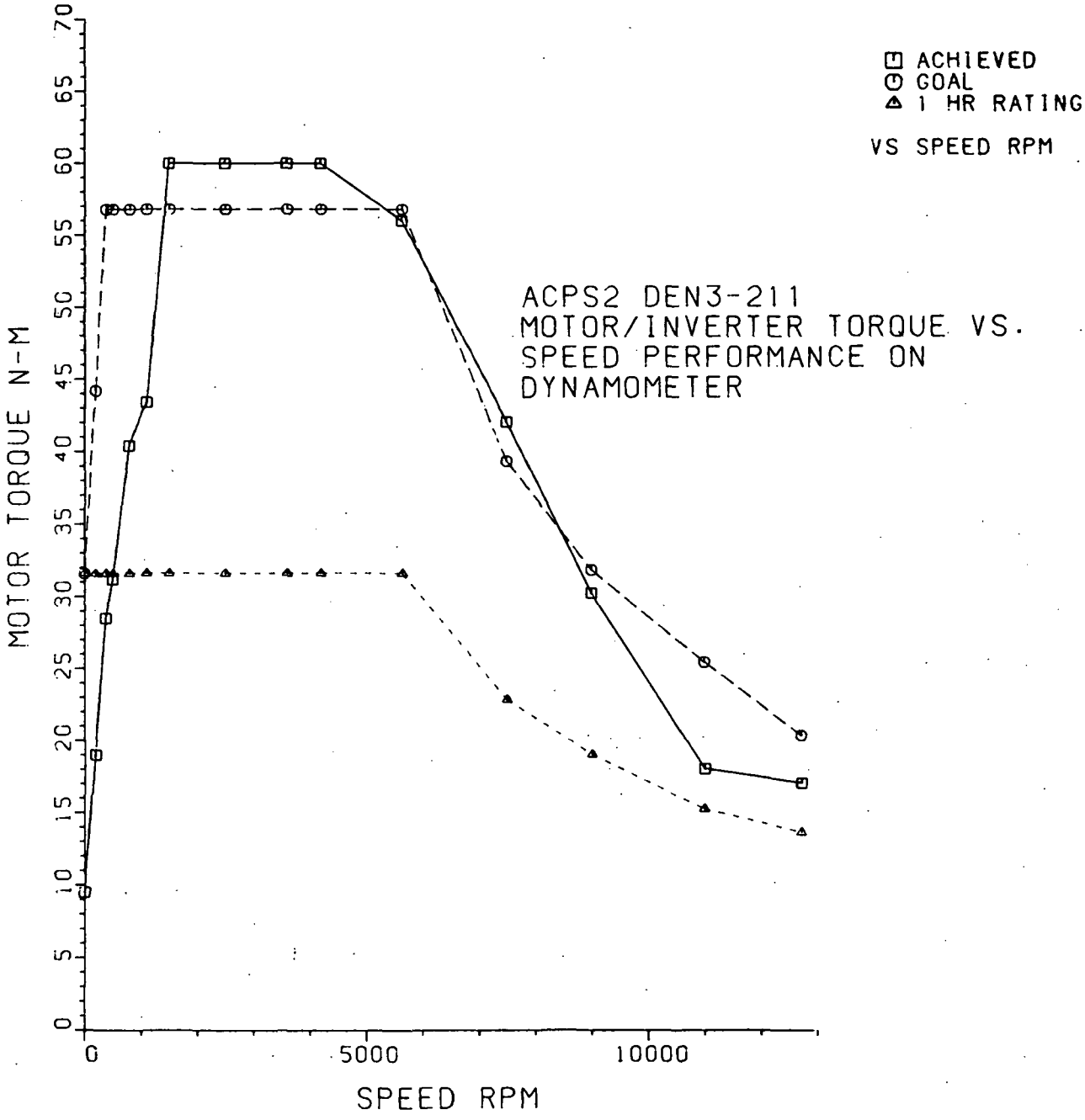

Figure 10.3.1 Motor/Inverter Torque/Speed Performance

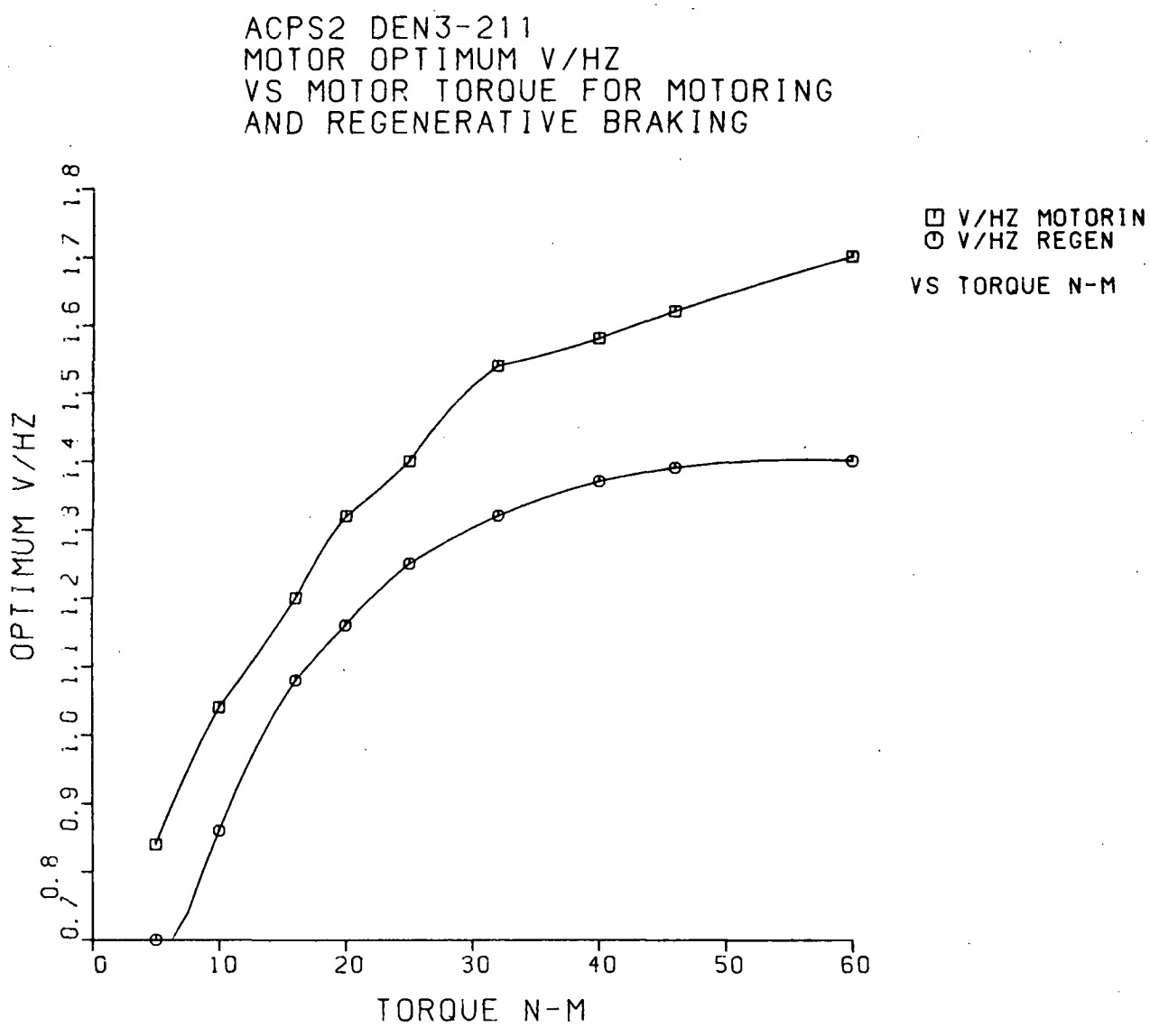
ACPS2 DEN3-211
MOTOR OPTIMUM V/HZ
VS MOTOR TORQUE FOR MOTORING
AND REGENERATIVE BRAKING
V/HZ MOTORIN
V/HZ REGEN
VS TORQUE N-M
OPTIMUM V/HZ
0.7
0.8
0.9
1.0
1.1
1.2
1.3
1.4
1.5
1.6
1.7
1.8
0
10
20
30
40
50
60
TORQUE N-M

Figure 10.3.2

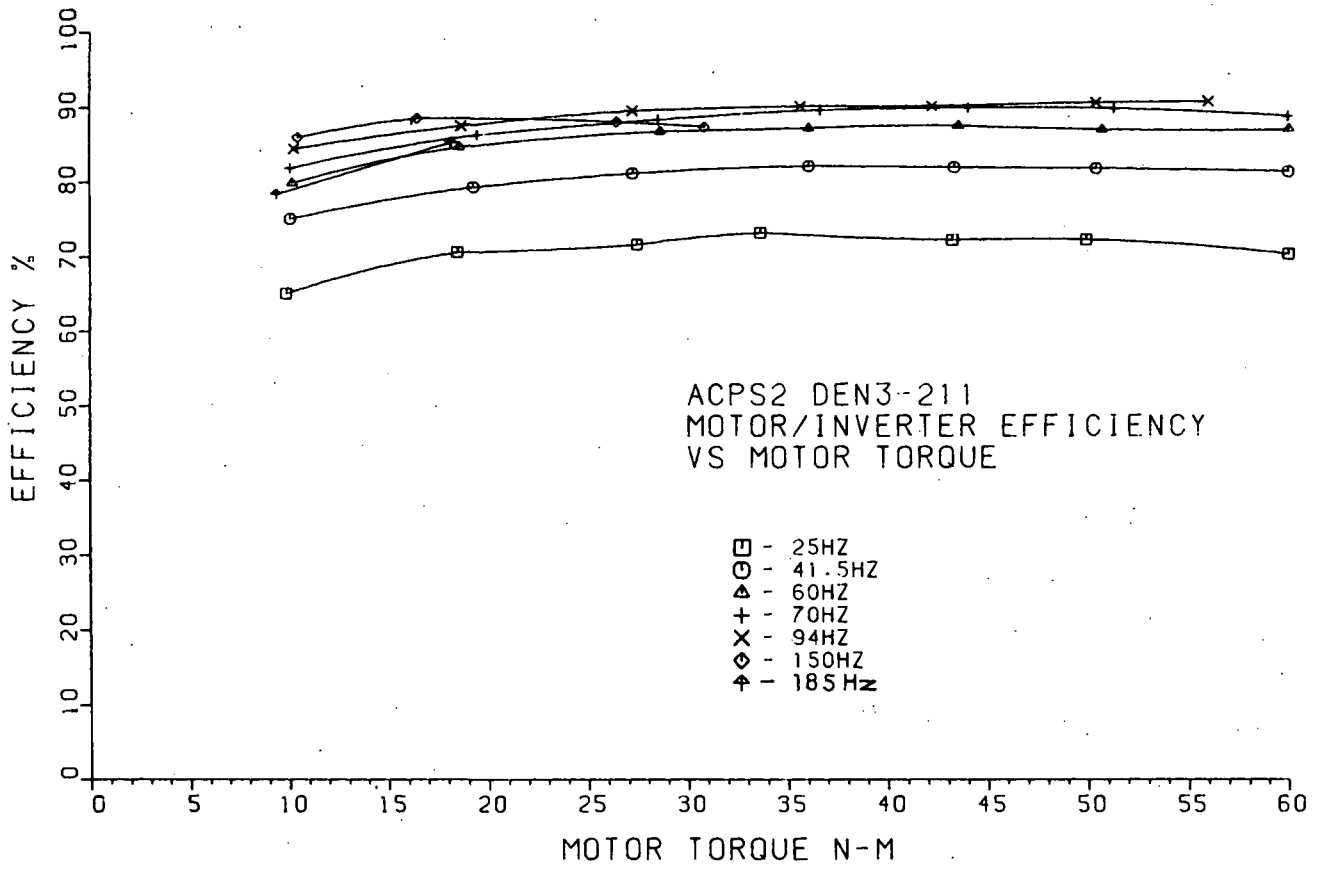

Figure 10.3.3 Motor/Inverter Efficiency Vs. Motor Torque

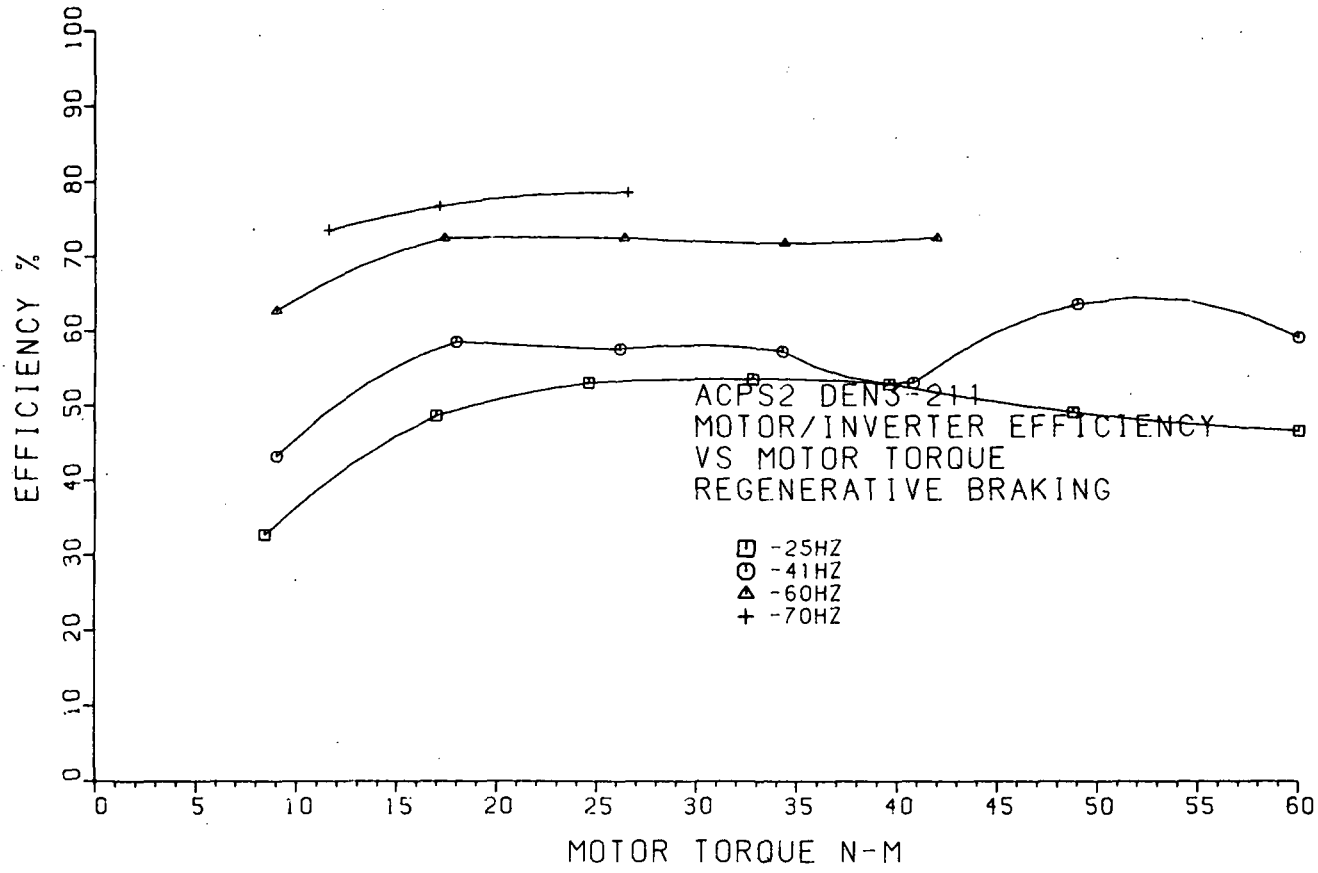

Figure 10.3.4 Motor/Inverter Efficiency Vs. Motor Torque, Regenerative Braking

For the above efficiency optimization effort, over 350 separate data points were collected by the data acquisition system. The resulting motor optimum V/Hz at different stator frequencies versus motor torque is plotted in Figure 10.3.2.

The optimum pulse number per motor stator cycle of 48 was also determined from these tests.

The combined motor/inverter efficiencies obtained at the optimum V/Hz versus motor torque is shown in Figure 10.3.3. These efficiencies show dramatic improvements over the Phase I motor/inverter efficiencies. In addition to numerous inverter circuit improvements, which have been described in Section 6, the increase in motor/inverter efficiency in Phase II can be attributed to the improved PWM scheme which reduces motor harmonic losses.

Only limited efficiency data was collected for regenerative braking because of scheduling deadlines for the propulsion system installation in the vehicle. These data are plotted versus motor torque in Figure 10.3.4. These efficiencies are also significantly higher than those in Phase I.

10.3.1.4 Inverter and Motor Thermal Performance

The purpose of this test was to ensure that the motor and inverter can meet their continuous power ratings without exceeding their thermal ratings. The test was run with the motor oil flow set to 0.5 gal./min. The inverter cover was in place and the inverter fan was running through a cowl which was designed to simulate the expected air flow rate along the inverter heat sink. Thermocouples were placed at strategic places in the inverter, on the motor case, and in the motor inlet and exit oil lines.

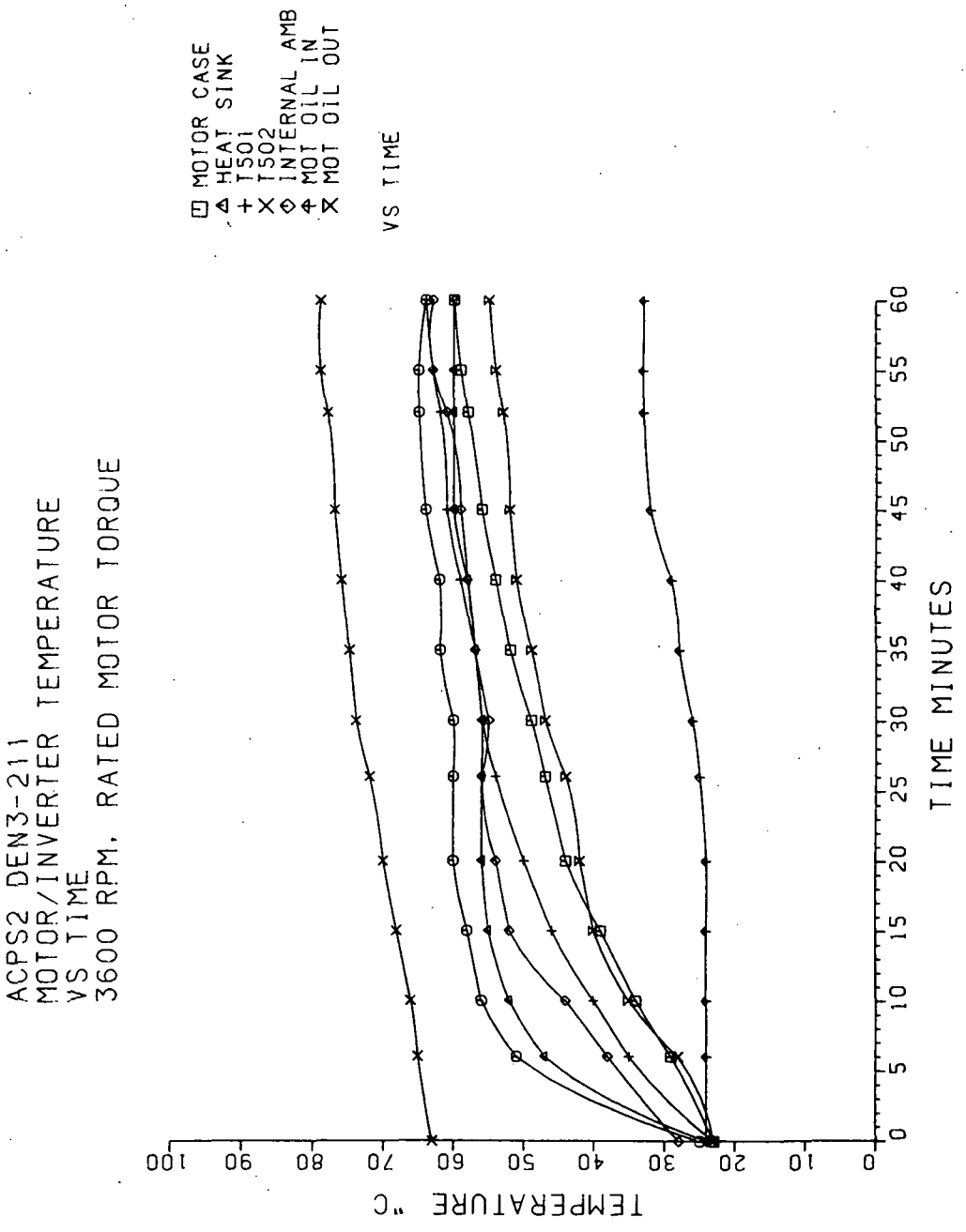

Figure 10.3.5 Motor/Inverter Component Temperatures Vs. Time, 3600 rpm, Rated Torque

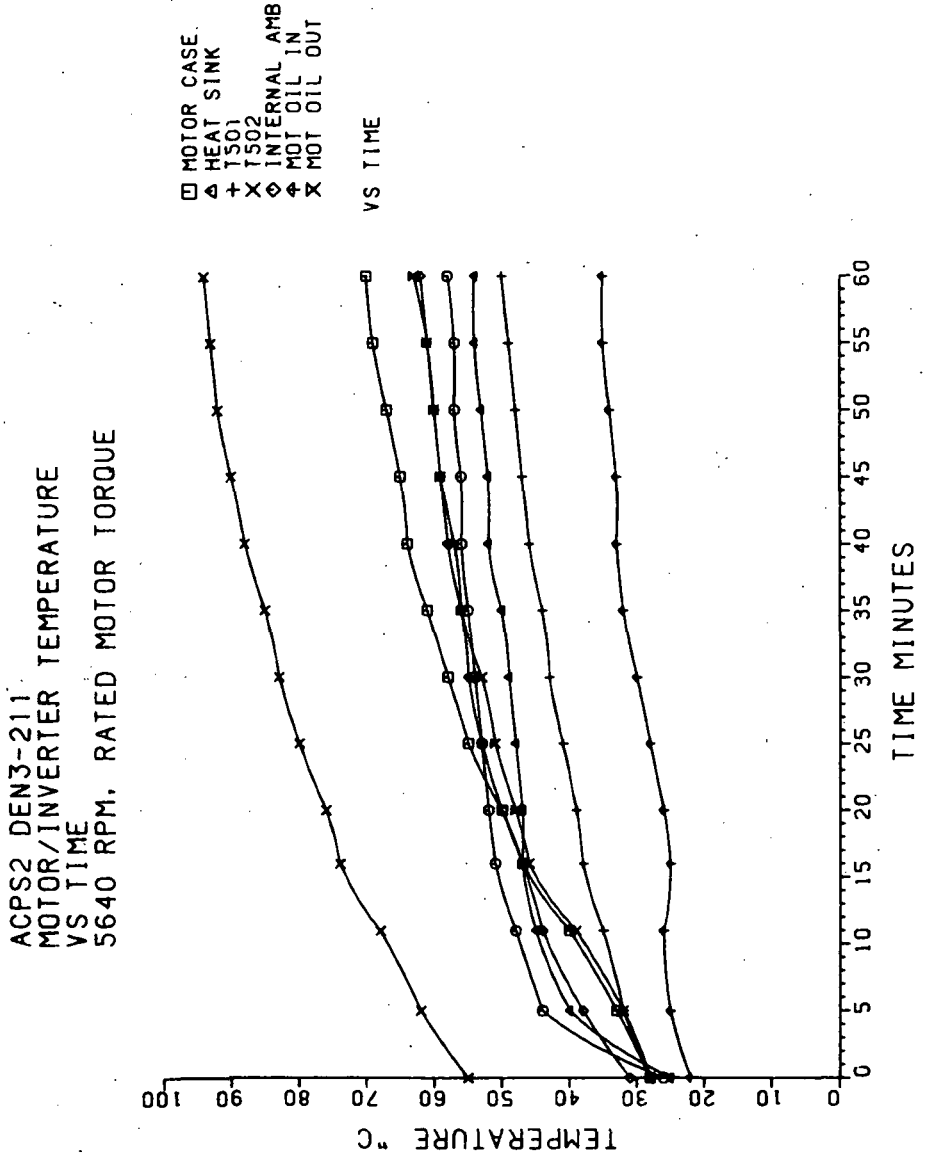

Figure 10.3.6 Motor/Inverter Component Temperature Vs. Time, 5640 rpm, Rated Torque

Two separate one-hour heat runs were made: one at rated torque and 3,600 motor rpm's and the other at rated torque and 5,640 rpm. The temperature vs. time of the various components monitored for the two above conditions are plotted in Figures 10.3.5 and 10.3.6. It was found that all of the inverter components ran within their thermal ratings.

Although the motor case temperature rise for both the above tests indicates acceptable performance, the result is inconclusive because of the unrepresentative oil system setup, which circulated oil through a heat exchanger. A more representative test, in which the motor/transaxle are run with a closed oil system is described in Section 10.3.3. A discussion of the motor thermal performance for the above motor test is given in Section 5.

10.3.2 AC Drivetrain Testing and Characterization (Transaxle/Motor/Inverter/Controller)

During these tests, the total propulsion system performance was characterized on the dynamometer. Final system adjustments were made prior to vehicle installation. Specific areas of testing in this phase are listed below.

- Final system efficiencies were measured throughout the torque-speed range in low and high gears. Independent transaxle efficiency tests were later run to confirm calculated efficiency for this component and to help fil in any gaps in the system efficiency maps.

- The system was run in "normal" mode and stable operation was verified.

- The thermal performance of the system was checked.

- The gearshift sequence was refined.

10.3.2.1 System Efficiency

This test was intended to generate system efficiency maps over the system operating range. Additional system efficiency information was obtained by combining the results of the torque table tests with the transaxle alone tests.

The combined motor/inverter/transaxle efficiencies for low gear are plotted in Figure 10.3.7. Those for high gear are plotted in Figure 10.3.8. The high gear curves were supplemented with data from separate torque table and transaxle alone tests to form a more complete efficiency map. Although the efficiencies shown are improved from Phase I, more marked improvements are

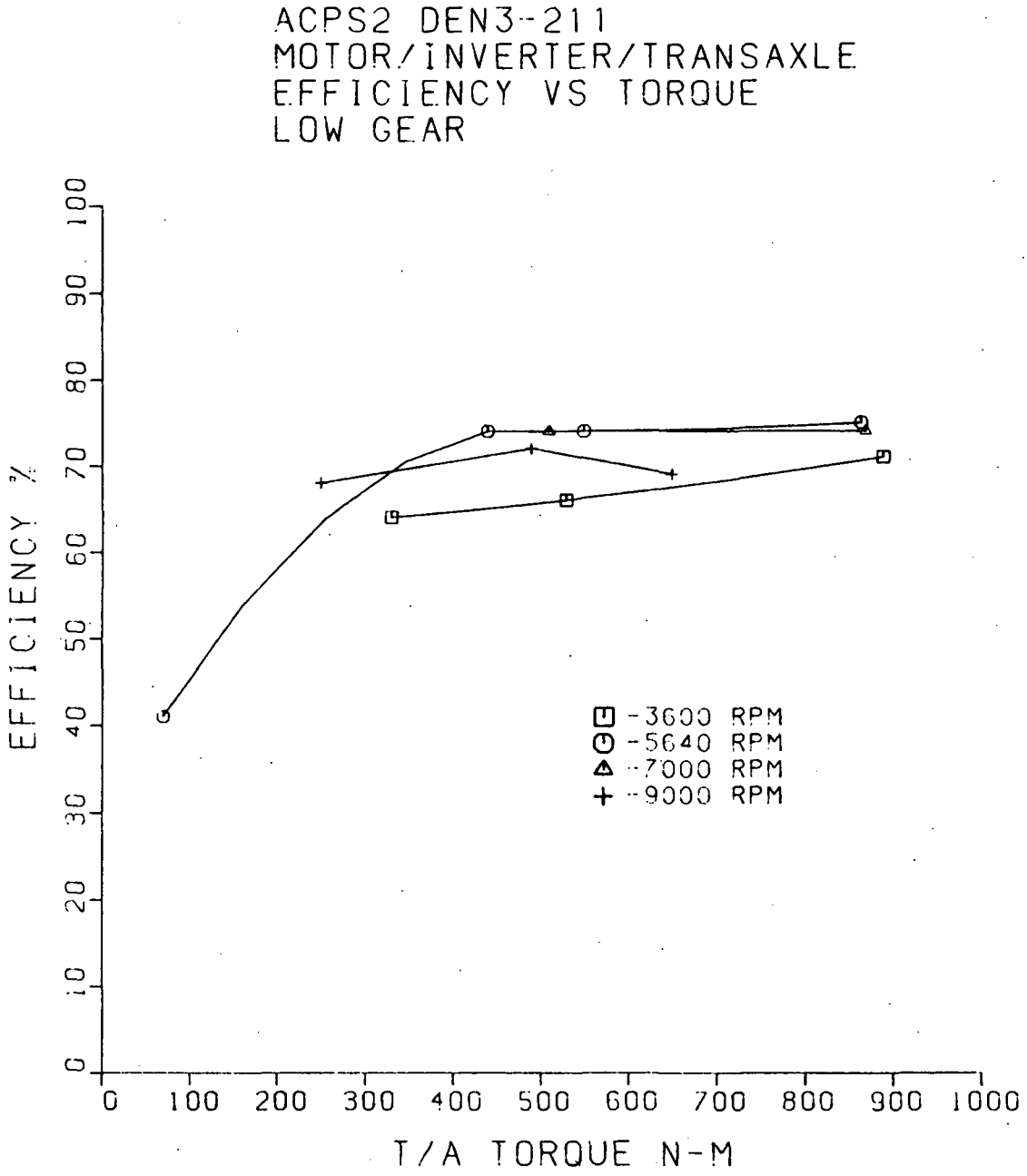
ACPS2 DEN3--211
MOTOR/INVERTER/TRANSAXLE
EFFICIENCY VS TORQUE
LOW GEAR
EFFICIENCY %
0
10
20
30
40
50
60
70
80
90
100
0
100
200
300
400
500
600
700
800
900
1000
T/A TORQUE N-M
-3600 RPM
-5640 RPM
-7000 RPM
-9000 RPM

Figure 10.3.7

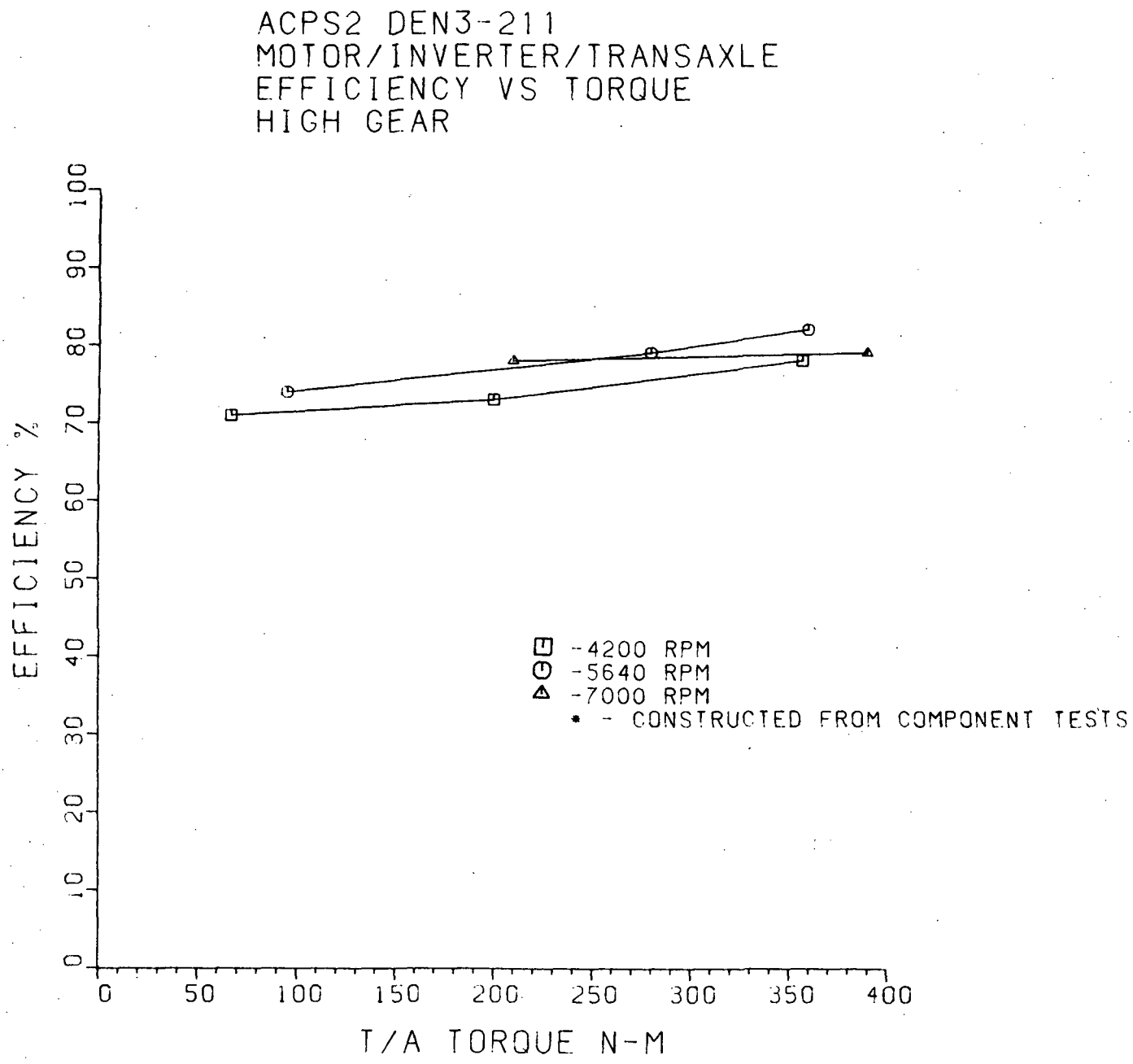
ACPS2 DEN3-211
MOTOR/INVERTER/TRANSAXLE
EFFICIENCY VS TORQUE
HIGH GEAR
EFFICIENCY %
0
10
20
30
40
50
60
70
80
90
100
0
50
100
150
200
250
300
350
400
T/A TORQUE N-M
-4200 RPM
-5640 RPM
-7000 RPM
* - CONSTRUCTED FROM COMPONENT TESTS

Figure 10.3.8

possible with improvements in the transaxle which were discussed in Section 4.

10.3.2.2 Temperature Effects

The purpose of this test was to determine the temperature rise of system components, and to evaluate the closed oil cooling system while running continuously at various power levels. Except for the closed cooling system, this test was similar to that run during the torque table test. A fan was provided to simulate normal vehicle air flow on the transaxle. One continuous test was run at 5,640 rpm for 25 minutes. (Further testing was not permitted due to the vehicle installation deadline.) The test was run in low gear, as this was the expected worst case.

The temperature versus time of the system components are shown in Figure 10.3.9.

The component temperatures, as shown, are well within their thermal ratings and, thus, safe thermal performance in the vehicle was predicted.

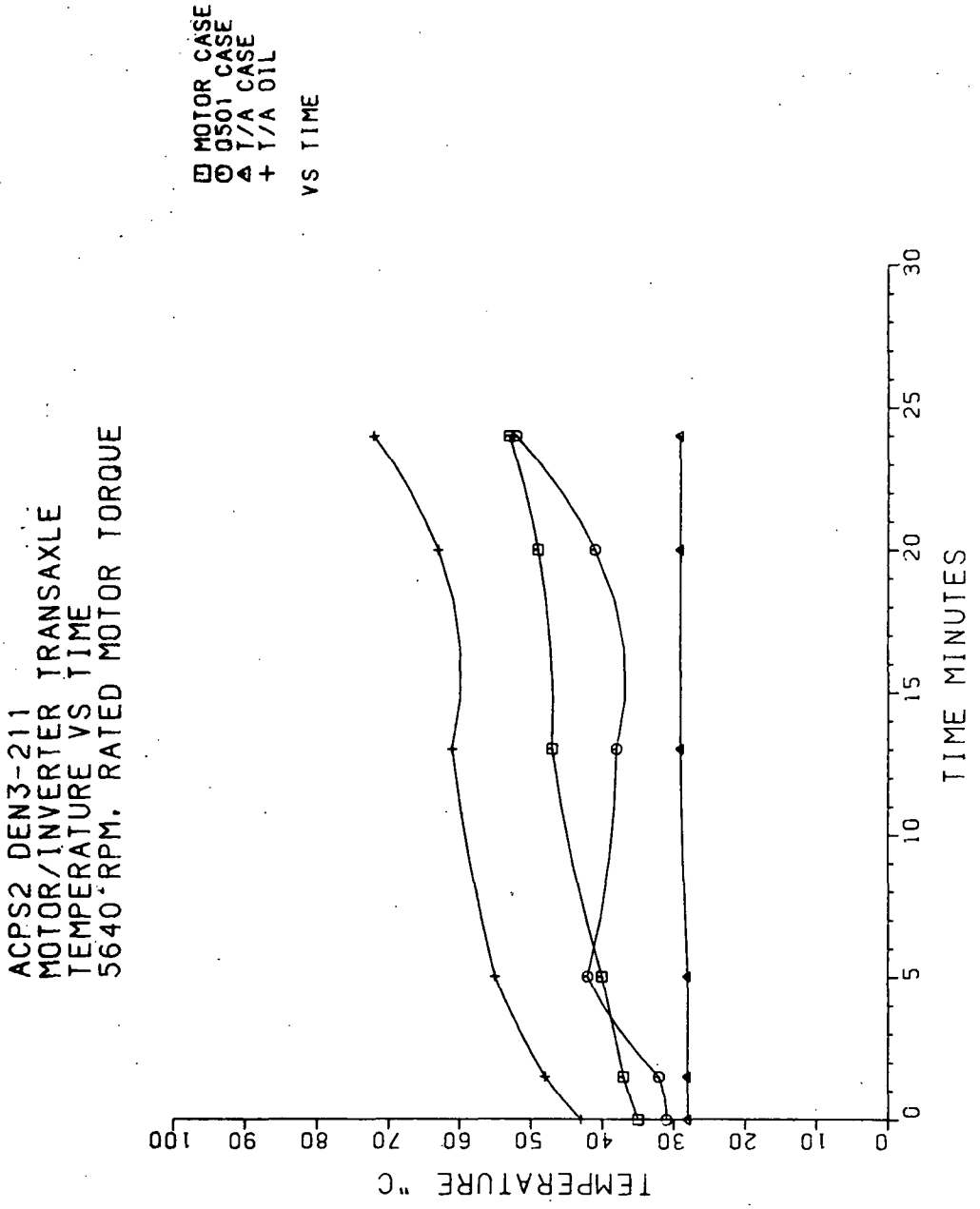

Figure 10.3.9 System Component Temperature Vs. Time Closed Motor/Transaxle Oil Circulation

10.3.2.3 Shift Sequence Refinement and Testing

The purpose of this test was to ensure stable operation of the system during the gearshifting sequence. Most of the gearshift refinement was done during the vehicle tests on chassis dynamometer rolls and on the road, and only initial gearshift checkout was done on the dynamometer. Thus, these tests are described in Section 11 on the vehicle tests.

11.0 VEHICLE TESTS

11.1 Overview of Tests

This section details the vehicle performance tests for the propulsion system. Testing involved:

- general driveability,
- adjustment to and evaluation of the gearshift and startup sequence,
- maximum regenerative braking,
- acceleration and gradeability,
- steady-state high speed, and
- expended energy on a per km or per drive cycle basis.

Guidelines for much of the testing is from SAE J227a recommended practice and from NASA TM-73757 Appendices D and E. Except for the general driveability and the gearshift and startup, the testing took place at Eaton's Marshall Proving Grounds.

A summary of tests performed is given below:

11.1.1 General Driveability

The general driveability test emphasized safe vehicle operation as well as handling, performance, and driving impressions. This activity was accomplished near Eaton's Engineering and Research Center in Southfield, Michigan, where developmental work and instrument checks could be made.

11.1.2 Gearshift and Startup

Much of the gearshift and startup tests were developmental in nature. The shift sequence was refined on chassis dynamometer rolls, where motor speed, clutch pressures, and shift actuations could be monitored with a strip chart recorder. Initial startup tests were also done on the chassis dynamometer. Final evaluation of both gearshift and startup were done on the road.

11.1.3 Regenerative Braking

This test was conducted at the Proving Grounds, where a level road surface was available to determine maximum regenerative braking. This determination is a function of the state of charge of the batteries and could be controlled manually by the driver/operator. The resultant rate of deceleration was the maximum that could be obtained in the regenerative mode.

11.1.4 Acceleration Tests

Acceleration tests were run on a level surface, one run each in opposite direction. Maximum acceleration on fully-

charged batteries was recorded. This test also included acceleration runs at battery states-of-charge of 60% and 30%. (The Standard SAE J227a specification of 20% capacity was not used because of the increased risk of damage to the EV-800 battery used in the test vehicle and the low energy available at 80% discharge.) This test determined the degree of comformance to the statement of work goals of 0 to 48 km/hr. (30 mph) within 8 seconds and from 40 to 88 km/hr. (25 to 55 mph) within 16 seconds. Also, from the acceleration data with fully-charged batteries, compliance to the gradeability requirement to attain a 64 km/hr. (40 mph) speed on a 4% grade and acceleration from rest to a speed of 64 km/hr. (40 mph) on a 4% grade within 305 m (1,000 ft.) was determined analytically. This data also was used to compute the maximum grade attainable at 8 km/hr. (5 mph).

11.1.5 High Speed Test

The high-speed run was conducted on the Proving Ground track. The speed goal was 105 km/hr. (65 mph), but since the run was made on the track, which isn't level at all points, a speed variation to a maximum of 113 km/hr. (70 mph) was allowed to assure a minimum of 105 km/hr. (65 mph) during the 5 km (3 mile) duration of the test.

11.1.6 Expended Energy

The expended energy test was run in two modes. One was a steady speed run conducted at three different speeds. The second run used the SAE Schedule D driving cycle as specified in J227a. The purpose of these tests was to measure the kw-hr per km demand for each driving test run. These tests were conducted on the level section of the track where opposite direction runs could be made.

11.1.7 Road Load Determination

Separate coast down and drawbar tests were performed in order to determine the vehicle road load. These tests were needed for proper interpretation of the peak acceleration and expended energy tests. It was found that the vehicle exhibited an abnormally high road load which degraded these test results.

11.2 Vehicle Preparation, Ambient Conditions, and Instrumentation

- The vehicle was tested in a normal and complete configuration.
- Front end alignment was checked as required before testing.

- The tests were conducted at test vehicle weight (TVW), which is curb weight plus approximately 227 kg (500 lbs.). Actual TVW was recorded before each test. Weight distribution was approximately 50/50%.

- Tires and tire pressure(s) were determined from ride handling development by Triad Services, Inc., and were 36 psi front and rear.

- Normal lubricants were used and maintained at proper levels.

- A log of mileage, test vehicle weight, tests run, system-on time, battery pack used, and any change in equipment or developmental tasks was maintained.

- The fifth wheel tire pressure was checked before each test series.

- Wind direction, wind speed, and ambient temperature in the track vicinity were recorded before each test series.

- Instrumentation calibration checks were done before critical tests.

Environmental Conditions

- Vehicle soak temperature for instrumented road tests ranged between 10-32°C (50-90°F).

- Wind velocity at the test site was not to exceed 16 km/hr. (10 mph), if possible.

- All tests on straightaways were run in opposite directions. Tests run on the closed track were not required to run in opposite directions unless otherwise specified.

- All measured performance tests were used as required on the vehicle to gather data.

Test Instrumentation

The following portable instruments were used as required on the vehicle to gather data.

- 4-Channel FM Cassette Recorder (abbreviated "CR")
  This unit, Teac Model R-61, has a bandwidth of 0.625 kHz and a calibration accuracy of 1% F.S. Analog signals were conditioned and scaled by conditioning circuits. One channel was for test identification control and three were for data acquisition.

- Eaton Mobile Test Laboratory
  This laboratory is a specially-converted G.M. van with computerized data reduction capabilities. The cassette tapes with test data were digitized on site with this facility so that immediate feedback on test results was possible.

- 4-Channel Portable Strip Chart Recorder (abbrev. "SCR")
  This unit, Gould Model TR444, has a bandwidth of 30 Hz @ 50 divisions and typically can be read to 4% F.S.

- Fifth Wheel (abbreviated "FW")
  This unit, Nucleus Model NC-7, can measure velocity to 241 km/hr. (150 mph) @ 0.5% accuracy and distance to $\pm$ 1 count. Analog velocity output and pulse train (accumulated sum proportional to distance) available along with digital readouts for velocity and distance.

- Portable Digital Voltmeter (abbreviated "DVM")

- Special Purpose Diagnostic Box (abbreviated "DB")
  This unit, built to monitor all important propulsion system variables used by the controller, is useful for monitoring torque demand, system temperature sensors, gear select status, motor speed, etc. It has four analog outputs where any signal can be output to the SCR or CR.

- Thermocouple Array (abbreviated "TCA")
  Independent thermocouples, a scanning switch, and portable analog "Minimite" meter monitored:
  - transaxle case
  - transaxle oil
  - front and rear battery pack internal ambient
  - ambient temperature in car

  Inverter heat sink temperature was read through the diagnostic box. Readings are recorded manually.

- A small gasoline-powered Honda portable generator, Model EM 400, provided 110 VAC 60 Hz instrumentation power (SCR, Analog power supply).

- Float Hydrometer for measuring battery electrolyte specific gravity.

Test Data

Table 11.1 shows the variables and data to be recorded. Such items as vehicle identification, battery identification, tire pressure and type, ambient temperature, wind velocity, etc., were routinely recorded.

TABLE 11.1

VARIABLE	ABBREV.	UNITS	MEASURING INSTRUMENT(S)	EXPECTED ACCURACY	COMMENTS
Veh. test weight	VTW	kg (lb)	Vehicle Scale	2% of F.S.	Measured for each test configuration w/instrumentation and passengers.
Veh. speed	VS	km/hr(mph)	FW	0.5 km/hr	Recorded on SCR, CR or manually for FW readout as test requires.
			FW, CR	1.0 km/hr	
Veh. distance	X	km(mi)	FW, Post processing of CR tape of Veh. speed.	0.02 km	Determined by digital integration of VS.
Bus Voltage	VBUS	Volts	Attenuator, isolation amp, SCR	5%	
			DVM, CR	1% of F.S.	
Bus Current	IBUS	amps	FW Bell ID 5031M, amplifier, SCR	5% of F.S.	
			DVM	2% of F.S.	
			CR	3% of F.S.	
Bus Power	PBUS	watts	Post processing of CR tape of VBUS, IBUS	4% of F.S.	Digitize FM recorded data product of IBUS, VBUS
All temperature	Temp.	^{o}C	TCA	2^{o}C	Thermocouples
Battery Energy	ENBAT	kwhr	Post processing of CR tape of VBUS, IBUS	3% of F.S.	Determined by digital integration of PBVS.
Time	t	sec	Stopwatch	0.2 sec.	
			SCR	0.2 sec.	Improved at higher paper feed speeds.
			CR	0.1 sec.	

Battery state-of-charge information was required for several tests. Table 11.2 relates temperature-compensated electrolyte specific gravity to defined percent capacity and pack open circuit voltage (VBUSOC).

Table 11.2 Globe Union EV-800 Battery

Specific Gravity	% Capacity	Pack Open Circuit Voltage (VBUSOC)
greater than 1260	100%	greater than 204V
1235 ±5	60%	199 ±1V
1215 ±5	30%	195 ±1V

The temperature effect on VBUSOC is +32 mv/°C, which can be ignored. VBUSOC was measured only after any surface charge caused by charging was removed by briefly loading the battery. VBUSOC was used to determine capacity for acceleration, deceleration, and steady-state speed tests. Accuracy is considered adequate for the propulsion system characterization tests performed in this plan.

11.3 General Driveability Tests (at ERC)

The purpose of this test was to check out initial vehicle performance, in particular, safety of operation and correct any malfunctions.

The test procedure was to operate the vehicle on limited access or low traffic volume roads and make observations regarding general driveability.

No quantitative goals were specified for this test except that the data recording meet the accuracy listed in Table I. Evaluations were made on a subjective basis by knowledgeable engineers. Standard handling tests, for instance, were not run at this stage. The main purpose was to uncover unusual or dangerous handling situations early in vehicle use.

11.3.1 Results

Two vehicle related problems were found during this test sequence. The first problem of too low rear ground clearance was fixed by substitution of a longer spring in the rear suspension system. However, a problem of mushy service brakes, which was caused by the moving of the master cylinder from the fore wall for the vehicle modification, persisted throughout the vehicle test phase. This problem was finally solved by stiffening the mounting brackets for the master cylinder and brake linkage components.

The overall vehicle handling including braking has been judged adequate for safe operation.

Other findings during this test sequence were as follows.

1. Response time to operator input of accelerator and decelerator controls was good. No operator/controller instabilities were noted and, except for the absence of motor braking torque with both the accelerator and brake pedals released, the vehicle had the feel of a conventional automobile in this respect.

2. Regenerative braking response was excellent and should take considerable wear away from the service brakes. The blending from regenerative to service braking was smooth and the transition between the two was imperceptible once the service brakes were rectified. A modification was made to regenerative braking in low gear so that peak motor torque is limited to half that allowed in high gear. This lower limit was added to give the operator the same brake pedal "feel" in both gears and also to reduce suspected high stress torques from the motor to the transaxle in low gear.

3. Although transaxle gearshifting was smooth relative to some existing automatic transmissions in conventional automobiles, there was considerable dead time (2 seconds) during the upshift, when the vehicle was unpowered. In addition, occasional inverter tripouts which momentarily disabled the vehicle were noted. Overall shift quality is discussed in the next section.

4. Vehicle startup from standstill was adequately smooth, but zero speed starting torque was inadequate and a hesitation was noted before full vehicle acceleration was achieved. Startup refinement is discussed in section 11.4.

11.3.2 Gearshift Refinement and Testing

During this test sequence the speed and smoothness of the gearshift was improved to the extent possible with the existing transaxle and motor controller. The final gearshift quality was then evaluated to determine design limitations and to make recommendations for future work.

Testing was facilitated by the diagnostic box, which allowed changing of program constants without reprogramming the controller EPROM.

An oscillogram taken on the dynamometer rolls for the final upshift sequence is shown in Figure 11.1. The time intervals shown, along with the shift speed and motor torque demand during shifting could be entered from the diagnostics box during testing.

Referring to Figure 11.1, the upshift sequence is described as follows:

1. As the vehicle accelerates to a predetermined upshift speed, the shift sequence is begun by deenergizing the high gear clutch solenoid, so that the high gear clutch starts engaging. This action is started before releasing the low gear clutch, because of the relatively long engagement time compared to release time of the clutches.

2. After the interval, "KLAPU," has passed, the low gear solenoid is deenergized, which starts the release of the low gear clutch. During the "KLAPU" interval the low gear clutch is still engaged, so the motor torque demand is allowed to respond to operator demand from the accelerator. Thus, the "KLAPU" interval is intended to minimize the time when both clutches are disengaged.

3. During the interval, "KRLS," the motor torque demand is brought to zero. This interval is needed to allow for the actual release of the low gear clutch.

4. After the "KRLS" interval, the motor torque demand is set at the preset negative value which, with both clutches now released, forces the motor into a downward slew. This motor slewing is done until the motor speed becomes "synchronous" with the transmission input shaft speed in high gear. Near synchronous speed is achieved without a speed sensor on the transmission, because the vehicle inertia prevents vehicle speed from changing appreciably during the shift interval and, thus, the motor target speed can be calculated to be its low gear upshift speed divided by the high gear/low gear ratio change of 2.68.

5. When the motor has slewed to the target "synchronous" speed, the motor torque demand is set to zero until the total shift time interval "SHCNT" is passed. The "SHCNT" interval is the time from deenergization of the high gear solenoid to final engagement of the high gear clutch. At this time the shift is considered over and motor torque demand control is turned back to the operator. Operator accelerator control is resumed gradually so that step torque demands are not applied.

Although the above strategy resulted in reasonably smooth shifting most of the time, problems of consistency and reliability were apparent. In addition the upshift time was objectionably long, with the above slew interval lasting two seconds. Two limitations were discovered.

First, it was found that the high gear clutch engagement time varied between 1.2 to 2.5 seconds. This wide variation necessitated that the time intervals, "KLAPU" and "SHCNT" be set for the longest possible shift. Thus, the "KLAPU" interval was shortened to allow enough motor slew time when the high gear clutch comes in fast, and "SHCNT" was lengthened to allow for the longest clutch engagement time. An objectionably long shift resulted.

The second limitation to a fast shift was the long slew time of the motor. Although a theoretical slew time of 300 ms is possible with the unloaded motor, the slip loop microprocessor sample time slowed it to 600 ms.

It was not possible to address the above two limitations within the time and budget constraints of this phase of the program. They are prime candidates for follow-on work.

The strategy used for downshift is the same as for upshift except the motor speed must increase during the slewing period. For downshift the high gear/low gear solenoid overlap time has a separate designation "KLAPD," to provide independence in specifying this interval for upshift and downshift.

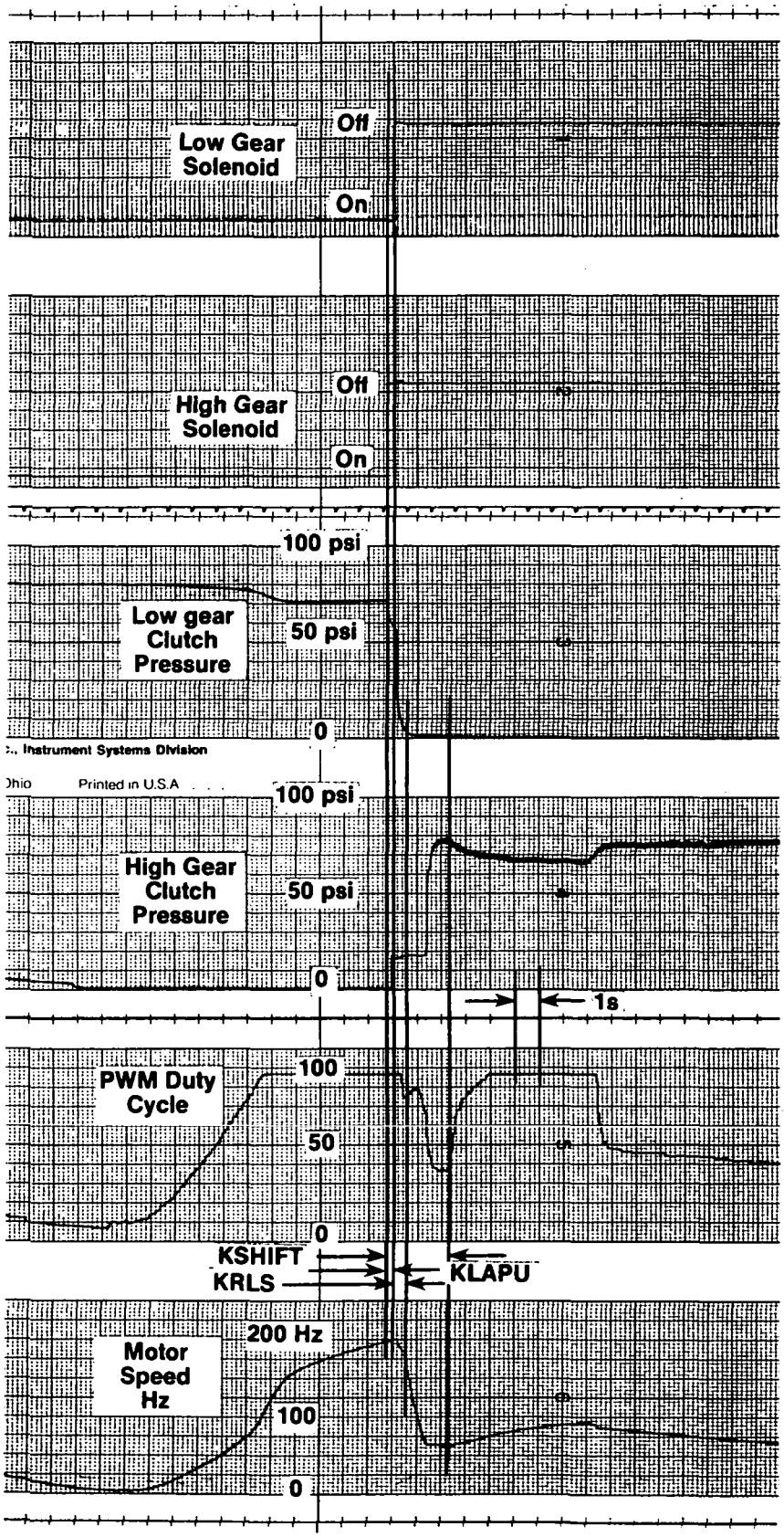

Figure 11.1 Vehicle Upshift Sequence

The controller logic provides for a downshift from high gear only if the vehicle speed is below 20 mph and the accelerator is depressed. Thus, for a normal deceleration to a full stop, the transmission will remain in high gear. This strategy avoids significant problems of jerkiness while downshifting with the brake pedal depressed.

The same problems described with upshift also apply for downshift and would need addressing in a future system.

11.3.3 Vehicle Startup

The vehicle startup was improved during this test phase, however, fundamental problems with reliability and achieving high starting torque were discovered which could not be solved in this time frame.

The test for evaluating startup took place on the roll dynamometer for getting instrumented results and on the road to determine actual performance. An initial evaluation of more fundamental problems was done by a simple computer simulation of the induction motor with vehicle inertia and basic control loops.

Adequate smoothness during startup was obtained by installation of a simple lag type digital filter in the controller calculation of duty cycle for the PWM waveform. This filter prevents abrupt changes in the motor flux level and helps stabilize the system at low torques.

However, this filter introduces a lag in the vehicle step response and detracts from its acceleration capability. In addition, the filter does not eliminate harmful resonances at high torque levels. Thus, it was necessary to restrain torque demand at zero vehicle speed.

By performing a simple simulation of the system under startup conditions it was possible to gain insight to some fundamental problems with this approach. Figure 11.2 shows a simulated vehicle startup under full closed loop V/Hz and slip control, which is ideally the case with this system. It is seen that the system is fairly stable with the motor current well within rated motor values. Thus, it would seem that the fundamental control approach is sound.

However, if voltage is allowed to take discrete steps, it is seen from Figure 11.3 that serious resonances arise. In Figure 11.3 the motor slip control is simulated but an input voltage step was assumed. This second case is a more realistic situation which reflects the digital quantizing error in the controller. These errors become more serious at slow speed because the smallest increment of change in controller duty cycle represents a large percentage of the operating value.

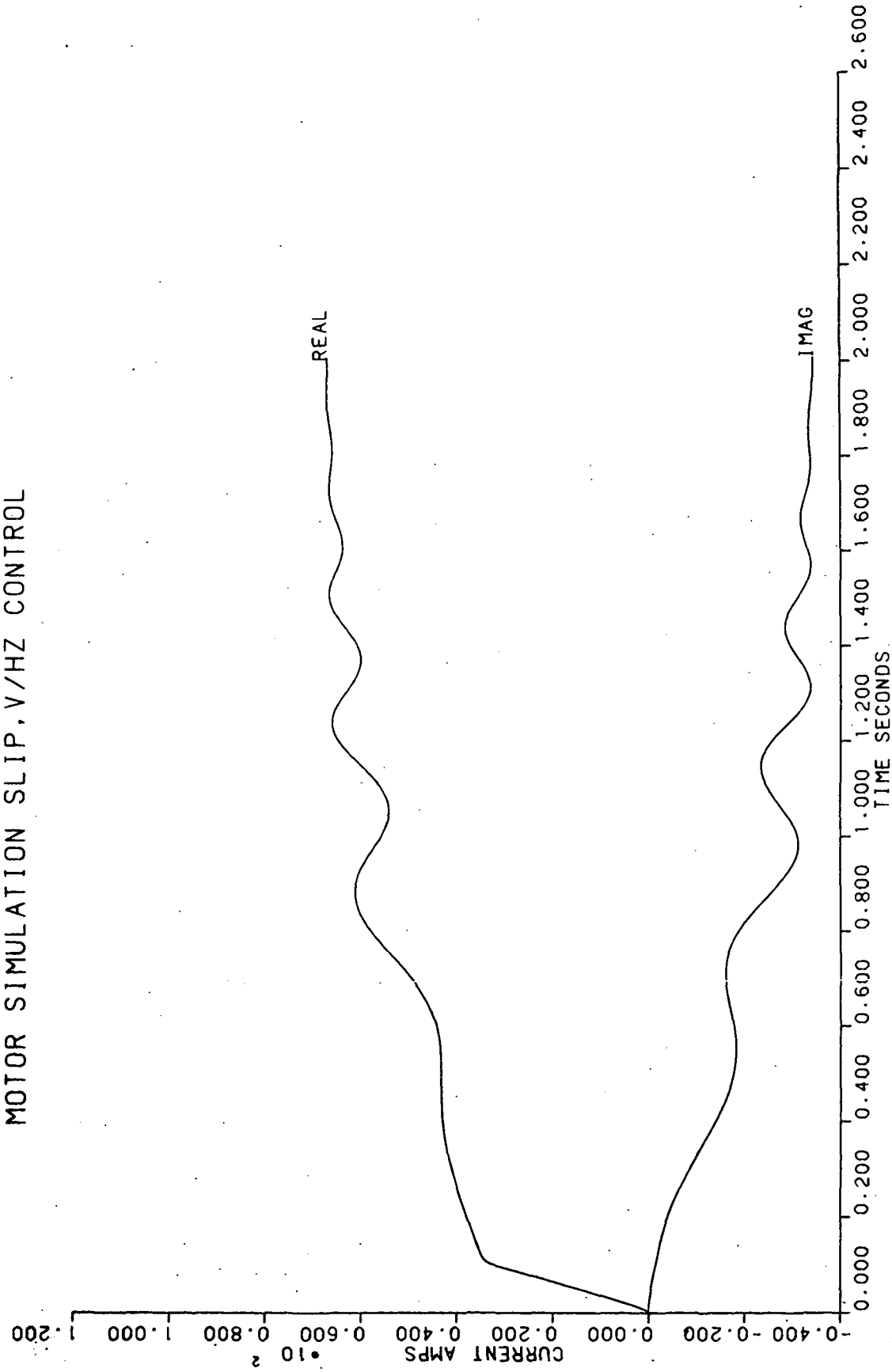

Figure 11.2 Motor Startup Simulation, V/Hz plus Slip Control

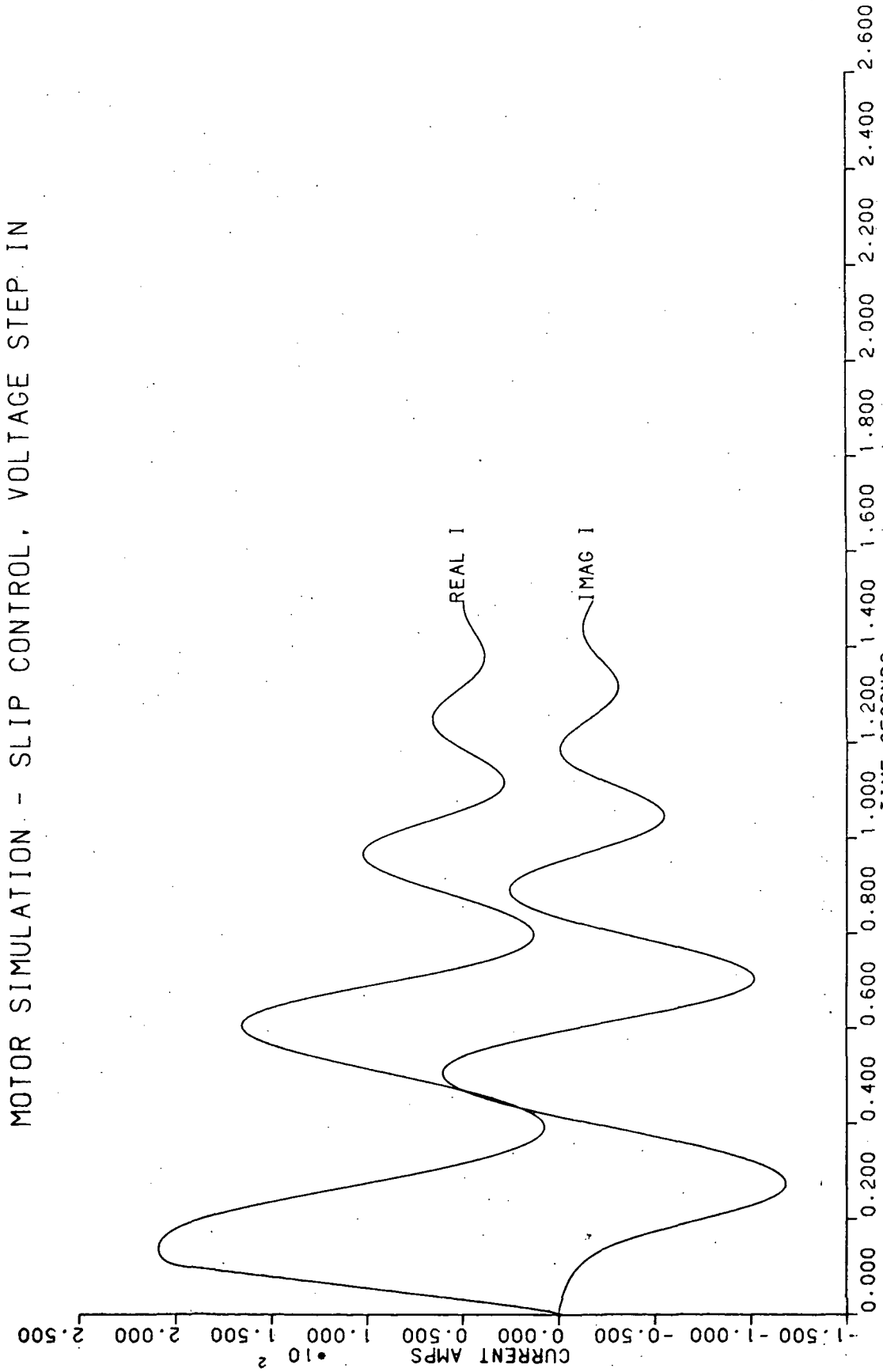

Figure 11.3 Motor Startup Simulation, Slip Control Only

The above analysis is by no means a complete evaluation of all aspects of the startup and control problems, and further work is needed to gain a full understanding. However, limitations in the control approach are now apparent and the need for further work in this area to obtain good low speed performance can be ascertained.

11.4 Proving Ground Tests

The following tests were conducted at the Marshall Proving Grounds. At this point no further adjustments were made to improve driveability.

11.4.1 Road Load Determination

These test results are reported first because knowledge of the vehicle road load is essential for interpretation of most other test results. Two methods of road load determination were attempted.

1. Coast down tests at Marshall
2. Low speed draw bar tests at ERC.

11.4.1.1 Coast down Tests

These tests were difficult to perform at Marshall, because of the lack of a sufficiently long straightaway to coast between the required 55 mph to 18 mph speeds. Thus, it was necessary to break each test up into two speeds - one between 55 mph and 30 mph, and another between 40 mph and 18 mph. The tests were conducted in opposite directions on the skid pad and the attached straightaway segment of the track.

An attempt was made to follow the EPA recommended procedure for this test except that time and the onset of bad weather did not permit the full 14 runs in each direction. In addition, the recommended 45 minute warmup was deleted in order to obtain the same vehicle road load that was encountered during the other tests.

The ambient temperature during these tests was 10°C, which resulted in a high rolling resistance. However, this temperature is approximately that also encountered during the expended energy and "D" cycle tests.

The composite velocity versus time from these tests is shown in Figure 11.4.1. The spread in the points is attributed to running the test in different directions, and to the fact that each run was necessarily split into a high speed and a low speed coast down.

Applying the "least squares" best curve fit thorough the data points in Figure 11.4.1 yielded a rolling resistance

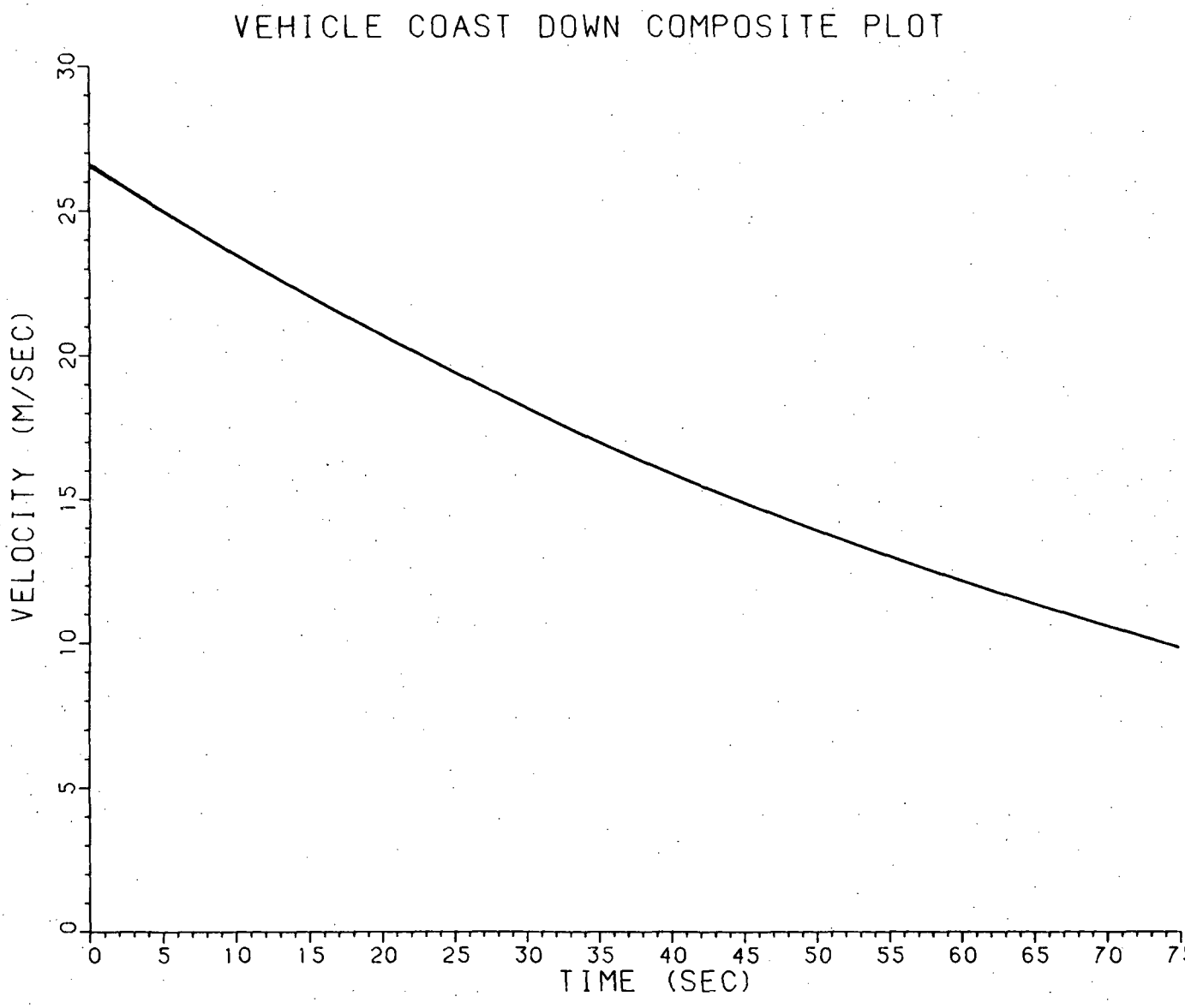
VEHICLE COAST DOWN COMPOSITE PLOT
VELOCITY (M/SEC)
0
5
10
15
20
25
30
TIME (SEC)
0
5
10
15
20
25
30
35
40
45
50
55
60
65
70
75

Figure 11.4.1

of 47.5 lbs and a drag coefficient of .467. No direct comparison of rolling resistance with the ETV-1 test vehicle[2] is available, because coastdown tests on this vehicle were performed with brakes removed. However, it is believed that this rolling resistance coefficient of .013 lbs/lb is about 25% higher than the ETV-1 and is attributed mainly to the low ambient temperature during testing.

The aerodynamic drag coefficient of .467 is 14% higher than the standard Escort and 45% higher than had been attained on the ETV-1 and on some production vehicles.[3] The high aerodynamic drag could be due to the custom grill or the A-frame that was mounted on the bumper to tow the vehicle.

The total road load computed at 45 mph for the Eaton vehicle is 195 wh/mile, which is 37% higher than that reported on the ETV-1 for this speed.

11.4.1.2 Draw Bar Tests

In order to get an independent determination of rolling resistance, the vehicle was towed at slow speed by a lift truck, and the towing force was measured by a force transducer. Multiple runs were made on a flat surface in the opposite directions. The ambient temperature was 4°C. The vehicle tires were allowed to cool to ambient temperature.

The rolling resistance determined from this test by averaging the force for each direction was 57 lbs. or 20% higher than that determined from the coastdown test and could be due to the lower ambient conditions.

11.4.1.3 Effects of High Road Load

In order to appreciate the added energy consumption of a high road load, two energy flow distribution diagrams are drawn for the Eaton system for steady state driving at 45 mph. The first diagram in Figure 11.4.2a shows predicted energy flow using the road load as measured on the coastdown test. The second diagram, Figure 11.4.2b, assumes that the ETV-1 road load of 142 wh/mile could be achieved. The component efficiencies shown were taken from the dynamometer tests. Comparison of the two diagrams shows that the road load alone in (a) is nearly equal to the total expended energy in (b).

11.4.2 Regenerative Braking Test

The purpose of this test was to determine the maximum deceleration of the test vehicle using the regenerative braking system only. The test was conducted on the skid pad at the Marshall Proving Ground.

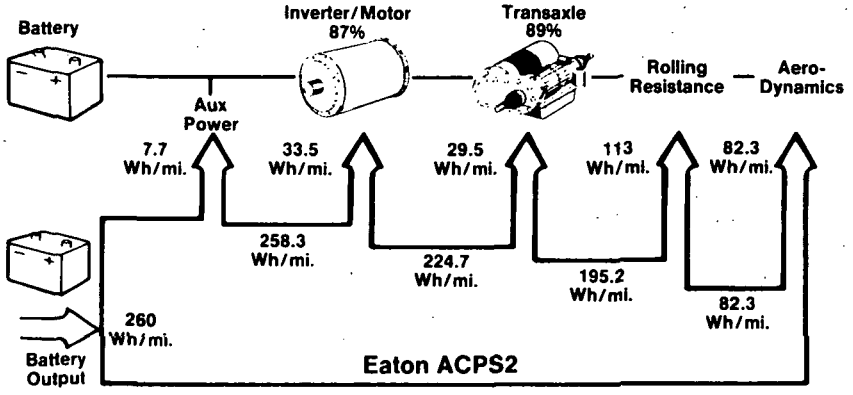

(a) Actual Road Load

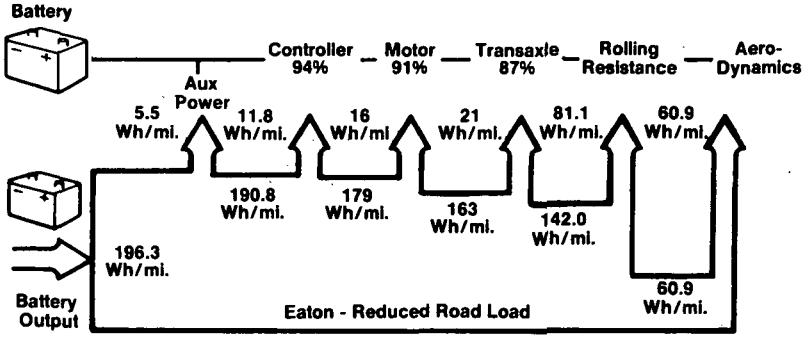

(b) Reduced Road Load

Figure 11.4.2 Energy Flow Distribution at a Steady 45 mph Speed

The test procedure was as follows:

- The vehicle was run until the battery capacity was 60%. As a check, VBUSOC was approximately 199 ±1 volt.

- To minimize brake drag, braking was done with the emergency brake while positioning the vehicle for the test. Absence of serious brake drag was checked by jacking up the car and spinning the wheels by hand.

- The car was accelerated to 70 km/hr (44 mph) and coasted down to 65 km/hr (40 mph). Using the diagnostic control box, the regen control was manually dialed in to maximum allowable range. Service brakes were not used. The vehicle was decelerated to 10 km/hr (6 mph).

- The test was repeated for three runs in each direction.

Figure 11.4.3a-f shows the battery amps, volts, instantaneous power, recovered energy, vehicle speed, and distance traveled versus time for this test. The elapsed time to brake from 40 mph to 6 mph was 19 seconds. The braking distance was 528 feet.

Regenerative braking efficiency can be calculated by dividing the recovered energy to the battery from Figure 11.4.3d (153,672 joules) by the vehicle initial minus its final kinetic energy - 247,000 joules. This efficiency is calculated to be 62%.

11.4.3 Acceleration And Gradeability Test

The purpose of this test was to determine the maximum acceleration of the test vehicle on a level road. From this data gradeability performance was computed. The determination of conformance to the acceleration goal of 0 to 48 km/hr (30 mph) within 8 seconds and from 40-88 km/hr (25-55 mph) within 16 seconds was made. The ability to attain a goal speed of 65 km/hr (40 mph) within a goal distance 305 m (1000 ft.) on a 4% grade was determined by computation from the speed time curve for maximum acceleration. Also the maximum grade attainable at 8 km/hr (5 mph) was computed.

11.4.3.1 Acceleration on Level Ground

The test was conducted on the dry skid pad at the Marshall Proving Ground. The battery state of charge was 100%. The vehicle was accelerated with full travel accelerator pedal to 89 km/hr (55 mph). An opposite direction run within 5 minutes of the previous run was made. This test was repeated for reduced battery states of charge.

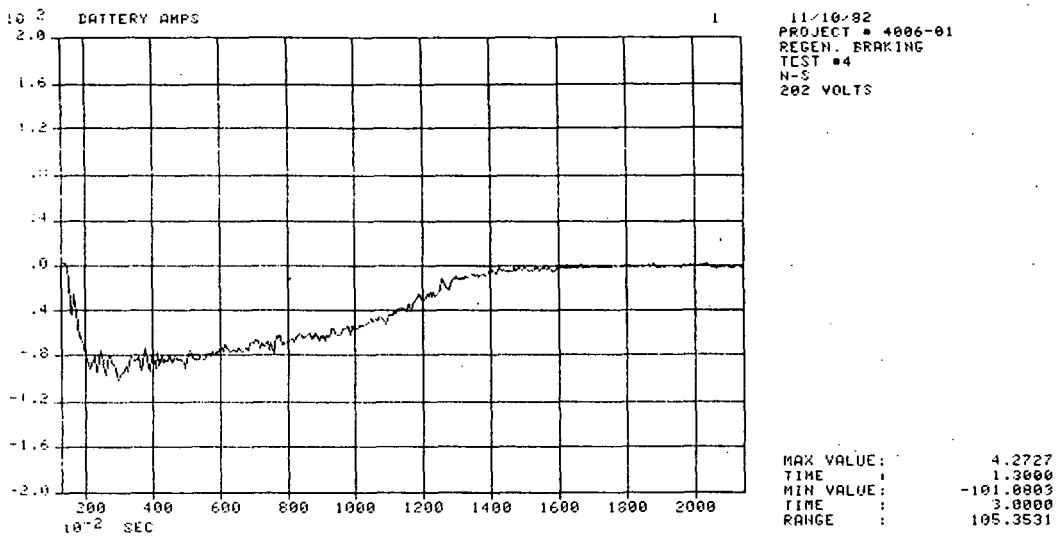

Figure 11.4.3a Battery amps Regenerative Braking Test

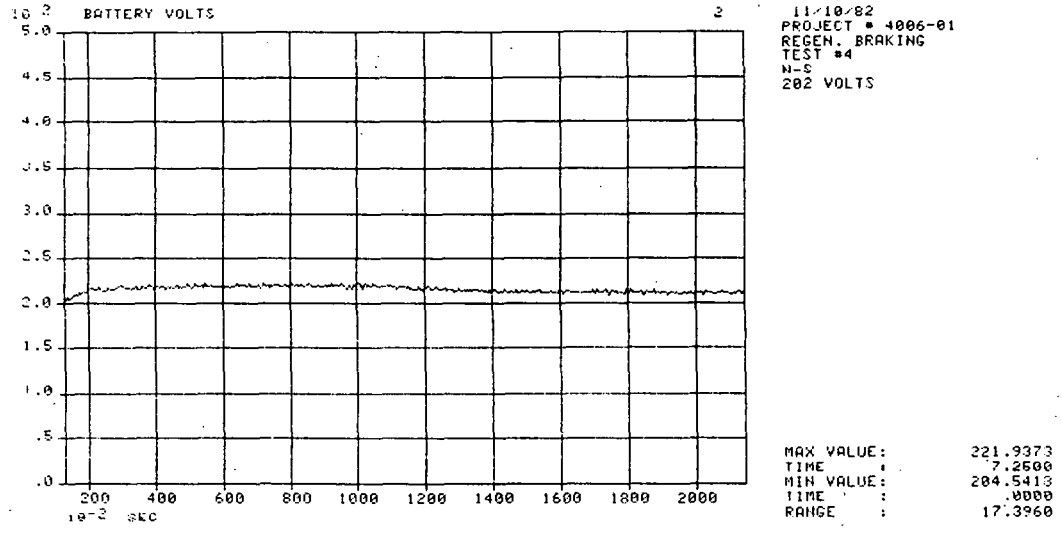

Figure 11.4.3b Battery Volts, Regenerative Braking Test

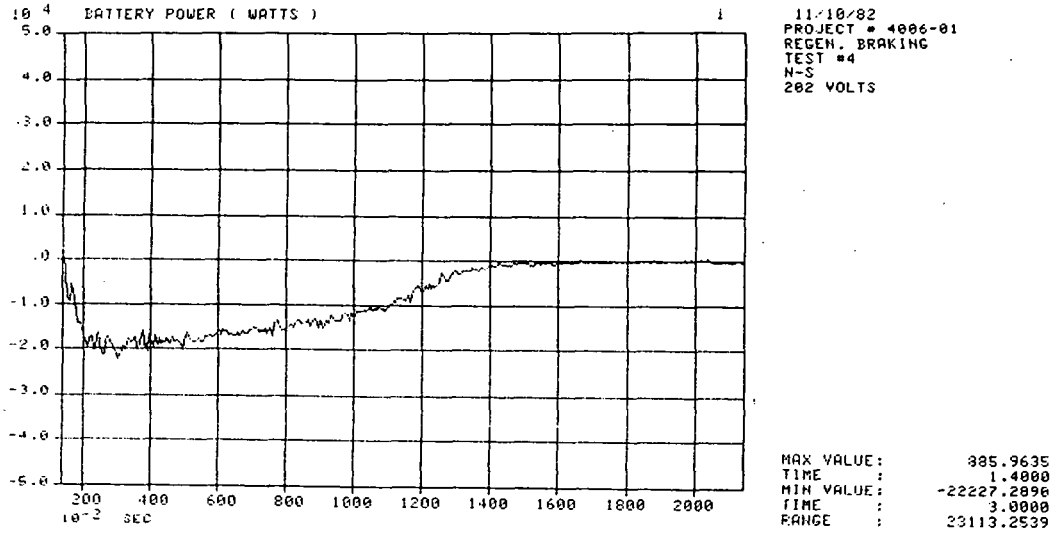

Figure 11.4.3c Battery Power, Regenerative Braking Test

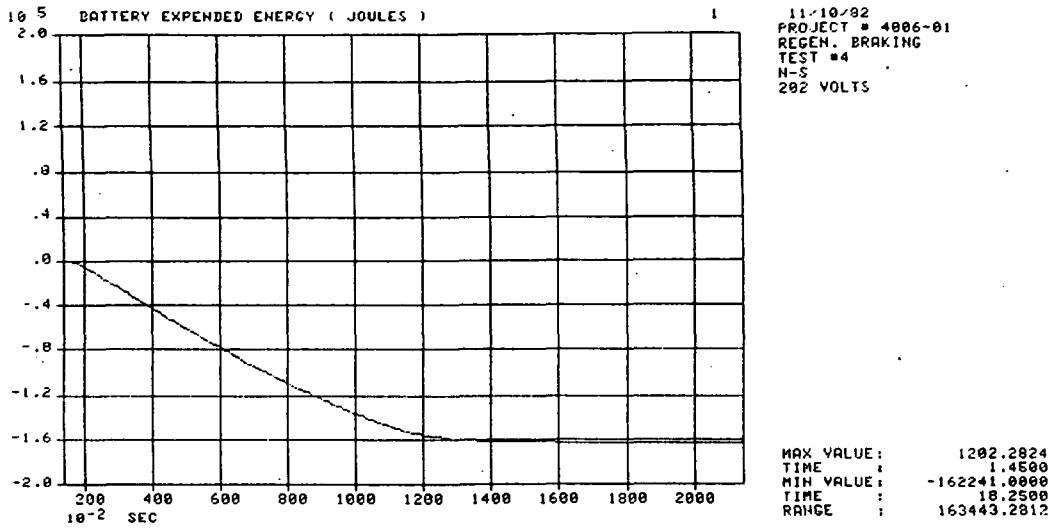

Figure 11.4.3d Recovered Energy, Regenerative Braking Test

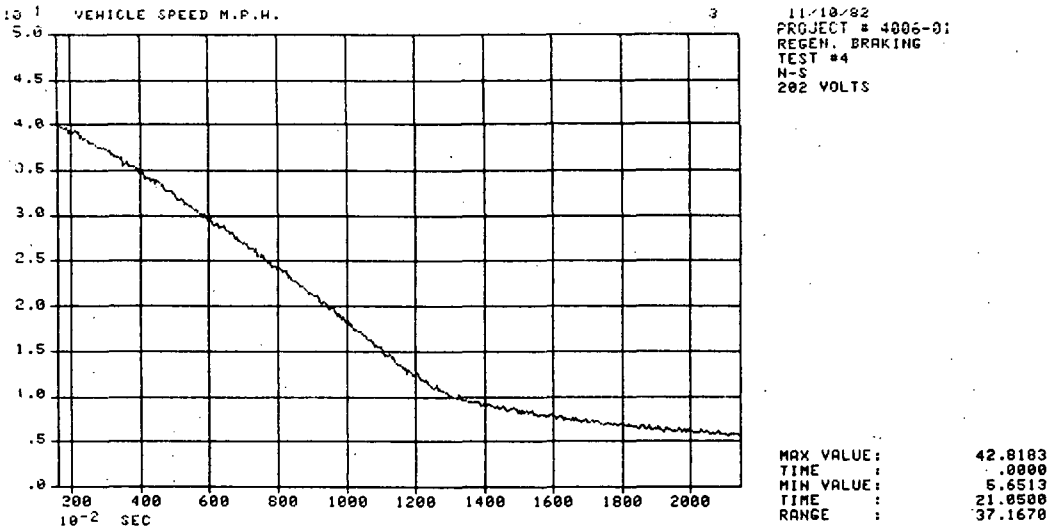

Figure 11.4.3e Vehicle Speed, Regenerative Braking Test

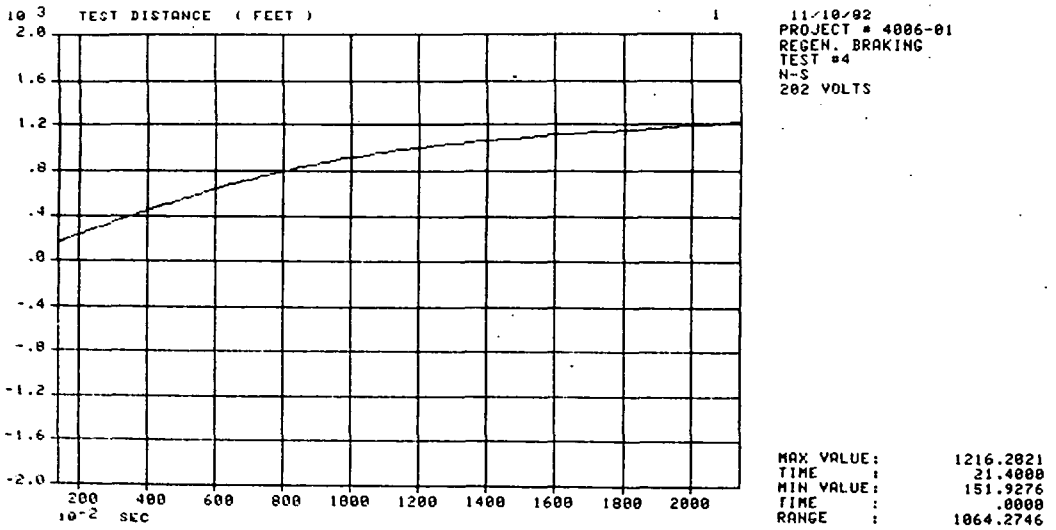

Figure 11.4.3f Vehicle Distance Traveled Regenerative Braking Test

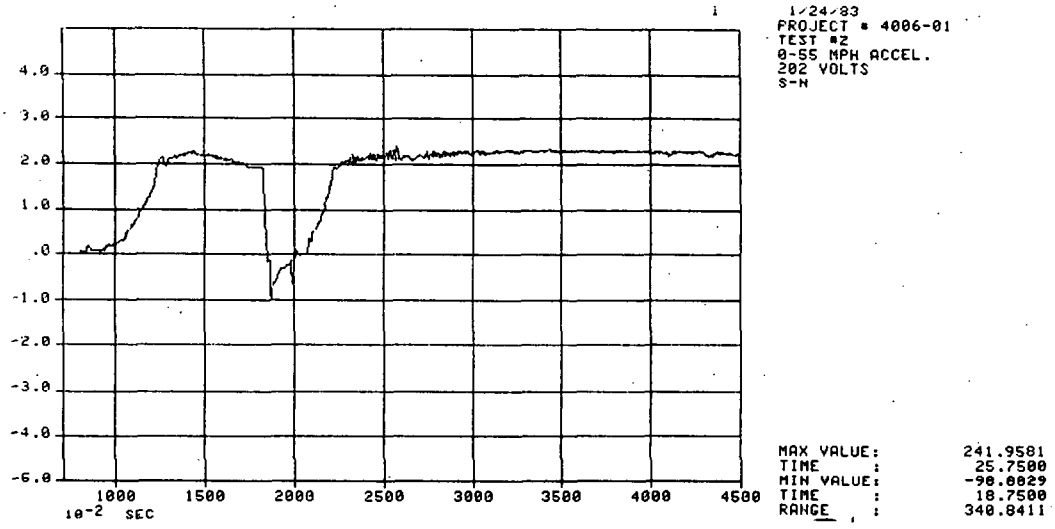

Figure 11.4.4a Battery amps Vs. Time Acceleration on Level Grade

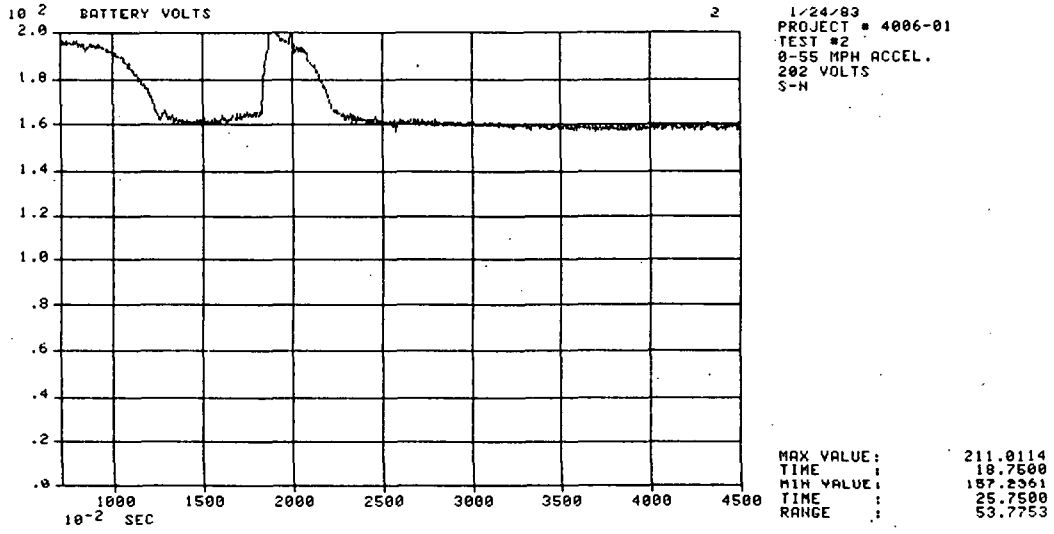

Figure 11.4.4b Battery Volts Vs. Time Acceleration on Level Ground

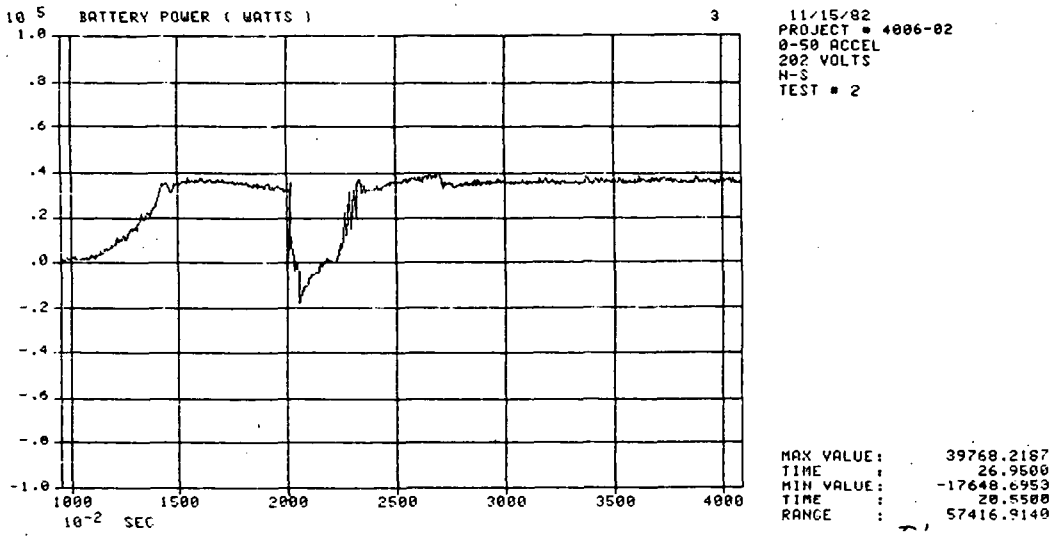

Figure 11.4.4c Battery Power Vs. Time, Acceleration on Level Grade

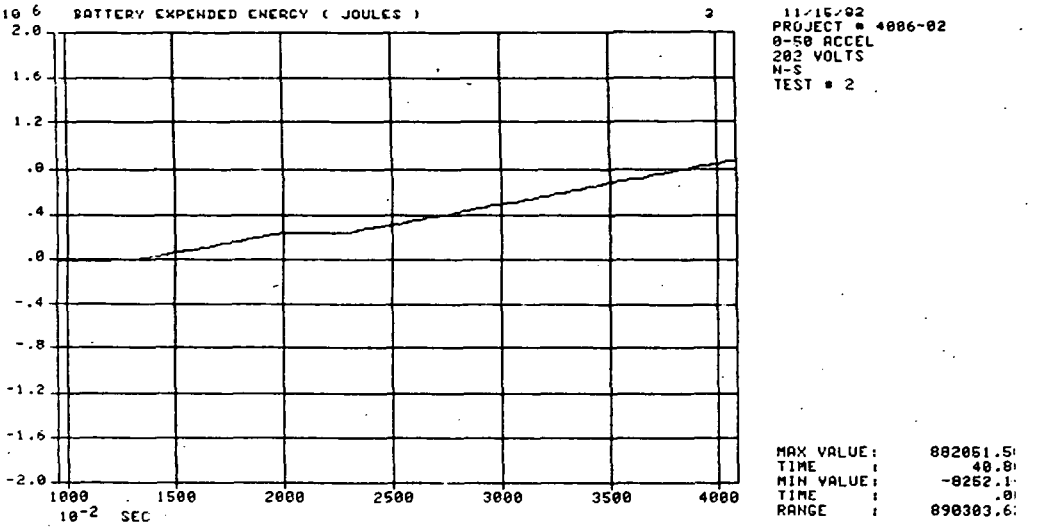

Figure 11.4.4d Battery Expended Energy Vs. Acceleration on Level Grade

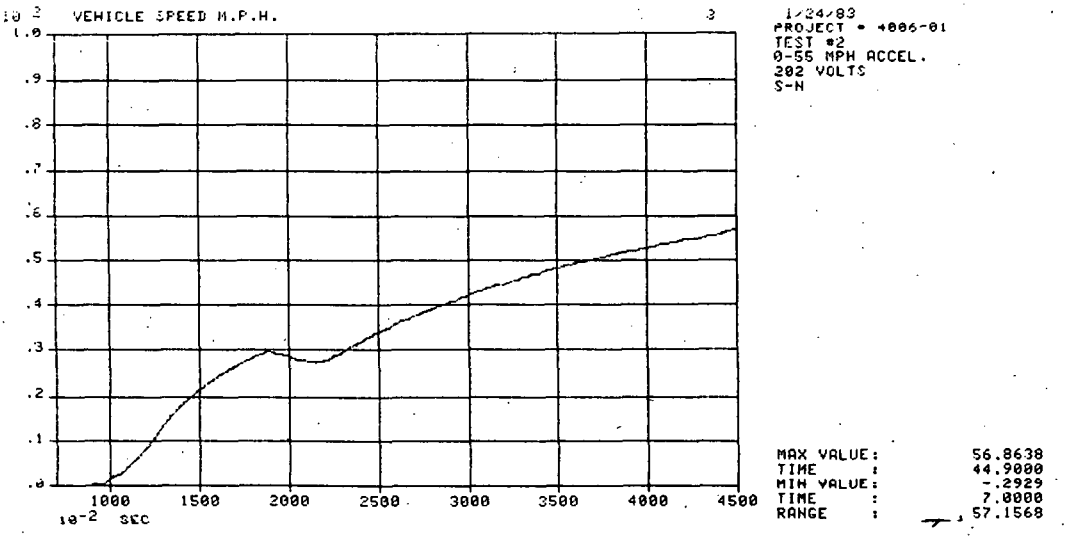

Figure 11.4.4e Vehicle Speed, Vs. Time Acceleration on Level Grade

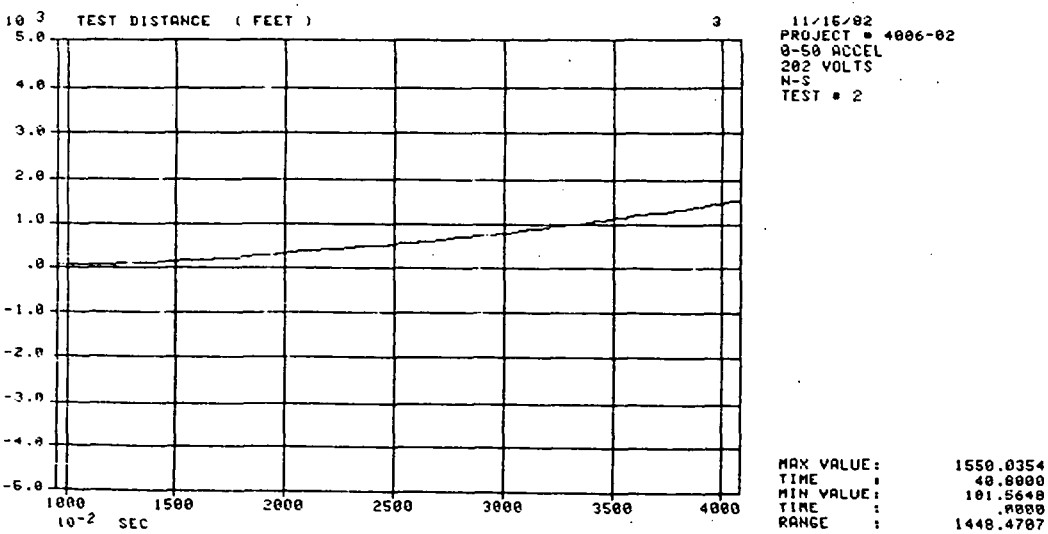

Figure 11.4.4f Distance Traveled Vs. Time Acceleration on Level Grade

Figure 11.4.4 shows the battery amps, volts, instantaneous power, expended energy and vehicle speed and distance for this test.

The acceleration goal of 0 to 48 Km/hr was nearly met, having achieved this speed just before the upshift in 8.5 seconds. This goal could have been easily surpassed with improved startup as outlined in section 8.4, which adds one to two seconds to the total acceleration. Abnormally high road load and lower than expected low gear transaxle efficiency also degraded the performance of this test.

The acceleration goal of 40 Km/hr to 88 Km/hr in 16 seconds was missed by 11 seconds as 27 seconds were needed for the test. The principle factors in this disappointing performance were high vehicle road load and the 2.5-second shift time, which is noted in Figure 11.4.4e.

The propulsion system capability to accelerate a light road load vehicle within the design goals is evident from the instantaneous power curve in Figure 11.4.4c. It is seen, except for lapses during the gearshift and startup, that a steady 38 kw is output from the battery packs. This power level meets the peak power requirment in the design goal, and thus shows the true acceleration capability of the system.

11.4.3.2 Computed Performance Values

By using the speed-time data plotted in the acceleration tests, the required performance values can be derived and compared with the goals.

11.4.3.2.1

Goal: Maintain 65 km/hr (40 mph) on a +4% grade.

Calculation: On a 4% grade, rolling and aerodynamic resistance at a given speed is essentially identical to the resistance encountered on level grade. If a vehicle has an acceleration a_L on a level road at speed v, it will have an acceleration a_G on a grade angle θat speed v of

$$a_G = a_L - g \sin \theta \text{ (all else being equal)}$$

where g = acceleration of gravity = 35.1 km/hr/sec = 21.8 mph/sec = 32.0 ft/sec^2

A 4% grade is equivalent to $\theta = 2.3^o$. Since $a_G = 0$ for this calculation:

$$a_L = g \sin \theta = (35.1)(\sin 2.3^o) = 1.403 \text{ km/hr/sec}$$
$$= (21.8)(\sin 2.3^o) = 0.871 \text{ mph/sec}$$

From the level road data, the maximum acceleration at 65 km/hr, a_1, was computed by differentiation.

A plot of acceleration versus speed is for the maximum acceleration test shown in Figure 11.4.5. It is seen that at 65 km/hr (40 mph) acceleration is approximately 1.5 mph/sec and thus this goal is more than adequately met.

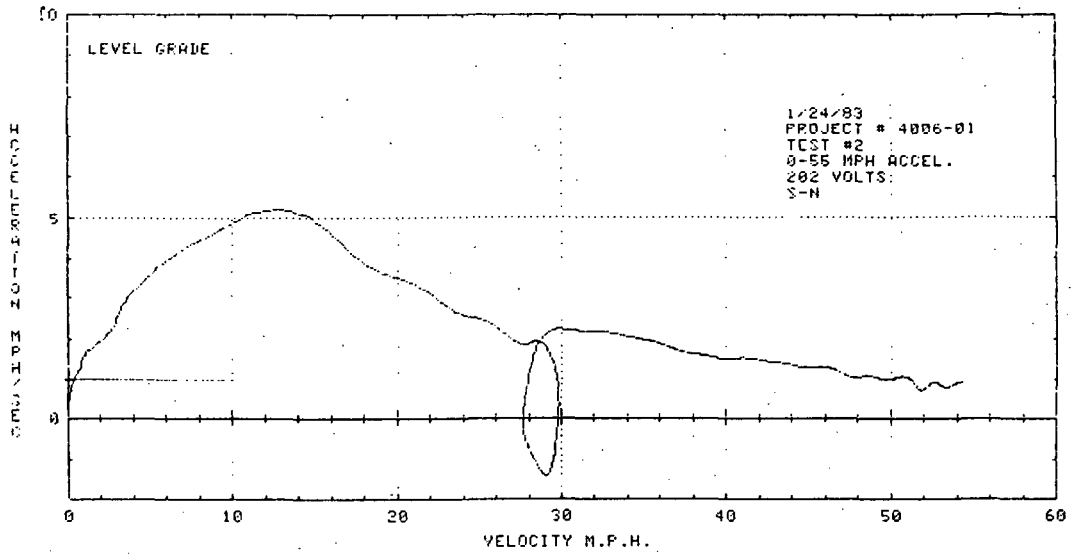

Figure 11.4.5 Vehicle Max. Acceleration Vs. Speed on Level Grade

11.4.3.2.2

Goal: Accelerate to 65 km/hr (40 mph) within 305m (1000 ft) on a 4% grade.

At a given speed, a 4% grade simply introduces a fixed offset of g sin 2.3^{o} to the curve in Figure 11.4.5 since aerodynamics and frictional drag are functions of velocity. The resulting fixed offset is shown in Figure 11.4.6.

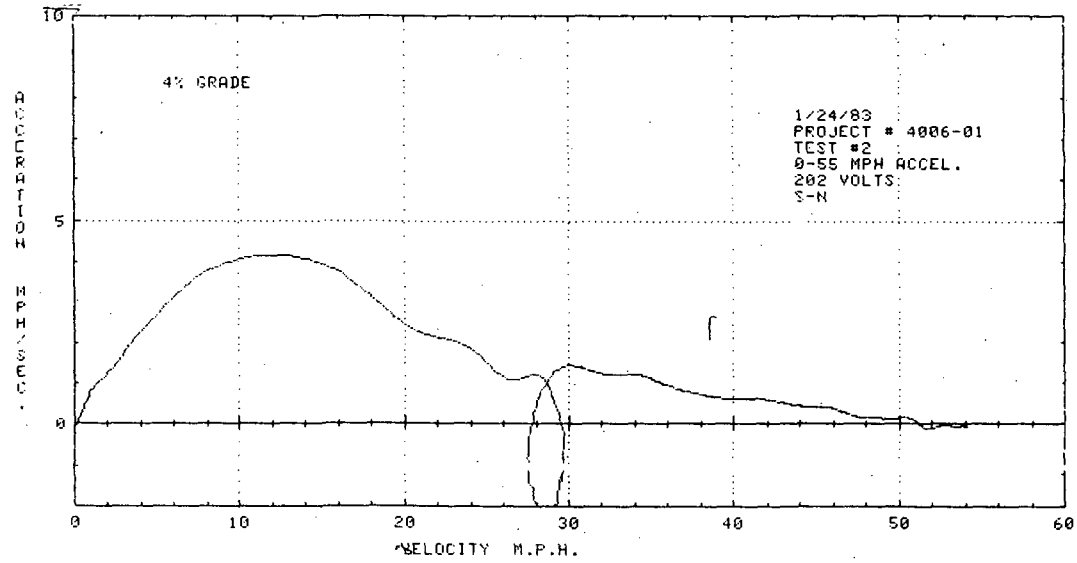

Figure 11.4.6 Vehicle Max. Acceleration Vs. Speed, Computed for 4% Grade

Using the maximum acceleration values from this curve, a recursive relationship for velocity vs. time on a 4% grade can be set up as follows:

$$V_t = ag(V_{t-T}) \cdot T + V_{t-T}$$

where T is some sufficiently small time increment. A curve of V_G versus time t can now be developed and is shown in Figure 11.4.7.

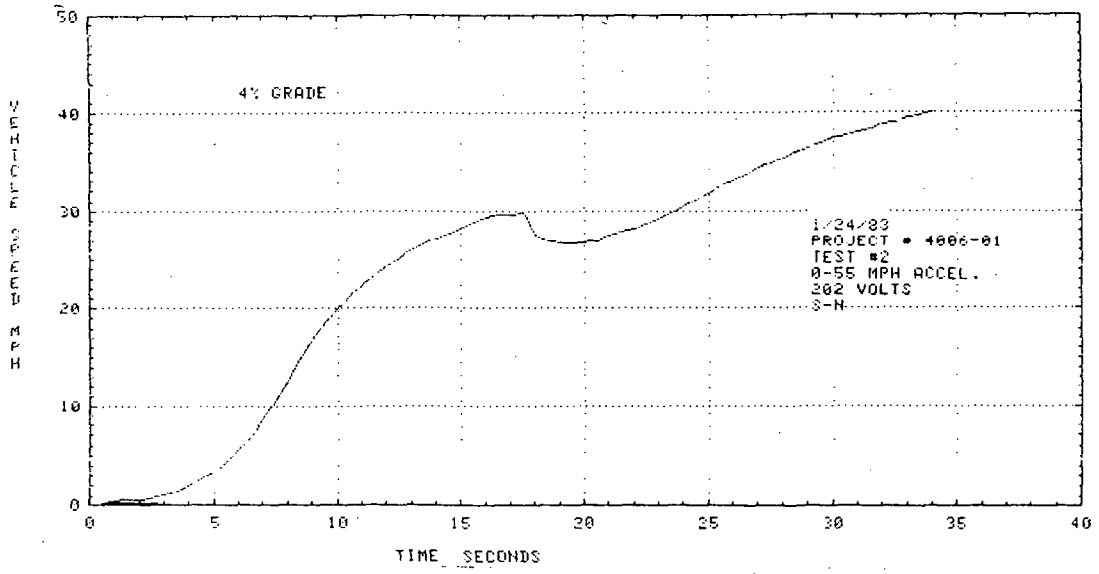

Figure 11.4.7 Vehicle Speed Vs. Time Computed for 4% Grade

Finally, computer numerical integration of V_G is done to yield a distance X:

$$X = \int_0^{t_f} V_G dt$$

If X is less than 305 meters (1000 ft), the goal is satisfied. The actual numerical integration of V_G yielded an X of 361 m (1186 ft.), which falls short of the goal by 56 m.

The input velocity data, recorded on cassette tape, was filtered to reduce noise but preserve at least 1 Hz bandwidth. With all processing steps done by computer with high resolution, accuacy of results approached instrumentation accuracy.

11.4.3.2.3

Goal: Find the maximum grade attainable.

Calculation: Maximum grade is computed at low vehicle speed where rolling resistance and aerodynamic losses are minimal. The equation $\theta = \sin^{-1}(aL/g)$ was used to obtain maximum gradeability at 8 km/hr (5 mph) from the level road velocity-time data. The maximum angle was

$$\theta = \sin^{1} \frac{3.5 \text{ mph/sec}}{4.8 \text{ mph/sec}} = 9.2^{o}$$

and thus the maximum gradeability was g = 16%. This grade value is an indication of the maximum torque capability of the system. This gradeability is not presently achievable at startup because of the problems described in Section 11.3.3.

11.4.4 Speed Test

The purpose of this test was to conduct a high-speed run for a specified distance to attain the goal speed of 105 km/hr (65 mph).

The test was run on the test track at Marshall Proving Grounds.

The vehicle was slowly accelerated to 105 km/hr (65 mph) to ease battery drain.

Then the vehicle was successfully operated between 105 km/hr (65 mph) and 113 km/hr (70 mph) for a minimum distance of 5 km (3 miles) in order to maintain an average speed of at least 105 km/hr (65 mph). This distance is almost two full laps (3.2 mi.) around the test track.

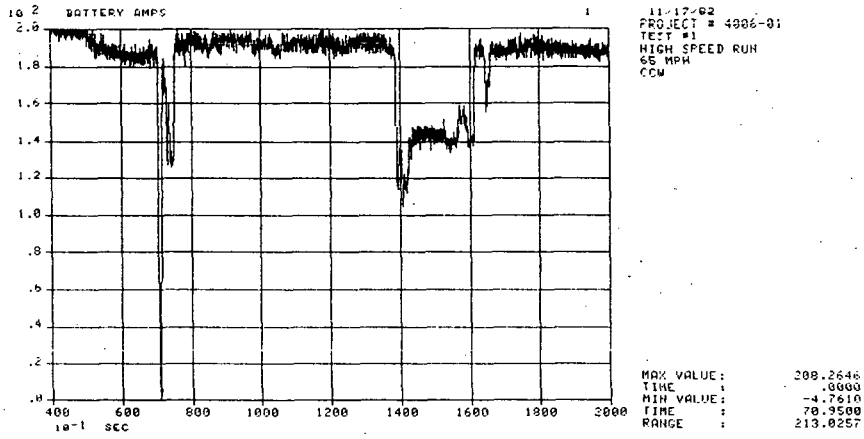

Figure 11.4.8a Battery amps Vs. Time, High Speed Run

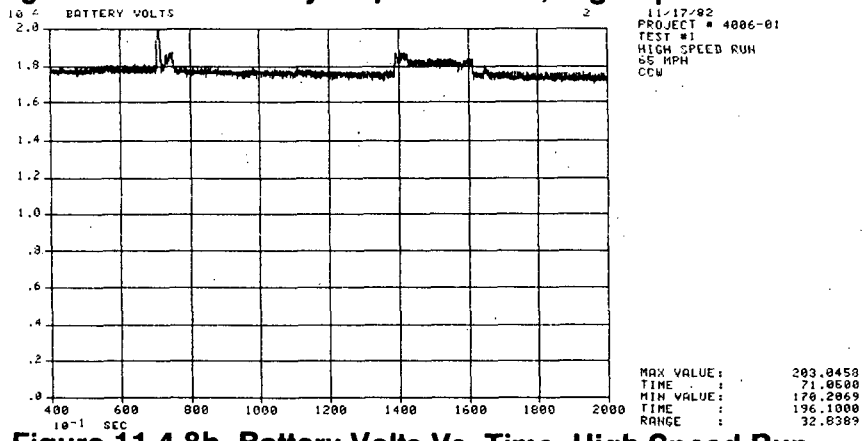

Figure 11.4.8b Battery Volts Vs. Time, High Speed Run

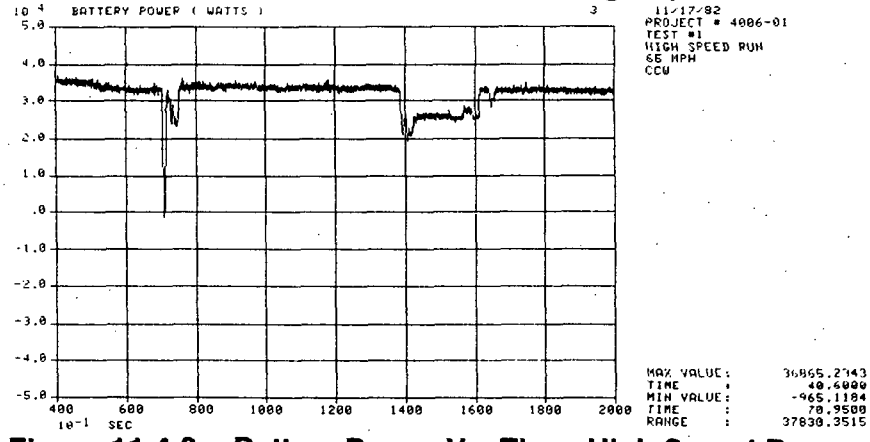

Figure 11.4.8c Battery Power Vs. Time, High Speed Run

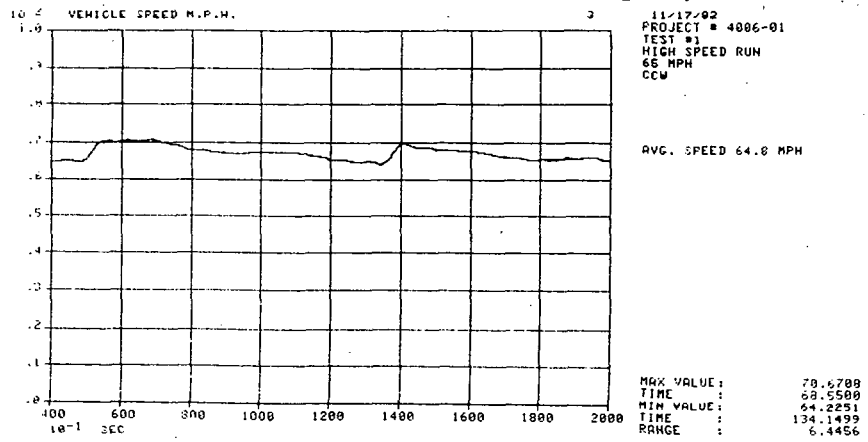

Figure 11.4.8d Vehicle Speed Vs. Time, High Speed Run

The initial battery state of charge was 100%. Vehicle gross test weight was 3460 lbs.

Figure 11.4.8a-d shows the battery current, voltage, instantaneous power, and vehicle speed for this test. The average expended energy in watt-hrs/km is also shown.

11.4.5 Expended Energy Test

The purpose of this test was to measure the amount of energy expended during steady state speeds and during a controlled driving cycle. The results were recorded in w-hr/km and w-hr/mi.

11.4.5.1 Expended Energy for Steady State Speeds

This test was conducted on the skid pad and a portion of the straightaway at Marshall Proving Ground.

The vehicle was run at nominal steady state vehicle speeds as follows:

-- 80 km/hr (50 mph)
-- 72 km/hr (45 mph)
-- 56 km/hr (35 mph)
-- 40 km/hr (25 mph)

Two runs in each direction for each speed were made.

The 25 mph run was done in both low gear and high gear. All other tests were run in high gear.

A bar graph, indicating the expended energy in W-h/mi is shown by the solid bars in Figure 11.4.9. The relatively high numbers shown are attributed mainly to the high road load that was measured for this vehicle and partly to the lower than expected transaxle efficiency.

In order to indicate the possible improvement in expended energy with the more optimistic road load, a separate set of bars with horizontal hatching is plotted in Figure 11.4.9 which represent a calculated expended energy based on component dynamometer efficiency tests and assuming an equivalent road load to the ETV-1. The energy consumption figures for the ETV-1 are also shown in Figure 11.4.9 for comparison. These last figures for the Eaton system are shown to be close to those obtained with the ETV-1 at every speed and are predicted to exceed the ETV-1 with future improvements to transaxle efficiency.

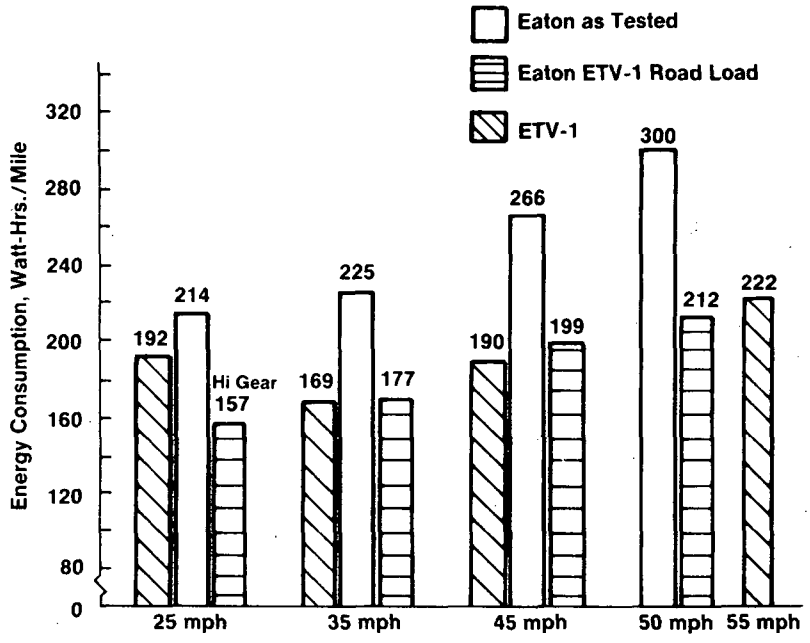

Figure 11.4.9 ACPS 2 Vehicle Energy Consumption Constant Speed

11.4.6 Expended Energy on SAE J227A/D Driving Cycle

This test was performed by driving this cycle a minimum of four (4) times running in the opposite direction after each cycle on the section of the track shown as a solid line in Figure 11.4.10.

1 Lap = 1.6 miles

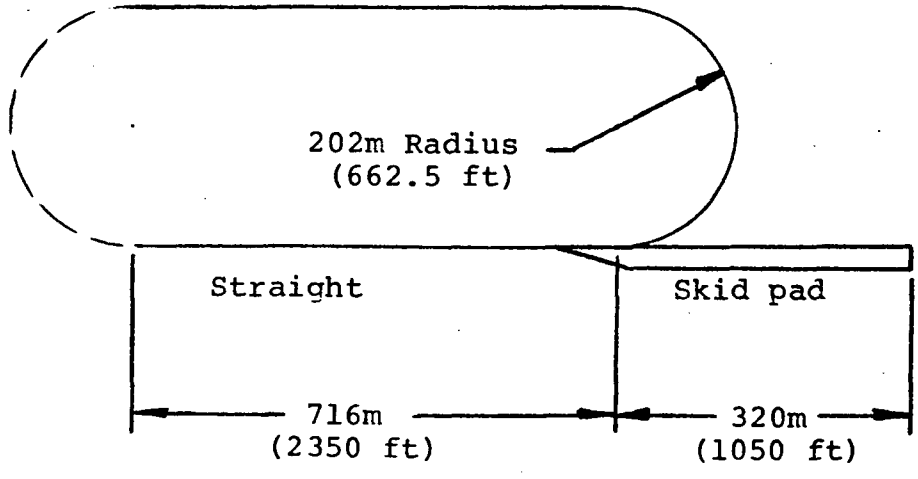

Figure 11.4.10

Figure 11.4.11a-e shows the battery current, voltage, instantaneous power, instantaneous wh/mile, expended energy, and vehicle speed and distance for this test. The energy consumption over the cycle can be calculated by dividing the total energy expended by the distance traveled. These numbers are shown in Figure 11.4.12, first by taking system regeneration into account and then neglecting recovered energy during regeneration. 100% regeneration efficiency by the battery pack is assumed in these results. The actual portion of available energy which is absorbed by the power source is a function of the type of batteries being used.

The cross-hatched bars in each case are the actual test result values. These relatively high values are due partly to high road load and transaxle efficiency problems and partly to running the test around a curved track. The detriments of the curved track can be seen by the next set of bars, which substitute energy consumption figures from the constant 45 mph speed test for the cruise portion of this test. A small improvement can be noted. The effects of high road load are seen by the solid bars, in which the predicted energy consumption figures assuming the ETV-1 road load were substituted for the cruise portion of the cycle. It is seen that a considerable improvement can be gained from reducing the road load. Again the energy consumption on this cycle for the ETV-1 for the case without regeneration is included for comparison. The Eaton system with a lighter road load is shown to be more efficient during this cycle.

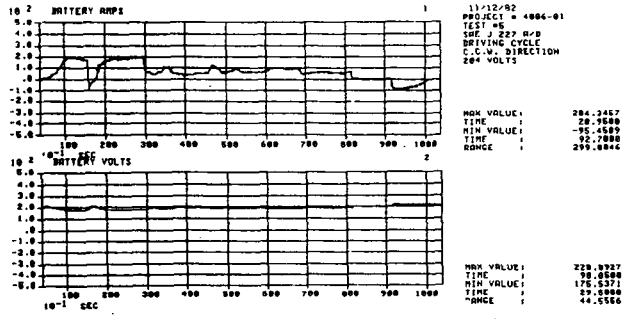

Figure 11.4.11.a Battery amps and Volts Vs. Time SAE J227a/D Cycle

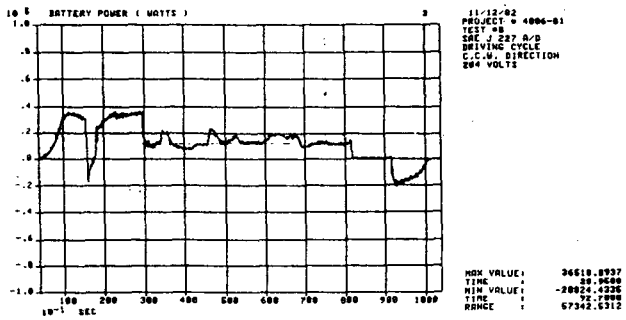

Figure 11.4.11.b Battery Power Vs. Time, SAE J227a/D Cycle

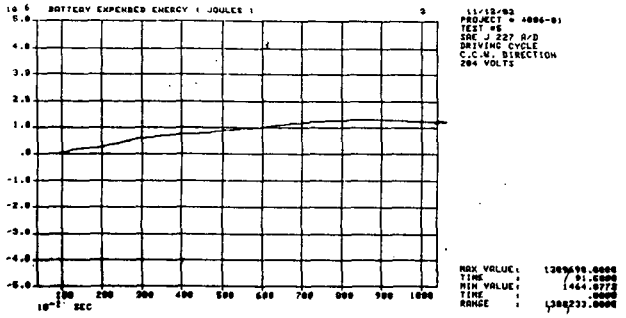

Figure 11.4.11.c Battery Expended Energy Vs. Time, J227a/D Cycle

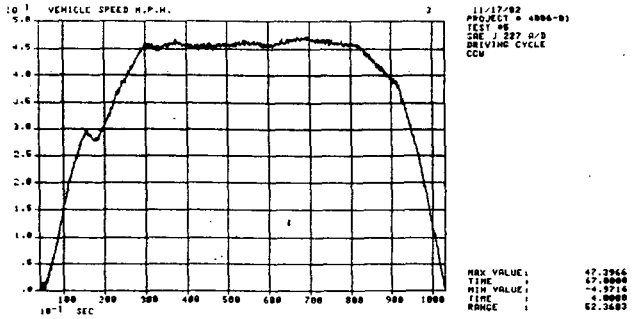

Figure 11.4.11.d Vehicle Speed Vs. Time, J227a/D Cycle

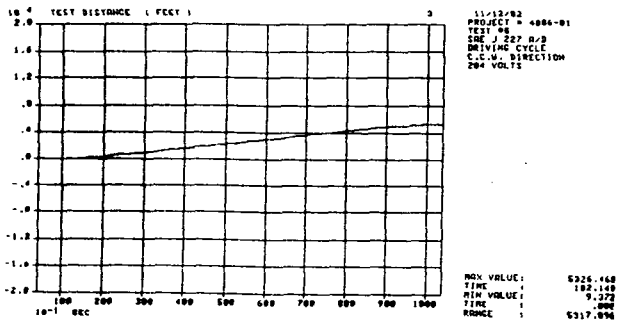

Figure 11.4.11.e Distance Traveled Vs. Time J227a/D Cycle

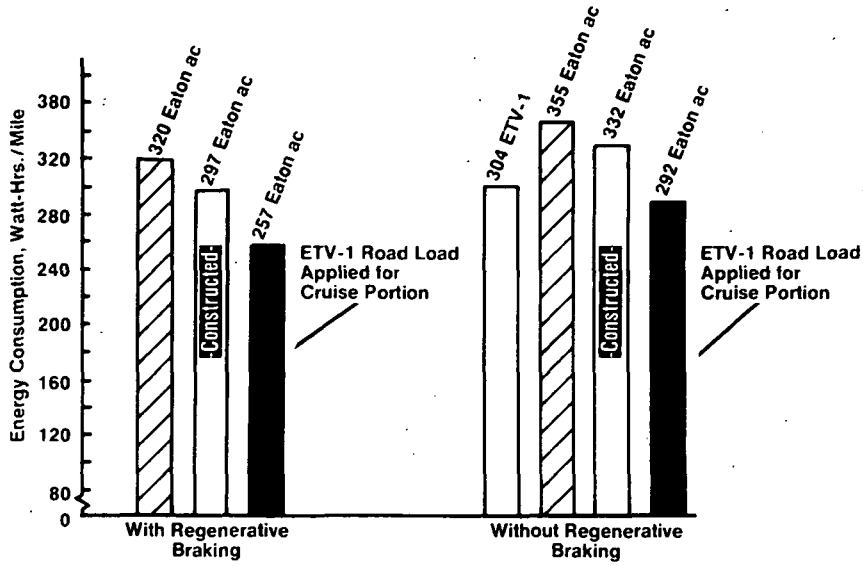

Figure 11.4.12 Energy Consumption Over J227A/D Cycle

11.4.7 Braking Test

The purpose of this test was to establish brake system capabilities regarding stopping distance for vehicle speeds from 80 km/hr (50 mph) and 48 km/hr (30 mph). This test was done prior to improvements made to the service brakes as described in Section 11.2. Hence, the vehicle stopping capability, although judged adequate during this test, has since been improved.

The test was conducted on the skid pad at the Marshall Proving Ground. The brakes were inspected to make sure they were in good condition.

The vehicle test weight was 3640 lbs.

Tire pressures were 36 psi on all four tires.

The first test was run from 48 km/hr (30 mph) to a full stop with regenerative braking active. Stopping distance was 21 m (70 ft.).

For the same initial speed, the above test was repeated but without regenerative braking, and the required stopping distance of 21 m was met.

The second test was run from 80 km/hr (50 mph) to ful stop with regenerative braking active. The stopping distance was 60 m (197 ft.).

This test was also repeated without regenerative braking, and the same 60 m stopping distance was obtained.

Each test was run three times.

12.0 CONCLUSIONS

This report describes work relating to Phase 2 development and testing of an ac propulsion system for an electric vehicle. The system, which consists of a 2-speed automatic mechanical transaxle, 18.6 kw ac induction traction motor, 33.6 kw inverter and overall logic controller, was installed and evaluated in a converted Mercury Lynx rolling test bed vehicle. An on-board charger and an auxiliary dc to dc converter were integrated into the inverter/controller package.

1. The system concept of an ac propelled electric vehicle is feasible.

2. A multi-speed transmission pays large dividends in reducing motor and inverter weight and cost, and in achieving high performance and efficiency from the vehicle on the road.

3. Vehicle performance relative to goals is encouraging. The propulsion system achieved the specified power and torque except at start and very low speed. Those vehicle performance goals not met resulted from higher than expected road load from the test vehicle.

4. More starting and low speed (below 10 mph) torque are required from the propulsion system. The motor is believed to be capable of this torque, but a more thorough study of the startup control methods is required to achieve it.

5. The transaxle efficiency, as tested during Phase 2, was below that of Phase I due to the unexpected effect of design changes which otherwise met their objectives to reduce size, weight and cost. It should be possible to restore the efficiency to the Phase I levels of mid 90's in high gear and high 80's in low gear.

6. Assuming those efficiencies can be restored to the mechanical transaxle, the overall propulsion system efficiency is projected to be superior to the dc ETV-1 baseline vehicle system for the same vehicle road load.

7. Although driveability and gear shifting were adequate to conduct the tests and evaluation in the vehicle, more work is required to reduce shift times and to better integrate the electronic and hydraulic shift control system.

8. The electrical regenerative braking function of the ac system is functionally excellent. Subjectively it feels smoother and more stable than the vehicle's hydraulic power braking system.

9. A choice of 192 volt battery bus for a lead-acid traction battery is very close to optimal for a 25 hp system.

10. Reliability of an ac system is projected good. Not a single failure of the inverter, logic controller or sensors was encountered during several weeks of road and track testing.

11. The feasibility of combining an on-board charger (sharing inverter components) and the auxiliary dc to dc 192 volt to 12 volt converter into inverter/controller package is proven. The size of this total package is comparable with state of the art dc vehicle systems with all these functions included.

12. Overall system cost is sensitive to main transistor cost. The cost of main transistor fell to 37% compared to those for Phase I. Transistors in the $60 each range are needed to compete with dc systems on first cost, and this figure is expected to be within reach in two years time.

REFERENCES

Section 6

1. "Advancing Power Transistors and Their Applications to Electronics Power Converters," Fuji Application Note, 1981.

2. "A PWM Transistor Inverter for an AC Electric Vehicle Drive" J. M. Slicker, 1981 IAS-IEE Conference Record.

3. "Design of Solid State Power Supplies" 1981, Van Norstrand pp 68-85.

4. A. H. Weinberg, "A Boost Regulator With a New Energy Transfer Principle" Proceedings of the Spacecraft Power Conversion Electronics Seminar, Sept. 1974.

5. L. H. Dixon and C. J. Baranowski, "Designing Multi-Output Converters With a Coupled-Inductor Current-Driven Topology," Proceedings of Powercon 8, April 1981.

6. D. Nathasingh and C. H. Smith, "A New High-Flux, Low-Loss Magnetic Material for High Frequency Applications," Proceedings of Powercon 7, March 1980.

Section 11

1. "Environmental and Safety Engineering Staff Automotive Emissions and Fuel Economy Office Procedure." Appendix C "Coastdown Procedure for Determining Alternate Dynamometer Road Load Horsepower Setting."

2. JPL publication 81-93 (DOE/CS54209-3), Performance Testing and System Evaluation - Phase III Final Report of the DOE ETV-1 Electric Vehicle.

3. D. Simanaitis, "Seeking Light at the End of the Tunnel" Road and Track, Aug. 1982.

Appendix D

1. Kreith, Frank; Principles of Heat Transfer; 3rd edition; Intext Press Inc., New York, 1973.

2. Newberger, Joel; Thermal System Approach to Heat Sink Selection AHAM Inc., Rancho California, 1979.

3. Steinberg, Dave S.; Cooling Techniques for Electronic Equipment John Wiley & Sons Inc., New York, 1980.

APPENDIX A

TEST STAND DESCRIPTION

APPENDIX A - TEST STAND DESCRIPTION
Computer and Instrumentation

The following describes the automatic data acquisition equipment used for measuring, recording and reporting steady state propulsion system performance. Two reasons for implementing the automatic data acquisition system are:

a. Increased visibility of the device being tested. Important system information is displayed in real time to allow the engineer to concentrate on the significance of a test rather than on the mechanics of data acquisition.

b. Improved reliability and accuracy of test results. An automatic acquisition system reduces the chance for human error, reduces time skew of a set of data measurements, and allows results to be reported on a larger sample of data than would be available if the data were collected manually.

The measurement accuracy goal for propulsion system power outputs and efficiencies is +/- 2 percent of reading. This goal places tight requirements on the acquisition system error budget. The feasibility of making measurements to these accuracies was demonstrated in the Phase I propulsion system development. The instrumentation approach in Phase II is largely the same, with a computer controlled 12 bit analog-to-digital converter replacing the meter readouts used earlier. The data acquisition system accuracy meets or exceeds the required accuracy on all critical data channels.

The AC propulsion system test stand consists of the basic elements shown in Figure A.1; the test stand control console and dynamometer, the propulsion system control console ("diag box"), the propulsion system itself, data transducers, signal conditioning instrumentation interface, the test stand computer, the VAX-11/780 host computer and numerous mechanical fixtures. The propulsion system consists of the motor controller, power inverter, and AC motor and transaxle.

To perform steady state measurements, the engineer sets up the propulsion system operation through the control consoles. The data acquisition system collects information at the propulsion system and it's control console, and at an assortment of test stand transducers. Propulsion system performance is displayed and updated continuously on the test stand CRT terminal. On operator command, the displayed data is copied at the local printer and/or stored on the host computer.

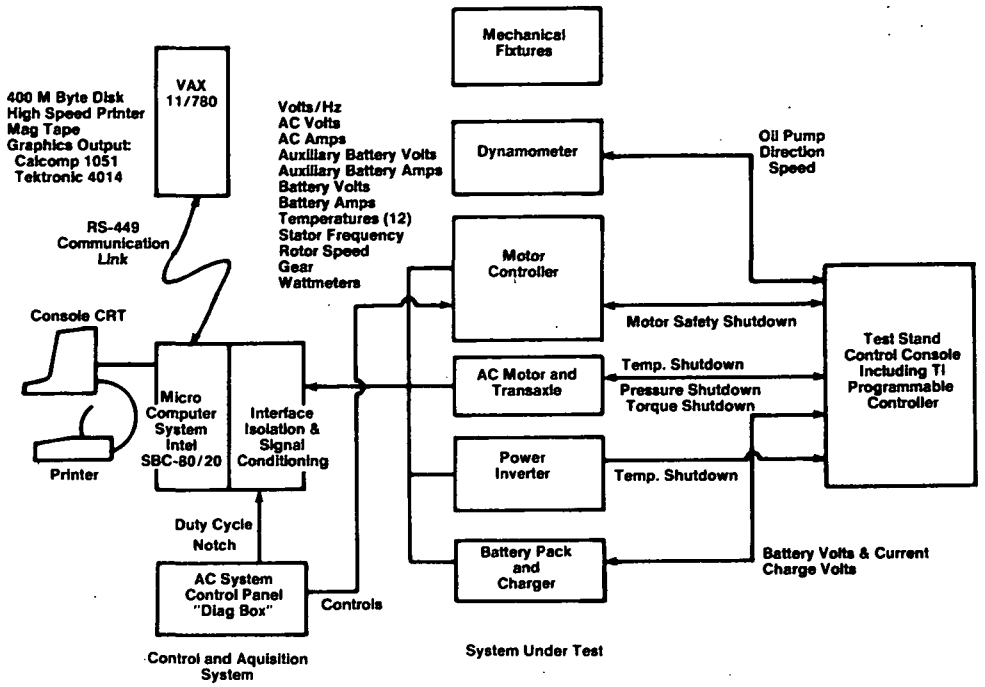

Figure A.1 AC Propulsion System Test Stand For Steady State Measurements

The following describes the test stand computer and the signal conditioning instrumentation interface. The test stand computer hardware is based on the industry standard Intel MULTIBUS microcomputer bus, the Intel SBC 80/20-4 single board computer and an array of interface cards compatible with the MULTIBUS. The computer hardware is identified at the board level in Figure A.2. All boards are standard products of Intel, Data Translation or Monolithic Systems Corporation and are identified with the manufacturer's part numbers in the block diagram. The 12 bit A/D converter is configured for +/- 10 volt single-ended input operation and is described in a copy of the manufacturer's specifications in Table A.1.

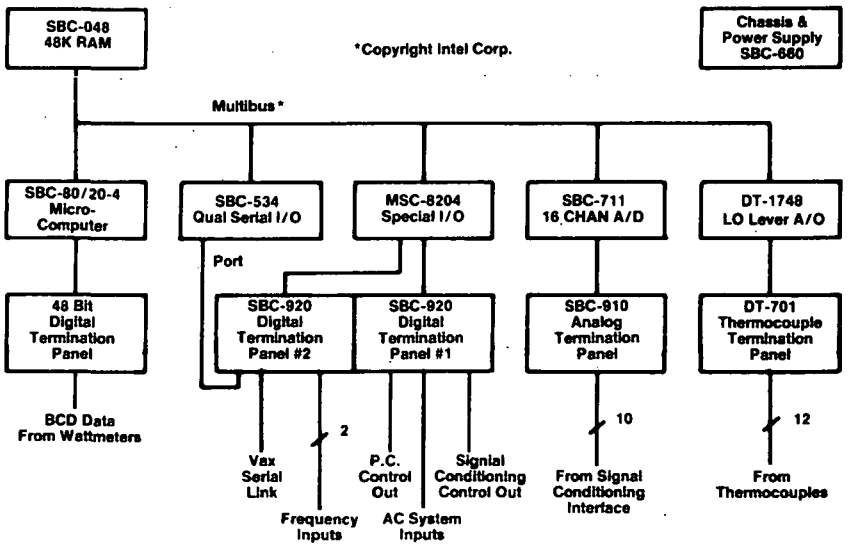

Figure A.2 Test Stand Computer Hardware Block Diagram

One interface board was designed and constructed to perform rate measurements, expand the digital I/O of the computer and to hold the Advanced Micro Devices AMD-9511 arithmetic processor integrated circuit. This board is based on the Monolithic Systems Corp. interface card for the MULTIBUS (MSC-8204). The AMD-9511 math processor enables 32 bit floating point arithmetic to be performed at speeds 3-6 times faster than would be possible using math functions implemented in software.

The signal termination and conditioning electronics provide a means to physically connect the test stand sensors and to process analog sensor signals to a form compatible with the computer system. The signal conditioning provides high voltage isolation as well as flexible analog signal processing on independent channels. The circuitry is packaged two channels per 3.5 by 6.5 inch printed circuit board. The circuitry and a high quality power supply is housed in a card rack. Signal processing functions implemented for each channel include:

- Zero and calibration voltage insertion ahead of the isolation amplifier. Digital command signals from the test stand computer control the isolation amp input.

- High input impedance instrumentation amplifier with input electrically isolated from output.

- Adjustable isolator zero offset and gain.

- Active lowpass filter with 80db/decade roll-off and resistor selectable breakpoints from 1.5 Hz to 1 Khz.

- RMS-to-DC conversion (optional)

- Final stage buffer amplifier

Figure A.3 is a block diagram of a typical instrumentation interface printed circuit board. Figure A.4 is a set of hardware block diagrams showing instrumentation for specific data channels. Table A.2 lists the transducers used on the test stand.

The acquisition system displays a single torque channel representing motor output for the Motor tests or transaxle output for the Motor/Transaxle tests. The remainder of the test stand instrumentation is the same for either test.

The VAX host computer is used for software development and storage of test stand computer programs and measurement data. The 8080 microcomputer programs are written in Pascal, C and 8080 assembler using a development package from Whitesmiths, Ltd. running on the VAX. Special software is provided to download programs and upload data between the VAX and the test stand computer. Measurement data displayed at the test stand terminal is also stored on the VAX for off-line analysis and display. No mass data storage is provided at the test stand.

POWER REQUIREMENTS:	V_{cc} = +5V, ±5%. I_{cc} = 1.7A maximum.
ENVIRONMENTAL REQUIREMENTS	
Operating Temperature:	0° to 55°C (32° to 131°F).
Relative Humidity:	To 90%, without condensation.
PHYSICAL CHARACTERISTICS	
Width:	30.48 cm (12.00 inches).
Depth:	17.15 cm (6.75 inches).
Thickness:	1.27 cm (0.50 inch).
Weight:	454 gm (16 ounces).
ADDRESSING:	Reserves a block of 16 contiguous memory locations relative to a jumper-selectable memory base address. Programming information is provided in Chapter 3.
ANALOG INPUT	
Number of Channels:	8 differential or 16 single-ended; expandable to 16 differential or 32 single-ended using two plug-in 8:1 multiplexers (Harris H181BA or equivalent).
Resolution:	12-bits (0.025%), bipolar or unipolar.
S/H Aperature Time:	<20 nanoseconds.
S/H Uncertainty:	5 nanoseconds.

Multiplexer Input Voltage Ranges:

Gain X	A/D Input Range +5V	+10V	±5V	±10V	
1	+5V	+10V	±5V	±10V	Jumper Selectable
2	+2.5V	+5V	±2.5V	±5V	
4	1.25V	+2.5V	±1.25V	±2.5V	Programmable
8	0.625V	+1.25V	±0.625V	±1.25V	

Input Impedance:	Power Off: 680 ohms. Power On: > 100 megohms.
Input Current Range:	4 to 20 mA using customer-installed discrete 250-ohm ±1% 1/4W resistors; resistor temperature coefficient must be <0.01%/°C.
Source Impedance:	Balanced: <5000 ohms. Unbalanced: <1000 ohms.
Common Mode Rejection (CMR):	60 dB (differential input).
Common Mode Voltage (CMV):	±10.24V (signal plus common mode).
Input Overvoltage Protection:	±28V (dc); 28V peak ac.
Overall Accuracy (25°C):	0.05% FSR ± 1/2 LSB (gain X1). 0.07% FSR ± 1/2 LSB (gain X2, X4, X8). (Includes 3σ noise, linearity, offset gain, and dynamic response errors.)
Temperature Coefficient:	0.0025% FSR/°C (Gain X1). 0.0030% FSR/°C (Gain X2, X4, X8).
A/D Conversion Speed:	28 kHz.
THROUGHPUT*	
Sample Rate (Single Channel):	17 kHz.
Channel-to-Channel Rate:	16 kHz.
EXTERNAL TRIGGER:	TTL compatible; 1.5 μsec (minimum) pulse width, better than 50 nsec rise time.
INTERNAL PACER CLOCK:	Crystal-controlled accuracy 0.05%; divider provides range of $\frac{1000}{2^n}$ msec where n = 0 through 10.

INTERFACE CONNECTORS:

Interface	No. of Pins	Pin Centers in.	Pin Centers mm	Mating Connectors
P1 Multibus	86	0.156	3.96	CDC VPB01E43A00A1
P2 ±15V Aux Power	60	0.1	2.54	CDC VPB01B30A00A2 TI H3-11130
J2 1st 8/16 Input Channels	50	0.1	2.54	3M 3415-0000 or TI H3-12125
J3 Expander 8/16 Input Channels	50	0.1	2.54	Same as J2

*Assuming 2-MHz CPU clock. Includes time required to transfer data from the SBC 711 to system memory.

Table A-1

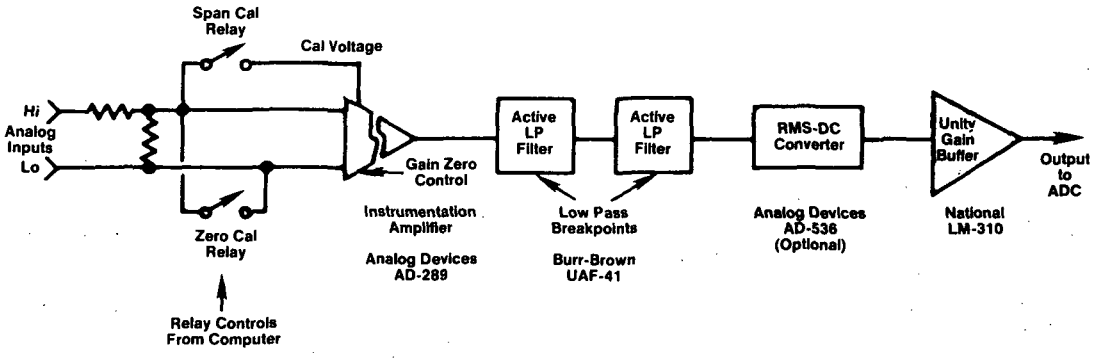

Figure A.3 Hardware Block Diagram for Instrumentation Signal Conditioning Interface

TABLE A.2 Test Stand Transducers & Instruments

Item	Manufacturer	Model No.	Property Control No.
Coax Shunt	T & M	F10,000-40	G-0037
Coax Shunt	T & M	F10,000-40	G-0036
Coax Shunt	T & M	F10,000-40	Eaton E548
Wideband Transformer	Pearson	301X	Eaton E363
Torque Table	Lebow	5528-150	Serial No. 165
Torque Sensor	Himmelstein	9-02T (1-4)	USG G-0033
Torque Sensor	Himmelstein	9-02T (2-3)	USG G-0034
Torque Signal Conditioner	Daytronics	3378	USG G-0049
Wattmeter	Clarke-Hess	255	USG G-0032
Wattmeter	Clarke-Hess	255	USG G-0031
V/Hz Meter	Eaton	-	Eaton E-695

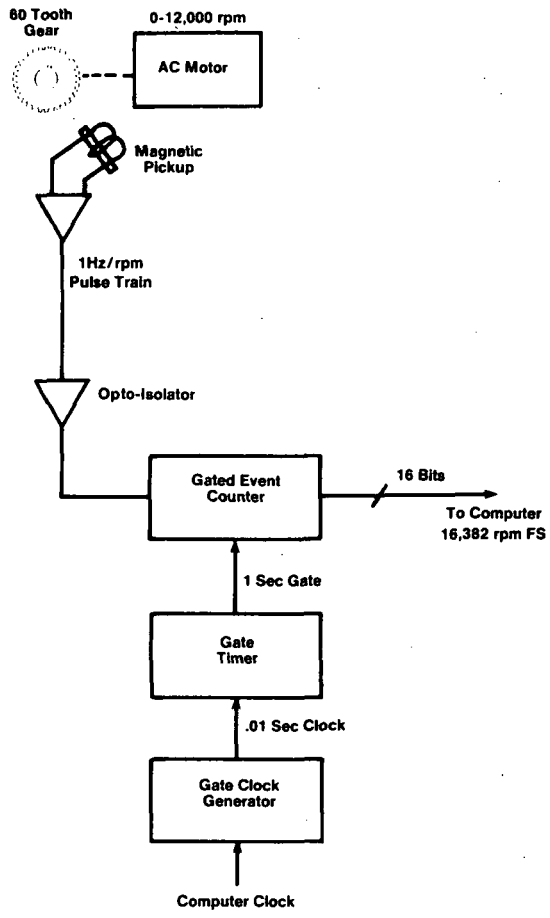

Figure A.4a Motor Speed Channel Block Diagram

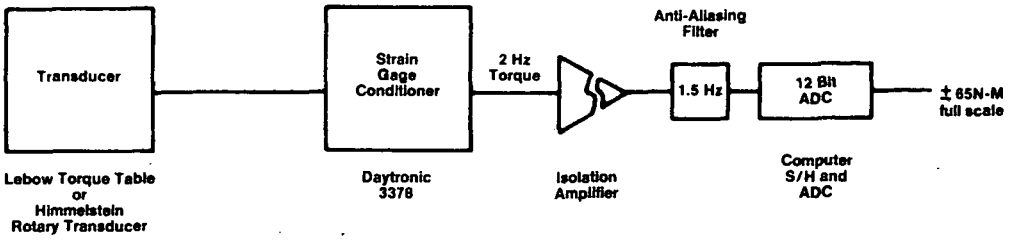

Figure A.4b Traction Battery Current Channel Block Diagram

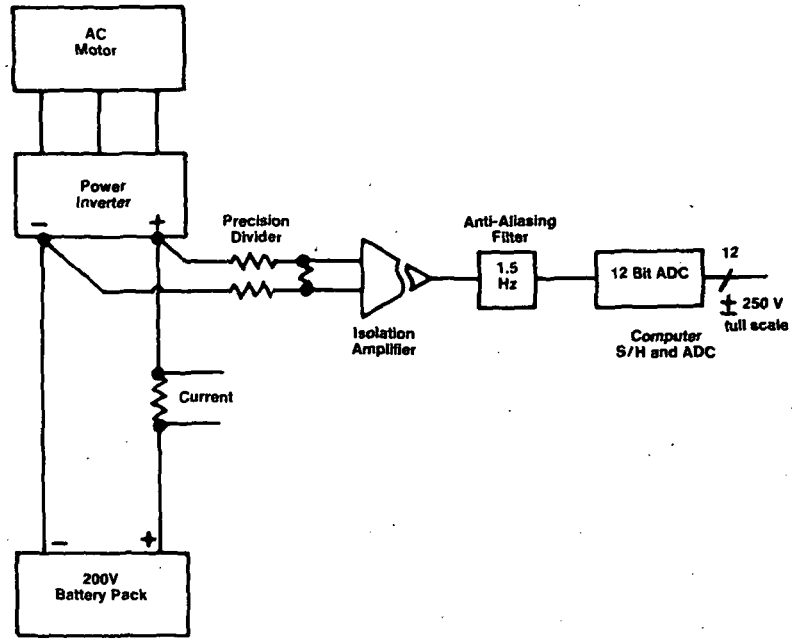

Figure A.4c Traction Battery Volts Channel Block Diagram

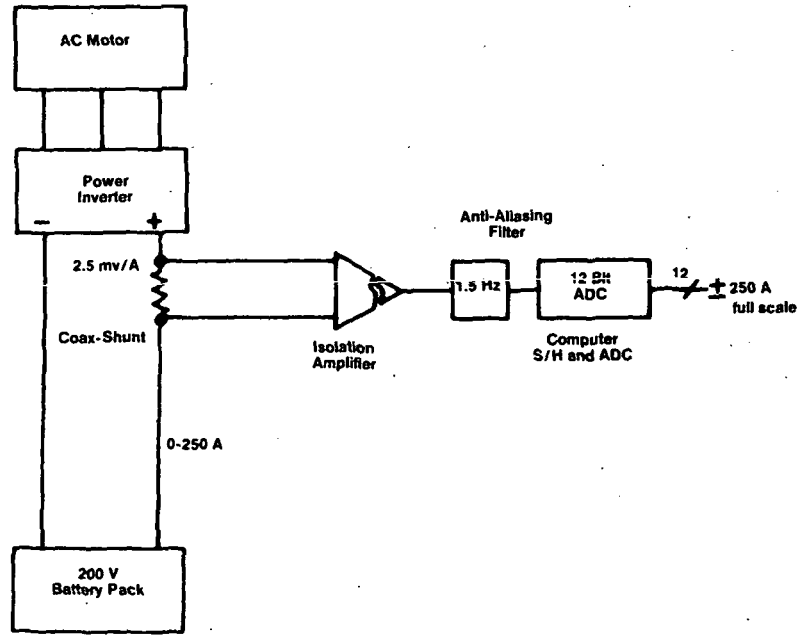

Figure A.4d AC Watts Measurement Block Diagram

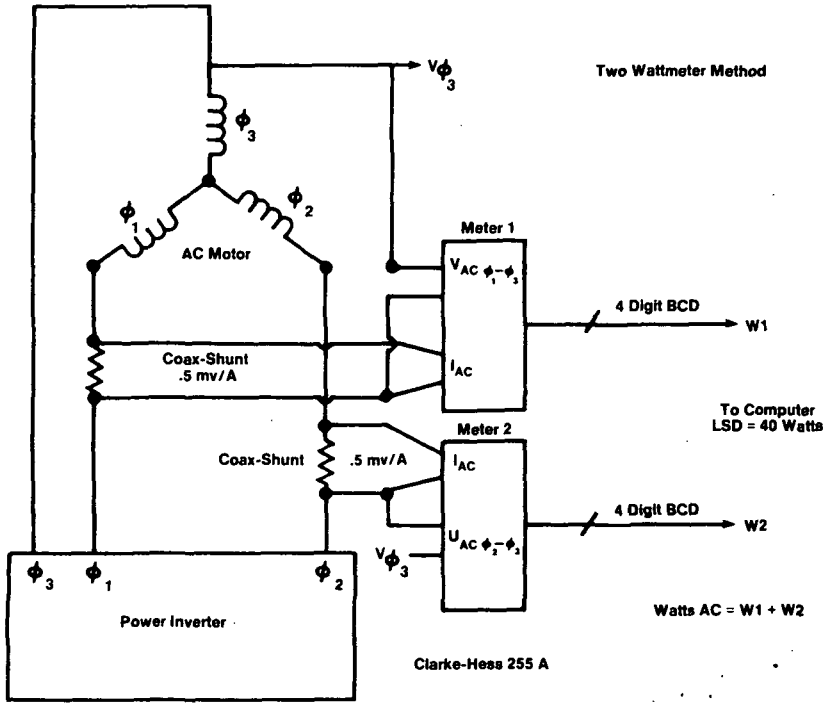

Figure A.4e Torque Channel Block Diagram

APPENDIX B

CONTROLLER SOFTWARE PSEUDO-CODE

MODULES
****

I	ASSIGN	NOTE: ASSIGN COMPILED IN DEFINITIONS AT END OF LISTING
II	RAMLOC	NOTE: RAMLOC COMPILED IN DEFINITIONS AT END OF LISTING
III	MRESET	
IV	MINPRO	
V	MCAP	
VI	EXCHG	
VII	MCHARG	
VIII	MTORQ	
IX	MTRQLM	
X	MSHIFT	
XI	MVPHZ	
XII	MSLIP	
XIII	MDUTCY	
IXX	MWAVE	
XX	MDRIVE	
XXI	EXEND	
XXII	IFRTRG	
XXIII	IFRCLC	
XXIV	IFSGEN	
XXV	ICOMM	
XXVI	S1MLT	
XXVII	S1DIV	
XXVIII	SDCYS	
IXXX	SADSPL	
XXX	STEMP	
XXXI	SCURVE	
XXXII	SSHIFT	
XXXIII	SKDATA	
XXXIV	SWAVLD	
XXXV	SCHDCY	
XXXVI	MWVTBL	
XXXVII	CRVTBL	
XXXVIII	MCNST	
IXXXX	IVCTRS	

```
*************************************************************
*                                                           *
*         AC2 CONTROLER SOFTWARE PSUEDO-CODE                *
*                                                           *
*************************************************************


TITLE    'MRESET.SRC'
********************

RESET MODULE CONTAINS:
 INITIALIZATION OF MICRO AND VARIABLES,
 RAM AND PROM VERIFICATION, AND DISPLAY CHECK
*
*        BEGIN
*          DISABLE INTERRUPTS
*          DEFINE STACK_PTR
*          INHIBIT INVERTER AND ENABLE HI_GEAR
*          INITIALIZE PARALLEL I/O PORTS
*          INITIALIZE SERIAL I/O PORT
*          RESET FR CIRCUIT
*          INITIALIZE OUTPUT CAPTURE REGISTER
*          INITIALIZE INPUT CAPTURE REGISTER
*          TEST RAM INTEGRITY
*          TEST DISPLAY INTEGRITY
*          RESET FASTIV FLAG
*          CAPACITY COUNTER = 1
*          SET RESTART FLAG
*          SELECT HI_GEAR
*          COPY ROM TABLES INTO RAM--CALL SKDATA
*          DIAGNOSTICS_BOX_STATUS_WORD = $80
*          ENABLE INTERRUPTS
*        END_BEGIN

TITLE    'MINPRO.SRC'
********************

MERGES MUX/ADC READ AND CONDITIONING OF INPUTS.
MAINLINE EACH CHANNEL FOR #SAMPLE FLEXIBILITY.
USE "DEAD TIME", ALSO FRCALC D/DT CHECK, DIG WORD PROCESSING,
FAULT PROCESSING, AND DUMMY PROCESSING.
*
*        AUXVLO BIT CLEAR SERVICE ROUTINE
*
*        PROCESS SAMPLED AMBIENT TEMPERATURE
*
*        PROCESS SAMPLED BUS VOLTAGE
*
*        PROCESS SAMPLED BUS CURRENT
*
*        PROCESS SAMPLED HEAT SINK TEMPERATURE
*
*        PROCESS SAMPLED BATTERY TEMPERATURE
*
```

```
*         PROCESS SAMPLED MOTOR TEMPERATURE
*
*         PROCESS SAMPLED ACCEL RATE
*
*         PROCESS SAMPLED DEACCEL RATE
*
        END

        TITLE     'MCAP.SRC'
        ********************

;BATTERY CAPACITY METER
;ESTIMATES ORIGONAL CHARGE LEVEL
;ACOUNTS FOR BATT CHARGE AND DISCHARGE RATES
;INDICATES PRESENT LEVEL OF CHARGE ON DASH LEDS
;
;
;KAMP8S         EQU         0DA98H         = 55960
;KDIVSR         EQU         064H           = 100
;KSCALE         EQU         0A3H
;
;
*         BEGIN
*
*         IF_ROTOR SPEED = 0
*           IF_IBUSF > 2AMPS
*             CAPCN = KCAPCN------------->: NR CYCLES BEFORE UPDATE
*           ELSE                          :
*             CAPCN1 = CAPCN1 - 1         :
*             IF_CAPCN1 = 0               :
*               AMP8S =  (KCAP1)(VBUSOC) - KCAP2
*                 IF_AMP8S <= 0           :
*                   AMP8S = 0             :
*                 END_IF                  :
*               AMP8S.CAL/SCALE           :
*             END_IF                      :
*           END_IF                        :
*         ELSE                            :
*           CAPCN = KCAPCN<---------------: NR CYCLES BEFORE UPDATE
*         END_IF
*         IF_ACCFLG = 1                     NOTE:FLAG SET IN IRQ1
*           CLR ACCFLG
*           IF_IBS8CM < KSCALE
*             AMP8S = AMP8S + (KSCALE - IBS8CM)
*             IF_OVERFLOW
*               AMP8S = KAMP8S (FULL BATT CHARGE LIMIT)
*             END_IF
*           ELSE
*             IBS8CM = IBS8CM - KSCALE
*             AMP8S = AMP8S - IBS8CM
*             IF_NEGATIVE
*               AMP8S = 0
*             END_IF
*           END_IF
```

```
*         ELSE BRANCH TO END
*         END_IF
*         BTTPFC = (KCAP3)(BATTPF) + KCAP4
*         CAPI = (AMP8S/KAMP8S)(BTTPFC)
*         CAP = CAPI
*         IF_RMNDR > 0.5
*           CAP = CAP + 1
*         ELSE
*           IF_CAP > 7
*             CAP = 7
*             IF_CAP = 0
*               CAP = 1
*           END_IF
*         END_IF
*         IF_CHARGE MODE                          NOT USED NOW THRU <
*           IF_I < 0
*             IF_CAPCN > 0
*               TOGGLE CAP LED
*             END_IF
*           END_IF
*         END_IF                                                    <
*         OUTPUT CAP TO OLAT2
*         END
;
;


        TITLE    'EXCHG.SRC'
        ********************

         EXECUTIVE MODULE SELECTING CHARGE MODE
         IF CHARGE DOOR OPEN - ENTER CHARGE MODE
         AND FORCE NEUTRAL


        TITLE    'MCHARG.SRC'
        ********************

        MODULE CHARGE MODE

*         BEGIN
*           INDICATE CHARGE MODE
*           IF 110 OR 220 VAC CHARGING MODE
*             IF CURRENT CHARGE MODE NOT THE SAME AS PREVIOUS CHARGE MODE
*               CHARGE_FLAG = 0
*             END_IF
*             RECORD CURRENT CHARGE MODE AS PREVIOUS CHARGE MODE
*           ELSE
*            CHARGE_ERROR = 1
*            CHARGE_FLAG = 0
*           END_IF
*           IF CHARGE_FLAG = 0
*             CYCLE_COUNTER = KCYCNT
*             CHARGE_FLAG = 1
*             DISABLE CHARGER
```

```
*           END_IF
*           IF CHARGE_FLAG = 1
*             CYCLE_COUNTER = CYCLE_COUNTER - 1
*             IF CYCLE_COUNTER NOT= 0
*               CHARGE_FLAG = 2
*               CHARGE_DUTY_CYCLE = KMNDCC
*             END_IF
*           END_IF
*           IF CHARGE_FLAG = 2
*             LOAD CHARGE WAVEFORM INTO BUFFER_RAM--CALL SWAVLD
*             STROBE OUT THE BUFFER_RAM_FULL SIGNAL
*             SET CHARGE_FLAG = 3
*           END_IF
*           IF CHARGE_FLAG = 3
*             IF THE BUFFER_RAM IS EMPTY
*               ENABLE CHARGER
*               CYCLE_COUNTER = KCYCNT
*               IBUSCM = 0
*               VBUSCM = 0
*               CHARGE_FLAG = 4
*             END_IF
*           END_IF
*           IF CHARGE_FLAG = 4
*             IF CYCLE_COUNTER NOT= 0
*               IBUSCM = :IBUSF: + IBUSCM
*               VBUSCM = VBUSF + VBUSCM
*               CYCLE_COUNTER = CYCLE_COUNTER - 1
*             ELSE
*               IBUSCH = IBUSCM / KCYCNT
*               VBUSCH = VBUSCM / KCYCNT
*               IF CHARGE_DUTY_CYCLE > KTHDCX
*                 IF IBUSF > 0
*                   NO_CHARGE_FLAG = 1
*                   CHARG_ERROR = 1
*                 END_IF
*               ELSE
*                 IF IBUSF > 0
*                   NO_CHARGE_FLAG = 1
*                 ELSE
*                   NO_CHARGE_FLAG = 0
*                 END_IF
*                 CALCULATE CHARGE_DUTY_CYCLE--CALL SCHDCY
*                 IF CHARGE_DUTY_CYCLE < KMNDCC
*                   CYCLE_COUNTER = KCYCNT
*                   SET CHARGE_FLAG = 1
*                 ELSE_IF CHARGE_DUTY_CYCLE > KMXDCX
*                   CHARGE_ERROR = 1
*                 ELSE
*                   CHARGE_FLAG = 2
*                 END_IF
*               END_IF
*             END_IF
*           END_IF
*         JUMP TO MDRIVE
*         END_BEGIN
```

```
TITLE    'MTORQ.SRC'
******************

CALCULATE TRQDM LIMITS
*
*        BEGIN
*          IF RESET FLAG IS SET
*            IF ACCELF < KACLMN
*              CLEAR RESET FLAG
*            END_IF
*            TRQCM = $80
*            DISABLE DRIVE
*          ELSE
*            IF DRIVE IS INHIBITTED
*              DELAY 200 MS
*              DUTCYO = 0
*              FRHYS = 50 HZ
*            ELSE
*              FRHYS = 0 HZ
*            END_IF
*            IF FRCLCF < KFRCO + FRHYS
*              IF ACCELF < KACLMN
*                TRQCM = $80
*                DISABLE DRIVE
*              ELSE
*                TRQCM =  + ACCELF
*                ENABLE DRIVE
*              END_IF
*            ELSE_IF DECEL < KDCLMN
*              IF ACCELF < KACLMN
*                TRQCM = KDCLCS
*              ELSE
*                TRQCM = $80 + ACCELF
*              END_IF
*              ENABLE DRIVE
*            ELSE
*                IF LOGR
*                  DECELF = DECELF / 2
*                  TRQCM = DECELF + :KDCLCS:
*                ELSE
*                  TRQCM = DECELF +: KDCLCS:
*                END_IF
*              ENABLE DRIVE
*            END_IF
*          END_IF
*        END_BEGIN
*
```

```
        TITLE    'MTRQLM.SRC'
        ********************

        CALCULATE TRQDM LIMITS

LIMIT       MACRO       ARG1,ARG2,ARG3          :SUBROUTINE *******
            LOCAL       NOLIM
              LDAA              ARG2              :"A" = ABSCISSA
              LDX               #ARG1             :"X" = CURVE
              JSR               SCURVE            :"B" = ORDINATE
              CMPB              >TRQCMT           :FLAGS: CURVE -TRQCMT
              BHS               NOLIM             :BR IF CURVE >OR= TRQCMT
                STAB            >TRQCMT
                LDAA            #ARG3             :CWRNT = OVERLIMIT MASK
                STAA            >CWRNT
NOLIM
        ENDM
*
*        BEGIN                                    :MAIN MODULE *******
*          TRQCMT = :TRQCM:
*          CWRNT = $00
*          LIMIT TRQCMT TO CURVE3(AMBTPF)
*          LIMIT TRQCMT TO CURVE4(HSTPF)
*          LIMIT TRQCMT TO CURVE5(BATTPF)
*          LIMIT TRQCMT TO CURVE6(MOTTPF)
*          LIMIT TRQCMT TO CURVE7(VBUSF)
*          LIMIT TRQCMT TO CURVE8(IBUSF)
*          LIMIT TRQCMT TO  CURVE9(FRCLCF)
*          IF MOTORING/REGENERATION TRANSITION
*            TRQCMT = 0
*            CWRNT = TQRATE
*          ELSE_IF TRQCMT < :TRQCMO:
*            IF TRQCMT <   (:TRQCMO: - KTQDL)
*              TRQCMT = :TRQCMO: - KTQDL
*              CWRNT = TQRATE
*            END_IF
*          ELSE
*            IF TRQCMT > ( :TRQCMO: + KTQDL)
*              TRQCMT = :TRQCMO: + KTDPL
*              CWRNT = TQRATE
*            END_IF
*          END_IF
*          CWRN =  (CWRN "AND" $20) "OR" CWRNT
*          IF DECELF > 0
*            XF = CURV13(FRCLCF)
*            TRQCMT = XF * TRQCMT
*          END_IF
*          TRQDM = TRQCMT "OR" SIGN(TRQCM)
*          TRQCMO = TRQDM
*        END_BEGIN
*
```

```
TITLE    'MSHIFT.SRC'
*********************
SHIFT LOGIC
*
*    BEGIN
*      IF NEUTRAL REQUESTED
*        IF FR ~ 0
*          FORCE NEUTRAL
*        ELSE
*          DO NOTHING
*        END_IF
*      ELSE_IF PARKBRAKE REQUESTED
*        FORCE NEUTRAL
*      ELSE_IF SHIFT IN PROGRESS
*        SHIFT GEARS--CALL SSHIFT
*      ELSE_IF REVERSE REQUESTED
*         IF FR ~  0
*           FORCE REVERSE
*         ELSE IF REVERSE NOT SELECTED
*           FORCE NEUTRAL
*        ELSE
*          DO NOTHING
*         END_IF
*       ELSE_IF DRIVE REQUESTED
*        IF FR ~  0
*          FORCE LO_GEAR
*         ELSE_IF MANUAL MODE OR REVERSE SELECTED
*           FORCE NEUTRAL
*         ELSE_IF LO_GEAR SELECTED
*           IF FR > KFRSHU
*             UPSHIFT
*           END_IF
*         ELSE
*           IF FR < KFRSHD
*            IF ACCELF > 0
*              DOWNSHIFT
*            ELSE_IF INTEGER(FRCLCF) < KFRCO
*              DOWNSHIFT
*            ELSE
*              DO NOTHING
*            END_IF
*           END_IF
*        END_IF
*       ELSE_IF LO_GEAR_ONLY REQUESTED
*         IF FR ~  0
*           FORCE LO_GEAR
*         ELSE_IF REVERSE SELECTED
*           FORCE NEUTRAL
*        ELSE_IF HI_GEAR SELECTED
*          IF FR < KFRSHD
*            DOWNSHIFT
*          END_IF
```

```
*             ELSE
*               DO NOTHING
*             END_IF
*           ELSE
*             IF FR ~  0
*               FORCE HI_GEAR
*             ELSE_IF REVERSE SELECTED
*               FORCE NEUTRAL
*           ELSE
*             DO NOTHING
*           END_IF
*         END_IF
*       END_BEGIN


      TITLE    'MVPHZ.SRC'
      ********************

      CALC VPHZI FROM CURVE EQUATIONS
      ON ENTERING NEED: TRQDM, VBUSF

*
*       NOTE:  MACHINE VPHZ = 100 * REAL VPHZ
*
*
*       BEGIN
*         VPHZCH = F1(TRQDM)
*         VPHZAV = (VBUSF * 73) / FS
*         IF VPHZCH F VPHZAV
*           VPHZ = VPHZCH
*         ELSE
*           VPHZ = VPHZAV
*         END IF
*       END BEGIN
*


      TITLE    'MSLIP.SRC'
      ********************

      SLIP CALCULATION MODULE
      SETS SLIP TO MAINTAIN MINIMUM FS AND
       CALCULATES NEW VPHZ WHEN IN THIS MODE
      ON ENTERING NEED: VPHZ, TRQDM, FRCLCF

*       BEGIN
*         SLPTMP = (:TRQDM: * KMOT * 2) / (VPHZ)**2
*         IF SLPTMP > $6.0
*           SLPTMP = $6.0
*         END IF
*         FSLP = (TRQDM "AND" $80) "OR" SLPTMP
*       END BEGIN
```

```
TITLE    'MDUTCY.SRC'
*********************

COMPUTE DUTCY W/DEL DUTCY,AND SCALED DUTCY.
DETERMINE W/HYSTEREIS NN BASED ON DUTCY
ENTER WITH: FS, VPHZCH, VBUSF, DUTCY, DUTCYI
EXIT WITH:  DUTCY, DUTCIO, DUTCYS, NNF, NOTCHI
*
*        BEGIN
*          DUTCY = DUTF1 * DUTCY + DUTF2 * DUTCYI  ; FILTER
*          DUTCYO = DUTCY
*          DUTCYI = (FS * VPHZCH) / VBUSF
*          IF TRQDM > = $80 (ACCELL MODE)
*            DIVSR = 85
*          ELSE (REGEN MODE)
*            DIVSR = 79
*          DUTCYI =  DUTCYI * (373 - FRCLCF)  / DIVSR
*          IF DUTCYI> 100%
*            DUTCYI= 100%
*          ELSE_IF DUTCYI< KDCYSU
*            DUTCYI= KDCYSU
*          ELSE
*            DO NOTHING
*          END_IF
*          SCALE DUTCY FOR WAVE TABLE
*          SELECT NOTCH NUMBER
*          SELECT WAVE TABLE INDEX
*        END_BEGIN


TITLE   'MWAVE.SRC'
*******************

WAVE GENERATING SCHEME
ON ENTERING MODULE MUST HAVE: NNF,DUTCYS,NOTCHI(W/ ZNW)
NNF          == FINAL NOTCH NUMBER
DUTCYS          == SCALED DUTCY CYCLE
NOTCHI        == NOTCH INDEX REGESTER


TITLE    'MDRIVE.SRC'
*********************

ENABLES/DISABLES INVERTER DRIVERS
FAULT SHUTDOWN
STROBES OUTPUT LATCHES



TITLE    'EXEND.SRC'
*******************

END EXECUTIVE BLOCK
COMPLETES CHARGE/DRIVE MODE DECISION LOOPS
FLASHES LED, WATCHDOG RETRIGGER, RESTARTS CHARGE IN EVENT OF A FAULT
```

```
TITLE    'IFRTRG.SRC'
*********************

IRQ INTERRUPT HANDELING ROUTINE
FR MEASURE TRIGGER OR ZERO DETECT
IRQ1 PULSE SHOULD BE >60 USEC AND <120 USEC
DECRIMENT ALL TIMERS TO ZERO
INPUT MCAP IBUSS CONDITION DATA


TITLE    'IFRCLC.SRC'
*********************

INPUT CAPTURE OF INITIAL OR FINAL COUNTER VALUE FOR FR MEASURE
INHIBITED IN CHARGE MODE.


TITLE    'IFSGEN.SRC'
*********************

FS OUTPUT FREQUENCY GENERATION
OCF MUST BE CHECKED AT LEAST AT 90 USEC INTERVALS


TITLE    'ICOMM.SRC'
*********************

SCI COMMUNICATION INTERRUPT SERVICE ROUTINE


TITLE    'S1MLT.SRC'
*********************

MULTIPLY 16*8
ON CALL: MULTIPLICAND IN D
          MULTIPLIER IN MULT
ON RETURN: PRODUCT IN D
            PRODUCT(LOW) IN PROD


TITLE    'S1DIV.SRC'
*********************

DIVIDES 16 BIT NUMBER BY AN 8 BIT NUMBER
GIVING A 16 BIT QUOTIENT AND 8 BIT HEX FRACTION
ON CALL: LO(DIVIDEND) IN B
          HI(DIVIDEND) IN A
          8 BIT DIVISOR IN DIVSR
ON RETURN: LO(QUOTIENT) IN B
            HI(QUOTIENT) IN A
            8 BIT HEX FRACTION IN RMNDR
            IF DIVSR = 00, QUOTIENT = FFFF.FF
REG AFFECTED: A,B,SPAD-SPAD+2
```

```
        TITLE   'SDCYS.SRC'
        ********************

        SUBROUTINE SCALES DUTY CYCLE FOR PROPER USE IN MWAVE
        ENTER WITH: DUTCY IN ACCA
        EXIT WITH:  DUTCYS IN RAM MEM


        TITLE   'SADSPL.SRC'
        ********************

        SUBROUTINE A/D AVERAGE SAMPLE

        CALLING SEQUENCE
                A = # OF SAMPLES
                B = UNDEFINED
                X = ANALOG TO DIGITAL CONVERTER CHANNEL ADDRESS
        RETURNING SEQUENCE
                A = CHANGED
                B = AVERAGED SAMPLE
                X = UNCHANGED



*
*        BEGIN:
*          LOOP_COUNTER = LIMIT
*          A/D_SUM = 0
*          REPEAT:
*            TRIGGER ANALOG TO DIGITAL CONVERTER
*            DELAY 130 uSECS
*            A/D_SUM = A/D_SUM + A/D_SAMPLE
*            LOOP_COUNTER = LOOP_COUNTER - 1
*            UNTIL LOOP_COUNTER = 0
*          END REPEAT
*          AVERAGED_SAMPLE = A/D_SUM / LOOP LIMIT
*        END BEGIN



        TITLE   'STEMP.SRC
        ******************

        SUBROUTINE TEMPERATURE PROCESSING

        CALLING SEQUENCE
                A = UNDEFINED
                B = RAW TEMPERATURE
                X = UNDEFINED
        RETURNING SEQUENCE
                A = CHANGED
                B = NORMALIZED TEMPERATURE
                X = CHANGED
```

```
        TITLE   'SCURVE.SRC'
        ********************

        SUBROUTINE CURVE HANDLER
        CALLING SEQUENCE
                A = ABSCISSA
                B = UNDEFINED
                X = CURVE TABLE BASE ADDRESS
        RETURNING SEQUENCE
                A = UNDEFINED
                B = ORDINATE
                X = UNDEFINED

*        BEGIN
*          NODE = 0
*          DO FOREVER
*            IF ABSCISSA <OR= BRKPT$(NODE)
*            THEN
*              ORDINATE = { ABSCISSA * M$(NODE)  / 256} + B$(NODE)
*            ELSE
*              NODE = NODE + 1
*              CONTINUE
*            END IF
*          END DO
*        END BEGIN
*


        TITLE   'SSHIFT.SRC'
        ********************

        SUBROUTINE SHIFT LOGIC
*        BEGIN
*          DUTF1=KDUTF3
*          DUTF2=KDUTF4
*          IF RELEASE_COUNTER = 0
*            TRQDM = F(FRCLCF)
*          ELSE_IF LAP COUNTER = 0
*            IF UPSHIFT
*              FORCE HI_GEAR
*            ELSE
*              FORCE LO_GEAR
*            END IF
*            RELEASE_COUNTER = KRLS
*            LAP_COUNTER = $FF
*            TRQDM = $80
*          ELSE_IF LAP_COUNTER <OR= $7F
*            IF OVERLAP
*              ENABLE LO_GEAR
*              ENABLE HI_GEAR
*            END IF
*          ELSE
*            TRQDM = $80
*          END IF
```

```
*           IF SHIFT COMPLETE
*             INDICATE SHIFT COMPLETE
*             SET TRQCMO = 00
*             DUTF1=KDUTF1
*             DUTF2=KDUTF2
*           END IF
*         END BEGIN
*         LOCAL SUBROUTINE SSHTRQ
*         BEGIN
*           IF UPSHIFT
*             IF FRCLCF <OR= KFRSHU * 0.374
*               TRQDM = $00
*             ELSE
*               TRQDM = KTQUS
*             END IF
*           ELSE
*             IF FRCLCF > KFRSHD * 2.67
*               TRQDM = $00
*             ELSE
*               TRQDM = KTQDS
*             END IF
*           END IF
*         END BEGIN


          TITLE   'SKDATA.SRC'
          **********************

          TRANSFER MODIFY CONSTANTS FROM EPROM TO RAM
          NEEDED ON ENTRY:
           KLNGTH (NUMBER OF CONSTANTS)
           KSTART (PROM START ADDRESS)

*
*          TRANSFER PARAMETERS USED BY SKDATA
*
KSTART    EQU      RESETW           :STARTING ADDRESS OF ROM CONSTANTS
KEND      EQU      KEXCY            :ENDING ADDRESS OF ROM CONSTANTS
KLNGTH    EQU      KEND-KSTART      :LENGTH OF ROM CONSTANTS TABLE
          ENABLES/DISABLES INVERTER DRIVERS
          FAULT SHUTDOWN
          STROBES OUTPUT LATCHES
*
*          DUTF1=KDUTF1                          :SETUP DUTCY FILTER FOR
*          DUTF2=KDUTF2                          :DRIVE MODE TIME CONSTANTS
*
          END
```

```
        TITLE   'SWAVLD.SRC'
        ********************

        CHARGE MODE WAVE LOADING SUBROUTINE
*        BEGIN
*          PTR = BUFFER_RAM_BASE_ADDRESS
*          PERIOD_COUNTER = KPERD
*          DO
*          PERIOD_LENGTH_COUNTER = 0
*           DO
*             BUFFER_RAM(PTR) = $01
*             PTR = PTR + 1
*             PERIOD_LENGTH_COUNTER = PERIOD_LENGTH_COUNTER + 1
*           UNTIL PERIOD_LENGTH_COUNTER = CHARGE_DUTY_CYCLE
*           DO
*             BUFFER_RAM(PTR) = $00
*             PTR = PTR + 1
*             PERIOD_LENGTH_COUNTER = PERIOD_LENGTH_COUNTER + 1
*           UNTIL PERIOD_LENGTH_COUNTER = KRSLN
*           PERIOD_COUNTER = PERIOD_COUNTER - 1
*         UNTIL PERIOD_COUNTER = 0
*        END_BEGIN
*



        TITLE   'SCHDCY.SRC'
        ********************

*        BEGIN
*          VBUSCR = CURVE2(BATTPF)
*          IF VBUSCH >OR= VBUSCR
*            CHARGE_DUTY_CYCLE = CHARGE_DUTY_CYCLE - 1
*          ELSE
*            XF = $FF
*            CWRNT = $00
*            LIMIT XF TO CURVE10(AMBTPF)
*            LIMIT XF TO CURVE11(HSTPF)
*            LIMIT XF TO CURVE12(BATTPF)
*            CWRN = (CWRN "AND" $8F) "OR" CWRNT
*            MXICH = (MXICH * XF) / $0100
*            IF IBUSCH > MXICH
*              CHARGE_DUTY_CYCLE = CHARGE_DUTY_CYCLE - 1
*            ELSE
*              CHARGE_DUTY_CYCLE = CHARGE_DUTY_CYCLE + 1
*            END_IF
*          END_IF
*        END_BEGIN
        LOCAL SUBROUTINE CALCULATE CHARGE DUTY CYCLE
LIMIT   MACRO   ARG1,ARG2,ARG3
        LOCAL   NEXT
        LDAA                ARG2                :"A" = PARAMETER
        LDX                 #ARG1               :"X" = CURVE
```

```
        JSR             SCURVE
        CMPB            >XF                 :FLAGS: CURVE - XF
        BHS             NEXT                :BR IF CURVE >OR= XF
          STAB            >XF
          LDAA            #ARG3             :CWRNT = OVERLIMIT MASK
          STAA            >CWRNT
NEXT
        END_MODULE


        TITLE   'MWVTBL.SRC'
        ********************

        WAVE TABLE VALUES FOR MWAVE
        REDUCED TO 24 NOTCH VALUES ONLY.


        TITLE   'CRVTBL.SRC'
        ********************

        CURVE TABLE FOR SCURVE

*       VPHZCH = F(TRQDM)
*
CURVE1
*       VBUSCR = F(BATTP)
*
CURVE2
*       :TRQ: = F(AMBTPF)
*
CURVE3
*       :TRQ: = F(HSTPF)
*
CURVE4
*       :TRQ: = F(BATTPF)
*
CURVE5
*       :TRQ: = F(MOTTPF)
*
CURVE6
*       :TRQ: = F(VBUSF)
*
CURVE7
*       :TRQ: = F(IBUSF)
*
CURVE8
*       :TRQ: = F(FRCLCF)
*
CURVE9
*       XF = F(AMBTPF)
*
CURV10
*       XF = F(HSTPF)
*
```

```
CURV11
*       XF = F(BATTPF)
*
CURV12
*       XF = F(FRCLCF)
*
CURV13
*       XF = F(FRCLCF)


        TITLE   'IVCTRS.SRC'
        ********************

        INTERRUPT VECTORS
        SWI
        NMI
        RESET
```

```
*********************************************************
*                                                       *
*  AC2 SOFTWARE LOGICAL PROGRAM SYMBOL DEFINITIONS      *
*                                                       *
*********************************************************


THIS SECTION IS A COMPILATION OF SYMBOL AND DEFINITION TABLES
FROM THE FOLLOWING MODULES

TITLE   'RAMLOC.SRC'
********************
RAMLOC MODULE CONTAINS ALL RAM ALLOCATIONS

TITLE   'MCNST.SRC'
********************
CONTROLER CONSTANTS

TITLE   'ASSIGN.SRC'
********************
ASSIGNMENT SYMBOL TABLE


ACCELF      RMB     1           ; IDX_18--ACCEL DEMAND FINAL (AXXX%)
ACCFLG      RMB     1           ;--RESERVED FOR USE IN MCAP.SRC (ACCUM FLAG)--
ACLD        RMB     1           ;DUMMY ACCELERATOR INPUT
ADSUM       RMB     2           ;A/D AVERAGING SUM
AMBTPF      RMB     1           ; IDX_30--AMBIENT TEMPERATURE (DEG C)
AMP8S       RMB     2           ;SCALED CUM AMPS, MCAP
AMTQL       EQU     %00000001   ;AMBIENT TEMPERATURE TORQUE LIMIT
ANLERR      EQU     %00010000   ;ANALOG ERROR
B$          EQU     3           ;INTERCEPT
BATTPF      RMB     1           ; IDX_32--BATTERY TEMPERATURE (DEG C)
BFINX       RMB     1           ;INDEX BUFFER
BFRMFL      EQU     $2003       ;BUFFER RAM FULL
BITCNT      RMB     2           ;BIT COUNTER
BRKPT$      EQU     0           ;BREAK POINT
BTTPFC      RMB     1           ; IDX_34--SCALING/TEMP FACTOR--<MCAP>
BTTQL       EQU     %00000100   ;BATTERY TEMPERATURE TORQUE LIMIT
BUFWD1      RMB     1           ; IDX_21--INPUT BUFFER WORD
BWVOUT      EQU     $1000       ;BUFFER RAM BASE ADDRESS
CAPCN       RMB     1           ;CAPACITY CNTR, MCAP
CFLT1       RMB     1           ; IDX_1D--CONTR. FAULT WORD 1
CFLT1L      RMB     1           ; IDX_25--CONTROLLER FAULT WORD 1 LATCHED
CFLT2       RMB     1           ; IDX_1E--CONTR. FAULT WORD 2
CFLT2L      RMB     1           ; IDX_26--CONTROLLER FAULT WORD 2 LATCHED
CHARFG      EQU     %00000111   ;CHARGE FLAG
CHG110      EQU     %01000000   ;110 VAC CHARGING REQUESTED
CHG220      EQU     %10000000   ;220 VAC CHARGING REQUESTED
CHRERR      EQU     %00100000   ;CHARGE ERROR
CHRIND      EQU     %00001000   ;CHARGE MODE SELECTED
CHRVOL      RMB     1           ;CHARGE VOLTAGE (110 OR 220)
CMSTAT      RMB     1           ;SERIAL COMMUNICATION STATUS
CNST        RMB     1           ; IDX_20--CONTR. STATUS WORD
```

```
CNT             EQU     SPAD
CNTR1           RMB     2       ;COUNTER #1--(2 BYTES--CHARGE MODE ONLY)
COUNT           EQU     SPAD+2  ;COUNTER
CUMCNT          RMB     1       ;CUMULATIVE CNTR, MCAP, IN IRQ1 (MCAP)
CWRN            RMB     1       ; IDX_1F--CONTR. WARN WORD
CWRNT           EQU     SPAD+3  ;TEMPORARY WARN WORD
CYCNT           RMB     1       ;CYCLE COUNTER
DCLD            RMB     1       ;DUMMY DEACCELERATOR INPUT
DCYCH           RMB     1       ; IDX_2B--DUTY CYCLE (%)--<MCHARGE>
DCYM            RMB     1       ;MANUAL DUTY CYCLE
DECELF          RMB     1       ; IDX_19--DECEL DEMAND FINAL (DXXX%)
DELTFS          RMB     2       ;STATOR FREQUENCY HALF PERIOD LENGTH
DFSRMN          RMB     1       ;DELTFS REMAINDER
DIACN           RMB     1       ;DIAGNOSTIC BOX CONTROL STATUS WORD
DIVCNT          RMB     1       ;DIVIDE COUNTER
DIVSR           RMB     1       ;DIVISOR
DLY130          EQU     31      ;# OF 4 µSEC DELAYS FOR A/D CONVERGANCE
DRIVE           EQU     %00001000 ;DRIVE REQUESTED
DUTCY           RMB     1       ; IDX_15--DUTY CYCLE (XXX%)
DUTCYI          RMB     1       ;INTERMEDIATE DUTCY CALCULATION
DUTCYO          RMB     1       ;OLD DUTY CYCLE
DUTCYS          RMB     2       ;DUTY CYCLE SCALED
DUTF1           RMB     1       ;DUTCY FILTER CONSTANT STORAGE #1
DUTF2           RMB     1       ;DUTCY FILTER CONSTANT STORAGE #2
DVDH            EQU     SPAD    ;DIVIDEND HIGH BYTE
DVDL            EQU     SPAD+1  ;DIVIDEND LOW BYTE
DYMSK1          RMB     1       ;DUMMY MASK #1
DYMSK2          RMB     1       ;DUMMY MASK #2
FASTIV          EQU     %01000000 ;FAST I OR V ERROR
FLGWRD          RMB     1       ; IDX_1C--FLAG WORD (COMPOSITE)
FRCLCF          RMB     2       ; IDX_10--FINAL CALC ROTOR FREQ. (HZ)
FRD             RMB     1       ;DUMMY ROTOR FREQUENCY
FREX            EQU     %00001000 ;FR EXCEEDED
FRFLG           RMB     1       ;ROTOR FREQUENCY CALCULATION FLAGWORD
FRTQL           EQU     %00000000 ;ROTOR FREQUENCY TORQUE LIMIT(WAS #10)
FRZERO          EQU     %00000010 ;ZERO FR
FS              RMB     2       ; IDX_12--STATOR FREQ. (HZ)
FSLP            RMB     1       ; IDX_14--SLIP FREQ. (+-HZ)
FSLPM           RMB     1       ;MANUAL SLIP FREQUENCY
HGOREQ          EQU     %00010000 ;HI_GEAR_ONLY REQUEST
HGRSEL          EQU     %00001000 ;HI_GEAR_SELECTED
HIGEAR          EQU     %10000000 ;HI_GEAR ENABLE
HSTPF           RMB     1       ; IDX_31--HEAT SINK TEMPERATURE (DEG C)
HSTQL           EQU     %00000010 ;HEAT_SINK TEMPERATURE TORQUE LIMIT
IBS8CM          RMB     2       ;SCALED IBSCUM FOR W-SEC, MCAP
IBSCUM          RMB     2       ;CUMULATIVE IBUS, MCAP, IN IRQ1 (MCAP)
IBUSCH          RMB     1       ; IDX_2A--BUS CURRENT AVE (-A)--<MCHARG>
IBUSCM          RMB     2       ;CUMULATIVE BUS CURRENT
IBUSD           RMB     1       ;DUMMY BUS CURRENT
IBUSF           RMB     1       ; IDX_1B--BUS CURRENT FINAL (+-AMPS)
ICR             EQU     $0D     ;INPUT CAPTURE REGISTER
INBUF1          EQU     $2005   ;INPUT BUFFER #1
```

```
INBUF2      EQU     $2006       ;INPUT BUFFER #1
INHCB       EQU     %10000000   ;DRIVE ENABLE
INHIB       EQU     %00000001   ;DRIVE_INHIBIT'
K24         EQU     $18         ;DO LOOP ARGUMENT IN S1DIV.SRC
KACLMN      FCB     01          ; THRESHOLD OF ACCEL MODE
KACLMX      RMB     1           ; IDX_3D--MAXIMUM ACCELERATION
KACLMX      FCB     90          ; MAXIMUM ACCELERATION / 2
KAMBFN      RMB     1           ; IDX_3F--AMB TEMP FAN TURN ON POINT (DEG C)
KAMBFN      FCB     028H        ; 40 C   AMBIENT TEMP THRESHOLD FOR FAN ACTUATION
KAMBTP      FCB     046H        ; 70 C   AMBIENT TEMP. SHUTDOWN LIMIT
KAMBTP      RMB     1           ; IDX_40--AMB TEMP OVERLIMIT POINT (DEG C)
KBATTP      FCB     03CH        ; 60 C   BAT TEMP. SHUTDOWN LIMIT
KBATTP      RMB     1           ; IDX_4A--BATTERY TEMP OVERLIMIT POINT (DEG C)
KCHRCY      FDB     0EA60H      ; 10 MIN. NOM.  CHARGE RESTART TIME AFTER FAULT
KCYCNT      RMB     1           ; IDX_45--INITIAL COUNTER VALUE--<MCHARG>
KCYCNT      FCB     0FFH        ; INITIAL COUNTER VALUE IN MCHARG
KDCLCS      FCB     $80         ; COAST DECEL (SIMULATE ENGINE BRAKING)
KDCLCS      RMB     1           ; IDX_51--COAST DECEL
KDCLMN      FCB     01          ; THRESHOLD OF DECEL MODE
KDCLMX      FCB     $2D         ; MAXIMUM DEACCELERATION / 2
KDCLMX      RMB     1           ; IDX_3E--MINIMUM ACCELERATION
KDCYSU      FCB     $12         ; START UP DUTY CYCLE
KDCYSU      RMB     1           ; IDX_53--STARTUP DUTY CYCLE LIMIT (2.55 %)
KDLDCY      FCB     $0F         ; DUTCY RATE OF CHANGE LIMIT
KDLNCH      FCB     08H         ; FS HYSTERISIS FOR NOTCH SELECTION
KDUTF1      FCB     $80         ; DIGITAL FILTER CONSTANT #1
KDUTF2      FCB     $7E         ; DIGITAL FILTER CONSTANT #2
KEND        EQU     KEXCY       ;ENDING ADDRESS OF ROM CONSTANTS
KEXCY       FCB     04H         ; NUMBER OF EXEC CYCLES BEFORE FAULT LATCHES
KEXCY       RMB     1           ; IDX_5F--NUMBER OF EXEC CYCLES BEFORE FAULT
                                  LATCHES
KFRCO       FCB     $10         ; LO SPEED CUTOUT
KFRCO       RMB     1           ; IDX_50--LOW SPEED CUTOUT
KFRSHD      RMB     1           ; IDX_54--ROTOR FREQ. DOWNSHIFT POINT (HZ)
KFRSHD      FCB     55          ; 55 HZ
KFRSHU      FCB     $C8         ; 200 HZ
KFRSHU      RMB     1           ; IDX_55--ROTOR FREQ. UPSHIFT POINT (HZ)
KHSFN       FCB     $28         ; 40 C   HS TEMP. THRESHOLD FOR FAN ACTUATION
KHSFN       RMB     1           ; IDX_48--HEAT SINK TEMP FAN TURN ON POINT
                                  (DEG C)
KHSTP       FCB     06EH        ; 110 C   HS TEMP. SHUTDOWN LIMIT
KHSTP       RMB     1           ; IDX_49--HEAT SINK TEMP OVERLIMIT POINT
                                  (DEG C)
KI110       FCB     $03         ; 06 A, CHARGE CURRENT CLAMP ($  2)
                                  FOR 110 V

KI110       RMB     1           ; IDX_43--MAX CHARGE CURRENT IN 110 VAC
KI220       FCB     $08         ; 16 A, CHARGE CURRENT CLAMP ($  2)
                                  FOR 220 V
KI220       RMB     1           ; IDX_44--MAX CHARGE CURRENT IN 220 VAC
KIBMAX      FCB     0FDH        ; +250 A   FASTIV CURRENT TRIGGER
KLAPD       FCB     $B0         ; 480 MS  LAP DOWNSHIFT
KLAPD       RMB     1           ; IDX_56--DOWNSHIFT LAP VALUE (10 MS/STEP)
KLAPU       FCB     $A0         ; 960 MS LAP UPSHIFT
```

```
KLAPU     RMB     1          ; IDX_57--UPSHIFT LAP VALUE (10 MS/STEP)
KLNGTH    EQU     KEND-KSTART;LENGTH OF ROM CONSTANTS TABLE
KLOWFS    FDB     $0401      ; LOW FS CROSS OVER POINT
KLOWFS    RMB     2          ; IDX_5D--MIN STATOR FREQ ALLOWED
KMNDCC    FCB     02         ; MINIMUM DUTY CYCLE
KMNDCC    RMB     1          ; IDX_3C--MINIMUN DUTY CYCLE
KMNIBS    FCB     05AH       ; -180 A  CURRENT SHUTDOWN LIMIT
KMNIBS    RMB     1          ; IDX_47--NEGATIVE BUS CURRENT LIMIT (A)
KMNVBS    RMB     1          ; IDX_42--MIN BUS VOLTAGE LIMIT (V)
KMNVBS    FCB     07DH       ; 125 V  MIN VBUS SHUTDOWN LIMIT
KMODFG    FCB     0FFH       ; FF = MODIFIABLE,  00 = NONMODIFIABLE
KMOT      FCB     138        ; MOTOR SLIP SCALING CONSTANT
KMOT      RMB     1          ; IDX_5B--MOTOR SLIP SCALING CONSTANT
KMOTTP    FCB     0BEH       ; 190 C   MOTOR TEMP. SHUTDOWN LIMIT
KMOTTP    RMB     1          ; IDX_4B--MOTOR TEMP OVERLIMIT POINT (DEG C)
KMXDC1    FCB     $15        ; 110 V DCYCH CLAMP LIMIT
KMXDC1    RMB     1          ; IDX_4E--110 V MAX DCYCH--<MCHARG>
KMXDC2    RMB     1          ; IDX_4F--220 V MAX DCYCH--<MCHARG>
KMXDC2    FCB     $15        ; 220 V DCYCH CLAMP LIMIT
KMXVBS    FCB     248        ; 248 V  MAX VBUS SHUTDOWN LIMIT
KMXVBS    RMB     1          ; IDX_41--MAX BUS VOLTAGE LIMIT (V)
KNTCH     EQU     0
KPERD     EQU     1920/KRSLN ;NUMBER OF PERIODS IN CHARGE MODE
KPLIBS    RMB     1          ; IDX_46--POSITIVE BUS CURRENT LIMIT (A)
KPLIBS    FCB     0F8H       ; +240 A  CURRENT SHUTDOWN LIMIT
KRLS      FCB     $28        ; CLUTCH RELEASE TIME (10 MS/COUNT) (200 MS)
KRLS      RMB     1          ; IDX_52--CLUTCH RELEASE TIME CONSTANT
KRSLN     EQU     60         ;PERIOD RESOLUTION IN CHARGE MODE
KSHFT     FCB     $F0        ; 1 SEC NOM.  OVER ALL SHIFT TIME
KSHFT     RMB     1          ; IDX_3B--SHIFT DELAY ($64 = 1 SEC)
KSTART    EQU     RESETW     ;STARTING ADDRESS OF ROM CONSTANTS
KTHDC1    FCB     $3B        ; 110 V DCYCH THRESHOLD LIMIT
KTHDC1    RMB     1          ; IDX_4C--110 V THRESHOLD DCYCH--<MCHARG>
KTHDC2    FCB     $3B        ; 220 V DCYCH THRESHOLD LIMIT
KTHDC2    RMB     1          ; IDX_4D--220 V THRESHOLD DCYCH--<MCHARG>
KTQDL     FCB     $10        ; TORQUE RATE OF CHANGE
KTQDS     FCB     $90        ; TORQUE DEMAND (ACCEL) DURING DOWNSHIFT
KTQDS     RMB     1          ; IDX_58--DOWNSHIFT MOTOR TORQ VALUE
KTQUS     FCB     $20        ; TORQUE DEMAND (DECEL) DURING UPSHIFT
KTQUS     RMB     1          ; IDX_59--UPSHIFT MOTOR TORQ VALUE
KVBMAX    FCB     248        ; 248 V  FASTIV VOLTAGE TRIGGER
LAPCNT    RMB     1          ;UNDER / OVER LAP COUNTER
LAT1      RMB     1          ; IDX_23--LATCH 1 VALUE STROBED
LAT2      RMB     1          ; IDX_24--LATCH 2 VALUE STROBED
LEDCNT    RMB     1          ;LED COUNTER
LGOREQ    EQU     %00000100  ;LO_GEAR_ONLY REQUESTED
LGRSEL    EQU     %00000100  ;LO_GEAR_SELECTED
LOGEAR    EQU     %01000000  ;LO_GEAR ENABLE
M$        EQU     1          ;SLOPE
MANMOD    EQU     %00100000  ;MANUAL MODE
MODE      RMB     1          ; IDX_22--MODE OF VEHICLE
MODED     RMB     1          ;DUMMY MODE WORD
MOTTPF    RMB     1          ; IDX_33--MOTOR TEMPERATURE (DEG C)
MOTTPR    RMB     1          ; IDX_39__RAW ANALOG SAMPLED MOTOR TEMPERATURE
```

```
MTTQL       EQU     %00001000   ;MOTOR TEMPERATURE TORQUE LIMIT
MULT        RMB     1           ;MULTIPLIER
NCHCT1      RMB     1           ;NOTCH COUNTER PHASE 1
NCHCT2      RMB     1           ;NOTCH COUNTER PHASE 2
NCHCT3      RMB     1           ;NOTCH COUNTER PHASE 3
NCHCTX      EQU     7
NCHSPD      RMB     2           ;NOTCH SCRATCH PAD
NCHTBL      RMB     30          ;NOTCH TABLE RAM
NEUTRL      EQU     %00011110   ;NEUTRAL' REQUESTED
NNF         RMB     1           ; IDX_36--NOTCH NUMBER FINAL
NNM         RMB     1           ;MANUAL NOTCH NUMBER
NOCHR       EQU     %00100000   ;CHARGE MODE - TRICKLE CHARGE ONLY
NOTCHI      RMB     2           ;NOTCH INDEX REGISTER
NTCH        EQU     1
OCFCNT      RMB     1           ;OUTPUT CAPTURE FLAG COUNTER
OCR         EQU     $0B         ;OUTPUT CAPTURE REGISTER
OLAT1       RMB     1           ;OUTPUT LATCH 1 WORD
OLAT2       RMB     1           ;OUTPUT LATCH 2 WORD
P1DDR       EQU     $00         ;PORT 1 DATA DIR REG
P2DDR       EQU     $01         ;PORT 2 DATA DIR REG
PH1CNT      RMB     1           ;PHASE 1 COUNTER
PH2CNT      RMB     1           ;PHASE 2 COUNTER
PH3CNT      RMB     1           ;PHASE 3 COUNTER
PHXCNT      EQU     6
PORT1       EQU     $02         ;PORT # 1
PRKBRK      EQU     %00000001   ;PARK_BREAK' REQUESTED
PROD        RMB     1           ;LSB OF PRODUCT
PROMST      EQU     $F000       ;PROM START ADDRESS
PWCNT       EQU     BITCNT+1    ;PULSE WIDTH COUNTER
RAMEND      EQU     $17F        ;USER RAM END ADDRESS
RAMERR      EQU     %00000010   ;RAM ERROR
RAMST       EQU     $080        ;USER RAM START ADDRESS
RBUFF       RMB     1           ;BUFFER REGISTER
RDADC       EQU     $2004       ;READ A/D CONVERTER
RDR         EQU     $12         ;UART RX DATA REG
RESETW      RMB     1           ; IDX_3A--RESET WORD ($EE -> CLRCFLT1/CFLT2,
RESETW      FCB     00          ; EE = CLEAR CFLT1,2    FF = RESET CONTROLLER
REVREQ      EQU     %00000010   ;REVERSE REQUESTED
REVSEL      EQU     %00000001   ;REVERSE / FORWARD' SELECTED
RLSCNT      EQU     CNTR1       ;CLUTCH RELEASE COUNTER--(2 BYTE--MOTORING
                                 MODE ONLY)
RMCR        EQU     $10         ;UART RATE/MODE REGISTER
RMNDR       RMB     1           ;REMAINDER
RPM         RMB     2           ; IDX_2E--RPM (XXXX0 MOTOR RPM)
RSTFR       EQU     $2001       ;RESET FR CIRCUIT
RUNMOD      EQU     %00100000   ;RUN_MODE / STARTUP_MODE'
SACCEL      EQU     4           ;# OF ACCEL RATE SAMPLES
SAMBTP      EQU     8           ;# OF AMBIENT TEMPERATURE SAMPLES
SBATTP      EQU     8           ;# OF BATTERY TEMPERATURE SAMPLES
SCRPAD      RMB     07          ;SCRATCHPAD RAM
SDECEL      EQU     4           ;# OF DECEL RATE SAMPLES
SHCNT       RMB     1           ;SHIFT COUNTER
SHERR       EQU     %10000000   ;SHIFT ERROR
SHFLG       EQU     %00010000   ;SHIFT
```

```
SHSTP       EQU     8           ;# OF HEAT SINK TEMPERATURE SAMPLES
SIBUS       EQU     4           ;# OF BUS CURRENT SAMPLES
SIP         EQU     %01000000   ;SHIFT_IN_PROGRESS
SLPTMP      EQU     SPAD+4      ;TEMPORARY SLIP VALUE
SMOTTP      EQU     8           ;# OF MOTOR TEMPERATURE SAMPLES
SPAD        RMB     8           ;SCRATCH PAD RAM
SPARE1      RMB     1           ; IDX_29__(WAS MXICH)
SPARE2      RMB     1           ; IDX_37--SPARE
SPARE3      RMB     1           ; IDX_5A--SPARE--
SPARE4      RMB     1           ; IDX_5C--SPARE WAS (KFRSU)
SPLCTR      RMB     1           ;TEMPERATURE SAMPLING COUNTER
STKTOP      RMB     1           ;TOP OF STACK
STRL1       EQU     $2005       ;STROBE LATCH #1
STRL2       EQU     $2006       ;STROBE LATCH #2
STRMX0      EQU     $2004       ;AMBIENT TEMPERATURE        (CH 0)
STRMX1      EQU     $2014       ;BUS VOLTAGE                (CH 1)
STRMX2      EQU     $2024       ;BUS CURRENT                (CH 2)
STRMX3      EQU     $2034       ;ACCELERATION RATE          (CH 3)
STRMX4      EQU     $2044       ;DEACCELERATION RATE        (CH 4)
STRMX5      EQU     $2054       ;HEAT SINK TEMPERATURE      (CH 5)
STRMX6      EQU     $2064       ;BATTERY TEMPERATURE        (CH 6)
STRMX7      EQU     $2074       ;MOTOR TEMPERATURE          (CH 7)
SVBUS       EQU     8           ;# OF BUS VOLTAGE SAMPLES
TBLCNT      RMB     1           ;TABLE COUNTER
TBLI        EQU     2
TCSR        EQU     $08         ;TIMER CONTROL AND STATUS REGISTER
TDR         EQU     $13         ;UART TX DATA REG
TEMP1       RMB     2           ;TEMPORARY STORAGE #1
TEMP2       RMB     2           ;TEMPORARY STORAGE #2
TGGL11      RMB     2           ;FIRST TOGGLE POINT PHASE 1
TGGL12      RMB     2           ;SECOND TOGGLE POINT PHASE 1
TGGL21      RMB     2           ;FIRST TOGGLE POINT PHASE 2
TGGL22      RMB     2           ;SECOND TOGGLE POINT PHASE 2
TGGL31      RMB     2           ;FIRST TOGGLE POINT PHASE 3
TGGL32      RMB     2           ;SECOND TOGGLE POINT PHASE 3
TGGLX1      EQU     0
TGGLX2      EQU     4
TPD         RMB     1           ;DUMMY TEMPERATURE
TQRATE      EQU     %10000000   ;TORQUE RATE LIMIT
TRCSR       EQU     $11         ;UART TX/RX, CONTROL, AND STATUS REG
TRGFR       EQU     $2002       ;TRIGGER FR CIRCUIT
TRQCM       EQU     SPAD+7      ;TORQUE COMMAND INITIAL
TRQCMO      RMB     1           ;TORQUE COMMAND OLD
TRQCMT      EQU     SPAD+6      ;TORQUE COMMAND WITH TEMP. LIMITS
TRQDM       RMB     1           ; IDX_2D--TORQUE DEMAND (+/- % OF RATED)
VBUSCH      RMB     1           ; IDX_28--BUS VOLTAGE AVE (V)--<MCHARG>
VBUSCM      RMB     2           ;CUMULATIVE BUS VOLTAGE
VBUSCR      RMB     1           ; IDX_27--CROSSOVER BUS VOLTAGE (V)--
                                  <MCHARG>
VBUSD       RMB     1           ;DUMMY BUS VOLTAGE
VBUSF       RMB     1           ; IDX_1A--BUS VOLTAGE FINAL (VOLTS)
VITQL       EQU     %01000000   ;VOLTAGE / CURRENT TORQUE LIMIT
VPHZ        RMB     1           ; IDX_17--VOLTS / HERTZ (SCALED)
VPHZCH      RMB     1           ; IDX_38--VPHZ CHART (100 HZ)
VPHZIU      RMB     1           ; IDX_35--VPHZI UNSCALED (100 HZ)
```

```
WAVCNT      RMB     2       ;WAVE COUNT (CURRENT BUFFER RAM ADDRESS)
WAVOUT      RMB     2       ;WAVE OUTPUT COUNTER
WAVWRD      RMB     1       ;WAVE WORD
WMSK11      RMB     1       ;WAVE MASK HIGH PHASE 1
WMSK12      RMB     1       ;WAVE MASK LOW PHASE 1
WMSK21      RMB     1       ;WAVE MASK HIGH PHASE 2
WMSK22      RMB     1       ;WAVE MASK LOW PHASE 2
WMSK31      RMB     1       ;WAVE MASK HIGH PHASE 3
WMSK32      RMB     1       ;WAVE MASK LOW PHASE 3
WMSKX1      EQU     2
WMSKX2      EQU     3
WRNCNT      RMB     1       ;WARN COUNTER
WTCHDG      EQU     $2000   ;WATCH DOG TIMER RETRIGGER
XF          EQU     SPAD+6  ;X FACTOR (IN MCHARG)
ZNW         RMB     1       ;ZERO NOTCH WIDTH
```

```
*****************************************
*                                       *
*        DEFINITION LISTING OF          *
*        MEMORY LOCATIONS FOR RAM       *
*                                       *
*****************************************
```

ACCELF	00F8	ACCFLG	0095	ACLD	0083	ADSUM	00E6
AMBTPF	0110	AMP8S	00D6	AMTQL	0001	ANLERR	0010
BATTPF	0112	BFINX	008F	BFRMFL	2003	BITCNT	00B8
BRKPT$	0000	BTTPFC	0114	BTTQL	0004	BUFWD1	0101
BWVOUT	1000	B$	0003	CAPCN	00D5	CFLT1	00FD
CFLT1L	0105	CFLT2	00FE	CFLT2L	0106	CHARFG	0007
CHG110	0040	CHG220	0080	CHRERR	0020	CHRIND	0008
CHRVOL	00D8	CMSTAT	008E	CNST	0100	CNT	00CD
CNTR1	0091	COUNT	00CF	CUMCNT	00C8	CURV10	FFB2
CURV11	FFB7	CURV12	FFBC	CURV13	FFC1	CURVE1	FF53
CURVE2	FF76	CURVE3	FF7B	CURVE4	FF80	CURVE5	FF85
CURVE6	FF8A	CURVE7	FF8F	CURVE8	FF99	CURVE9	FFA3
CWRN	00FF	CWRNT	00D0	CYCNT	0094	DCLD	0084
DCYCH	010B	DCYM	0086	DECELF	00F9	DELT2	FB76
DELTFS	0096	DFSRMN	009C	DIACN	008C	DIVCNT	009E
DIVSR	00C6	DLY130	001F	DRIVE	0008	DUTCY	00F5
DUTCYI	00E9	DUTCYO	00E2	DUTCYS	00E0	DUTF1	00EA
DUTF2	00EB	DVDH	00CD	DVDL	00CE	DYMSK1	008A
DYMSK2	008B	EXCHG	F312	EXEND	FA20	FASTIV	0040
FLGWRD	00FC	FRCLCF	00F0	FRD	0088	FREX	0008
FRFLG	0090	FRTQL	0000	FRZERO	0002	FS	00F2
FSLP	00F4	FSLPM	0085	HGOREQ	0010	HGRSEL	0008
HIGEAR	0080	HSTPF	0111	HSTQL	0002	IBS8CM	00CB
IBSCUM	00C9	IBUSCH	010A	IBUSCM	00D9	IBUSD	0082
IBUSF	00FB	ICOMM	FC56	ICR	000D	IFRCLC	FB2A
IFRTRG	FA9A	IFSGEN	FC2D	INBUF1	2005	INBUF2	2006
INHCB	0080	INHIB	0001	IVCTRS	FFF0	K24	0018
KACLMN	FFCF	KACLMX	011D	KAMBFN	011F	KAMBTP	0120
KBATTP	012A	KCHRCY	FFC8	KCYCNT	0125	KDCLCS	0131
KDCLMN	FFD0	KDCLMX	011E	KDCYSU	0133	KDLDCY	FFCB
KDLNCH	FFCC	KDUTF1	FFCD	KDUTF2	FFCE	KEND	FFF7
KEXCY	013F	KFRCO	0130	KFRSHD	0134	KFRSHU	0135
KHSFN	0128	KHSTP	0129	KI110	0123	KI220	0124
KIBMAX	FFC7	KLAPD	0136	KLAPU	0137	KLNGTH	0025
KLOWFS	013D	KMNDCC	011C	KMNIBS	0127	KMNVBS	0122
KMODFG	FFCA	KMOT	013B	KMOTTP	012B	KMXDC1	012E
KMXDC2	012F	KMXVBS	0121	KNTCH	0000	KPERD	0020
KPLIBS	0126	KRLS	0132	KRSLN	003C	KSHFT	011B
KSTART	FFD2	KTHDC1	012C	KTHDC2	012D	KTQDL	FFD1
KTQDS	0138	KTQUS	0139	KVBMAX	FFC6	LAPCNT	00DE
LAT1	0103	LAT2	0104	LEDCNT	0093	LGOREQ	0004
LGRSEL	0004	LOGEAR	0040	MANMOD	0020	MCAP	F27F
MCHARG	F35E	MDRIVE	F9B3	MDUTCY	F730	MINPRO	F080
MODE	0102	MODED	0080	MOTTPF	0113	MOTTPR	0119
MRESET	F000	MSHIFT	F5ED	MSLIP	F6F5	MTORQ	F495
MTRQLM	F509	MTTQL	0008	MULT	00C4	MVPHZ	F6CC
MWAVE	F7FB	M$	0001	NCHCTX	0007	NCHSPD	00C1
NCHTBL	0140	NEUTRL	001E	NNF	0116	NNM	0087

NOCHR	0020	NOTCHI	00BF	NTCH	0001	NTCH24	FF1E
OCFCNT	009D	OCR	000B	OLAT1	00E4	OLAT2	00E5
P1DDR	0000	P2DDR	0001	PH2CNT	00AD	PH3CNT	00B5
PHXCNT	0006	PORT1	0002	PRKBRK	0001	PROD	00C5
PROMST	F000	PWCNT	00B9	RAMEND	017F	RAMERR	0002
RAMST	0080	RBUFF	008D	RDADC	2004	RDR	0012
RESETW	011A	REVREQ	0002	REVSEL	0001	RLSCNT	0091
RMCR	0010	RMNDR	00C7	RPM	010E	RSTFR	2001
RUNMOD	0020	S1DIV	FCFA	S1MLT	FCE7	SACCEL	0004
SADSPL	FD51	SAMBTP	0008	SBATTP	0008	SCHDCY	FEA4
SCRPAD	015E	SCURVE	FD91	SDCYS	FD26	SDECEL	0004
SHCNT	00DF	SHERR	0080	SHFLG	0010	SHSTP	0008
SIBUS	0004	SIP	0040	SKDATA	FE64	SLPTMP	00D1
SMOTTP	0008	SPAD	00CD	SPARE1	0109	SPARE2	0117
SPARE3	013A	SPARE4	013C	SPLCTR	00E8	SPOLL	FC45
SSHIFT	FDC9	STEMP	FD83	STKTOP	017F	STRL1	2005
STRL2	2006	STRMX0	2004	STRMX1	2014	STRMX2	2024
STRMX3	2034	STRMX4	2044	STRMX5	2054	STRMX6	2064
STRMX7	2074	SVBUS	0008	SWAVLD	FE80	TBLCNT	00C3
TBLI	0002	TBLSLN	FF4F	TCSR	0008	TDR	0013
TEMP1	0098	TEMP2	009A	TGGL11	009F	TGGL21	00A7
TGGL31	00AF	TGGLX1	0000	TGGLX2	0004	TPD	0089
TQRATE	0080	TRCSR	0011	TRGFR	2002	TRQCM	00D4
TRQCMO	00DD	TRQCMT	00D3	TRQDM	010D	VBUSCH	0108
VBUSCM	00DB	VBUSCR	0107	VBUSD	0081	VBUSF	00FA
VITQL	0040	VPHZ	00F7	VPHZCH	0118	VPHZIU	0115
WAVCNT	00BA	WAVOUT	00BC	WAVWRD	00B7	WMSK11	00A1
WMSK21	00A9	WMSK31	00B1	WMSKX1	0002	WMSKX2	0003
WRNCNT	00E3	WTCHDG	2000	XF	00D3	ZNW	00BE

APPENDIX C

WAVEFORM MODULATION SCHEME

APPENDIX C - WAVEFORM MODULATION SCHEME

The pulse-width modulation scheme consists of the following set of rules applied to a carrier pulse train which is traveling at some multiple of the stator frequency.

1. The carrier frequency is an integer multiple of 3 times the stator frequency. This rule provides a means of referencing the pulse train applied to each phase so that the unmodulated waveform puts zero voltage on the motor.

2. The center of each pulse of the carrier waveform in held stationary and both edges of the pulse are modulated an equal amount. This rule effectively doubles the pulse rate applied to the motor, as seen by the line-line voltage Figure A.C.1, where two pulses are applied to the motor for every pulse in the carrier wave.

3. The modulating function (sin V_et +0/) is evaluated at the center of each pulse. This rule fixes the least amount of distortion as compared to evaluating the waveform at the beginning of the pulse, etc.

4. The modulating functions for each motor phase are shifted from each other by 120°.

The resulting modulation of the carrier wave for each motor phase is shown in Figure A.C.1 for a carrier frequency of 12 times the stator frequency. In practice the carrier frequency was fixed at 48 times the stator frequency.

Fourier analysis of this PWM scheme shows that for less than 60% of the available line voltage, the lowest theoretical harmonic appearing in the voltage waveform is at twice the carrier frequency, which turns out to be the 96th harmonic in this case. At higher applied voltages, the modulated carrier pulses start merging and a sideband harmonic appears at the carrier frequency. Eventually the waveform degrades to a squarewave at the stator frequency.

Motor currents resulting from this PWM scheme are shown in section 6.2 "Inverter Performance Results."

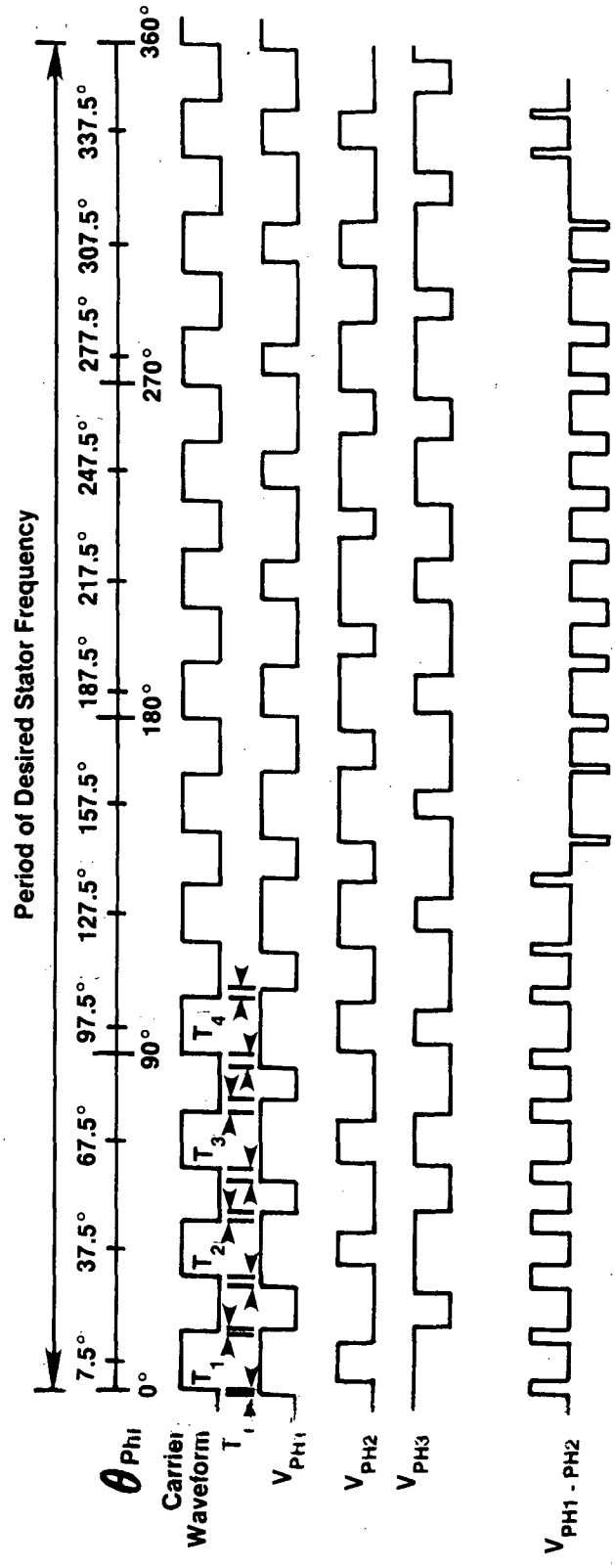

Figure A.C.1 Pulse-Width Modulation Scheme for Twelve Pulses/Stator Cycle

APPENDIX D

THERMAL ANALYSIS

APPENDIX D - THERMAL ANALYSIS

Purpose

This analysis was performed in order to predict the inverter package thermal performance as well as to provide recommendations for the improvement of the package thermal design.

Technical Details

The thermal analysis of the AC inverter package was performed using the SPICE Electrical Network Analysis Program, the component layout for the inverter package, at the time of this analysis is shown in Figure A.D.1.

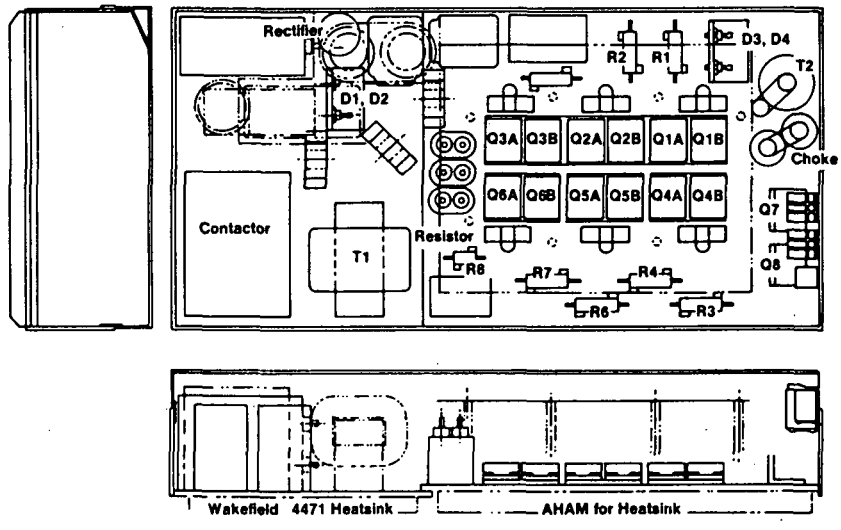

Figure A.D.1 Inverter Layout for Thermal Analysis

The following requirements for the operation of the system were specified:

- 50°C ambient external air temperature maximum
- 65°C internal case air temperature maximum
- 3 modes of operation
  - Charging - Free convection air cooling--550 watts total dissipation
  - Continuous - Forced convection air cooling--850 watts total dissipation
  - Overload (2 minutes) - Forced convection air cooling--1350 watts total dissipation.

An initial analysis showed that the inverter heatsink would be nonisothermal. To account for the heatsink temperature variation and the location of the component heat inputs, the heatsink was divided into a 40 node structure as shown in Figure A.D.2.

4.5 in.	1.5in.	4.0in	3.75in.	4.0 in.	4.0 in.	4.0 in.	4.25 in.	
101 o	106 o	111 o (Rectifier)	116 o	121 o	126 o (R2)	131 o (R1) (D3,D4)	136 o	3.0 in.
102 o	107 o	112 o (D1,D2)	117 o	122 o (R3)	127 o	132 o	137 o (T2)	2.5 in.
103 o	108 o	113 o	118 o	123 o (Q3A,Q3B)	128 o (Q2A,Q2B)	133 o (Q1A,Q1B)	138 o (Choke)	2.75 in.
104 o (contactor)	109 o	114 o (T1)	119 o (R8)	124 o (Q6A,Q6B)	129 o (Q5A,Q5B)	134 o (Q4A,Q4B)	139 o (Q7)	3.25 in.
105 o (contactor)	110 o	115 o (T1)	120 o	125 o (R7)	130 o (R6)	135 o (R4, R3)	140 o (Q8)	3.5 in.

Figure A.D.2 Heatsink Nodal Division

Each of the heat generating electrical components in the inverter package was represented using a thermal circuit analogy such as in Figure A.D.3. Standard heat transfer techniques (see References 1-3) were used in calculating values for the thermal circuit parameters. Component power dissipations for the three operating modes are shown in Figure A.D.4.

Figure A.D.3 Thermal/Electrical Analogy

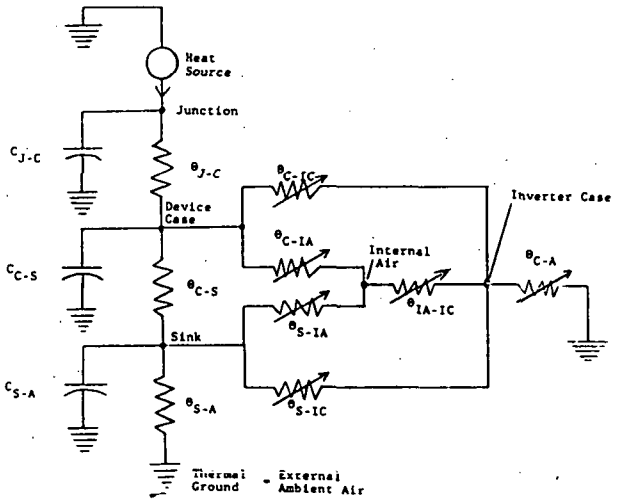

Initial data runs revealed several overheating components, as summarized in Figure A.D.5a. Also, forced convection air cooling was found to be necessary in all three modes of inverter operation. Several recommendations (see next section) were made to correct the overheating problems. The results of the analysis on the corrected geometry (Figure A.D.5b) show that the overheating problems are eliminated (with an air velocity of 1140 LFM over the inverter heatsink). The accuracy of these analyses is estimated at ±15 percent.

Data runs were also performed on the corrected geometry for air velocities of 180 LFM, 360 LFM, and 600 LFM. The results of these and the 1140 LFM run are shown in Figures A.D.6a through A.D.6j. This data was used in developing airflow requirements for various sections of the heatsink.

Conclusions and Recommendations

The following changes to the inverter package were recommended as a result of the thermal analysis:

- Provide forced convection air cooling over the inverter heatsink in all 3 modes of operation.

- Provide limited airflow over the top of the inverter case in all 3 modes of operation. (Approximately one third of the airflow over the heatsink.)

- Maintain thickness of Wakefield Series 120 thermal joint compound, the original method of mounting the transistors called for bolting them to an aluminum block, which had been joined to the main heatsink with a thermal epoxy. The devices are now bolted directly to the heatsink using a thermal conductive gasket, between 0.001 and 0.002 in. by providing adequate clamping (screw) torque at the following interfaces:

  - Transistor - Aluminum Block interface (Q1-Q6)
  - Diode - Aluminum Block interface (D1-D4)
  - Transistor - Angle Bar interface (Q7-Q8)
  - Rectifier - Heatsink interface
  - PCB transistor - Aluminum bus interface

- Route aluminum heatsink bus from PCB transistors to cabinet walls.

- Enlarge aluminum angle mounting brackets for transistors Q7-Q8.
- Alter mounting of diodes to reduce thermal resistance from diode case to heatsink (D1-D4).

- Use rectifier package with lower power dissipation and/or lower junction to case thermal resistance.

- Thermally insulate the following components to reduce internal case air heating:

  - Transistors (Q1-Q6)
  - Resistors (all RH-50 type)
  - Transformer (T1)
  - Aluminum Heatsink bus on PCB transistors.

The heatsink temperature maps in Figure A.D.6 should be consulted when developing airflow requirements for various sections of the inverter heatsink. These maps show that air velocities below 1140 LFM will provide adequate cooling in many areas of the heatsink.

COMPONENT POWER DISSIPATION

	DEVICE DISSIPATION (WATTS)											
Operating Mode	Q1-Q6 Transistor	Q1-Q6 Diode	PCB Transistor	D1-D2	D3-D4	Q7-Q8	R1-R7	T1	T2	Choke	Contactor	R8
Charging	Q6 A&B only 85 total	Q6A&B only 15 total	2.5 each	86 total	10 total	20 total	R6 & R7 only 100 total	200	14	14	--	50
Continuous	per pair (A&B) 67 each	per pair (A&B) 12 each	9.0 each	15 total	40 total	40 total	R1-R6 18 each	40	24	24	25	8
Overload	per pair (A&B) 115 each	per pair (A&B) 20 each	10.8 each	15 total	40 total	50 total	R1-R6 25 each	70	24	24	25	14

Figure A.D.4

Figure A.D.5A

INITIAL ANALYSIS RESULTS (1140 LFM)
T_{AMB} = 50°C

	DEVICE												
	Q1-Q6 Transistor	Q1-Q6 Diode	PCB Transistor	D1-D2	D3-D4	Q7-Q8	Rectifier	R1-R8	T1	T2	Choke	Contactor	Case air
Maximum Operating Temperature (°C) per data sheet specifications	150	150	150	125	125 assumed	200	175	250	200 assumed	200 assumed	200 assumed	125	65
Maximum Operating Temperature -Charging (°C)	116	119	136	175	78	78	187	131	96	73	70	--	62
Maximum Operating Temperature -Continuous (°C)	117	120	84	92	163	163	--	99	82	98	83	59	77

Figure A.D.5B

FINAL ANALYSIS RESULTS (1140LFM)
T_{AMB} = 50°C

Maximum Operating Temperature -Charging (°C)	95	94	69	123	63	81	89	87	198	68	66	--	60
Maximum Operating Temperature -Continuous (°C)	100	99	112	65	106	118	--	85	83	88	79	106	62
Maximum Overload Temperature	115	115	106	71	108	129	--	87	85	90	--	--	63

ALL UNITS (°C)

				(65.2)	(65.2)	(65.2)	
57.9	67.2	81.9 (89.0)	63.9	59.1	56.1	56.2 (62.9)	55.7
58.0	67.4	83.8 (123.2)	65.6	61.5	57.2	55.8	57.4 (68.4)
58.0	67.1	79.0	68.7	66.8	59.5	56.1	57.5 (66.3)
58.2	68.9	87.8 (196.0)	76.8 (84.4)	80.4 (94.8)	63.8	57.0	57.6 (81.0)
58.3	69.0	90.0 (198.2)	73.6	79.2 (86.8)	70.9 (78.4)	58.1	57.6 — Heatsink Temp. (81.0) — Operating Devi temp.
				(68.9)	(68.9)	(68.9)	

T_{AMB} = 50.0

$T_{AIR_{INT}}$ = 60.2

Figure A.D.6A

TEMPERATURE PROFILE MAP
CHARGING MODE $-V_{AIR}$ = 1140 LFM

ALL UNITS (°C)

				(101.1)	(101.1)	(101.1)	
53.2	54.6	56.6	59.7	67.5	74.0 (76.7)	78.2 (81.2) (105.8)	67.0
53.7	55.2	58.3 (65.3)	61.2	73.8 (76.6)	77.3	78.1	69.9 (88.1)
54.6	55.8	58.4	63.0	83.2 (94.6)	88.1 (99.5)	87.3 (98.8)	70.8 (78.8)
56.5 (104.7)	57.0	60.7 (82.4)	64.2 (65.4)	82.6 (94.1)	88.8 (100.2)	88.2 (99.6)	72.1 (118.1)
57.3 (105.5)	57.6	61.3 (83.0)	62.2	71.6	79.5 (82.3)	81.9 (84.6)	71.7 — Heatsink Temp. (117.1) — Operating Dev. Temp.
				(112.3)	(112.3)	(112.3)	

T_{AMB} = 50.0

$T_{AIR_{INT}}$ = 61.6

TEMPERATURE PROFILE MAP

CONTINUOUS MODE -V_{AIR} = 1140 LFM

Figure A.D.6B

ALL UNITS (°C)

				(66.9)	(66.9)	(66.9)	
66.7	78.5	95.6 (102.7)	73.9	67.0	62.0	60.9 (67.5)	60.3
66.6	78.7	97.6 (136.9)	76.0	69.9	63.5	60.7	62.1 (73.3)
66.4	78.1	92.9	79.8	76.1	66.4	61.5	62.5 (71.3)
66.2	79.1	102.1 (210.3)	88.7 (96.3)	91.0 (105.5)	71.5	62.6	62.6 (86.1)
65.6	75.5	104.0 (212.2)	85.7	90.4 (97.9)	79.4 (87.0)	64.0	62.7 — Heatsink Temp. (86.2) — Operating Devi Temp.
				(72.3)	(72.3)	(72.3)	

T_{AMB} = 50.0

$T_{AIR_{INT}}$ = 67.5

TEMPERATURE PROFILE MAP
CHARGING MODE $-V_{AIR}$ = 600 LFM

ALL UNITS (°C)

				(104.6)	(104.6)	(104.6)	
57.8	60.0	63.1	67.8	78.4	86.8 (89.5)	90.7 (93.3) (118.1)	78.1
58.4	60.8	65.0 (71.9)	69.6	85.5 (88.2)	90.7	91.4	81.1 (99.0)
59.5	61.6	65.3	71.7	95.7 (107.1)	102.5 (113.9)	91.6 (113.1)	82.4 (90.0)
61.7 (109.8)	63.0	67.9 (89.6)	73.1 (74.4)	95.3 (106.7)	103.6 (115.0)	102.9 (114.4)	84.3 (129.8)
62.6 (110.8)	63.6	68.7 (90.3)	71.1	83.6	93.9 (96.6)	96.4 (99.1)	84.1 — Heatsink Temp (129.6) — Operating Dev Temp.
				(104.6)	(140.6)	(104.6)	

T_{AMB} = 50

$T_{INT_{AIR}}$ = 67.8

TEMPERATURE PROFILE MAP
CONTINUOUS MODE - V_{AIR} = 600 LFM

Figure A.D.6D

ALL UNITS (°C)

				(67.5)	(67.5)	(67.5)	
72.1	85.1	103.1 (110.2)	80.6	72.7	66.8	64.6 (71.1)	63.9
71.9	85.1	105.1 (144.4)	82.8	75.9	68.5	64.7	65.9 (77.0)
71.5	84.3	100.3	86.8	82.5	71.7	65.7	66.4 (75.2)
70.9	84.6	109.5 (217.7)	96.2 (103.8)	98.1 (112.6)	77.2	67.0	66.5 (90.1)
69.9	78.5	111.1 (219.3)	93.2	97.7 (115.3)	85.5 (93.0)	68.6	66.7 — Heatsink Temp. (90.2) — Operating Devi Temp.
				(73.2)	(73.2)	(73.2)	

T_{AMB} = 50.0

$T_{AIR_{INT}}$ = 72.0

TEMPERATURE PROFILE MAP
CHARGING MODE $-V_{AIR}$ = 360 LFM

Figure A.D.6E

ALL UNITS (°C)

				(105.4)	(105.4)	(105.4)	
61.2	64.0	67.8	74.1	86.4	95.8 (98.6)	99.1 (101.3) (126.2)	86.0
61.9	64.8	69.8 (76.7)	76.0	93.9 (96.6)	100.2	100.6	89.2 (106.7)
63.0	65.7	70.2	78.3	104.5 (115.9)	112.4 (123.9)	111.4 (122.9)	90.8 (98.0)
65.2 (113.4)	67.1	72.9 (94.5)	79.8 (81.0)	104.2 (115.6)	113.8 (125.3)	113.1 (124.6)	93.1 (138.2)
66.2 (114.3)	67.3	73.6 (95.3)	77.7	92.2 (92.2)	104.0 (106.7)	106.6 (109.3)	93.0 — Heatsink Temp (138.1) — Operating Dev Temp.
				(121.3)	(121.3)	(121.3)	

T_{AMB} = 50

$T_{INT_{AIR}}$ = 67.8

TEMPERATURE PROFILE MAP
CONTINUOUS MODE -V_{AIR} = 360 LFM

Figure A.D.6F

ALL UNITS (°C)

				(68.6)	(68.6)	(68.6)	
85.4	100.1	119.9 (126.9)	96.4	87.1	79.2	74.7 (81.1)	74.0
84.9	99.9	121.8 (160.9)	98.9	90.8	81.4	75.6	76.2 (87.3)
83.9	98.4	116.8	103.3	98.1	85.2	77.2	77.0 (85.7)
82.3	97.0	122.7 (233.9)	113.1 (120.7)	114.8 (129.2)	91.5	79.0	77.3 (100.8)
80.2	85.4	126.5 (234.7)	110.2	114.8 (122.4)	100.4 (108.0)	80.9	77.7 — Heatsink Temp. (101.2) — Operating Devi Temp.
				(75.5)	(75.5)	(75.5)	

T_{AMB} = 50

$T_{AIR_{INT}}$ = 82.7

TEMPERATURE PROFILE MAP
CHARGING MODE $-V_{AIR}$ = 180 LFM

Figure A.D.6G

ALL UNITS (°C)

				(108.0)	(108.0)	(108.0)	
71.2	75.3	80.6	90.1	95.8	117.3 (120.1)	118.9 (120.2) (145.6)	105.4
71.8	76.1	82.7 (89.5)	92.3	114.1 (116.8)	122.5	122.2	108.7 (125.2)
72.9	76.8	83.1	94.8	125.4 (136.9)	135.6 (127.1)	134.3 (145.8)	110.8 (117.2)
74.9 (123.1)	77.8	85.7 (107.4)	96.5 (97.7)	125.4 (136.8)	137.7 (149.1)	136.9 (148.3)	114.1 (158.3)
75.6 (123.7)	76.3	86.2 (107.9)	94.3	113.0	127.8 (130.5)	130.6 (133.3)	114.4 — Heatsink Temp. (158.6) — Operating Devi Temp.
				(125.9)	(125.9)	(125.9)	

T_{AMB} = 50

$T_{INT_{AIR}}$ = 83.1

TEMPERATURE PROFILE MAP
CONTINUOUS MODE -V_{AIR} = 180 LFM

Figure A.D.6H

	DEVICE								
	Q1-Q6 Transistor	Q1-Q6 Diode	PCB Transistor	D1-D2	D3-D4	Q7-Q8	R1-R8	T1	Case Air
Max Recommended Operating Temp. (°C)	150	150	150	125	125 assumed	200	250	200 assumed	65
Max Temperature at 1140 LFM (°C)	115	115	106	71	108	129	87	85	63
Max Temperature at 600 LFM (°C)	130	129	110	77	121	141	102	92	69
Max Temperature at 360 LFM (°C)	141	139	111	82	129	150	112	97	73
Max Temperature at 180 LFM (°C)	165	163	113	95	149	170	137	110	84

SUMMARY - INVERTER OVERLOAD OPERATION

Figure A.D.6J

APPENDIX E

MECHANICAL MODIFICATION NOTES, CALCULATIONS AND DEFINITIONS

NOTES

1. EV 1300 battery weighs 75 lbs. The EV 800 which is being used for the first vehicle build weighs 51 lbs.

2. Comparable weights for the vehicle with EV 800 batteries are:

Distribution	Total	Front	Rear
Curb	2819	1489	1330
Design	3319	1641	1678
GVW	3519	1653	1866

3. Johnson's parabolic formula.

$$C_3 = \frac{S_y}{4n^2E}$$

where: S_y = yield stress
n = beam end restraint
E = modulus of elasticity

The values for P were taken from tables for steel S_y = 15,000 psi.

4. The 24-inch crush length is based on actual crush data generated on a production Escort (Lynx).

5. The crush length is for transversely oriented battery plates determined by crash tests.

6. After impact battery box length L_B = 2 crushed batteries + 2 battery box wall thickness + crushed front end sheet metal.

7. From crash tests of similar cars with battery pack dynamics.

8. Computer study of hatch back structural analysis by Alan Cross, Triad Services.

9. 9.459 is the moment of inertia of the reinforced rear rails plus a small contribution by the floor plan. The 0.7 denominator is the added stiffness of body structure.

10. There are 66 stainless steel hollow rivets in shear.

$$\text{AREA} = \frac{}{4}(0.18^2 - 0.125^2) = 0.0132 \text{ in}^2$$

For EV 1300 batteries and battery box

$$WT = 8 \times 75 + 40 = 640$$

$$S_s = \frac{640 \times 30}{66 \times 0.0132} = 22{,}038 \text{ psi}$$ (For a 30g deceleration)

Allowable S_S = 60,000 psi for 18 and 8 stainless steel

Therefore $\frac{22,038}{60,000}$ = 36% or 24 active rivets are required.

11. The increased rail section height for the rear suspension and battery pack results in a more than adequate bending moment improvement (174% greater versus 134% required). However, at the front wheel centerline the increased bending moment due mainly to the front battery pack is 58% over the production loading whereas the section structural modification (added gusset) resulted in a moment increase of 42%. These values are for EV 1300 (heavy) batteries. When the bending moment comparison is made for EV 800 batteries, which will be used initially in the test vehicles, the bending moment increases 32% over production which is less than the 42% structural increase. Therefore, the front wheel centerline structure is adequate for the EV 800 battery loading whereas the use of EV 1300 may be marginal.

12. Torsional loading refers to one side jounce opposite side rebound twisting of the trailing arms and rubber suspension bushings. In this case the torsional stiffness does not permit rebound to be reached when the opposite side is in jounce.

13. Lynx tire is P165-80R13, Citation tire is P185-80R13. The Lynx tires were considered adequate for the test vehicle loading. Ride handling was also adequate for tire pressures of 35 psi front and rear. The Citation tires could be used if, in future ride performance tests, upgrading is needed.

14. Ride and Handling Definitions

Reference Steer Angle - Deg/g

The angle from straight ahead the wheel plane attains when at 60 mph the lateral acceleration is 1.0g. The test is run at a large turn radius and a small steer angle where Ackerman can be neglected and the tire slip angle(1) is in the linear range.

Total Understeer - Deg/g

The difference in front and rear tire slip angles during a 1.0g turn at 60 mph for the above reference steer angle. The value shown includes the effects of suspension compliance, system geometry, tire characteristics, weight distribution, roll rate, etc., and equates them to an equivalent two-wheeled, mass-centered vehicle where the load sensitivity is zero and the system is rigid and noncompliant. The tires are also identical and inflated to the same pressure. The desired steer characteristic (oversteer or understeer) is a small amount of understeer for most passenger car conditions.

(1) Tire Slip Angle - angle formed between the direction of travel of the center of tire contact and the line of intersection of the wheel plane with the road surface.

Yaw Velocity Reponse Time - Sec.
Yaw velocity is the rate the car body rotates about an axis perpendicular to the ground with respect to a steady state (constant steer angle) direction change. Typically the body will oscillate toward a steady state condition. The time it reaches 95% of its steady state condition on the first leg of its rotation is the response time See Figure A.E.1.

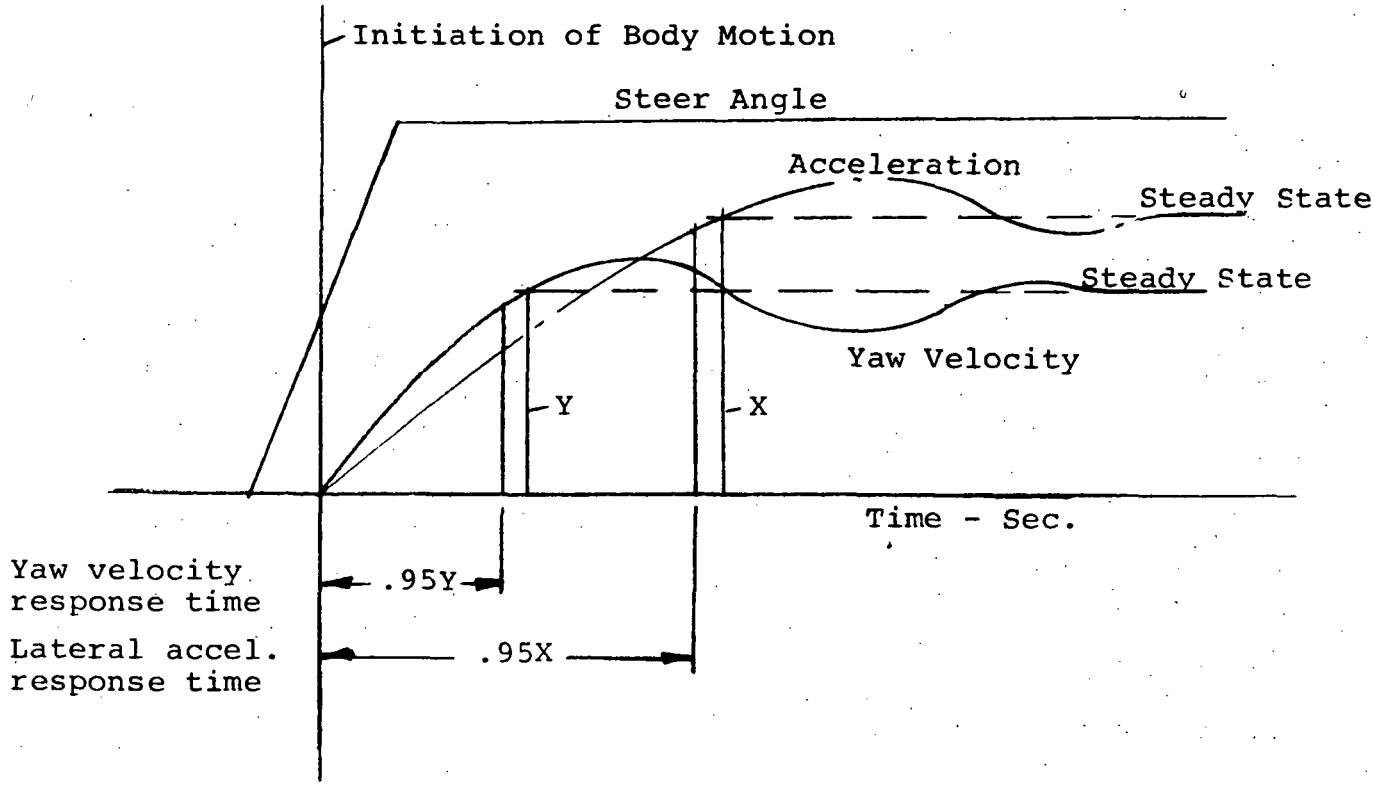

Figure A.E.1

Lateral Acceleration Response Time - Sec.
The lateral acceleration during a fixed turn angle will oscillate to a steady state condition similar to the yaw velocity but usually lags it. The response time is similarly computed at 95% of its steady state value on the first leg of acceleration. See Figure A.E.1.

1. Report No	2. Government Accession No.	3. Recipient's Catalog No.
NASA CR- 168244		

4. Title and Subtitle	5. Report Date
AC PROPULSION SYSTEM FOR AN ELECTRIC VEHICLE - PHASE 2 INTERIM REPORT	June 1983
	6. Performing Organization Code
7. Author(s)	8. Performing Organization Report No.
J. M. Slicker	ERC TR #83024
	10. Work Unit No.
9. Performing Organization Name and Address Eaton Corporation Engineering & Research Center 26201 Northwestern Highway, P. O. Box 766 Southfield, MI 48037	11. Contract or Grant No. DEN3-211
	13. Type of Report and Period Covered Contractor Report
12. Sponsoring Agency Name and Address National Aeronautics and Space Admin. Washington, D.C. 20546	14. Sponsoring Agency Code DOE/NASA/0211-1

15. Supplementary Notes

Project Manager N. Sargent, Transportation Propulsion Division
NASA-Lewis Research Center, Cleveland, OH

16. Abstract

A second-generation prototype ac propulsion system for a passenger electric vehicle was designed, fabricated, tested, installed in a modified Mercury Lynx vehicle and track tested at the Contractor's site. The system consisted of a Phase 2, 18.7 kw rated ac induction traction motor, a 192-volt, battery powered, pulse-width-modulated, transistorized inverter packaged for under rear seat installation, a 2-axis, 2-speed, automatically-shifted mechanical transaxle and a microprocessor-based powertrain/vehicle controller. A diagnostics computer to assist tuning and fault finding was fabricated. Dc-to-mechanical-system efficiency varied from 78% to 82% as axle speed/torque ranged from 159 rpm/788 nm to 65 rpm/328 nm. Track test efficiency results suggest that the ac system will be equal or superior to dc systems when driving urban cycles. Additional short-term work is being performed under a third contract phase (AC-3) to raise transaxle efficiency to predicted levels, and to improve starting and shifting characteristics. However, the long-term challenge to the system's viability remains inverter cost. A final report on the Phase 2 system, describing Phase 3 modifications, will be issued at the conclusion of AC-3.

17. Key Words (Suggested by Author(s))		18. Distribution Statement
Electric Vehicle	Drivetrain	Unclassified - unlimited
Alternating Current	Powertrain	DOE Category UC-96
Propulsion System	Inverter	

19. Security Classif. (of this report)	20. Security Classif. (of this page)	21. No. of Pages	22. Price*
Unclassified	Unclassified		

* For sale by the National Technical Information Service, Springfield, Virginia 22161

NASA-C-168 (Rev. 10-75)